DEUQUA EXCURSIONS

issn 2625-8129
An open-access journal by the German Quaternary Association
Editor-in-chief: Henrik Rother

DEUQUA Special Publications

FROM WEICHSELIAN ICE-SHEET DYNAMICS TO HOLOCENE LANDSCAPE CHANGES IN WESTERN POMERANIA AND MECKLENBURG

Field trips on geology, geomorphology and geoarchaeology

Guest editors: Heiko Hüneke, Andreas Börner, and Sebastian Lorenz

International Field Symposium
of the **INQUA Peribaltic Working Group**
7–13 September 2019 in Greifswald, Germany

Copernicus Publications
The Innovative Open Access Publisher

DEUQUA Special Publications

An open-access journal of the German Quaternary Association

Editor-in-chief 2018: Christopher Lüthgens

Die Deutsche Quartärvereinigung (DEUQUA) e.V. ist ein Zusammenschluss deutschsprachiger Quartärwissenschaftler. Der Verein hat zum Ziel die Quartärwissenschaft zu fördern, sie in der Öffentlichkeit zu vertreten, den Kontakt zu angewandter Wissenschaft zu intensivieren sowie öffentliche und politische Gremien in quartärwissenschaftlichen Fragestellungen zu beraten. Desweiteren hat der Verein sich zur Aufgabe gemacht, die Kontaktpflege der Quartärforscher untereinander und zu verwandten Organisationen im In- und Ausland zu betreiben.

The German Quaternary Association (Deutsche Quartärvereinigung, DEUQUA e.V.) is the official union of German-speaking Quaternary scientists. The aim of the association is to support Quaternary science, to present it to the public, to intensify contacts to the applied sciences, and to provide advice to public and political authorities on issues related to Quaternary science. Furthermore, the association supports networking among Quaternary scientists and neighbouring disciplines at home and abroad.

Copernicus Publications
The Innovative Open Access Publisher

Copernicus Publications
Bahnhofsallee 1e
37081 Göttingen
Germany

Phone: +49 551 90 03 39 0
Fax: +49 551 90 03 39 70

publications@copernicus.org
http://publications.copernicus.org

Printed in Germany.
Schaltungsdienst Lange o.H.G.

ISSN 2625-8129

Published by Copernicus GmbH (Copernicus Publications) on behalf of the German Quaternary Association (DEUQUA).

Image credits:
Top: Sea cliff and morphology of the Jasmund Peninsular from southeast (Photo: Martin Meschede)
Bottom left: Königsstuhl, coastal cliff of Jasmund, imbricated chalk (Photo: Paul Mehlhorn)
Bottom center: The valley of the meandering Tollense River near Kessin (Photo: Sebastian Lorenz)
Bottom right: View from Großer Werder at Lake Krakower Obersee (Photo: Sebastian Lorenz)

Excursion route

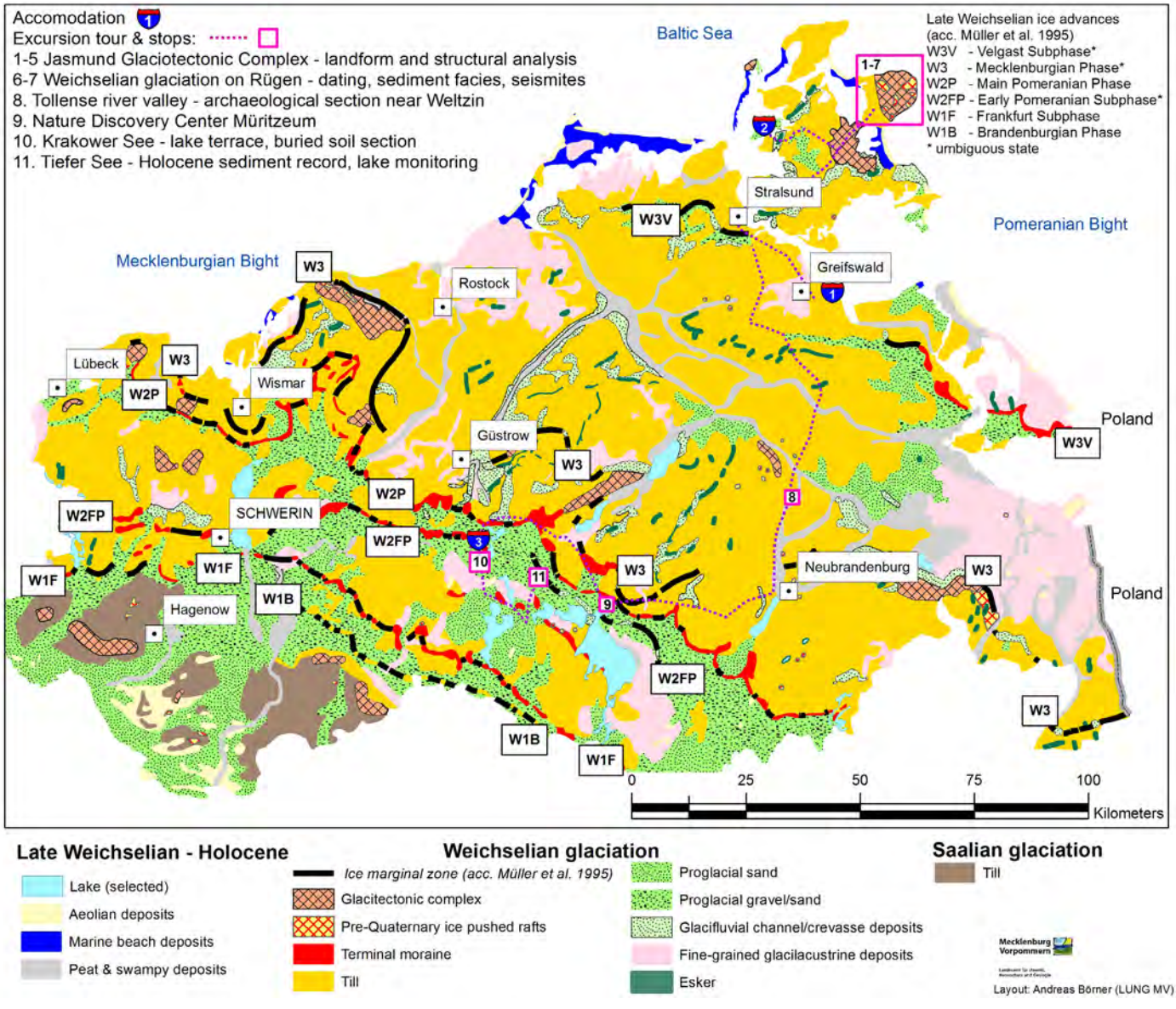

Excursion route during the International Field Symposium of the Peribaltic Working Group from 7 to 13 September 2019 in Greifswald. Simplified geological map of Mecklenburg-Western Pomerania modified by A. Börner (2019, based on Bremer, 2002; Müller et al., 1995; and Müller, 2004b); for details and references, see the introduction of this volume.

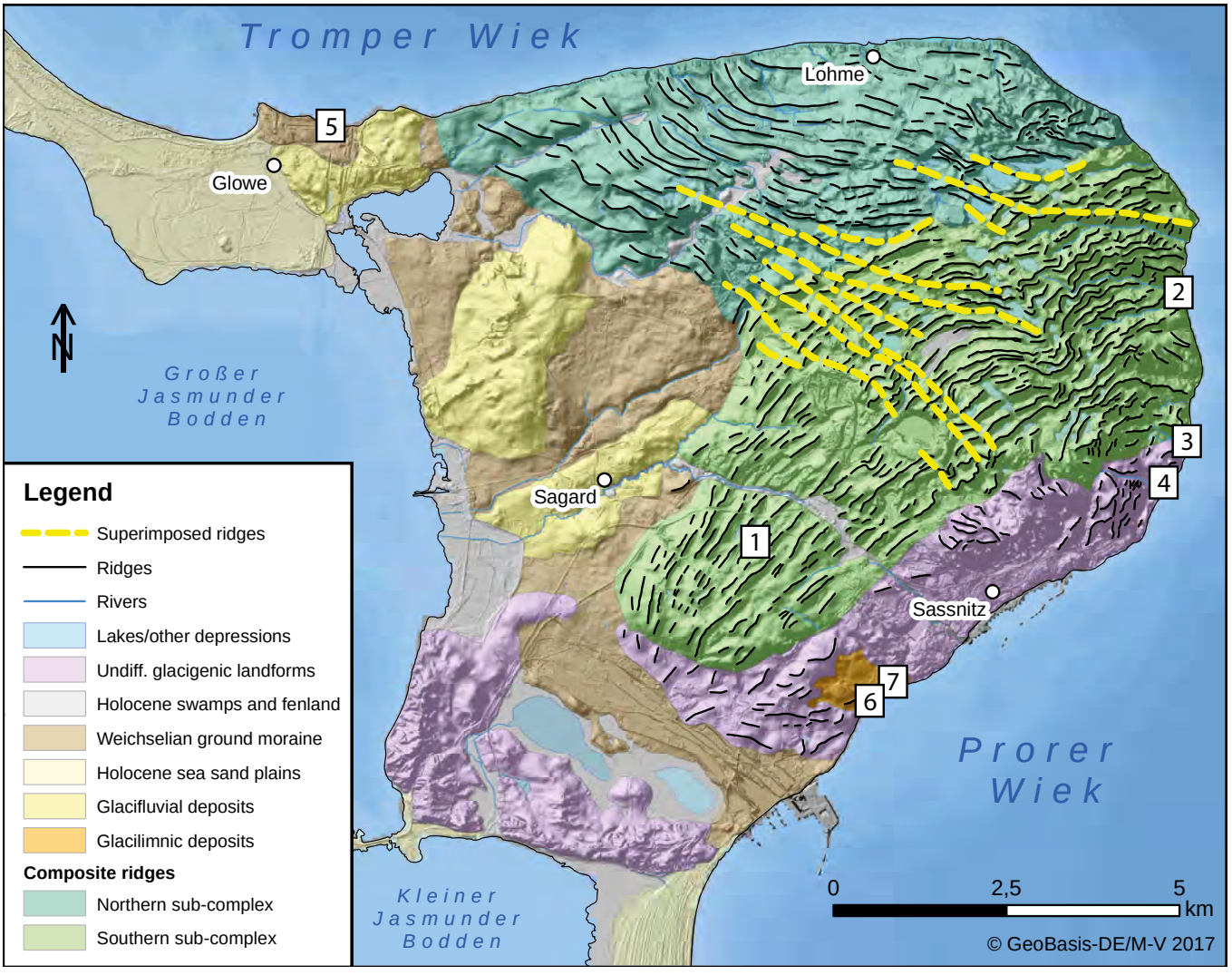

Location of stops 1 to 7 on Jasmund (Rügen) during the International Field Symposium of the Peribaltic Working Group from 7 to 13 September 2019 in Greifswald. Geomorphological map of the Jasmund peninsula with hillshaded digital elevation model as background (modified from Gehrmann, 2018); for details and references, see stop 1 of this volume (Gehrmann and Harding, 2019). The surrounding seabed is based on a digital elevation model of the German Baltic Sea (Tauber, 2012a, b).

DEUQUA Spec. Pub., 2, 1–10, 2019
https://doi.org/10.5194/deuquasp-2-1-2019

Open Access DEUQUA Special Publications

The Quaternary sequence of Mecklenburg-Western Pomerania: areas of specific interest and ongoing investigations

Andreas Börner[1], **Anna Gehrmann**[2], **Heiko Hüneke**[2], **Michael Kenzler**[2], **and Sebastian Lorenz**[2]

[1]Geological Survey of Mecklenburg-Western Pomerania, LUNG M-V, Goldberger Strasse 12, 18273 Güstrow, Germany
[2]Greifswald University, Institute for Geography and Geology, Friedr.-Ludwig-Jahn Str. 17a, 17489 Greifswald, Germany

Correspondence: Andreas Börner (andreas.boerner@lung.mv-regierung.de)

Relevant dates: Published: 15 August 2019

How to cite: Börner, A., Gehrmann, A., Hüneke, H., Kenzler, M., and Lorenz, S.: The Quaternary sequence of Mecklenburg-Western Pomerania: areas of specific interest and ongoing investigations, DEUQUA Spec. Pub., 2, 1–10, https://doi.org/10.5194/deuquasp-2-1-2019, 2019.

Abstract: This paper aims to combine the knowledge of more than 100 years of Quaternary research in Mecklenburg-Western Pomerania (Geinitz, 1922; Deecke, 1907; Schulz, 1967, 1971; von Bülow, 2000; Rühberg et al., 1995; Müller et al., 1995; Katzung, 2004; Kenzler et al., 2015, 2018) including a summary of the areas of specific interest, a general overview of the most recent scientific results and of the ongoing investigations presented during the Field Symposium of the INQUA PeriBaltic Working Group 2019.

Dedication

This article is dedicated to Werner Schulz (1932–2018) and all active Quaternary field geologists for their important input during the last decades.

1 Quaternary sedimentary record and environmental change in northeastern Germany

1.1 Early and Middle Pleistocene (2.6–0.3 Ma)

The oldest Pleistocene deposits are located in the SW of Mecklenburg-Western Pomerania (MWP) and consist of fluvial gravel (von Bülow, 2000) with a mixed provenance of northern and southern source area (lydites and porphyrites). These fluvial deposits ("Loosen-Formation") were assigned to the Early Pleistocene (Rühberg et al., 1995; von Bülow and Börner, 2019; see Fig. 1). In the buried, over-deepened erosional channels near Hagenow (SW Mecklenburg), the base of the Pleistocene is found at a maximum depth of 550 m. Here, the greatest thickness of Pleistocene deposits in MWP (427 m) has been observed. Glaciofluvial sands overlie the oldest cold climate sediments at the base of this channel structure. Proglacial deposits of an Elsterian ice advance (400–320 ka; Litt et al., 2007) indicate the change to the first complete glacial–interglacial cycle. During the Elsterian deglaciation, glaciolacustrine sediments were deposited, such as the more than 100 m thick fine-grained sequence of the "Lauenburg Clay" in the lower Elbe area (SW Mecklenburg, Müller, 2004a). Palynological data from the upper part of the Lauenburg Clay sequence indicate the change from sub-arctic climate conditions to the warmer climate of the Holsteinian Interglacial (320–300 ka; German Stratigraphic Commission, 2016).

1.2 The Holsteinian Complex (320–300 ka)

In the area of MWP, the Holsteinian marine transgression occurred during pollen zone 4 and finished after Holsteinian pollen zone 5 (according to the pollen zones of Erd, 1973). The related marine-brackish deposits are not only restricted to the system of over-deepened Elsterian chan-

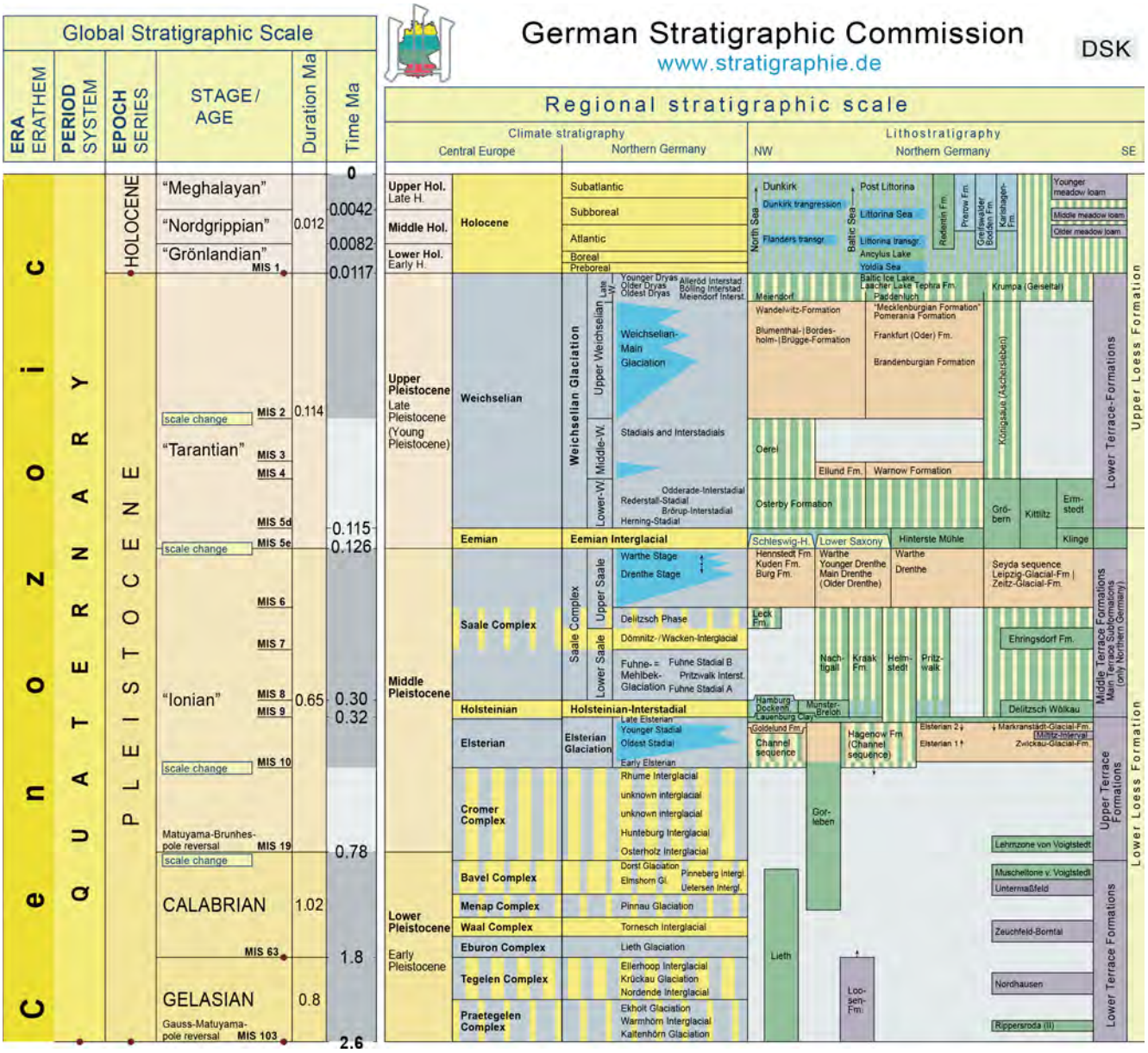

Figure 1. Quaternary stratigraphy of northern Germany (modified after German Stratigraphic Commission, 2016; cf. Bittmann et al., 2018).

nels and basins, but also locally distributed across central Mecklenburg and the eastern adjacent area between Anklam and Neubrandenburg. Throughout the "Holsteinian Complex", fluvial deposits of southerly provenance are intercalated (Müller et al., 1995; von Bülow, 2000).

1.3 The Saalian Complex (300–126 ka)

Above the late Holsteinian deposits, silt layers occur at several localities with a pollen spectrum indicating cold, arctic climate conditions. These silts are classified as the Fuhne cold stage (Fig. 1). During the course of the first Saalian ice advance (MIS 6), coarse proglacial sands were deposited, increasing in thickness towards the south. A similar tendency has also been noted with regard to the respective Saalian till sheets (Müller et al., 1995). The "Drenthe" ice advance deposited a highly variable, frequently very thick qsD-till sheet, often containing lenses and rafts of redeposited allochthonous pre-Quaternary materials of Jurassic, Cretaceous and Tertiary ages. For large areas of MWP, this Saalian ice advance is responsible for the palaeo-morphology of the pre-Pleistocene substrate surface (Müller, 2004c). In the easterly parts of MWP, the clay-rich qsD-till constitutes a characteristic marker unit, with its green to blue-green matrix (incorporation of Tertiary clay) and high flint content (Cretaceous). Further inland, a compact Saalian till sheet is present,

which splits further to the south into two individual till layers (qsD, qsWA), which may be separated locally by sand and gravel lenses possibly of englacial origin. Based on numerous drillings that have been sampled during the last 50 years, the conventional subdivision of the Saalian into a "Drenthe" and "Warthe" substage has proved to be valid (Fig. 1; Müller et al., 1995). In the northeasternmost parts of MWP (e.g. Rügen), this qsWA-till forms the main unit of the Saalian glaciation. For example, on the island of Rügen and in the coastal areas of Western Pomerania, only a discontinuous layer of Saalian till has been found (on Rügen mainly of the "Warthe substage").

1.4 The Eemian Interglacial (126–115 ka)

At several locations in MWP, Eemian sequences are preserved. For example, the transition from the Saalian deglaciation into the early Eemian (including the initial Eemian marine transgression) is documented in a sequence at the cliff of Klein Klütz Höved west of Wismar (Strahl et al., 1994; Menzel-Harloff and Meng, 2015; Kenzler et al., 2018). Furthermore, a lacustrine sequence comprising the complete transition from the Eemian into the Early Weichselian is well-documented at the outcrop "Hinterste Mühle" in Neubrandenburg (Rühberg, 1998 ; Rühberg et al., 1998; Börner et al., 2018), and the Eemian profiles of Banzin and Beckentin in the southwest of Mecklenburg have recently been investigated, yielding new palaeoecological and U–Th data (Börner et al., 2015; Rother et al., 2019). Hence, the number of sites with proven lacustrine Eemian deposits has increased markedly during recent years.

Marine deposits of Eemian age are largely restricted to the present coastal areas (Menzel-Harloff and Meng, 2015; Börner et al., 2018; Kenzler et al., 2018). Therefore, the palaeogeography of the Eemian Sea differs significantly from that of the Holsteinian Sea, and it closely resembles the recent land–sea distribution (Müller, 2004a). The "Eemian Warnow bay" (Fig. 1), where marine mollusc-bearing sands of Eemian age were deposited (Gehl, 1961; Müller, 2004b; Börner et al., 2018), is an exception. Another relic of the Eemian Interglacial is the greenish-coloured reduction zone in the upper part of the "m1" till (qsWA) of the Stoltera cliff section NW of Rostock. This zone is interpreted as a result of Eemian weathering and pedogenesis (Ludwig, 1964).

1.5 The Early to Middle Weichselian (115–27 ka)

The Lower and the beginning of the Middle Weichselian period are characterised by a repeated alternation of stadials and interstadials (e.g. Hermsdorf and Strahl, 2008). The existence of an Early to Middle Weichselian ice advance (Warnow advance, Müller, 2004a, b; Obst et al., 2017) reaching MWP has so far not been incontestably confirmed (Kenzler et al., 2018). A possible correlation of this Warnow advance with the Danish Ristinge advance (56–46 ka) has been proposed by Houmark-Nielsen (2010). However, because no absolute age data are available for the Warnow advance, the exact stratigraphic position is still unknown. One reason for this lack of data is the absence of deposits of Early to Middle Weichselian age in MWP. Hence, this time period is poorly documented across this area.

Sedimentological and geochronological results indicate that no ice advance reached the island of Rügen during MIS 3 (57–29 ka; Kenzler et al., 2015, 2017). Lacustrine and fluvial depositional environments dominated the steppe-like landscape at that time. A cooling phase during the transition from MIS 3 to MIS 2, which was possibly associated with the Klintholm advance (32 ± 2 ka; Houmark-Nielsen, 2010) known from Denmark, preceded the Last Glacial Maximum (LGM) with its massive Scandinavian Ice Sheet (SIS) advances (Kenzler et al., 2017). New luminescence ages for sandur deposits genetically related to the Brandenburgian ice marginal position (Lüthgens et al., 2010a, b, 2011) raised the possibility of a two-folded LGM in NE Germany (Lüthgens et al., 2011; Hardt et al., 2016), casting doubt on the traditional interpretations of the main Weichselian ice advances in this area.

1.6 The Last Glacial Maximum (27–13 ka)

We still only have limited knowledge about the depositional environments and processes, the oscillation of the SIS during the LGM and early Late Glacial, and especially the deglaciation sequence of NE Germany between 25 and 14 ka, which has only been locally dated. The first unequivocal evidence of a Weichselian ice advance reaching MWP has been dated at about 25–20 ka (Kenzler et al., 2015, 2017, 2018; Pisarska-Jamroży et al., 2018). This time roughly coincides with the palaeo-geographical reconstructions of the SIS extent in the southwestern Baltic Sea area by Hughes et al. (2016). This Late Weichselian glaciation created new landforms, such as end moraines, dead-ice holes or drumlins. Morphostratigraphical evidence, combined with provenance analyses of the till fine gravel (4–10 mm) content (TGL 25232, 1971), provides the basis for a subdivision into distinct classes (Nordic crystalline, Palaeozoic limestone and so on). The lowest member of the glacial sequence is the till sheet of the Brandenburgian Phase (W1B), together with its proglacial outwash deposits. Nearby the southern ice marginal zone till deposits of the W1B are often absent, which might be explained, at least partly, by solifluction and smoothing of the morphology due to the strong periglacial conditions during MIS 2 (Rühberg et al., 1995). The oscillating character of the W1 glaciation is documented in the deposits and end moraines of the Frankfurt(Oder) subphase (W1F), which is classified in NE Germany as a W1 readvance. In MWP both W1 subphases (W1B and W1F) are preserved together in a single till layer with no clear lithostratigraphical differences (Rühberg and Krienke, 1977). After a subsequent short deglaciation phase, the SIS readvanced into NE Ger-

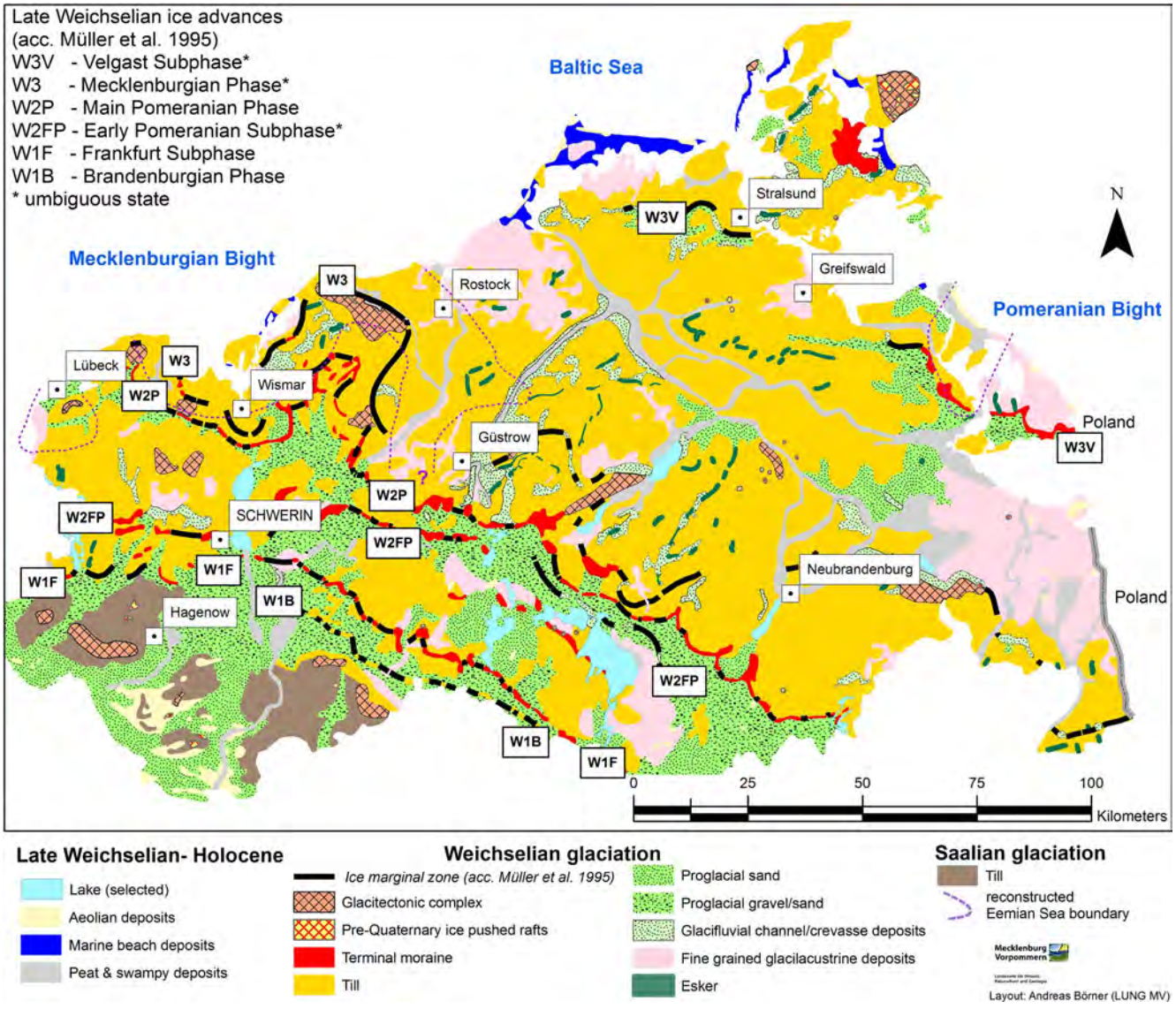

Figure 2. General geological map of Mecklenburg-Western Pomerania (based on Bremer, 2002; Müller, 2004b).

many (W2 – Pomeranian advance, Müller et al., 1995), which took place in two separated phases associated with distinct geomorphological features, such as different end moraines. The early Pomeranian advance (W2FP) pushed locally more southward as the "Pomeranian main advance" (W2P, Fig. 2), whereas the main Pomeranian advance formed pronounced end moraines, representing the main watershed between the catchment area draining into the Baltic Sea and the Elbe river catchment area flowing into the North Sea. The most important gravel and sand resources of MWP are related to the large proglacial outwash plain of the Pomeranian sandur areas. Based on recent work along the gas pipeline trenches crossing MWP (e.g. Börner et al., 2011; Börner and Müller, 2012), the place of the third Late Weichselian readvance of the "Mecklenburgian phase" (W3, Rühberg, 1987, Müller et al., 1995, Müller, 2004a), including the Velgast substage (W3V, Bremer, 2000), in the stratigraphic hierarchy remains controversial.

1.7 The Late Weichselian deglaciation and the Holocene (13–0 ka)

The landscape and the soil development in NE Germany show a clear relationship between the successive stages of the retreating SIS and the development of periglacial conditions (Liedtke, 1993). A first phase of intensified dead-ice melting, associated with intensive soil erosion, correlates with the Earliest Dryas and Bølling–Meiendorf (Terberger et al., 2004). Evidence for the presence of periglacial conditions and related soft-sediment deformations is found numerous in the soil profiles (Kopp, 1965, 1970). These "periglacial trans-

formed" soils display zones of distinct signs of periglacial transformation, such as a high concentration of clay/silt, which resulted from congelifraction and other processes. The *Geschiebedecksand* "pebble cover sand" represents a stratigraphic marker of periglacial origin due to frost heave, deflation, aeolian sedimentation and finally destratification (Kopp, 1970). The transformation, duration and intensity of climate conditions during the Weichselian deglaciation and Holocene period, as well as the soil formation, have been investigated in detail on the Pomeranian outwash plains (Küster and Preusser, 2010) and were found to be mainly influenced by intensive aeolian deflation and deposition. Within the covers and layer, a brunic Arenosol has been identified in MWP (Lorenz et al., 2002, 2019; Kaiser et al., 2009), which is associated with the Allerød "Finow soil" in NE Brandenburg (Schlaak, 1993, 1998). The development of a dense vegetation cover during the Early Holocene resulted in stabilisation of the landscape surface and subsequent soil formation. Often the dead-ice melting was followed by the formation of small lakes. Near Dobbertin at the Mildenitz river basin, the late glacial melting of buried dead ice occurred 14.5 kyr ago (Zawiska et al., 2014). The melting phase resulted in a reshaping of the lake basin morphology by new depressions, which were filled by glaciofluvial in- and outlets. Radiocarbon ages of buried birch trunks and basal peat indicate a first peat formation soon after the beginning of the Weichselian Late Glacial period ("Meiendorf-Interstadial", Fig. 1). The postglacial river–lake system in NE Germany was part of an immature drainage framework located along the Weichselian belt of northern central Europe. Frequent and abrupt changes in flow direction and the presence of numerous stagnant ice depressions occurred in the river valley (Lorenz and Schult, 2004; Kaiser et al., 2007; Błaszkiewicz, 2011). During the Allerød interstadial, the lake levels declined and fluvial activity decreased. As a consequence of the expansion of *Betula–Pinus* forests, soil erosion decreased and mainly organic sediments were deposited in the basins.

The oldest known human settlement in NE Germany, the elk-hunter camp at the Endingen archaeological site west of Stralsund, has been physically dated to the early Allerød (Kaiser et al., 1999). Remains of giant deer and horse indicate the existence of open parts in the landscape (Benecke, 2000). The pollen succession from a limnic section shows a palynostratigraphy ranging from the "Bølling" (*Hippophae* phase) to the middle Allerød. The tephrostratigraphy of lake sediments at the Endinger Bruch site provides the first age model for the Late Glacial palynological records of NE Germany (Lane et al., 2012). The cryptotephra contained six tephra layers of volcanic eruptions from Germany and Iceland spanning from the open vegetation phase I (Bølling) to the Early Holocene *Betula–Pinus* forest phase (Preboreal, 10.5 ka). Especially the Laacher See Tephra (12.9 ka cal BP, Eifel Volcanic Field in NW Germany) is present in very high concentrations within sediments of the Allerød phase (Lane et al., 2012).

The Younger Dryas (YD) is associated with a marked increase in fluvial and aeolian sedimentation, and lake-level high stands (Lorenz, 2007; Kaiser et al., 2007). In the open landscape during the YD, the soil erosion activity increased again and fluvial dynamics enlarged. There are clear indications of increasing aeolian activity mainly in the second part of the YD cooling phase. The YD in NE Germany was followed by Early Holocene lake-level low stands and a subsequent stabilisation phase with decreasing silicate input and increasing organic lacustrine deposition. The soil erosion was reduced and probably the final melting of the last remnants of buried dead ice blocks took place in the Preboreal (Terberger et al., 2004). The infilling continued until peat accumulation and terrestrialisation of lake basins became widespread during the Middle to Late Holocene. Beginning in the Late Holocene, the anthropogenic influence became important mainly through an increase in sediment supply due to deforestation and a rise in agricultural land use. In addition, mill stowage, river course corrections and anthropogenic lake-level modifications have increased stepwise since the 12th century CE.

2 Areas of specific interest and ongoing research

The peninsula of Jasmund on Rügen, located in the southwestern Baltic Sea area, is a landform that displays large-scale glaciotectonic folding and thrusting (e.g. Steinich, 1972; Groth, 2003; Ludwig, 2011; Gehrmann and Harding, 2018). Late Cretaceous and Pleistocene deposits exposed along impressive sea cliffs form part of a major fold and thrust complex. It developed as a result of Late Weichselian glaciotectonism (ice-marginal glacial tectonics) associated with the highly dynamic Baltic Ice Stream. The latter drained the SIS in a south-westerly direction during the Late Weichselian and the peninsula of Jasmund was situated at its southern marginal zone (Lüthgens and Böse, 2011; Böse et al., 2012; Hughes et al., 2016; Hardt and Böse, 2018; Kenzler et al., 2018).

Detailed macro- and microstructural studies have developed a kinematic model to explain the bi-lobed structure and the internal architecture of the glaciotectonic complex (Gehrmann, 2018; Gehrmann et al., 2019). Sediment–landform associations and flow-direction criteria derived from a variety of glacial deposits have been used to reconstruct successive glacial advances and retreats of this mobile ice sheet across the peninsula of Jasmund. The age of main ice advances and minor fluctuations have been reconstructed by luminescence dating in combination with lithostratigraphic, sedimentological and micromorphological investigations of the (glacio-)fluvial, lacustrine and aeolian deposits (e.g. Steinich, 1992; Panzig, 1995; Ludwig, 2006; Müller and Obst, 2006; Kenzler et al., 2017; Kenzler and Hüneke, 2019). The microfabrics within the tills laid down by the SIS have been studied by means of two- and three-

dimensional analyses based on the microstructural mapping, which enables the identification and interpretation of the successive generations of fabrics in terms of a progressive, polyphase deformation history (Brumme, 2015; Brumme et al., 2019; Gehrmann et al., 2017, 2019; Mehlhorn et al., 2019). The orientation of these microfabrics can be directly related to changes in the regional ice-flow direction across the peninsula of Jasmund.

The strongly curved coastline of Western Pomerania is initially followed by a morphologically inconspicuous inland. The slightly undulating morainic areas with dominating ablation tills were most likely formed by rapid Late Weichselian glacier decay without oscillations from the ice margin of the Mecklenburgian Phase (Rühberg, 1987). Due to intense weathering, the predominantly loamy tills are characterised by cambic soils and partly hydromorphic Luvisols (Börner et al., 2012). From a regular network of subglacial channels, large ramified river valleys and mires emerged from the Late Weichselian onwards, mainly driven by a rising groundwater table since the Early Holocene, while lower river sections were influenced by the rising level of the Baltic Sea (Janke, 2002; Kaiser et al., 2012). A valley section of river Tollense near the village Weltzin about 25 km north of Neubrandenburg holds spectacular archaeological findings, attributed to violent conflicts in the Bronze Age about 3250 years ago (Jantzen et al., 2011; Lidke et al., 2018). Large quantities of human bones, arrowheads and other types of weapons, and metal findings have been preserved in the deposits of river Tollense. The assumed starting point of the battle is a pathway currently overgrown by peat, which crossed the river and surrounding mire (Jantzen et al., 2014). Results of archaeological excavations and interdisciplinary research on the found materials, as well as geoscientific results on the Bronze Age palaeoenvironment, are presented in Brinker et al. (2018), Flohr et al. (2015), Krüger et al. (2012), Lorenz et al. (2015), Price et al. (2017), and Lidke and Lorenz (2019).

The lake district of Mecklenburg ranges between the Weichselian ice marginal zones of the Brandenburgian and Pomeranian Phase with a broad variety of lakes and rivers (Rühberg, 1999; Kaiser et al., 2012; Janke, 2004). While some parts still belong to the Baltic Sea catchment, the larger lakes drain via tributary waters and eventually the river Elbe to the North Sea. Lake Müritz (113 km^2, 62.1 m a.s.l.) is the largest lake of the Mecklenburg lake district and represents together with the city of Waren/Müritz the tourist centre of the area (Rühberg, 1999; Grundmann, 1999). South and northwest of the city large interconnected lakes, the so-called "Upper Lakes", can be found as relics of vast Pleniglacial and Late Glacial palaeolakes (Kaiser, 1998). In the southeastern continuation of the lake district, smaller lakes and chains of lakes characterise the landscape (Küster et al., 2012). During the last decade, geoscientific research has focused on Holocene palaeohydrology and morphogenesis of lakes and river valleys, and the pedological tracing of land use history (Kaiser et al., 2012, 2015; Küster, 2014; Lampe et al., 2009). Typical sections of the lake landscapes are protected in the Müritz National Park, while the nature experience centre Müritzeum in Waren exhibits collections of indicator boulders, fossils, plants and animals (Küster, 2019).

The lacustrine basins of Krakower See and Tiefer See are genetically related to glaciofluvial incision very close to the ice margin of the Pomeranian Phase, followed by a delayed thawing of buried dead ice between the Meiendorf Phase and the Preboreal with remarkable lake-level fluctuations. Detailed palaeoenvironmental studies on lake sediments, and pedological and geomorphological studies on lake terraces, palaeosoils and adjacent river valleys have been used to reconstruct Weichselian Late Glacial and Holocene lake-level fluctuations and Holocene land-use history (e.g. Kaiser et al., 2007; Lorenz, 2008). While Krakower See exhibits two lake terraces with littoral landforms such as beach ridges and palaeosoils (Lorenz, 2007), Tiefer See basin is remarkably deeply incised with a narrow littoral zone, which allowed varve formation during long parts of the Holocene (Kienel et al., 2013). In addition to various sediment cores, Tiefer See was equipped with multi-purpose samplers and measuring devices to establish an interdisciplinary field laboratory for the ICLEA Helmholtz Institute (Schwab et al., 2017; Brauer et al., 2019). The applied combination of long-term high-resolution varve analyses with in situ sampling of present detrital components on the lake bottom and dendroecological analyses has revealed complex coupled processes working at different timescales (Czymzik et al., 2015; Dräger et al., 2014; Theuerkauf et al., 2015; van der Maaten et al., 2015).

Data availability. All data relevant for this contribution are presented within the article itself or the publications cited (key publications are Küster et al., 2012; Börner et al., 2012; Kenzler et al., 2017).

Author contributions. AB wrote the first draft of the manuscript and developed the illustrations. MK re-wrote part of the text and translated the stratigraphic table. AG, HH, MK and SL wrote the chapter about the regional geology of specific areas of interest. All authors contributed to the discussion and interpretation of the presented research results.

Competing interests. The authors declares that there is no conflict of interest.

Acknowledgements. We acknowledge support for the article processing charge from the DFG (no. 393148499) and the Open Access Publication Fund of the University of Greifswald. The contribution benefited from the critical comments of an unknown reviewer. We thank Marie-Elaine van Egmond (Halle) professional English proofreading.

Financial support. This research has been supported by the DFG (German Research Foundation, grant no. 393148499) and the Open Access Publication Fund of the University of Greifswald.

References

Benecke, N.: Die jungpleistozäne und holozäne Tierwelt Mecklenburg-Vorpommerns, Beiträge zur Ur- und Frühgeschichte Mitteleuropas, 23, 143 pp., 2000.

Bittmann, F., Börner, A., Doppler, G., Ellwanger, D., Hoselmann, C., Katzschmann, L., Sprafke, T., Strahl, J., Wansa, S., Wielandt-Schuster, U., and Subkommission Quartär der Deutschen Stratigraphischen Kommission: Das Quartär in der Stratigraphischen Tabelle von Deutschland 2016, Z. Dtsch. Ges. Geowiss., 169, 295–306, 2018.

Błaszkiewicz, M.: Timing of the final disappearance of permafrost in the central European Lowland, as reconstructed from the evolution of lakes in N Poland, Geol. Q., 55, 361–374, 2011.

Börner, A. and Müller, U.: Lithologie und Lithostratigraphie von oberfl ächennahen Tillhorizonten der OPAL-Trasse in Mecklenburg-Vorpommern [Lithology and lithostratigraphy of near surface till layers from OPAL pipeline trench in Mecklenburg-Western Pomerania], Brandenburg. Geowiss. Beitr., 19, 3–18, 2012.

Börner, A., Janke, W., Lampe, R., Lorenz, S., Obst, K., and Schütze, K.: Geowissenschaftliche Untersuchungen an der OPAL-Trasse in Mecklenburg-Vorpommern – Geländearbeiten und erste Ergebnisse, Brandenburg. geowiss. Beitr. 18, 9–28, Cottbus, 2011.

Börner, A., Janke, W., Lorenz, S., Pisarska-Jamrozy, M., and Rother, H.: Das Jungquartär im Binnenland Mecklenburg-Vorpommerns – glaziale Morphologie, Gewässernetzentwicklung und holozäne Landnutzungsgeschichte (Exkursion G am 13 April 2012), Jahresberichte und Mitteilungen des Oberrheinischen Geologischen Vereins, N.F., 94, 287–313, Stuttgart, 2012.

Börner, A., Hrynowiecka, A., Kuznetsov, V., Stachowicz-Rybka, R., Maksimov, F., Grigoriev, V., Niska, M., and Moskal-del Hoyo, M.: Palaeoecological investigations and ^{230}Th/U dating of Eemian interglacial peat sequence of Banzin (Mecklenburg-Western Pomerania, NE-Germany), Quatern. Int., 386, 122–136, 2015.

Börner, A., Hrynowiecka, A., Stachowicz-Rybka, R., Niska, M., Moskal-del Hoyo, M., Kuznetsov, V., Maksimov, F., and Petrov, A.: Palaeoecological investigations and ^{230}Th/U dating of the Eemian Interglacial peat sequence from Neubrandenburg-Hinterste Mühle (Mecklenburg-Western Pomerania, NE Germany), Quatern. Int., 467, 62–78, 2018.

Böse, M., Lüthgens, C., Lee, J. R., and Rose, J.: Quaternary glaciations of northern Europe, Quaternary Sci. Rev., 44, 1–25, 2012.

Bremer, F.: Geologische Übersichtskarte Mecklenburg-Vorpommern 1 : 500 000, 2. ed., Landesamt für Umwelt, Naturschutz und Geologie Mecklenburg-Vorpommern, Güstrow, 2000.

Brauer, A., Schwab, M. J., Brademann, B., Pinkerneil, S., and Theuerkauf, M.: Tiefer See – a key site for lake sediment research in NE Germany, DEUQUA Spec. Pub., this volume, 2019.

Brinker, B., Harten-Buga, H., Staude, A., Jantzen, D., and Orschiedt, J.: Perimortem Lesions on Human Bones from the Bronze Age Battlefield in the Tollense Valley: An Interdisciplinary Approach, in: Prehistoric Warfare and Violence – Quantitative and Qualitative Approaches, edited by: Dolfini, A., Crellin, R. J., Horn, C., and Uckelmann, M., 39–60, Springer, 2018.

Brumme, J.: Three-dimensional microfabric analyses of Pleistocene tills from the cliff section Dwasieden on Rügen (Baltic Sea Coast): Micromorphological evidence for subglacial polyphase deformation, PhD thesis, University of Greifswald, Germany, 250 pp., 2015.

Brumme, J., Hüneke, H., and Phillips, E.: Micromorphology and clast microfabrics of subglacial traction tills at the sea-cliff Dwasieden: evidence of polyphase syn- and post-depositional deformation, DEUQUA Spec. Pub., this volume, 2019.

Czymzik, M., Muscheler, R., Brauer, A., Adolphi, F., Ott, F., Kienel, U., Dräger, N., Słowinski, M., Aldahan, A., and Possnert, G.: Solar cycles and depositional processes in annual 10Be from two varved lake sediment records, Earth Planet. Sc. Lett., 428, 44–51, 2015.

Deecke, W.: Geologie von Pommern, Gebrüder Bornträger, 302 pp., 1907.

Dräger, N., Wulf, S., Kienel, U., Dulski, P., Ott, F., Słowinski, M., Theuerkauf, M., and Brauer, A.: High-resolution microfacies analysis and tephrochronology of varved sediments from Lake Tiefer See (NE Germany), Geophysical Research Abstracts, EGU2014–2411, 2014.

Erd, K.: Pollenanalytische Gliederung des Pleistozäns der Deutschen Demokratischen Republik, Z. Geol. Wissenschaft., 1, 1087–1103, 1973.

Flohr, S., Brinker, U., Schramm, A., Kierdorf, U., Staude, A., Piek, J., Jantzen, D., Hauenstein, K., and Orschiedt, J.: Flint arrowhead embedded in a human humerus from the Bronze Age site in the Tollense Valley, Germany – a high-resolution micro-CT study to distinguish antemortem from perimortem projectile trauma to bone, Int. J. Paleopathol., 9, 76–81, 2015.

Gehl, O.: Neue Ergebnisse über das marine Eem und zur Gliederung des Jungpleistozäns in NW-Mecklenburg, Geologie, 10, 396–408, 1961.

Gehrmann, A.: The multi-stage structural development of the Upper Weichselian Jasmund glacitectonic complex (Rügen, NE Germany), PhD thesis, University of Greifswald, Germany, 235 pp., 2018.

Gehrmann, A. and Harding, C.: Geomorphological Mapping and Spatial Analyses of an Upper Weichselian Glacitectonic Complex based on LiDAR Data, Jasmund Peninsula (NE Rügen), Germany, Geosciences, 8, 208, https://doi.org/10.3390/geosciences8060208, 2018.

Gehrmann, A., Hüneke, H., Meschede, M., and Phillips, E. R.: 3D microstructural architecture of deformed glacigenic sediments associated with large-scale glacitectonism, Jasmund Peninsula (NE Rügen), Germany, J. Quaternary Sci., 32, 213–230, https://doi.org/10.1002/jqs.2843, 2017.

Gehrmann, A., Meschede, M., Hüneke, H., and Pedersen, S. A. S.: Sea cliff at Kieler Ufer (Pleistocene stripes 11-16) – Large-scale architecture and kinematics of the Jasmund Glacitectonic Complex, DEUQUA Spec. Pub., this volume, 2019.

Geinitz, E.: Geologie Mecklenburgs – I. Teil, inklusive geologische Übersichtskarte von Mecklenburg, Hofbuchdruckerei Carl Hinstorff, 200 pp., Rostock, 1922.

German Stratigraphic Commission, Stratigraphic Table of Germany 2016, edited by: Menning, M. and Hendrich, A., Potsdam, 2016.

Groth K.: Zur glazitektonischen Entwicklung der Stauchmoräne Jasmund/Rüge, Schriftenreihe des Landesamtes für Umwelt, Naturschutz und Geologie Mecklenburg-Vorpommern, 3, 39–49, 2003.

Grundmann, L. (Ed.): Das Müritzgebiet – Ergebnisse der landeskundlichen Bestandsaufnahme im Raum Waren, Klink, Federow und Rechlin, in: Werte der deutschen Heimat 60, 282 pp., Leipzig, 1999.

Hardt, J. and Böse, M.: The timing of the Weichselian Pomeranian ice marginal position south of the Baltic Sea: A critical review of morphological and geochronological results, Quatern. Int., 478, 51–58, 2018.

Hardt, J., Lüthgens, C., Hebestreit, R., and Böse, M.: Geochronological and geomorphological investigation at the presumed Frankfurt ice marginal position in northeast Germany, Quaternary Sci. Rev., 154, 85–99, 2016.

Hermsdorf, N. and Strahl, J.: Eemian deposits in the Brandenburg area, Brandenburg, Geowiss. Beitr., 15, 23–55, 2008.

Houmark-Nielsen, M.: Extent, age and dynamics of Marine Isotope Stage 3 glaciation in the southwestern Baltic Basin, Boreas, 39, 343–359, 2010.

Hughes, A. L. C., Gyllencreutz, R., Lohne, Ø. S., Mangerud, J., and Svendsen, J. I.: The last Eurasian ice sheet – a chronological database and time-slice reconstruction, DATED-1, Boreas, 45, 1–45, 2016.

Janke, W.: Zur Genese der Flusstäler zwischen Uecker und Warnow (Mecklenburg-Vorpommern), Greifswalder Geographische Arbeiten, 26, 39–44, 2002.

Janke, W.: Holozän im Binnenland, in: Geologie von Mecklenburg-Vorpommern, edited by: Katzung, G., 265–284, Stuttgart, 2004.

Jantzen, D., Brinker, U., Orschiedt, J., Heinemeier, J., Piek, J., Hauenstein, K., Krüger, J., Lidke, G., Lübke, H., Lampe, R., Lorenz, S., Schult, M., and Terberger, T.: A Bronze Age battlefield? Weapons and trauma in the Tollense Valley, North-Eastern Germany, Antiquity, 85, 417–433, 2011.

Jantzen, D., Lidke, G., Dräger, J., Krüger, J., Rassmann, K., Lorenz, S., and Terberger, T.: An early Bronze Age causeway in the Tollense Valley, Mecklenburg-Western Pomerania – The starting point of a violent conflict 3300 years ago?, Bericht der Römisch-Germanischen Kommission, 95, 13–49, 2014.

Kaiser, K.: Die hydrologische Entwicklung der Müritz im jüngeren Quartär. Befunde und ihre Interpretation. Zeitschrift für Geomorphologie, N.F. Supplement-Band, 112, 143–176, 1998.

Kaiser, K., De Klerk, P., and Terberger, T.: Die "Riesenhirschfundstelle" von Endingen: geowissenschaftliche und archäologische Untersuchungen an einem spätglazialen Fundplatz in Vorpommern, E&G Quaternary Sci. J., 49, 102–123, https://doi.org/10.3285/eg.49.1.07, 1999.

Kaiser, K., Rother, H., Lorenz, S., Gärtner, P., and Papenroth, R.: Geomorphic evolution of small river-lake-systems in northeast Germany during the Late Quaternary, Earth Surf. Proc. Land., 32, 1516–1532, 2007.

Kaiser, K., Hilgers, A., Schlaak, N., Jankowski, M., Kühn, P., Bussemer, S., and Przegietka, K.: Palaeopedological marker horizons in northern central Europe: characteristics of Lateglacial Usselo and Finow soils, Boreas, 38, 591–609, 2009.

Kaiser, K., Lorenz, S., Germer, S., Juschus, O., Küster, M., Libra, J., Bens, O., and Hüttl, R. F.: Late Quaternary evolution of rivers, lakes and peatlands in northeast Germany reflecting past climatic and human impact – an overview, E&G Quaternary Sci. J., 61, 103–132, https://doi.org/10.3285/eg.61.2.01, 2012.

Kaiser, K., Kobel, J., Küster, M., and Schwabe, M. (Eds.): Neue Beiträge zum Naturraum und zur Landschaftsgeschichte im Teilgebiet Serrahn des Müritz-Nationalparks, Forschung und Monitoring, 4, 282 pp., 2015.

Katzung, G.: Geologie von Mecklenburg-Vorpommern, 580 pp., Stuttgart, 2004

Kenzler, M. and Hüneke, H.: Sea cliff at Glowe: Stratigraphy and absolute age chronology of the Jasmund Pleistocene sedimentary record, DEUQUA Spec. Pub., this volume, 2019.

Kenzler, M., Tsukamoto, S., Meng, S., Thiel, C., Frechen, M., and Hüneke, H.: Luminescence dating of Weichselian interstadial sediments from the German Baltic Sea coast, Quat. Geochronol., 30, 215–256, 2015.

Kenzler, M., Tsukamoto, S., Meng, S., Frechen, M., and Hüneke, H.: New age constraints from the SW Baltic Sea area – implications for Scandinavian Ice Sheet dynamics and palaeoenvironmental conditions during MIS 3 and early MIS 2, Boreas, 46, 34–52, 2017.

Kenzler, M., Rother, H., Hüneke, H., Frenzel, P., Strahl, J., Tsukamoto, S., Li, Y., Meng, S., Gallas, J., and Frechen, M.: A multi-proxy palaeoenvironmental and geochronological reconstruction of the Saalian-Eemian-Weichselian succession at Klein Klütz Höved, NE Germany, Boreas, 47, 114–136, 2018.

Kienel, U., Dulski, P., Ott, F., Lorenz, S., and Brauer, A.: Recently induced anoxia leading to the preservation of seasonal laminae in two NE-German lakes, J. Paleolimnol., 50, 535–544, 2013.

Kopp, D.: Die periglaziäre Deckzone (Geschiebedecksand) im nordostdeutschen Tiefland und ihre bodenkundliche Bedeutung, Berichte der Geologischen Gesellschaft in der DDR, 10, 739–771, 1965.

Kopp, D.: Kryogene Perstruktion und ihre Beziehung zur Bodenbildung im Moränengebiet, in: Periglazial, Löss – Paläolithikum im Jungpleistozän der DDR, edited by: Richter, H., Haase, G., Lieberoth, I., and Ruske, R., Petermann. Geogr. Mitt., 274, 269–279, 1970.

Krüger, J., Nagel, F., Nagel, S., Jantzen, D., Lampe, R., Dräger, J., Lidke, G., Mecking, O., Schüler, T., and Terberger, T.: Bronze Age tin rings from the Tollense valley in northeastern Germany, Praehist. Z., 87, 29–43, 2012.

Küster, M.: Holozäne Landschaftsentwicklung der Mecklenburgischen Seenplatte: Relief- und Bodengenese, hydrologische Entwicklung sowie Siedlungs- und Landnutzungsgeschichte in Nordostdeutschland, PhD thesis, University of Greifswald, Germany, 238 pp., 2014.

Küster, M.: The Müritzeum in Waren (Müritz): Natural History Museum and modern Nature Discovery Center, DEUQUA Spec. Pub., this volume, 2019.

Küster, M. and Preusser, F.: Late Glacial and Holocene aeolian sands and soil formation from the Pomeranian outwash plain (Mecklenburg, NE-Germany), E&G Quaternary Sci. J., 58, 156–163, https://doi.org/10.3285/eg.58.2.04, 2010.

Küster, M., Janke, W., Meyer, H., Lorenz, S., Lampe, R., Hübener, T., and Klamt, A.-M.: Zur jungquartären Landschaftsentwicklung der Mecklenburgischen Kleinseenplatte: Geomorphologis-

che, bodenkundliche und limnogeologische Untersuchungen am Krummen See bei Blankenförde (Mecklenburg), in: Forschung und Monitoring, Bd. 3, Nationalparkamt Müritz, 78 pp., Geozon, Greifswald, 2012.

Lampe, R., Lorenz, S., Janke, W., Meyer, H., Küster, M., Hübener, T., and Schwarz, A.: Zur Landschafts- und Gewässergeschichte der Müritz. Forschung und Monitoring, Band 2, Nationalparkamt Müritz, 94 pp., 2009.

Lane, C. S., Klerk, D. P., and Cullen, V. L.: A tephrochronology for the Lateglacial palynological record of the Endinger Bruch (Vorpommern, north-east Germany), J. Quaternary Sci., 27, 141–149, 2012.

Lidke, G. and Lorenz, S.: The Bronze Age battlefield in the River Tollense Valley – Conflict Archaeology and Holocene landscape reconstruction, DEUQUA Spec. Pub., this volume, 2019.

Lidke, G., Jantzen, D., Lorenz, S., and Terberger, T.: The Bronze Age battlefield in the Tollense Valley, Mecklenburg-Western Pomerania, northeast Germany – conflict scenario research, in: Conflict archaeology: Materialities of collective violence in late prehistoric and early historic Europe, edited by: Fernández-Götz, M. and Roymans, N., Themes in Contemporary Archaeology 5, 61–68, 2018.

Liedtke, H.: Phasen periglaziär-geomorphologischer Prägung während der Weichseleiszeit im norddeutschen Tiefland, Z. Geomorphol., 93, 69–94, 1993.

Litt, T., Behre, K.-E., Meyer, K.-D., Stephan, H.-J., and Wansa, S.: Stratigraphische Begriffe für das Quartär des norddeutschen Vereisungsgebietes, E&G Quaternary Sci. J., 56, 7–65, https://doi.org/10.3285/eg.56.1-2.02, 2007.

Lorenz, S.: Die spätpleistozäne und holozäne Gewässernetzentwicklung im Bereich der Pommerschen Haupteisrandlage Mecklenburgs, Dissertation Universität Greifswald, 349 pp., 2007.

Lorenz, S.: Durchbruchstalgenese im Bereich der Pommerschen Haupteisrandlage Mecklenburgs, Abhandlungen der Geologischen Bundesanstalt, 62, 183–188, 2008.

Lorenz, S. and Schult, M.: Das Durchbruchstal der Mildenitz bei Dobbertin (Mecklenburg) – Untersuchungen zur spätglazialen und holozänen Talentwicklung an Terrassen und Schwemmfächern, Meyniana, 56, 47–68, 2004.

Lorenz, S., Rother, H., and Kaiser, K.: Die jungquartäre Gewässernetzentwicklung der Krakower Seen und der Nebel (Mecklenburg) erste Ergebnisse, Greifswalder Geographische Arbeiten, 26, 79–82, 2002.

Lorenz, S., Schult, M., Lampe, R., Spangenberg, A., Michaelis, D., Meyer, H., Hensel, R., and Hartleib, J.: Geowissenschaftliche und paläoökologische Ergebnisse zur holozänen Entwicklung des Tollensetals, in: Tod im Tollensetal – Forschungen zu den Hinterlassenschaften eines bronzezeitlichen Gewaltkonfliktes in Mecklenburg-Vorpommern. Teil 1: Die Forschungen bis 2011 – Beiträge zur Ur- und Frühgeschichte Mecklenburg-Vorpommerns, edited by: Jantzen, D., Orschiedt, J., Piek, J., and Terberger, T., 50, 37–60, Landesamt für Kultur und Denkmalpflege, Schwerin, 2015.

Lorenz, S., Rother, H., Kenzler, M., and Kaphengst, S.: Late glacial to Holocene dune development at Lake Krakower See, DEUQUA Spec. Pub., this volume, 2019.

Ludwig, A. O.: Untersuchung des Pleistozäns der Ostseeküste von der Lübecker Bucht bis Rügen, Geologie, Beiheft 42, 143 pp., 1964.

Ludwig, A. O.: Cyprinenton und I1-Folge im Pleistozän von Nordost-Rügen und der Insel Hiddensee (südwestliche Ostsee), Z. Geol. Wissenschaft., 34, 349–377, 2006.

Ludwig, A. O.: Zwei markante Stauchmoränen: Peski/Belorussland und Jasmund, Ostseeinsel Rügen/Nordostdeutschland – Gemeinsame Merkmale und Unterschiede, E&G Quaternary Sci. J., 60, 31, https://doi.org/10.3285/eg.60.4.06, 2011.

Lüthgens, C. and Böse, M.: Chronology of Weichselian main ice marginal positions in north-eastern Germany, E&G Quaternary Sci. J., 60, 17, https://doi.org/10.3285/eg.60.2-3.02, 2011.

Lüthgens, C., Böse, M., and Krbetschek, M.: On the age of the young morainic morphology in the area ascribed to the maximum extent of the Weichselian glaciation in north-eastern Germany, Quatern. Int., 222, 72–79, 2010a.

Lüthgens, C., Krbetschek, M., Böse, M., and Fuchs, M.C.: Optically stimulated luminescence dating of fluvioglacial (sandur) sediments from north-eastern Germany, Quat. Geochronol., 5, 237–243, 2010b.

Lüthgens, C., Böse, M., and Preusser, F.: Age of the Pomeranian ice-marginal position in northeastern Germany determined by Optically Stimulated Luminescence (OSL) dating of glaciofluvial sediments, Boreas, 40, 598–615, 2011.

Mehlhorn, P., Winkler, L., Grabbe, F. C., Kenzler, M., Gehrmann, A., Hüneke, H., and Rother, H.: Coastal cliff at Lenzer Bach on Jasmund Peninsula, Rügen Island (Pleistocene Stripe 4): Reconstructed history of glacitectonic deformation based on fold geometry and microstructural mapping, DEUQUA Spec. Pub., this volume, 2019.

Menzel-Harloff, H. and Meng, S.: Spätsaalezeitliche und eemzeitliche Makrofaunen aus dem Kliffaufschluss Klein Klütz Höved (NW-Mecklenburg): mit Erstnachweisen von Belgrandia germanica (Gastropoda: Hydrobiidae), Pupilla loessica (Gastropoda: Pupillidae) und Lagurus lagurus (Mammalia: Cricetidae) für Mecklenburg-Vorpommern, E&G Quaternary Sci. J., 64, 82–94, https://doi.org/10.3285/eg.64.2.03, 2015.

Müller, U.: Alt- und Mittel-Pleistozän; Jung-Pleistozän – Eem-Warmzeit bis Weichsel-Hochglazial, in: Geologie von Mecklenburg-Vorpommern, edited by: Katzung, G., 226–242, Stuttgart, 2004a.

Müller, U.: Weichsel-Frühglazial in Nordwest Mecklenburg, Meyniana, 56, 81–115, 2004b.

Müller, U.: Das Relief der Quartärbasis in Mecklenburg-Vorpommern, Neubrandenburger Geologische Beiträge, 4, 67–76, 2004c.

Müller, U. and Obst, K.: Lithostratigraphy and bedding of the Pleistocene deposits in the area of Lohme (Jasmund/Rügen), J. Geol. Sci., 34, 39–54, 2006.

Müller, U., Rühberg, N., and Krienke, H.-D.: The Pleistocene sequence in Mecklenburg-Vorpommern, in: Glacial deposits in North-East Europe, edited by: Ehlers, J., Kozarski, S., and Gibbard, P., 501–514, Rotterdam, Balkema A.A. Publishers, 1995.

Obst, K., Nachtweide, C., and Müller, U.: Late Saalian and Weichselian glaciations in the German Baltic Sea documented by Pleistocene successions at the southeastern margin of the Arkona Basin, Boreas, 46, 18–33, 2017.

Panzig, W.-A.: Zum Pleistozän von Rügen, Terra Nostra, 6, 177–200, 1995.

Pisarska-Jamroży, M., Belzyt, S., Börner, A., Hoffmann, G., Hüneke, H., Kenzler, M., Obst, K., Rother, H., and van Loon, A. J.: Evidence from seismites for glacio-isostatically induced crustal faulting in front of an advancing land-ice mass (Rügen Island, SWBaltic Sea), Tectonophysics, 745, 338–348, 2018.

Price, T. D., Frei, R., Brinker, U., Lidke, G., Terberger, T., Frei, K. M., and Jantzen, D.: Multi-isotope proveniencing of human remains from a Bronze Age battlefield in the Tollense Valley in northeast Germany, Journal of Archaeological and Anthropological Science, https://doi.org/10.1007/s12520-017-0529-y, 2017.

Rother, H., Lorenz, S. , Börner, A., Kenzler, M., Siermann, N., Fülling, A., Hrynowiecka, A., Forler, D., Kuznetsov, V., Maksimov, F., and Starikova, A.: The terrestrial Eemian to late Weichselian sediment record at Beckentin (NE-Germany): First results from lithostratigraphic, palynological and geochronological analyses, Quatern. Int., 501, 90–108, 2019.

Rühberg, N.: Die Grundmoräne des jüngsten Weichselvorstoßes im Gebiet der DDR, Z. Geol. Wissenschaft., 15, 759–767, Berlin, 1987.

Rühberg, N.: Die eiszeitliche Schichtenfolge und Entwicklung im Gebiet um Neubrandenburg, in: Geologie der Region Neubrandenburg, edited by: Granitzki, K., 31–40, Neubrandenburg, 1998.

Rühberg, N.: Geologische Entstehung des Müritzgebietes, in: Die Müritz, Die Geschichte einer Landschaft und ihrer Bewohner rund um Deutschlands größten Binnensee, edited by: Müller, A., 24–30, Waren, 1999.

Rühberg, N. and Krienke, H.-D.: Zur Geschiebeführung der Weichselgrundmoräne im westlichen Odermündungsgebiet, Z. Geol. Wissenschaft., 5, 805–813, 1977.

Rühberg, N., Schulz, W., Bülow, W.v., Müller, U., Krienke, H.-D., Bremer, F., and Dann, T.: Mecklenburg-Vorpommern, in: Das Quartär Deutschlands, edited by: Benda, L., 95–115, Berlin, 1995.

Rühberg, N., Strahl, J., and Keding, E.: Die eiszeitliche Schichtenfolge und Entwicklung im Gebiet um Neubrandenburg, in: Geologie der Region Neubrandenburg, edited by: Granitzki, K., 31–40, Neubrandenburg, 1998.

Schlaak, N.: Studie zur Landschaftsgenese im Raum Nordbarnim und Eberswalder Urstromtal, Berliner Geographische Arbeiten, 76, 1–145, 1993.

Schlaak, N.: Der Finowboden – Zeugnis einer begrabenen weichselspätglazialen Oberfläche in den Dünengebieten Nordostbrandenburgs, Münchener Geographische Abhandlungen, A49, 143–148, 1998.

Schulz, W.: Abriß der Quartärstratigraphie Mecklenburgs, Archiv Freunde der Naturgeschichte Mecklenburgs, XIII, 99–119, 1967.

Schulz, W.: Die quartärgeologische Kartierung in den Bezirken Rostock, Schwerin und Neubrandenburg bis zum Jahre 1967, Petermanns Geogr. Mitt., 115, 307–315, 1971.

Schwab, M. J., Błaszkiewicz, M., Raab, T., Wilmking, M., and Brauer, A. (Eds.): ICLEA Final Symposium 2017: Abstract Volume & Excursion Guide, Scientific Technical Report STR 17/03, GFZ German Research Centre for Geosciences, https://doi.org/10.2312/GFZ.b103-17037, 2017.

Steinich G.: Endogene Tektonik in den Unter-Maastricht-Vorkommen auf Jasmund (Rügen), Geologie, Suppl. 21/22, 207 pp., 1972.

Steinich, G.: Die stratigraphische Einordnung der Rügen-Warmzeit, J. Geol. Sci., 20, 125–154, 1992.

Strahl, J., Keding, E., Steinich, G., Frenzel, P., and Strahl, U.: Eine Neubearbeitung der eem- und frühweichselzeitlichen Abfolge am Klein Klütz Höved, Mecklenburger Bucht, E&G Quaternary Sci. J., 44, 62–78, https://doi.org/10.3285/eg.44.1.07, 1994.

Terberger, T., De Klerk, P., Helbig, H., Kaiser, K., and Kühn, P.: Late Weichselian landscape development and human settlement in Mecklenburg-Vorpommern (NE Germany), E&G Quaternary Sci. J., 54, 138—175, https://doi.org/10.3285/eg.54.1.08, 2004.

TGL 25232: Fachbereichstandard Geologie – Analyse des Geschiebebestandes quartärer Grundmoränen, Zentrales Geologisches Institut, Berlin, 1971.

Theuerkauf, M., Dräger, N., Kienel, U., Kuparinen, A., and Brauer, A.: Effects of changes in land management practices on pollen productivity of open vegetation during the last century derived from varved lake sediments, Holocene, 25, 733–744, 2015.

van der Maaten, E., van der Maaten-Theunissen, M., Buras, A., Scharnweber, T., Simard, S., Kaiser, K., Lorenz, S., and Wilmking, M.: Can We Use Tree Rings of Black Alder to Reconstruct Lake Levels? A Case Study for the Mecklenburg Lake District, Northeastern Germany, PLoS ONE, 10, 0137054, https://doi.org/10.1371/journal.pone.0137054, 2015.

von Bülow, W.: Geologische Entwicklung Südwest-Mecklenburgs seit dem Ober-Oligozän, Schriftenreihe für Geowissenschaften, 11, 413 pp., Berlin, 2000.

von Bülow, W. and Börner, A.: Loosen Formation, in: LithoLex [Online-Database], BGR, Hannover, last updated: 21 January 2019, Record No. 10000021, available at: https://litholex.bgr.de, last access: 26 June 2019.

Zawiska, I., Lorenz, S., Börner, A., Niessner, D., Słowinski, M., Theuerkauf, M., Pieper, H., and Lampe, R.: Late-glacial to Early Holocene lake basin and river valley formation within Pomeranian moraine belt near Dobbertin (Mecklenburg-Vorpommern, NE Germany), Geophysical Research Abstracts, Vol. 16, EGU2014, 2014.

DEUQUA Spec. Pub., 2, 11–17, 2019
https://doi.org/10.5194/deuquasp-2-11-2019

Open Access DEUQUA Special Publications

Blieschow on Jasmund – geomorphology and glacigenic landforms: keys to understanding the deformation chronology of Jasmund

Anna Gehrmann[1] **and Chris Harding**[2]

[1]Institut für Geographie und Geologie, Universität Greifswald, Friedrich-Ludwig-Jahn-Str. 17a, 17487 Greifswald, Germany
[2]Department of Geological and Atmospheric Sciences, Iowa State University, Ames, IA 50011, USA

Correspondence: Anna Gehrmann (anna.gehrmann@uni-greifswald.de)

Relevant dates: Published: 15 August 2019

How to cite: Gehrmann, A. and Harding, C.: Blieschow on Jasmund – geomorphology and glacigenic landforms: keys to understanding the deformation chronology of Jasmund, DEUQUA Spec. Pub., 2, 11–17, https://doi.org/10.5194/deuquasp-2-11-2019, 2019.

Abstract: The late Weichselian glacitectonic framework of the Jasmund peninsula forms surface expressions of subparallel ridges and elongated valleys in between. Geomorphological mapping and landform analyses based on lidar-derived digital elevation models (DEMs) give rise to a revised genetic model for Jasmund, including three evolutional stages that are characterised by different ice flow patterns.

1 Glacial geomorphology of the Jasmund peninsula

The Jasmund peninsula is situated in the NE of Germany's largest island, the isle of Rügen. It is a major example of large-scale glacitectonic folding and thrusting (Groth, 2003; Müller and Obst, 2006; Ludwig, 2011; Gehrmann et al., 2017). The structural framework shows a glacitectonic complex, which was probably formed after the Last Glacial Maximum (MIS 2) in response to a readvance of the Scandinavian Ice Sheet (SIS) during the Pomeranian phase (W2, 17.6 ka BP) (Müller and Obst, 2006; Litt et al., 2007; Gehrmann and Harding, 2018). It has a surface expression in the form of two major sets of subparallel composite ridges (Fig. 1). These ridges can be well observed from the elevation Goldberg near Blieschow (54°31.254′ N, 13°34.996′ E). The southern set is arcuate, presumably concave to the former glacier margin in the southeast. It consists of SW–NE-trending ridges. Furthermore, in the northeastern district of the southern set, the crest lines show a crenulated character. The northern complex is arcuate, too, but concave to the NE. Its elongated landforms have an approximately NW–SE trend. The northern ridge set appears to be partly truncated and superimposed by the southern set.

Both composite ridge sets are locally covered by depressions, which often form lakes. The lakes are potential karst phenomena, kettle holes, or both (e.g. Paulson, 2001; Groth, 2003). The effect of these depressions is especially noticeable at the boundary between the southern and the northern ridge set and at the area SE of the highest elevation, Piekberg (160.9 m a.s.l.).

Areas forming morphological highs SE and SW of the southern ridge set (undifferentiated landforms) differ from the composite ridges by their chaotic ridge pattern. Although there is not yet a lot of evidence, these landforms might be interpreted as hummocky moraines (Gehrmann and Harding, 2018).

The western area of the Jasmund peninsula is characterised by glacifluvial deposits and till from a Weichselian ground moraine (W2 following Niedermeyer et al., 2010). Areas of Holocene swamps/fenland cover parts of the river valleys, the

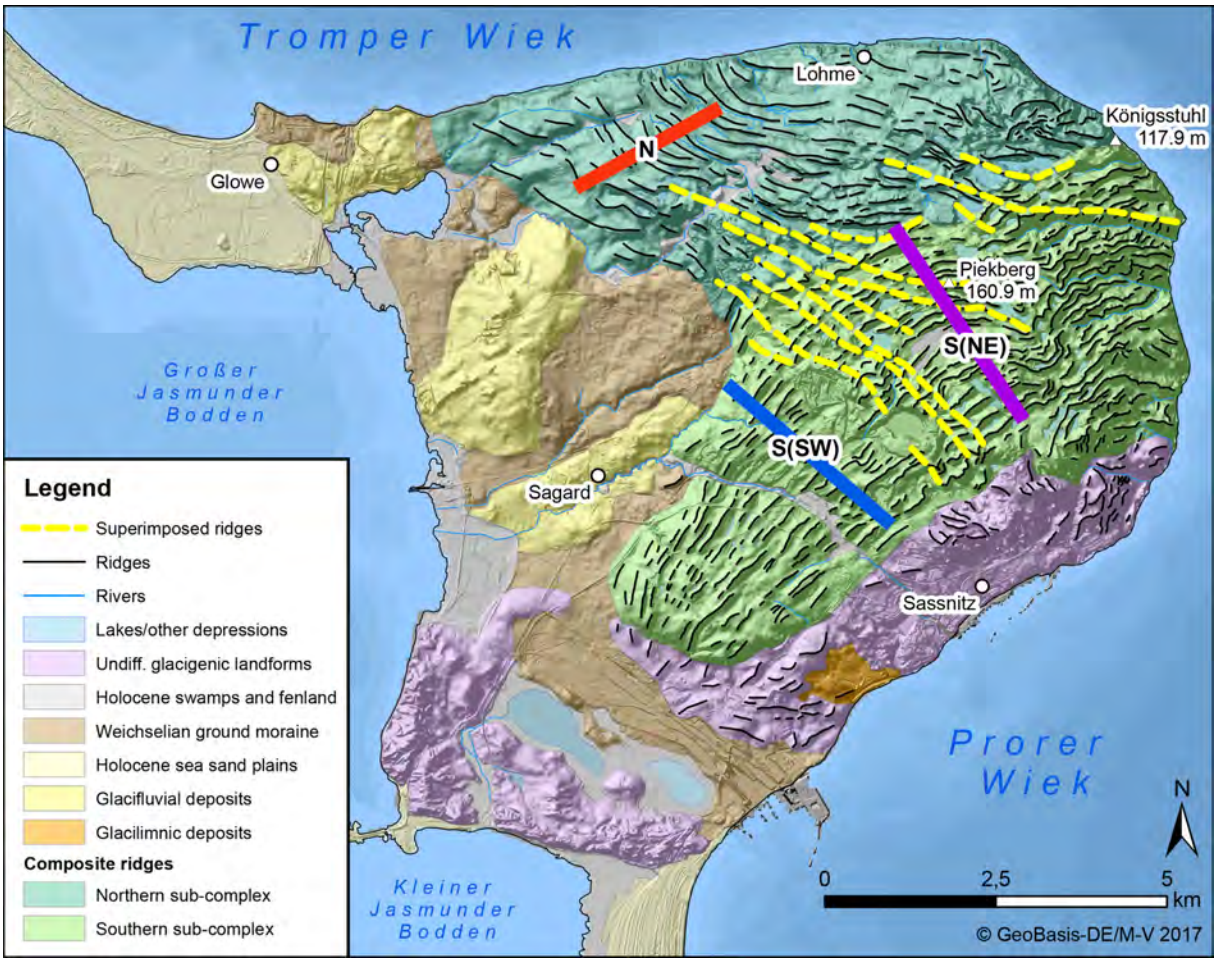

Figure 1. Geomorphological map of the Jasmund peninsula with the hillshaded DEM as background. The surrounding seabed of the Tromper and Prorer Wiek and the Großer and Kleiner Jasmunder Bodden are based on a DEM of the German Baltic Sea (see Tauber, 2012a, b). The profile tracks N, S(SW), and S(NE) show the position of the elevation profiles/periodograms in Fig. 3 (modified following Gehrmann, 2018).

shore to the western bay, and the elongated area between the morphological highs in the south. Holocene sea sand plains connect the Jasmund peninsula with the peninsulas in the NW and SE of Rügen.

2 Research history and evolutionary models of the Jasmund Glacitectonic Complex

The tectonic structure and development of Rügen has been investigated for more than a century. An early significant study was published by Credner (1893), who has already illustrated the surface structure of Jasmund, which is composed of differently oriented sets of subparallel ridges (Fig. 2).

Groth (2003) proposed a complex segmentation of the tectonic complex into five structural units, which are assigned to four developmental phases (Fig. 2). Initially, the majority of the southern structural sub-complex was formed by a glacial push from the SE, which was followed by a push from the NE/E that created the northern structural sub-complex and the southern part of the southern sub-complex. The deformation continued with a complicated reorganisation of the southernmost zone (push from the NE) and a final superposition of the entire complex.

Ludwig (1954/55, 2011) instead separated the Jasmund peninsula into three parts – a northern and a southern subcomplex, which are adjacent to a high central zone (Fig. 2). The model suggests a polyphase contraction of the deposits at the confluence between two major ice streams, which were active during the Pomeranian W2 phase. Pressure formed between the two competing flows and resulted in a loop-shaped accretion of thrust sheets, eventually forming a compressional arc that is convex to the east. This is thought to have been followed by a westward shift of the southern and northern thrust sheets induced by the increasing ice push.

The analysis of high-resolution digital elevation models (DEMs) derived from lidar data (provided by the LAiV M-V, Landesamt für innere Verwaltung Mecklenburg-

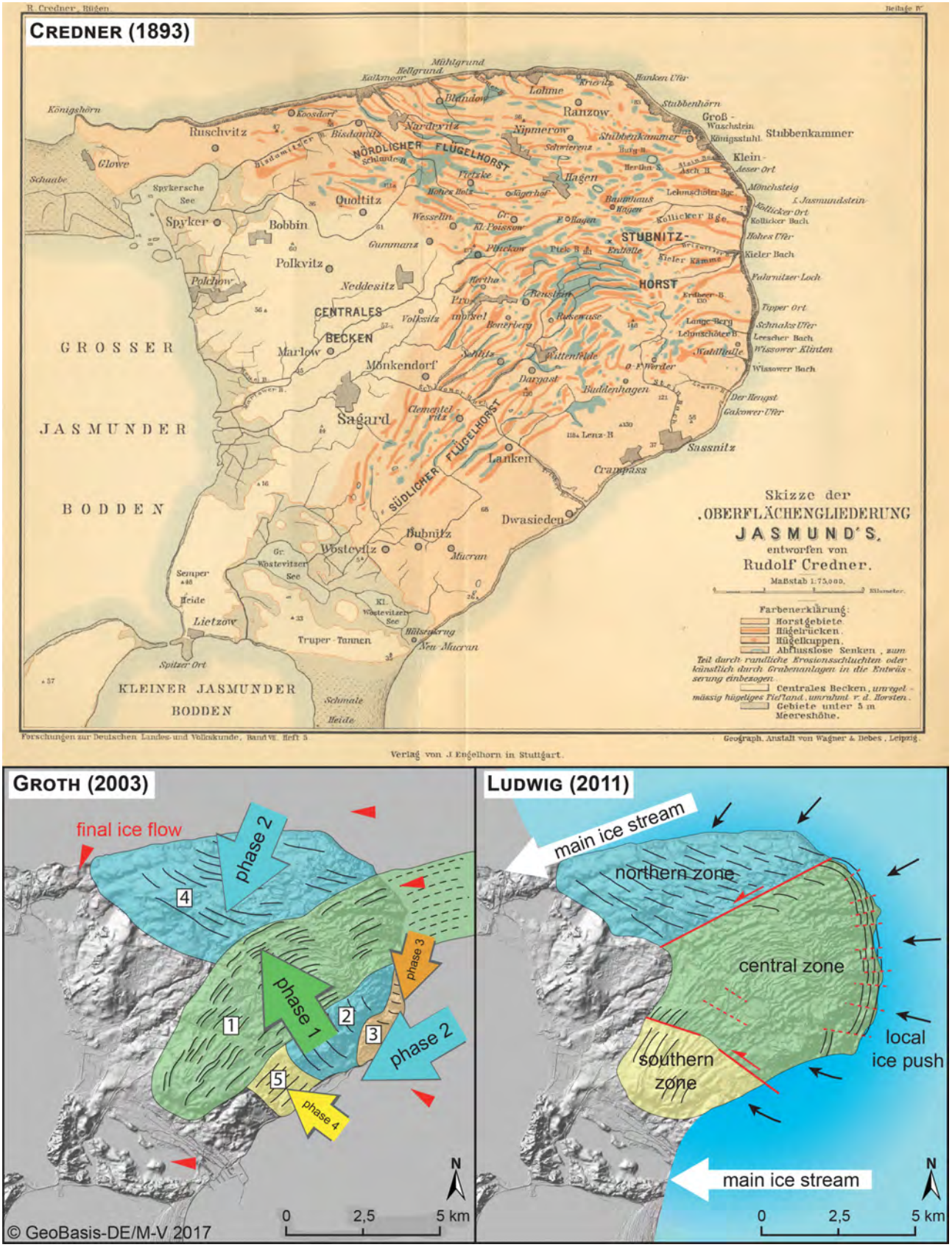

Figure 2. Three major models to interpret the structural conditions and development of the Jasmund peninsula, created by Credner (1893), Groth (2003), and Ludwig (2011).

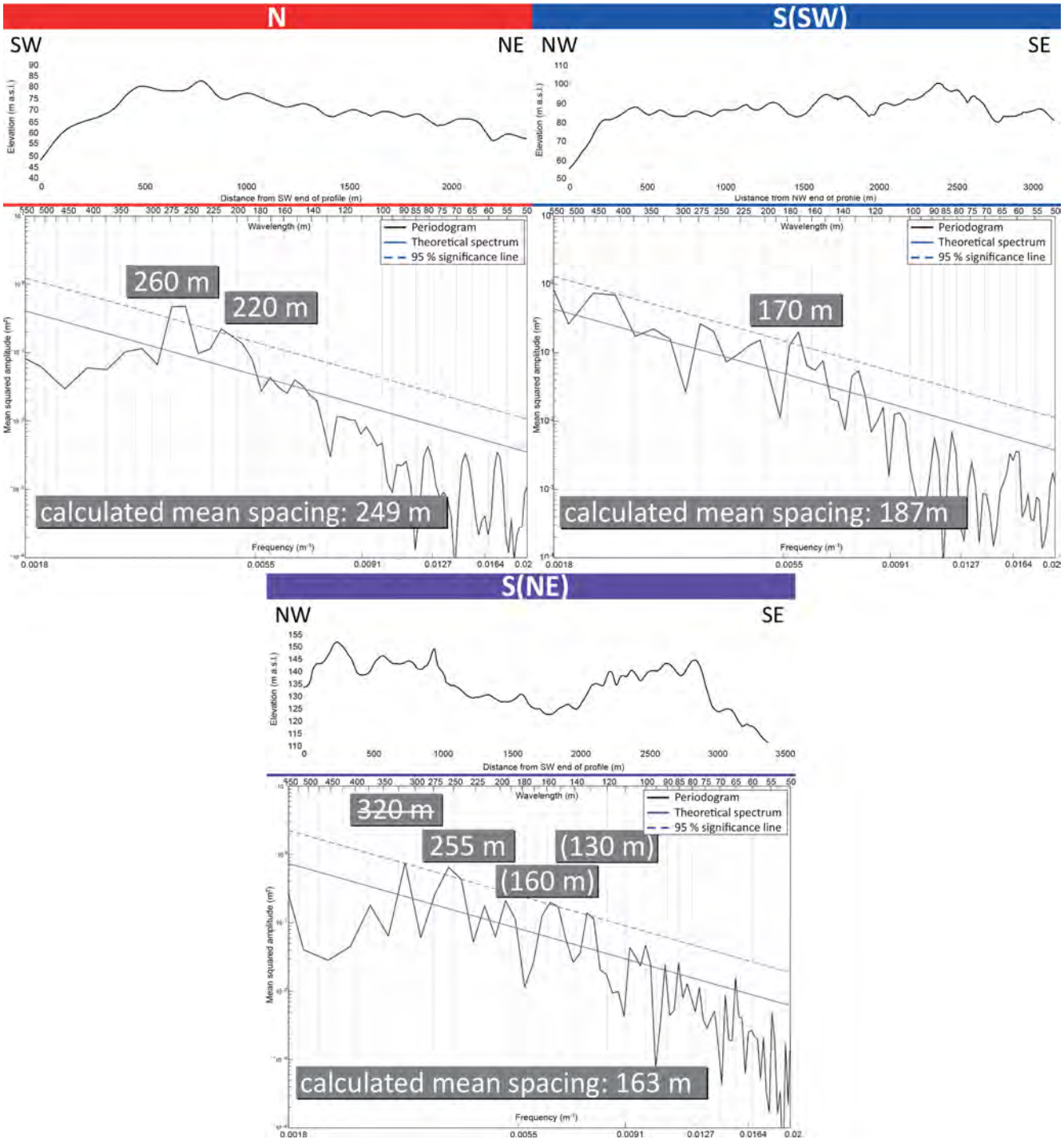

Figure 3. Elevation profiles and related periodograms of the profile tracks N (northern sub-complex), S(SW) (southwestern part of the southern sub-complex), and S(NE) (northeastern part of the southern sub-complex). The significant wavelengths are shown in grey boxes above the related peak. The struck through value in the S(NE) periodogram represents an outlier, and the values in parentheses are tangent to the 95 % significance line but still significant. Calculated mean spacing values in grey boxes support the results within the periodograms. The significant wavelengths of the S(NE) periodogram are representative of both the northern and the ridge domain; thus they indicate a superimposition of the northern sub-complex by the southern one (modified following Gehrmann and Harding, 2018).

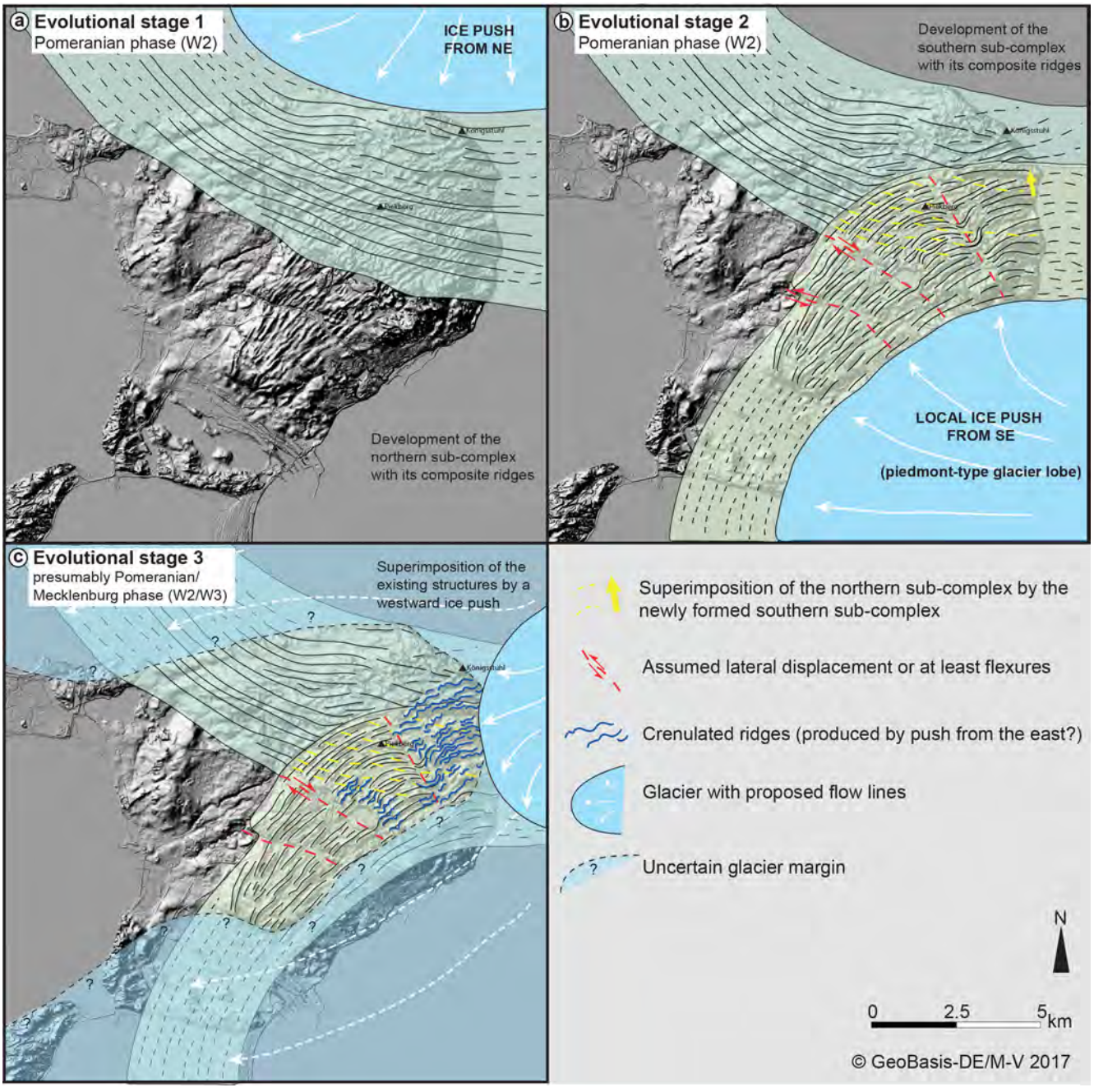

Figure 4. Multi-stage evolutional model of the Jasmund Glacitectonic Complex. **(a)** Formation of the northern sub-complex by a local ice push from the NE. **(b)** Development of the southern sub-complex by a local ice push from the SE leading to a partial truncation and superimposition of the northern ridge domain. **(c)** Minimum reconstruction of the ice front only touching the easternmost part of the glacitectonic complex (light blue) and assumed wider glacier extent, which to some extent envelopes the complex (transparent light blue). The local ice push from E/ENE reshapes the quasi-straight ridges to wavy forms (modified following Gehrmann and Harding, 2018).

Vorpommern) provides a novel research tool for sedimentological and tectonic studies at the Jasmund Glacitectonic Complex (Gehrmann and Harding, 2018). This analysis provides the basis for a re-examination of Jasmund's evolution and the development of a new structural model. The detailed assessment of the ridge morphometry is based on Bradwell et al. (2013), and the terrain analysis using Fourier transformations has been developed from Cline et al. (2015).

A number of transects were constructed in the northern and southern ridge domain perpendicular to the ridge crests (see the examples in Fig. 1). Performing a Fourier analysis of the waves formed by the trough–peak–trough elevation

changes along each ridge profile creates a frequency domain plot, called a periodogram, which plots the width of the wave (wavelength, trough-to-trough distance) on the x axis and the wavelength spectral power on the y axis (Fig. 3). Peaks of large spectral power values indicate that the peak's wavelength is potentially important. Wavelengths with a spectral power above the 95 % confidence line were considered to be statistically significant, resulting in a set of wavelengths that are dominant for a given profile.

The new evolutionary model created by Gehrmann and Harding (2018) suggests a multi-stage structural evolution for the Jasmund Glacitectonic Complex in the late Weichselian (Pomeranian phase, W2). The periodograms, as shown in Fig. 3, help to reveal the evolution of Jasmund's deformation stages. The dominant wavelength of the composite ridges in the northern sub-complex is about 260 m. The dominant wavelengths in the southern sub-complex are generally smaller, with 135 to 195 m. This could point to slight differences in formation time and mechanisms between the northern and southern ridge domain, with regard to exerted stresses and glacier velocities (Gehrmann and Harding, 2018). The ridges are periodically spaced, which is characteristic of even small fold-and-thrust belts like the Jasmund Glacitectonic Complex (see Benediktsson et al., 2010; Noble and Dixon, 2011) (Fig. 3).

The first evolutionary stage (Fig. 4a) is characterised by a local NE-to-SW push by a branch of the SIS forming the northern structural sub-complex and the related composite ridges. Composite ridges were formed during a single rapid ice advance, which created high pore-water pressure and resulted in extreme compressional deformation at the glacier margin (e.g. Benn and Evans, 2010).

The larger wavelengths of the northern ridge domain of around 260 m are still present in the eastern part of the southern ridge domain (Fig. 3c). One possible explanation is that this part of the southern ridge domain represents a zone of tectonic superimposition. Hence, the surface structures of the southern sub-complex were superposed over the northern structural sub-complex in a second evolutionary stage (Fig. 4b). A branch of the SIS might have pushed the local glacifluvial deposits from the SE towards the NW. Why the Pomeranian W2 ice stream moved from the SE to NW is still under debate (e.g. Ludwig, 2011; Gehrmann and Harding, 2018). Characteristic cross profiles of composite ridges with steep distal and flat proximal slopes can be observed in the northern sub-complex and in the southwestern district of the southern ridge domain. Ridges in the eastern district are rather symmetric, which is perhaps due to the northern ridge resisting the movement of the southern ridge set.

The ice stream induced a compressional deformation, presumably compensated for by lateral dislocation along slip faults or at least flexures (Fig. 4b). Ludwig (2011) described these structures as a result of a progressive glacier push and westward shift of the southernmost and northern zone of the Jasmund Glacitectonic Complex (see Fig. 2b). Gehrmann and Harding (2018) suggest that the shift along the central (assumedly dextral) fault is connected to the already existing northern sub-complex (see Fig. 4b). Nevertheless, it is possible that late Paleozoic faults (Wiek, Nord Jasmund, and Schaabe fault) played a role in the glacitectonic development of Jasmund, too (see e.g. Steinich, 1972; Seidel et al., 2018; Gehrmann and Harding, 2018).

The crenulated ridge shapes in the eastern district of the Jasmund Glacitectonic Complex may indicate a third evolutionary stage in the form of a local ice push from the E/ENE (Fig. 4c) (Gehrmann and Harding, 2018). Whether the glacier front only touched the eastern ridges of the glacitectonic complex or enveloped the entire complex has yet to be determined. However, the existence of the till complex on top of the glacitectonised sequence in the northern and southern sub-complex is an indicator that the ice eventually overrode the complex or at least its marginal zones.

Data availability. The data are publicly available via the thesis Gehrmann (2018) and the references therein online at https://nbn-resolving.org/urn:nbn:de:gbv:9-opus-24751 (last access: 22 July 2019).

Author contributions. CH and AG conceived and designed the methodology, performed the analysis, and wrote the article.

Competing interests. The authors declare that they have no conflict of interest.

Acknowledgements. We thank the Landesamt für innere Verwaltung Mecklenburg-Vorpommern, Abt. 3: Amt für Geoinformation, Vermessung und Katasterwesen (LAiV) for providing the lidar data and Jörg Hartleib for processing the lidar data and providing the DEM of Jasmund. In addition, he is thanked for a critical review of the contribution. We acknowledge support for the article processing charge from the DFG (no. 393148499) and the Open Access Publication Fund of the University of Greifswald.

Financial support. This research has been supported by the DFG (German Research Foundation, grant no. 393148499) and the Open Access Publication Fund of the University of Greifswald.

References

Benediktsson, Í. Ö., Schomacker, A., Lokrantz, H., and Ingólfsson, Ó.: The 1890 surge end moraine at Eyjabakkajökull, Iceland: a re-assessment of a classic glaciotectonic locality, Quaternary Sci. Rev., 29, 484–506, https://doi.org/10.1016/j.quascirev.2009.10.004, 2010.

Benn, D. I. and Evans, D. J. A.: Glaciers and Glaciation, Hodder Education, London, UK, 2010.

Bradwell, T., Sigguršsson, O., and Everest, J.: Recent, very rapid retreat of a temperate glacier in SE Iceland, Boreas, 42, 959–973, https://doi.org/10.1111/bor.12014, 2013.

Cline, M., Iverson, N., and Harding, C.: Origin of washboard moraines of the Des Moines Lobe: Spatial analyses with LiDAR data, Geomorphology, 246, 570–578, https://doi.org/10.1016/j.geomorph.2015.07.021, 2015.

Credner, R.: Rügen. Eine Inselstudie, Forschungen zur deutschen Landes- und Volkskunde, 7, 373–494, 1893.

Gehrmann, A.: The multi-stage structural development of the Upper Weichselian Jasmund Glacitectonic Complex (Rügen, NE Germany), Dissertation, Faculty of Mathematics and Natural Sciences, University of Greifswald, Germany, 2018.

Gehrmann, A. and Harding, C.: Geomorphological Mapping and Spatial Analyses of an Upper Weichselian Glacitectonic Complex based on LiDAR Data, Jasmund Peninsula (NE Rügen), Germany, Geosciences, 8, 1–24, https://doi.org/10.3390/geosciences8060208, 2018.

Gehrmann, A., Hüneke, H., Meschede, M., and Phillips, E. R.: 3D microstructural architecture of deformed glacigenic sediments associated with large-scale glacitectonism, Jasmund Peninsula (NE Rügen), Germany, J. Quaternary Sci., 32, 213–230, https://doi.org/10.1002/jqs.2843, 2017.

Groth, K.: Zur glazitektonischen Entwicklung der Stauchmoräne Jasmund/Rügen, Schriftenreihe des Landesamtes für Umwelt, Naturschutz und Geologie Mecklenburg-Vorpommern, 3, 39–49, 2003.

Litt, T., Behre, K.-E., and Meyer, K.-D.: Stratigraphische Begriffe für das Quartär des norddeutschen Vereisungsgebietes, Eiszeitalter und Gegenwart, 56, 7–65, https://doi.org/10.23689/fidgeo-1278, 2007.

Ludwig, A. O.: Eistektonik und echte Tektonik in Ost-Rügen (Jasmund), Wissenschaftliche Zeitschrift der Ernst-Moritz-Arndt-Universität Greifswald, Mathematisch-naturwissenschaftliche Reihe, 4, 251–288, 1954/55.

Ludwig, A. O.: Zwei markante Stauchmoränen: Peski/Belorussland und Jasmund, Ostseeinsel Rügen/Nordostdeutschland – Gemeinsame Merkmale und Unterschiede, E&G Quaternary Sci. J., 60, 31, https://doi.org/10.3285/eg.60.4.06, 2011.

Müller, U. and Obst, K: Lithostratigraphie und Lagerungsverhältnisse der pleistozänen Schichten im Gebiet von Lohme (Jasmund/Rügen), Zeit. geol. Wissenschaft., 34, 39–54, 2006.

Niedermeyer, R.-O., Kanter, L., Kenzler, M., Panzig, W.-A., Krienke, K., Ludwig, A. O., Schnick, H. H., and Schütze, K.: Die Insel Rügen (I) – Fazies, Stratigraphie, Lagerungsverhältnisse und geologisches Gefahrenpotenzial pleistozäner Sedimente der Steilküste Jasmund, in: Eiszeitlandschaften in Mecklenburg-Vorpommern. Exkursionsführer zur 35. Hauptversammlung der Deutschen Quartärvereinigung DEUQUA e.V. und der 12. Jahrestagung der INQUA PeriBaltic Working Group in Greifswald/Mecklenburg-Vorpommern, 13–17 September 2010, Greifswald, Germany, edited by: Lampe, R. and Lorenz, S., Geozon, Greifswald, Germany, 51, https://doi.org/10.3285/g0005, 2010.

Noble T. E. and Dixon, J. M.: Structural evolution of fold-thrust structures in analog models deformed in a large geotechnical centrifuge, J. Struct. Geol., 33, 62–77, https://doi.org/10.1016/j.jsg.2010.12.007, 2011.

Paulson, C.: Die Karstmoore in der Kreidelandschaft des Nationalparks Jasmund auf Rügen, Greifswalder Geographische Arbeiten, 21, 59–271, https://doi.org/10.23689/fidgeo-1978, 2001.

Seidel, E., Meschede, M., and Obst, K.: The Wiek Fault System east of Rügen Island: origin, tectonic phases and its relationship to the Trans-European Suture Zone, in: Mesozoic Resource Potential in the Southern Permian Basin, edited by: Kilhams, B., Kukla, P. A., Mazur, S., McKie, T., Mijnlieff, H. F., and van Ojik, K., Geological Society of London Special Publications, 469, https://doi.org/10.1144/SP469.10, 2018.

Steinich, G.: Endogene Tektonik in den Unter-Maastricht-Vorkommen auf Jasmund (Rügen), Supplement 71/72, Geologie, 20, 1–207, 1972.

Tauber, F.: Seabed relief in the German Baltic Sea: Arkona, Map 2946, 1 : 100 000, 54° N, Bundesamt für Seeschifffahrt und Hydrographie, Hamburg, Germany, 2012a.

Tauber, F.: Seabed relief in the German Baltic Sea: Pomeranian Bight, Map 2949 1 : 100 000, 54° N, Bundesamt für Seeschifffahrt und Hydrographie, Hamburg, Germany, 2012b.

DEUQUA Spec. Pub., 2, 19–27, 2019
https://doi.org/10.5194/deuquasp-2-19-2019

Open Access DEUQUA Special Publications

Sea cliff at Kieler Ufer (Pleistocene stripes 11–16) – large-scale architecture and kinematics of the Jasmund Glacitectonic Complex

Anna Gehrmann[1], Martin Meschede[1], Heiko Hüneke[1], and Stig A. Schack Pedersen[2]

[1]Institut für Geographie und Geologie, Universität Greifswald, Friedrich-Ludwig-Jahn-Str. 17a, 17487 Greifswald, Germany
[2]Geological Survey of Denmark and Greenland (GEUS), Øster Voldgade 10, 1350 Copenhagen, Denmark

Correspondence: Anna Gehrmann (anna.gehrmann@uni-greifswald.de)

Relevant dates: Published: 15 August 2019

How to cite: Gehrmann, A., Meschede, M., Hüneke, H., and Pedersen, S. A. S.: Sea cliff at Kieler Ufer (Pleistocene stripes 11–16) – large-scale architecture and kinematics of the Jasmund Glacitectonic Complex, DEUQUA Spec. Pub., 2, 19–27, https://doi.org/10.5194/deuquasp-2-19-2019, 2019.

Abstract: The Kieler Ufer cliff section is a structural key location in the late Weichselian thrust-dominated-to-fold–thrust-dominated glacitectonic complex of Jasmund. Restoration and balancing of geological cross sections from the eastern coast (southern sub-complex) enabled strain quantification and the illustration of stress orientation. The entire horizontal shortening of the Kieler Ufer section is 1280 m (51.6 %) at its minimum. The thrust faults generally inclined towards south indicate a local glacier push from the S/SSW, which fits well into the glacio-dynamic model suggested by Gehrmann and Harding (2018).

1 Introduction

The sea cliff Kieler Ufer (KU) is located on the east coast of Jasmund, and it is easily accessible via the stairs at the creek Kieler Bach (54°33.165′ N, 13°40.594′ E), which crosses the fault boundary between the imbricates S13 and S14 (Fig. 1a). The abbreviation S used in conjunction with a number stands for "section", and the section numbers S11 to S16 in the Kieler Ufer cliff profile have been adapted from the Pleistocene-stripe annotations given by Jaekel (1917). The horizontal length of the entire cross section is 1202 m. The highest point of the cliff profile is at the southernmost top of S15 (64 m a.s.l.).

The Kieler Ufer section represents a key area in the contractional fold-and-thrust system of Jasmund's southern structural sub-complex, which is a large imbricate fan with a number of individual thrust sheets and at least three duplex stacks (S01 to S23) (Gehrmann, 2018; Gehrmann and Harding, 2019). The large-scale glacitectonic folds and associated thrusts deforming both Upper Cretaceous (Maastrichtian) chalk and Pleistocene glacial deposits were formed in the Pomeranian W2 phase of the late Weichselian (see Kenzler and Hüneke, 2019). The detailed stratigraphy of the Maastrichtian chalk outlined by the flint-band numbers has been adapted from Steinich (1972). The Pleistocene sediments lie paraconformably on the chalk, parallel to this major lithostratigraphical boundary. The older glacial sediments (older than Pomeranian W2 phase) are subdivided into the tills/diamictons M1 and M2 that are separated and overlain by the units I1 and partly I2 with interbedded gravel, sand, and clay (e.g. Steinich, 1972; Panzig, 1995; Müller and Obst, 2006; Kenzler et al., 2015, 2016). These glacial deposits are cut by thrust faults at the trailing end of each imbricate in the SSW, below the large hanging-wall anticlines of the

southerly adjoining thrust sheets. The youngest M3 sediment complex (Pomeranian W2 phase/Mecklenburg W3 phase) lies unconformably upon a major erosion surface, which truncates the underlying glacitectonised sequence (chalk, M1, I1, M2, I2) (e.g. Steinich, 1972; Panzig, 1995; Müller and Obst, 2006; Niedermeyer et al., 2010). At the top of the Kieler Ufer cliff the M3 complex is only exposed in small patches. The tectonic setting at the Kieler Ufer shows an imbricate fan with six major thrust sheets subjected to fault-bend folding (Fig. 1b). The six thrust sheets S11 to S16 strike SSW–NNE and are exposed by the N–S-trending sea cliff at high angle.

Cross-section restoration and balancing is an increasingly applied kinematic-analysis technique in glacial environments. This was well demonstrated for instance by Croot (1987), Pedersen (2005), and Benediktsson et al. (2010). The restoration of the Kieler Ufer section has been performed on the single imbricates of the cliff profile in several experiments using different algorithms and bedding geometries until the best-fit interpretation could be used for shortening calculations and further interpretation (software: Move and the supplementary module 2-D Kinematic Modelling). The tectonic model, which best explains the geometry of the six thrust sheets at the Kieler Ufer is shown in Fig. 1. Regarding the structural evolution of classic fold-and-thrust belts, the restoration worked backwards from the distal to the proximal deformation area (see Pedersen, 2005). Thus, the youngest sheet S16 (closest to the foreland of the southern structural sub-complex) was first restored, and the oldest sheet S11 (closest to the hinterland) was restored in the end. Within the scope of the restoration, the individual thrust sheets (S11 to S16) have been renamed (KU1, KU2, KU3d1, KU3d2, KU3d3, KU4) according to the chronology of re-deformation (see Figs. 1 and 5). The orientation values of beds and faults were adapted from the best-fit model of the Kieler Ufer section, and they have been compared with those given by Steinich (1972).

2 The Kieler Ufer section as representative part of Jasmund's southern structural sub-complex

There are generally three individual thrust sheets: S16, S15, and S11 (KU1, KU2, and KU4). A duplex stack consisting of S14, S13, and S12 (KU3d1, KU3d2, and KU3d3) and the lowermost part of the thrust sheet S15 (KU2) are subject to debate. The highest point of the interpreted cross section is the hanging-wall anticline of S14 (166 m a.s.l.). Three different architectural surfaces occur between S11 and S16 (sensu stricto Pedersen, 2014) (Fig. 1b). The top of the cliff and minor zones, where the base-M3 unconformity occurs (mainly S12 and S16), are first-order surfaces. Another first-order surface is the décollement zone at ca. 120 m b.s.l. The ramps and upper flats between the sections are second-order surfaces. Considering the duplex stack, the intermediate flat at ca. 92 m b.s.l. (KU3d3) also belongs to the second-order surfaces. The bedding outlining the hanging-wall anticlines and the footwall syncline in S13 belong to the third order.

The Kieler Ufer section contains at least five satellite faults, which may have formed during the glacitectonic thrusting (Fig. 1b). Their age (post-, pre-, syn-tectonic) is difficult to determine, as they are truncated by the erosional unconformity at the cliff top. However, the interpretation can be related to the best-fit model using Move and the supplementary module 2-D Kinematic Modelling as well as comparisons with the faults in the surrounding sections. The reverse satellite fault in S16 dips steeply towards the SW, 235/70 (dip direction/dip), and shows an offset of at least 6 m. The satellite fault in S15 (presumably 250/47, 250/56) forms a vertical splay at a branch point about 7 m a.s.l. The offset at the main fault is about 10 m in the lowermost part. Above the branch point, the offset is less strong with ca. 3 to 4 m at each fault. The satellite fault in S13 may be moderately to steeply inclined towards the S (190/61), which is similar to that in S12. The northerly reverse fault in thrust sheet S11 is also assumed to have formed during glacitectonism of the southern structural sub-complex. It dips towards the SW by 72°. The southern reverse fault (205/80), on contrary, can certainly be interpreted as a pre-Quaternary structure, since it does not displace the chalk top and the Pleistocene beds above (Fig. 1b).

2.1 The youngest thrust sheets S16 (KU1) and S15 (KU2)

The footwall-ramp panel of the thrust sheet S16 contains flint bands and Pleistocene beds, which are gently inclined to the SSW (Fig. 2a). The beds steepen towards the centre of the tight hanging-wall anticline in the northern part. The Pleistocene deposits reach the cliff bottom, since their trend corresponds to the geometry of the moderately inclined footwall ramp below S16 and they are cut by the S15/S16 thrust fault only at or even closely below the cliff bottom (Figs. 1 and 2a). The frontal thrust fault of the Kieler Ufer section below S16 starts at the décollement at 120 m b.s.l. with a gentle-to-moderate inclination (210/38), and it becomes nearly vertical to the top of the cliff (210/79 and 210/80 following Steinich, 1972). The thrust plane is interpreted to have a slight listric shape.

The thrust sheet S15 is characterised by an open folded geometry both in the footwall-ramp panel and in the hanging-wall anticline (Figs. 1 and 2b). The beds of the southern anticline limb dip towards the SSW by 30° on average (210/30). Thus, they are more gently inclined than the beds in S16 (205/45). However, the thrust fault between S14 and S15 is much steeper between 0 and 51 m a.s.l. than the frontal thrust below S16, and therefore it truncates the Pleistocene beds at a higher level than in S16 (Fig. 2). Thus, the Pleistocene unit does not reach the beach level. The thrust fault between S15 and S16 is steeply inclined to the SSW (205/65), and

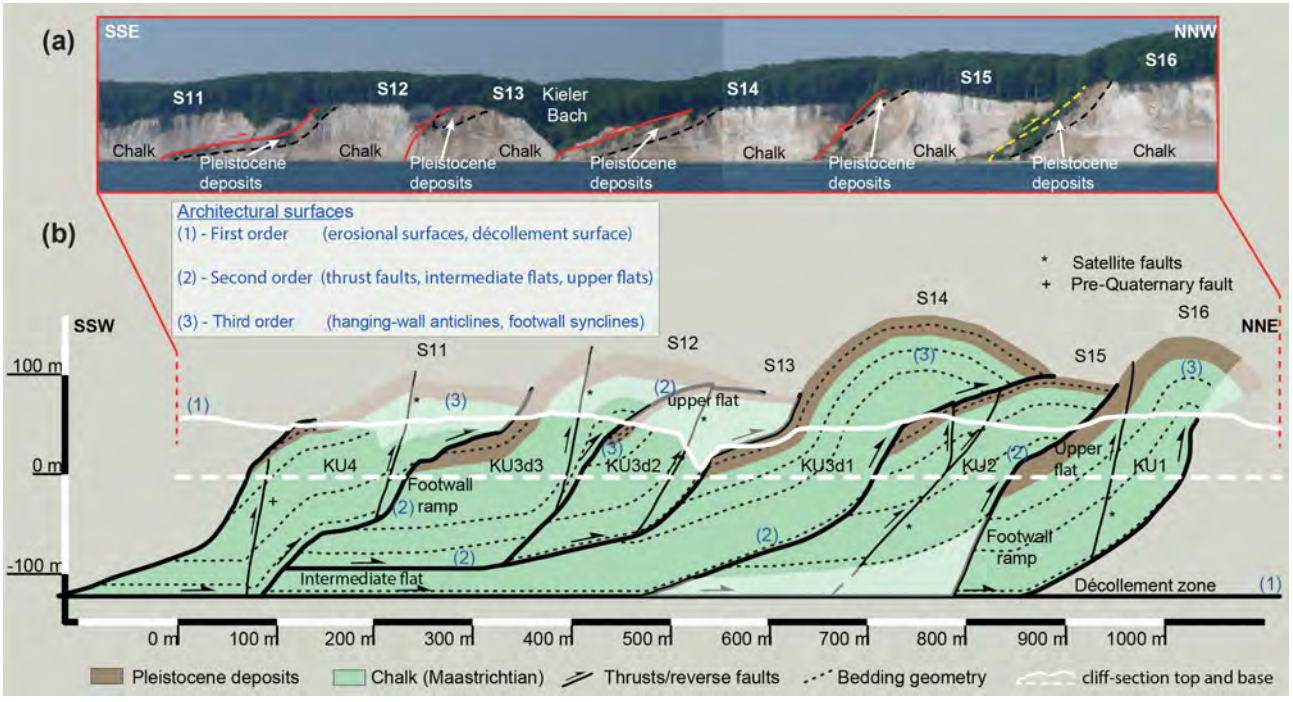

Figure 1. Structural conditions of the Kieler Ufer section (S11 to S16). **(a)** Overview of the thrust sheets S11 to S16 at the cliff coast. The red/yellow lines indicate thrust faults. The black dashed lines show the sedimentary boundary between Cretaceous chalk and Pleistocene glacigenic deposits. **(b)** Projected and interpreted cross section (simplified). Architectural surfaces are marked by numbers 1 to 3. Transparent fields represent approximate interpretations.

at a hinge point ca. 15 m above the cliff base it turns into a moderately inclined thrust fault (205/38). In fact, this part represents an upper flat, since it is parallel to the bedding in the S16 thrust sheet below. The inclinations from the best-fit model correspond well to the orientation 205/35 given by Steinich (1972).

2.2 Duplex stack S14–S13–S12 (KU3d1, KU3d2, KU3d3)

S14 is a long sheet with an open hanging-wall anticline (Figs. 1 and 3a). It is the lowermost element of the central duplex stack in the Kieler Ufer section and shows an S-type duplex segment (see inset in Fig. 3a). The flint bands gently dip towards the SSW (220/19), but the inclination increases towards the anticline core in the SSW (220/60). The thrust faults bounding S14 in the SSW and NNE are relatively steep in the cliff section, but they are more gently inclined below the cliff bottom, regarding the best-fit model. The frontal ramp starts at the décollement with an initially gentle inclination towards the SSW (210/21). At the hinge point at 37 m b.s.l. the inclination steepens (210/61). At another hinge point 53 m a.s.l., the thrust fault again turns into a gently inclined fault (210/24).

S13 is the very small central element of the duplex stack (Fig. 3b). It is also an S-type element. The bedding shows a gentle-to-moderate inclination (Fig. 3b). The upper flint bands of the chalk unit and the Pleistocene beds were dragged along the footwall ramp of S12 so that they form a slight footwall syncline in the trailing edge. The base of the thrust sheet is not the décollement or another flat. It is a gently inclined footwall ramp (220/12), which grows steeper at ca. 53 m b.s.l. (220/53). At 21 m a.s.l. the ramp may pass into the upper flat.

S12 is the upper segment of the duplex stack, also indicating an S-type element (Fig. 3c). The bedding of S12 shows a gentle inclination (225/07) until it exhibits a kink-like geometry at about section metre 360 (Fig. 3c). Northeast of this area the inclination is 225/53. Northeast of the satellite fault, the flint bands of the hanging-wall anticline show a succession of two smaller anticlines and a syncline in between, which may point to a thrust-fault geometry exhibiting a double ramp between section metre 445 and 500 rather than the simplified fault shown in Fig. 3c. S12 does not reach the décollement surface at 120 m b.s.l., but it reaches the intermediate flat at ca. 92 m b.s.l. At section metre 323 it turns into the actual footwall ramp of S13, which is gently inclined towards the SSW. The footwall ramp of S12 starts at section metre 349. It has a moderate inclination towards the S (190/45).

2.3 The oldest thrust sheet S11 (KU4)

The southernmost and oldest thrust sheet of the Kieler Ufer section is S11, which is an individual thrust sheet SSW of the

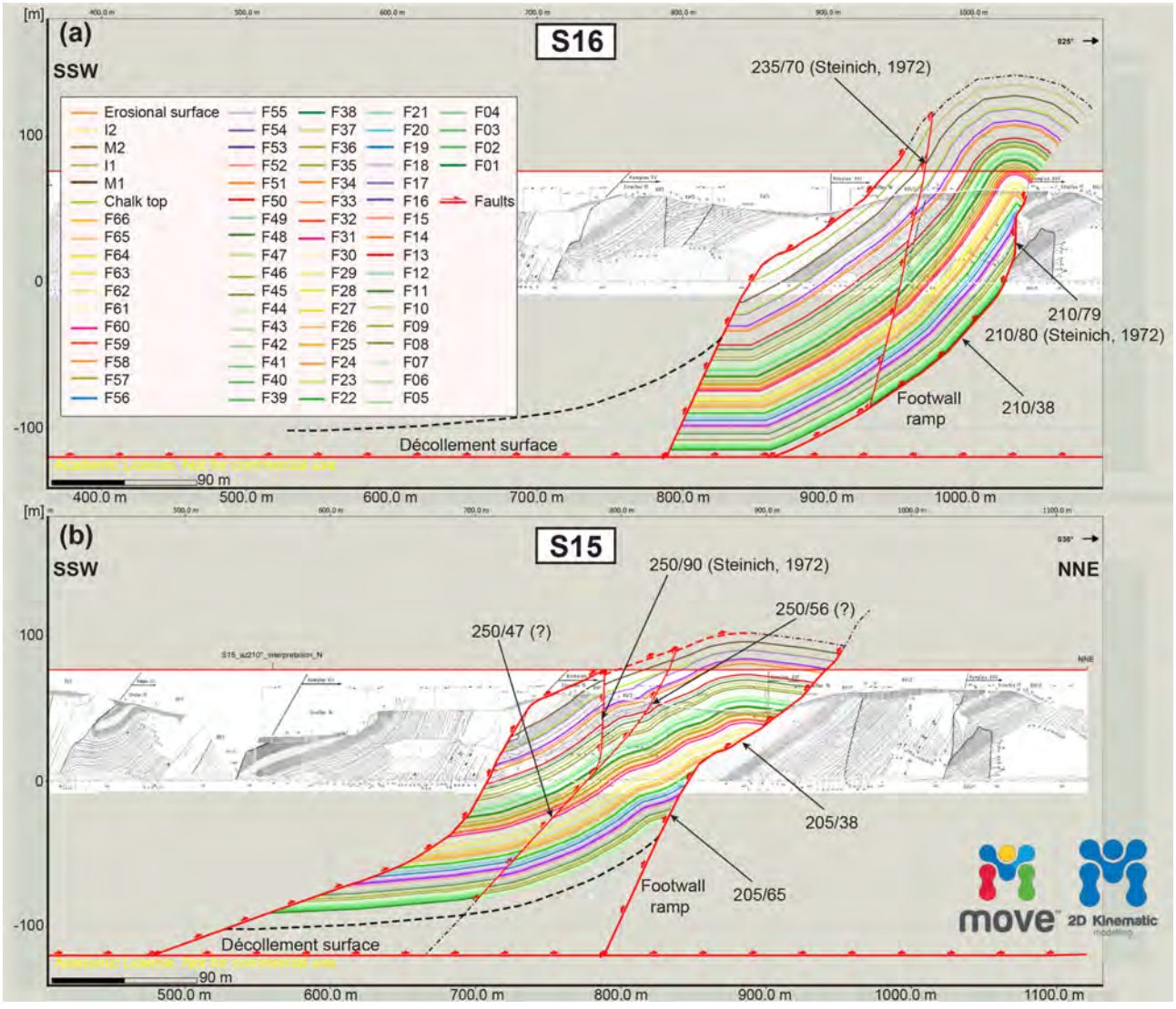

Figure 2. Detailed 2-D cross sections of the two youngest thrust sheets. **(a)** S16 with a horizontal length of 175 m at the cliff base but 294 m from its SSW to its NNE end. The thickness of the Cretaceous unit (flint bands F01 to F54) is 98 to 89 m, while the Pleistocene unit (M1, I1, and M2) is 24 m thick. **(b)** S15 with a horizontal length of 138 m at the cliff base and a total length of 427 m (max 477 m). The maximum thickness of the beds down to F01 is 128 m. The Pleistocene unit (M1 and I1) is ca. 21 to 12 m, while the chalk unit (F01 to F54) is at least 107 m. The coloured lines represent the flint bands of the chalk as well as horizons of the Pleistocene beds; the red lines are faults. The cross sections constructed by Steinich (1972) are shown in the background of each model.

duplex stack (Fig. 1). Due to the step-like geometry of the thrust fault between S11 and S12, the bedding also shows a kinking geometry (Fig. 4). In the SSW of S11, the beds are moderately inclined to the SSW (205/45), while the central beds are gently inclined (205/18). Farther north, the inclination gets steeper again to form the southern limb of the hanging-wall anticline. The hanging-wall anticline is characterised by two smaller anticlines comparable to the frontal edge of S12. This is a hint to a double-ramp configuration of the frontal thrust fault (Fig. 4). Below this structure, the ramp steeply dips to the SW (225/61). At a hinge point 57 m b.s.l. the ramp is only gently inclined (225/13). In its lowermost part, it forms the moderately inclined ramp between the décollement surface and the intermediate flat, on which S12 and S13 were translated.

3 The restored cross section: key to understanding Jasmund's glacitectonic evolution and kinematics

The kinematic analysis of the Kieler Ufer section led to strain quantification and the illustration of stress orientation. It includes strain partitioning and, hence, the separation of the shortening amount into folding and faulting. Cross-section restoration and balancing of the imbricate fans of the south-

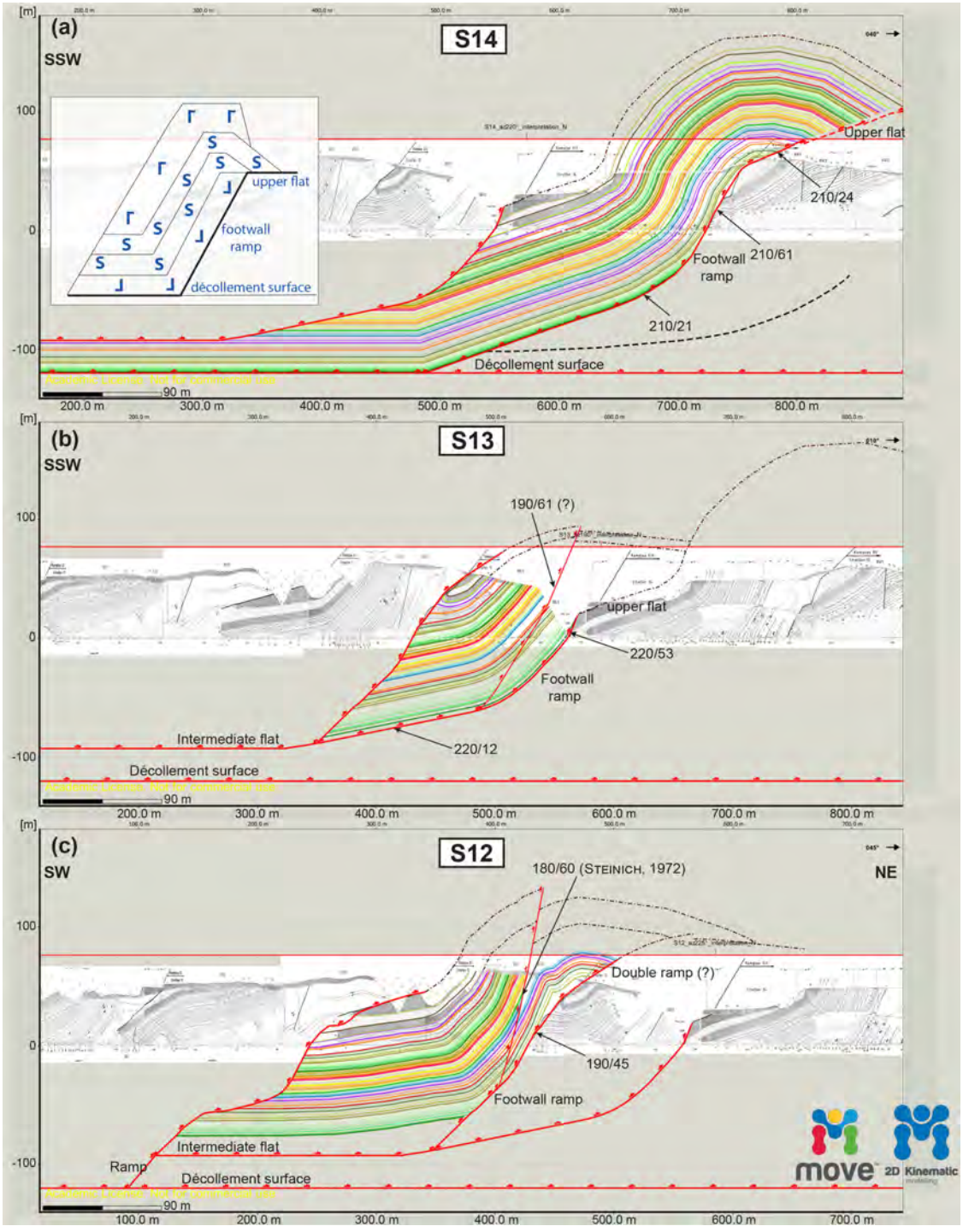

Figure 3. Detailed 2-D cross sections of the three duplex-stack elements. The schematic illustration of a duplex stack including the three different elements (L-, S-, and G-type) is given in **(a)** (modified following Pedersen, 2005). **(a)** S14 with a horizontal length of 178 m at the beach level but an entire horizontal length from the SSW end to the NNE end of ca. 820 m. The Cretaceous beds (F01 to F54) are 89 m thick at maximum. The thickness of the Pleistocene unit (M1, I1, and M2) is 22 m. **(b)** S13; the horizontal length is 131 m at the cliff base but 315 m from its SSW end to its NNE end. The chalk unit (F01 to F54) has a maximum thickness of 94 m. The Pleistocene deposits (M1, I1, and M2) are up to 14 m. **(c)** S12 with a horizontal length of 184 m at the cliff base. The entire horizontal length is 506 m. The entire bed thickness in the thrust sheet is 106 m from the F01 flint band to the topmost bed in the Pleistocene sequence. However, the bed thickness from the thrust-sheet base to the top is 131 m. The Cretaceous unit has a thickness of 81 m (F01 to F54/chalk top) but a of maximum 106 m. The Pleistocene sequence is ca. 25 m. The coloured lines represent the flint bands of the chalk as well as horizons of the Pleistocene beds; the red lines are faults. A detailed legend for the horizons and faults can be found in Fig. 2. The cross sections constructed by Steinich (1972) are shown in the background of each model.

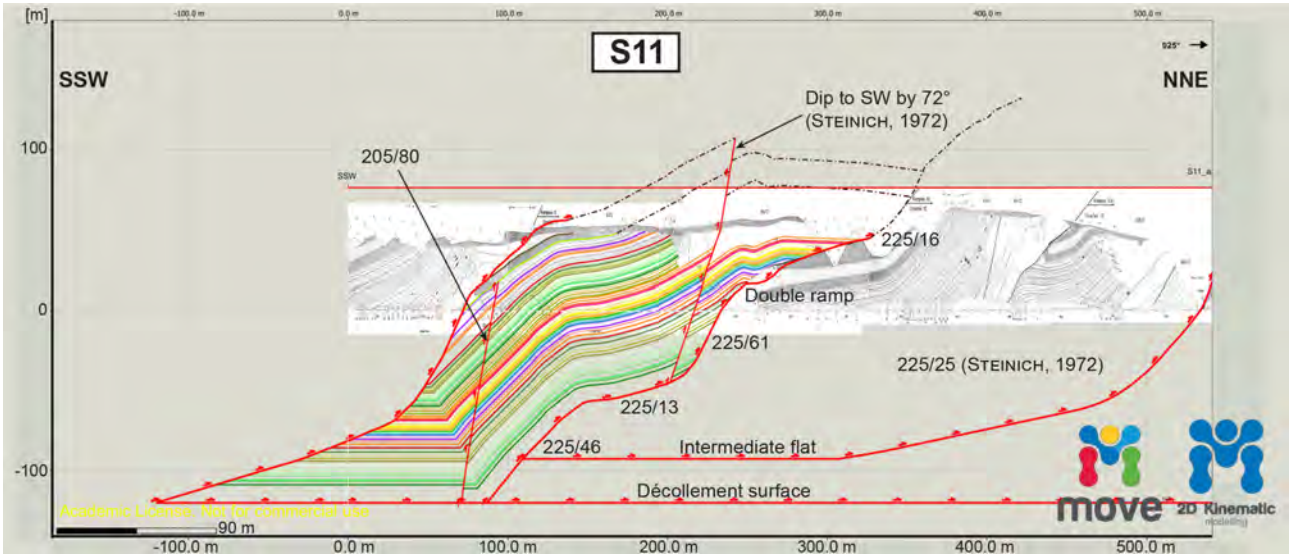

Figure 4. Detailed 2-D cross section of the oldest thrust sheet S11 in the Kieler Ufer section. The horizontal length is about 162 m. The entire thrust sheet has a horizontal length of 478 m from the southernmost to the northernmost end. The chalk deposits (F01 to F54) are about 100 m thick; the Pleistocene unit (M1 and I1) is at least 16 m. The coloured lines represent the flint bands of the chalk as well as horizons of the Pleistocene beds; the red lines are faults. A detailed legend for the horizons and faults can be found in Fig. 2. The cross sections constructed by Steinich (1972) are shown in the background of each model.

ern structural sub-complex revealed that the Kieler Ufer section had an initial length of at least 2482 m before its glacitectonic imbrication. Thus, the entire horizontal shortening of the Kieler Ufer section is 1280 m (51.6 %) at its minimum. This includes both folding and the translation along the flats and ramps. The process of folding constitutes only 20.5 % (263 m) of the entire deformation, while the translation part is even 79.5 % (1017 m). The amount of displacement along the individual thrust faults is 206 m (KU1), 164 m (KU2), 328 m (KU3d1), 521 m (KU3d2), 438 m (KU3d3), and 243 m (KU4). The stress was directed from the SSW to NNE. The orientation fits well into the glacio-dynamic model suggested by Gehrmann and Harding (2018). The glacier with a piedmont-type lobe mainly moved from the SE to NW in the second evolutionary stage and induced local stress in all sides due to the radial propagation in the unconfined ice-marginal zone (see e.g. Ó Cofaigh et al., 2003; Jónsson et al., 2014). This induced a local orientation change of the thrust faults from a dip to the SE in the inland zone of the southern sub-complex to the S/SW at the eastern cliff.

The final cross section of the Kieler Ufer section cannot be completely balanced. There are smaller restoration gaps in the northern parts of the restored sheets KU1, KU2, and KU3d1 (S16, S15, S14) (Fig. 5). A large gap can be seen in the northern end of KU3d2 (S13). Projection of the cliff sections has been considered in the modelling process to reduce such errors. The azimuth of the final large track of the Kieler Ufer section is 210°, adapted from the main orientation of the thrust faults or individually of the flint bands. The projection has been performed normal to the sections. However, the gaps represent volume loss during deformation rather than construction errors. Tectonic erosion may have occurred at the ramps, when the single sheets were thrust up, leading to small gaps in the frontal edge of the thrust sheets in the restored cross section. In addition, it has to be taken into account that the restored cross section only shows a 2-D interpretation. In particular, the large restoration gap in KU3d2 (S13) may point to a very complicated bedding and deformation history in the area of the Kieler Ufer section, which is highly likely related to interference between the northern and southern structural sub-complex. The specific complexity is confirmed by the high amount of shortening (51.6 %) and the duplex stack in the centre of the Kieler Ufer section.

4 The southern sub-complex of Jasmund in the context of glacitectonic-complex models

The Kieler Ufer section represents a structural key location in the thrust-dominated-to-fold–thrust-dominated glacitectonic complex of Jasmund (see Boulton et al., 1999). The specific geometric features of the constructed and restored cross section led to major information on the kinematics and deformation history, including the relationship between the northern and southern structural sub-complex of Jasmund.

The southern sub-complex exhibits a realistic décollement depth at mainly 120 m b.s.l., because the deformation in ancient glacitectonic complexes can extend to a depth of a few tens of metres up to 200 m (e.g. Aber et al., 1989; van der Wateren, 2003; Huuse and Lykke-Andersen, 2000; Vaughan-Hirsch and Phillips, 2017). Modern structurally similar glaci-

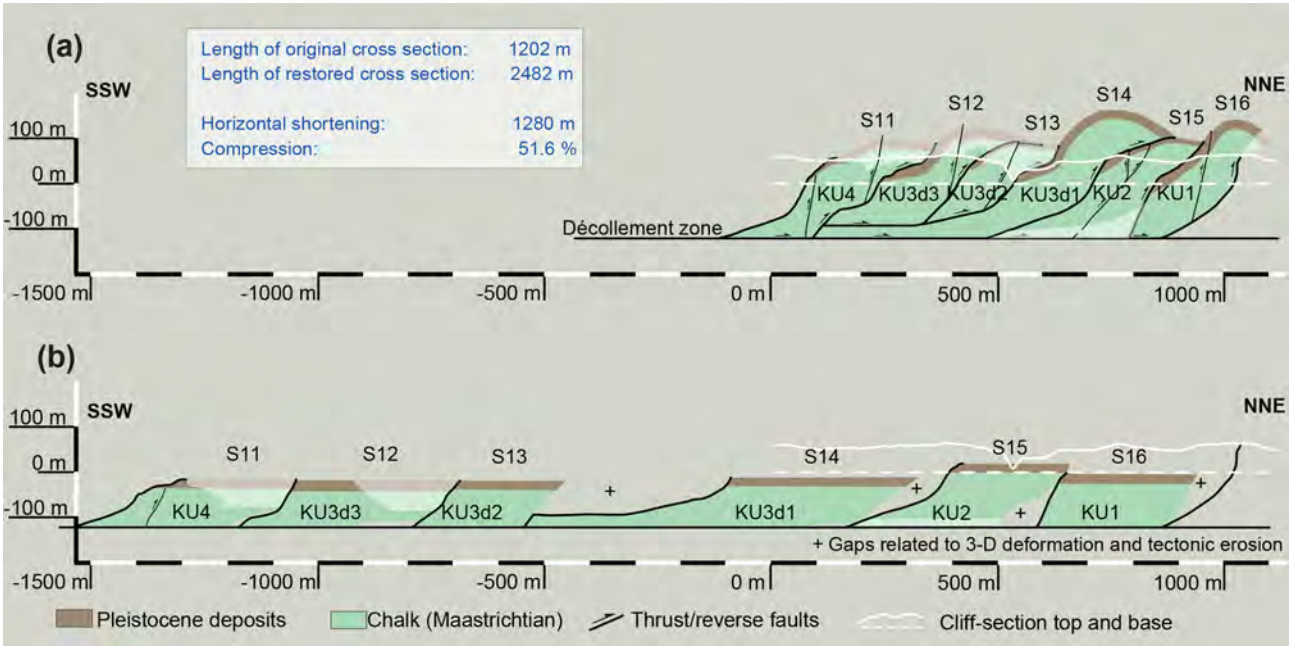

Figure 5. Interpretation and restoration of the Kieler Ufer section (S11 to S16) with horizontal-shortening results. **(a)** Cross section interpreted above and below the cliff boundaries (simplified). **(b)** Restored cross section indicating the configuration before the glacitectonic deformation of the southern structural sub-complex. The restored thrust sheets are additionally labelled with the new abbreviations KU1 to KU4, which represent the chronology of the restoration process.

tectonic landforms are generally smaller, with décollement depths of about 5 to 30 m (e.g. Boulton et al., 1999; Benediktsson et al., 2010).

Considering the classic separation of glacitectonic complexes into a proximal, central, and distal zone (e.g. Boulton et al., 1999; Pedersen, 2000), the Kieler Ufer section is part of the central zone, which is characterised by a highly complicated structural framework of duplex stacks and steeply dipping thrust faults implying a high-strain area with intensive thrusting and shortening. The Kieler Ufer section has the highest amount of horizontal shortening (51.6 %) compared to the other sections of the southern sub-complex. The highest elevations of the modelled southern structural sub-complex are at the hanging-wall anticlines of the central zone (e.g. S14: 166 m a.s.l.), which may confirm the intensive deformation and compression. Boulton et al. (1999) also described the more intensive folding and thrusting for the centre of the modern glacitectonic complex in front of Holmstrømbreen on Svalbard.

There are also substantial differences between Jasmund and previously described glacitectonic complexes when the entire southern sub-complex is considered. While most glacitectonic complexes indicate a significant strain decrease from the proximal to the distal end, the Jasmund Glacitectonic Complex is characterised by a constantly high strain. Normally, the length of the thrust sheets increases towards the foreland, which implies a greater degree of shortening towards the proposed ice margin (e.g. Pedersen, 2005; Vaughan-Hirsch and Phillips, 2017). However, such a trend cannot be seen in the southern sub-complex of Jasmund. Typically, the angle of the thrust faults and the offsets decrease towards the foreland (Dixon and Liu, 1992; Pedersen, 2005; Vaughan-Hirsch and Phillips, 2017). This is also not the case in the Jasmund Glacitectonic Complex. Even though the steepest thrust sheets are situated in the most proximal zone, there are still steeply to moderately inclined faults in the central and distal zone. This phenomenon can be explained with the complex relationship between the northern and southern structural sub-complex of Jasmund. Since the northern sub-complex was formed first by an earlier glacitectonically effective glacier in the SW Baltic Sea region, there already existed the structural framework of a glacitectonic complex in the north of the southern structural sub-complex. Thus, an obstacle in front of the deformation area has controlled the imbrication during the second stage (see Gehrmann and Harding, 2018). These circumstances intensively affected the deformation process of the southern sub-complex as well as its internal structure. There was no possibility to form gently inclined thrust faults in the distal foreland during the final deformation, as the northern sub-complex acted as a resistance. The stress induced by both the glacier and the northern sub-complex led to the documented highly complex architecture, which represents an exception from classic glacitectonic-complex models (unconfined). The structural configuration of Jasmund can be used as a model characteristic of confined glacitectonic complexes. It is all the more so an example of

various and intensive superimpositions in a multi-stage structural evolution (see Pedersen, 2000).

Data availability. The data are publicly available via the thesis Gehrmann (2018) and the references therein online at https://nbn-resolving.org/urn:nbn:de:gbv:9-opus-24751 (last access: 22 July 2019).

Author contributions. AG designed the methodology, performed the analysis, and prepared the manuscript with contributions from all co-authors.

Competing interests. The authors declare that they have no conflict of interest.

Acknowledgements. We acknowledge granting of software licences (Move™ suite) from Midland Valley Exploration Ltd for the years 2014 to 2018. Ralf-Otto Niedermeyer is thanked for his constructive review. We acknowledge support for the article processing charge from the DFG (no. 393148499) and the Open Access Publication Fund of the University of Greifswald.

Financial support. This research has been supported by the DFG (German Research Foundation, grant no. 393148499) and the Open Access Publication Fund of the University of Greifswald.

References

Aber, J. S., Croot, D. G., and Fenton, M. M.: Glaciotectonic Landforms and Structures, Kluwer, Dordrecht, 1989.

Benediktsson, Í. Ö., Schomacker, A., Lokrantz, H., and Ingólfsson, Ó.: The 1890 surge end moraine at Eyjabakkajökull, Iceland: a re-assessment of a classic glaciotectonic locality, Quaternary Sci. Rev., 29, 484–506, https://doi.org/10.1016/j.quascirev.2009.10.004, 2010.

Boulton, G. S., van der Meer, J. J. M., Beets, D. J., Hart, J. K., and Ruegg, G. H. J.: The sedimentary and structural evolution of a recent push moraine complex: Holmstrømbreen, Spitsbergen, Quaternary Sci. Rev., 18, 339–371, 1999.

Croot, D. G.: Glacio-tectonic structures: a mesoscale model of thin-skinned thrust sheets?, J. Struct. Geol., 9, 797–808, 1987.

Dixon, J. M. and Liu, S.: Centrifuge modelling of the propagation of thrust faults, in: Thrust Tectonics, edited by: McClay, K. R., Chapman & Hall, London, 53–70, 1992.

Gehrmann, A.: The multi-stage structural development of the Upper Weichselian Jasmund Glacitectonic Complex Rügen, NE Germany), Dissertation, Faculty of Mathematics and Natural Sciences, University of Greifswald, Germany, 2018.

Gehrmann, A. and Harding, C.: Geomorphological Mapping and Spatial Analyses of an Upper Weichselian Glacitectonic Complex based on LiDAR Data, Jasmund Peninsula (NE Rügen), Germany, Geosciences, 8, 208, https://doi.org/10.3390/geosciences8060208, 2018.

Gehrmann, A. and Harding, C.: Blieschow on Jasmund – Geomorphology and glacigenic landforms: keys to understanding the deformation chronology of Jasmund, DEUQUA Spec. Pub., this volume, 2019.

Huuse, M. and Lykke-Andersen, H.: Large-scale glaciotectonic thrust structures in the eastern Danish North Sea, in: Deformation of Glacial Materials, edited by: Maltman, A. J., Hubbard, B., and Hambrey, M. J., Geol. Soc. London Spec. Pub., 176, 293–305, https://doi.org/10.1144/GSL.SP.2000.176, 2000.

Jaekel, O.: Neue Beiträge zur Tektonik des Rügener Steilufers, Zeitschrift der Deutschen Geologischen Gesellschaft, 69, 81–176, 1917.

Jónsson, S. A., Schomacker, A., Benediktsson, Í. Ö., Ingólfsson, Ó., and Johnson, M.: The drumlin field and the geomorphology of the Múlajökull surge-type glacier, central Iceland, Geomorphology, 207, 213–220, https://doi.org/10.1016/j.geomorph.2013.11.007, 2014.

Kenzler, M. and Hüneke, H.: Sea cliff at Glowe: Stratigraphy and absolute age chronology of the Jasmund Pleistocene sedimentary record, DEUQUA Spec. Pub., this volume, 2019.

Kenzler, M , Tsukamoto, S., Meng, S., Thiel, C., Frechen, M., and Hüneke, H.: Luminescence dating of Weichselian interstadial sediments from the German Baltic Sea coast, Quat. Geochronol., 30, 251–256, https://doi.org/10.1016/j.quageo.2015.05.015, 2015.

Kenzler, M., Tsukamoto, S., Meng, S., Frechen, M., and Hüneke, H.: New age constraints from the SW Baltic Sea area – implications for Scandinavian Ice Sheet dynamics and palaeoenvironmental conditions during MIS 3 and early MIS 2, Boreas, 46, 34–52, https://doi.org/10.1111/bor.12206, 2016.

Müller, U. and Obst, K: Lithostratigraphie und Lagerungsverhältnisse der pleistozänen Schichten im Gebiet von Lohme (Jasmund/Rügen), Zeitschrift für geologische Wissenschaften, 34, 39–54, 2006.

Niedermeyer, R.-O., Kanter, L., Kenzler, M., Panzig, W.-A., Krienke, K., Ludwig, A. O., Schnick, H. H., and Schütze, K.: Die Insel Rügen (I) – Fazies, Stratigraphie, Lagerungsverhältnisse und geologisches Gefahrenpotenzial pleistozäner Sedimente der Steilküste Jasmund, in: Eiszeitlandschaften in Mecklenburg-Vorpommern, Exkursionsführer zur 35. Hauptversammlung der Deutschen Quartärvereinigung DEUQUA e.V. und der 12. Jahrestagung der INQUA PeriBaltic Working Group in Greifswald/Mecklenburg-Vorpommern, edited by: Lampe, R. and Lorenz, S., Geozon, Greifswald, 50–71, https://doi.org/10.3285/g0005, 2010.

Ó Cofaigh, C., Evans, D. J. A., and England, J.: Ice-marginal terrestrial landsystems: sub-polar glacier margins of the Canadian and Greenland high arctic, in: Glacial Landsystems, edited by: Evans, D. J. A., Arnold, London, 44–64, 2003.

Panzig, W.-A.: Zum Pleistozän Nordost-Rügens, in: Geologie des südlichen Ostseeraumes – Umwelt und Untergrund, edited by: Katzung, G., Hüneke, H., and Obst, K., Terra Nostra, Schriften der Alfred-Wegener-Stiftung, 6, 177–200, 1995.

Pedersen, S. A. S.: Superimposed deformation in glaciotectonics, B. Geol. Soc. DENMARK, 46, 125–144, 2000.

Pedersen, S. A. S.: Structural analysis of the Rubjerg Knude Glaciotectonic Complex, Vendsyssel, northern Denmark, Geol. Surv. Den. Greenl., 8, 1–192, 2005.

Pedersen, S. A. S.: Architecture of Glaciotectonic Complexes, Geosciences, 4, 269–296, https://doi.org/10.3390/geosciences4040269, 2014.

Steinich, G.: Endogene Tektonik in den Unter-Maastricht-Vorkommen auf Jasmund (Rügen), Geologie, 20, Supplement 71/72, 1–207, 1972.

van der Wateren, F. M.: Ice-marginal terrestrial landsystems: southern Scandinavian ice sheet margin, in: Glacial Landsystems, edited by Evans, D. J. A., Arnold, London, 166–203, 2003.

Vaughan-Hirsch, D. P. and Phillips, E. R.: Mid-Pleistocene thin-skinned glaciotectonic thrusting of the Aberdeen Ground Formation, Central Graben region, central North Sea, J. Quaternary Sci., 32, 196–212, https://doi.org/10.1002/jqs.2836, 2017.

DEUQUA Spec. Pub., 2, 29–33, 2019
https://doi.org/10.5194/deuquasp-2-29-2019

DEUQUA Open Access Special Publications

Sea cliff at Wissower Bach (Pleistocene stripe 5) – microstructural evidence of large-scale glacitectonism and glacier kinematics

Anna Gehrmann[1], **Heiko Hüneke**[1], **Martin Meschede**[1], **and Emrys Phillips**[2]

[1]Institut für Geographie und Geologie, Universität Greifswald, Friedrich-Ludwig-Jahn-Str. 17a, 17487 Greifswald, Germany
[2]British Geological Survey, The Lyell Centre, Research Avenue South, Edinburgh, EH14 4AP, UK

Correspondence: Anna Gehrmann (anna.gehrmann@uni-greifswald.de)

Relevant dates: Published: 15 August 2019

How to cite: Gehrmann, A., Hüneke, H., Meschede, M., and Phillips, E.: Sea cliff at Wissower Bach (Pleistocene stripe 5) – microstructural evidence of large-scale glacitectonism and glacier kinematics, DEUQUA Spec. Pub., 2, 29–33, https://doi.org/10.5194/deuquasp-2-29-2019, 2019.

Abstract: Soft-sediment thin sections from a SW-dipping thrust fault at the south-western limb of the Wissower Bach syncline (NE Rügen) give rise to the complicated glacitectonic environment in the south-western Baltic Sea region. Micromorphology, microstructural mapping, and macroscale information have led to the development of a detailed model for the evolution of the syncline during late Weichselian glacitectonism.

1 Macrostructural features of the Wissower Bach syncline

The Wissower Bach syncline (54°31.923′ N, 13°40.697′ E) is exposed in a ca. 200 m wide and 40 m high sea-cliff section 1.5 km north-east of Sassnitz. The syncline preserves Upper Cretaceous (Maastrichtian) chalk and a comprehensive Pleistocene sedimentary record (Fig. 1). The Pleistocene succession has been subdivided into at least three tills or diamictons (M1 to M3) with intercalated stratified units (I1 and I2) comprising gravel, sand, and clay (abbreviations adapted from Jaekel, 1917).

The NE-verging syncline (axial surface dips to the SW, 200–250/45–50 – dip direction/dip), which is very tight to the isoclinal, is moderately inclined and deforms both the chalk bedrock and unconsolidated pre-M3 Pleistocene glacigenic deposits (Fig. 1). The former lithostratigraphical boundary between the chalk and the Pleistocene record in the south-western limb has been modified by a SW/WSW-dipping (260/50) reverse fault. Glacitectonism of the Jasmund Peninsula occurred after accumulation of the I2, i.e. after the Last Glacial Maximum (MIS 2, marine isotope stage), with large-scale folding and thrusting occurring in response to a re-advance of the Scandinavian Ice Sheet during the Pomeranian W2 phase (around 18.5–16.0 ka) (e.g. Groth, 2003; Müller and Obst, 2006; Kenzler et al., 2015, 2016).

2 Microstructural features

Orientated soft-sediment thin sections from two samples (JA03, JA04) (Fig. 1b) were taken from the thrust fault at the south-western limb between Maastrichtian chalk (hanging wall) and Pleistocene deposits (footwall) (Gehrmann et al., 2017; see also van der Meer, 1993; Menzies, 2000). Micromorphology and microstructural mapping were used to understand the complicated glacitectonic environment in the south-western Baltic Sea region (see Phillips et al., 2011, 2013; Vaughan-Hirsch et al., 2013).

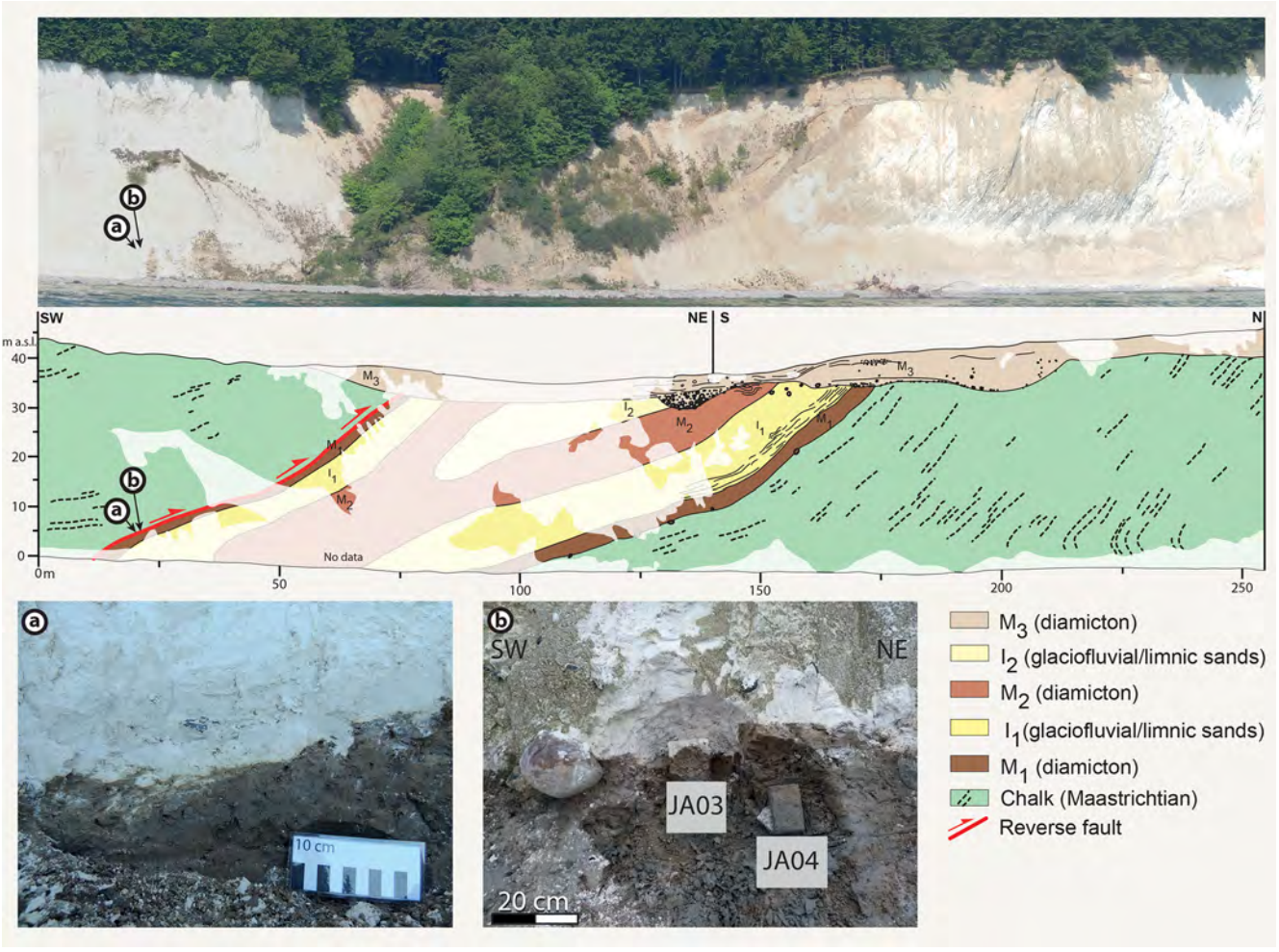

Figure 1. Panoramic image and geological cross section of the Wissower Bach syncline. At the south-western limb of the syncline there is a SW-dipping thrust fault between the Cretaceous chalk and the Pleistocene M1 diamicton below. **(a)** Tectonic contact between the chalk and the M1 diamicton. **(b)** Sample blocks JA03 and JA04 at the thrust fault (Gehrmann et al., 2017; abbreviations adapted from Jaekel, 1917).

Within the M1 diamicton which occurs immediately adjacent to the main fault, three different main fabrics were distinguished (Gehrmann et al., 2017). The dominant planar S1 fabric (oldest) dips approximately towards the north and is divided into the two sub-fabrics S1a (gently inclined) and S1b (steep) (Fig. 2). S2 is a linear fabric, dips to the south (perpendicular to S1), and can be divided into steeper (S2a) and more gently inclined (S2b) components. The youngest fabric, S3, is a planar-to-anastomosing subvertical foliation, which is interpreted as having formed in response to the dewatering of the till.

3-D analysis of the clast microfabrics has revealed that S1 shows a change of orientation with increasing proximity to the fault indicative of an anti-clockwise rotation of ~ 70 to 90° (Fig. 2). Adjacent to the chalk–diamicton boundary (JA03), S1 dips at a moderate angle towards the NW (S1a – 307/48, S1b – 307/55). In sample JA04, in contrast, S1 dips to the NE (S1a – 042/20, S1b – 042/54). The S2 domains are orientated perpendicular to S1. As with S1, the S2 fabric shows a pronounced change in orientation (anti-clockwise rotation) with decreasing distance to the chalk–diamicton boundary. In sample JA03, adjacent to the chalk–diamicton boundary, S2 is moderately inclined to the SE (S2a – 136/49, S2b – 136/31), whereas in sample JA04, S2 plunges towards the SW (S2a – 214/44, S2b – 214/68). In contrast to both S1 and S2, the S3 fabric shows a relatively consistent orientation in both samples indicating that the imposition of this foliation post-dated the deformation responsible for the rotation of the earlier-formed S1 and S2 fabrics.

3 The link between the microstructural architecture and large-scale glacitectonism

The combination of 3-D microstructural analysis and macroscale information of the Wissower Bach syncline gives rise to a detailed four-stage model of imbricate-fan forma-

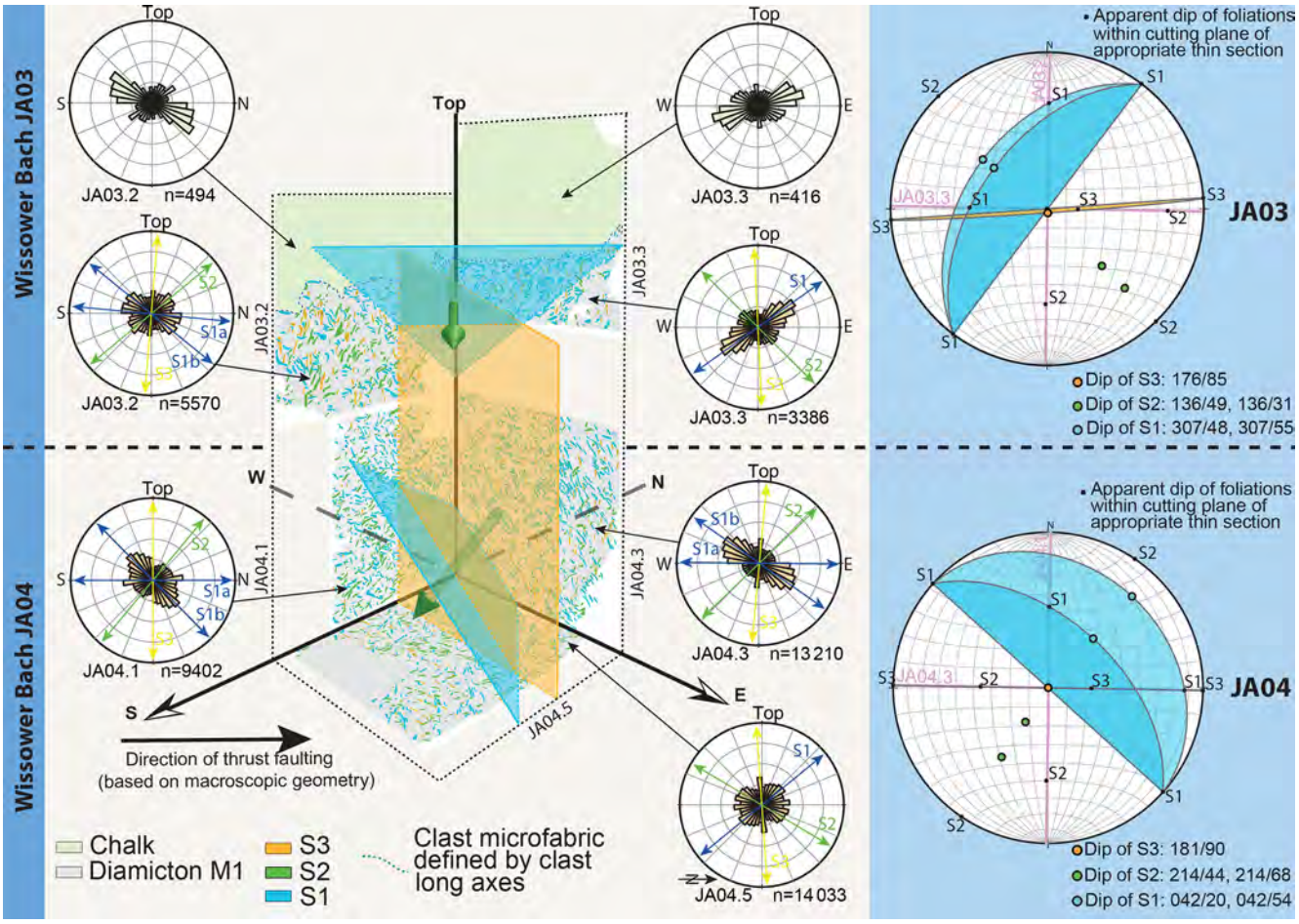

Figure 2. The 3-D model of the microfabric system at the faulted chalk–diamicton contact (samples JA03, JA04). The lower-hemisphere stereographic plots show the orientation of microfabrics S1–S3, their shape (linear/planar) and their spatial relationship to each other (Gehrmann et al., 2017).

tion by ice-push from the south (Fig. 3) (Gehrmann et al., 2017). The evolution starts with an overall sense of compressional movement to the NE leading to the formation of the Wissower Bach syncline (first stage). This was accompanied by flexural slip along the lithological boundary between the chalk and the diamicton, and the imposition of the S1 and S2 microfabrics within the M1 diamicton. The clast fabric developed as Riedel shears with the planar S1 fabric representing R shears (narrow zones of extension, kinematically corresponding to normal faults) and the linear fabric S2 indicating P shears that correspond to reverse faults, thus zones of compression (see Fossen, 2010).

Continued compression led to progressive folding and further tightening of the Wissower Bach syncline (second stage). This may have accompanied the overturning and localised thrusting on the southern limb of the syncline. During this deformation, the earlier-formed S1 microfabric was crenulated with axial surfaces of these microfolds occurring coplanar to the adjacent S2 fabric.

This folding was followed by the anti-clockwise rotation of the microfabrics in a narrow shear zone developed along the tectonic contact between the M1 diamicton and chalk; probably as the ice partly overrode the Jasmund Peninsula (third stage). This rotation of the microfabrics clearly records a change in the orientation in stress regime, possibly in response to changes in the local ice-movement direction as the glacier progressively overrode the peninsula. On a larger scale, during this stage of the ice sheet advance the top of the glacitectonised sequence was eroded, accompanied by the deposition of the M3 subglacial traction till (see Brumme et al., 2019).

The evolution ended in dewatering of the sediments and a late-stage reactivation (normal faulting due to gravitational relaxation) at the south-western limb of the Wissower Bach syncline as the ice retreated (fourth stage). The S3 domains represent anastomosing conduits or fluid pathways taken by the escaping porewater. This can be confirmed by the character of the contact between the chalk and the diamicton at both the macro- and microscale, which shows a ductile structure

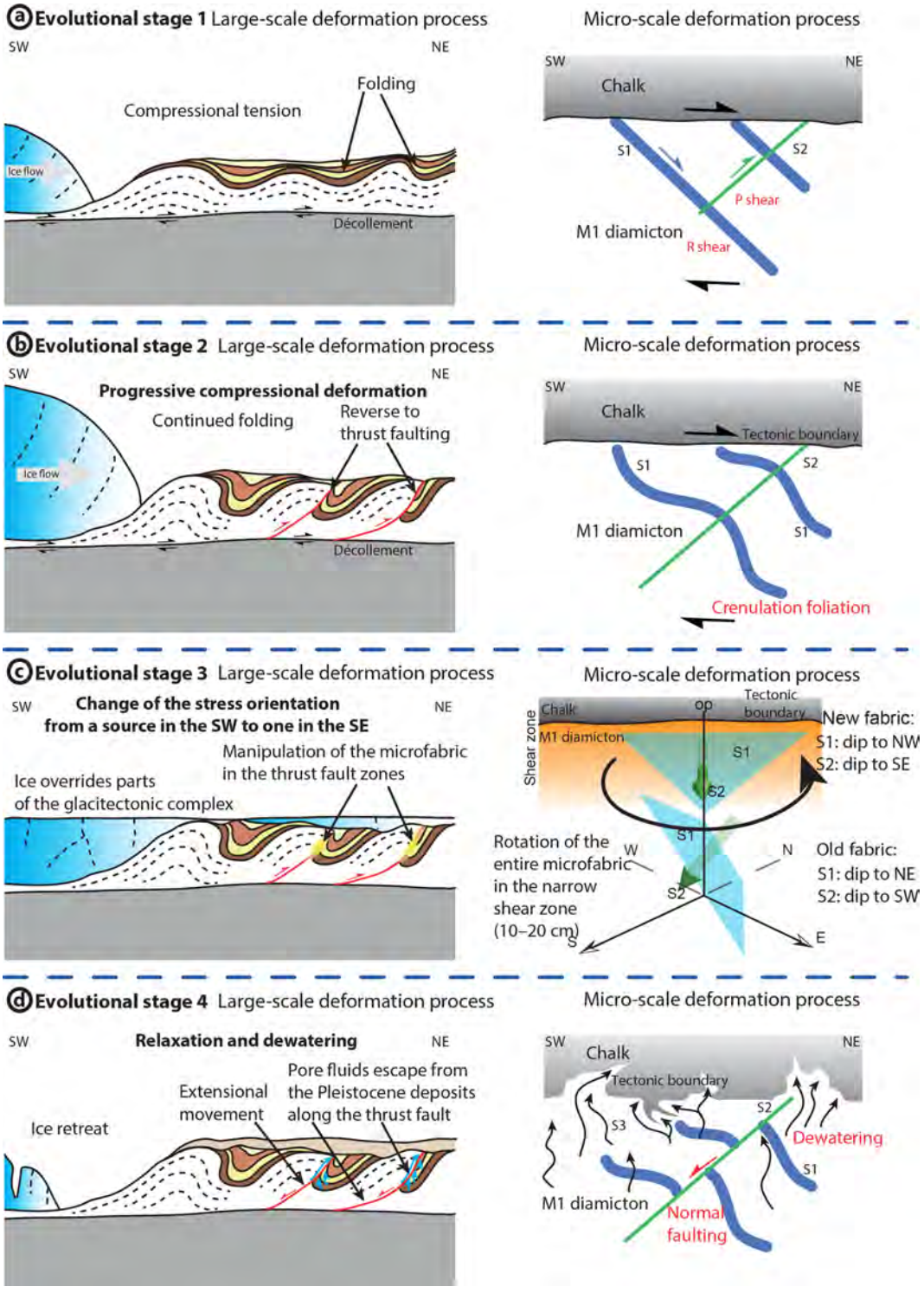

Figure 3. Four-stage evolutional model of the Wissower Bach syncline and adjacent structures including the microstructural development. **(a)** Stage 1: imposition of large-scale folds leading to the formation of the microfabrics S1 (dip to NE) and S2 (dip to SW) as part of a Riedel shear zone. **(b)** Stage 2: continuation of folding and thrusting leading to progressive deformation of S1 (crenulation) and S2 at microscale. **(c)** Stage 3: anti-clockwise rotation of S1 and S2 within the narrow shear zone (10–20 cm) of the thrust fault presumably by the partial overburden of the glacitectonic complex due to the proceeding ice. **(d)** Stage 4: retreat of the ice and associated relaxation ending in local microscale normal-fault movements along the S2 microfabric and dewatering of the M1 diamicton, which produces a ductile deformation of the tectonic boundary and formation of the S3 microfabric (Gehrmann et al., 2017).

and interfingering of both depositional units by porewater escape. Also during the fourth stage, the S2 foliation has been reactivated. Locally, it displays normal faults which crosscut and dislocate the earlier-developed S1 domains. This microstructural relationship records a generally south-directed extension during a late phase of the proposed polyphase deformation history recorded by the M1 diamicton.

Data availability. The dataset can be found in the database of the Institute for Geography and Geology of the University of Greifswald (Chair of Regional and Structural Geology) and in Gehrmann et al. (2017).

Author contributions. AG, HH, and EP designed the methodology and performed the analysis. AG prepared the article with contributions from all co-authors.

Competing interests. The authors declare that they have no conflict of interest.

Acknowledgements. The Nationalparkamt Vorpommern is thanked for granting the approval to work in the Jasmund National Park. We thank Sylvia Weinert (University of Greifswald) for careful preparation of the thin sections. The constructive comments of an unknown reviewer substantially improved our article. We acknowledge support for the article processing charge from the DFG (no. 393148499) and the Open Access Publication Fund of the University of Greifswald.

Financial support. This research has been supported by the DFG (German Research Foundation, grant no. 393148499) and the Open Access Publication Fund of the University of Greifswald.

References

Brumme, J., Hüneke, H., and Phillips, E. R.: Micromorphology and clast microfabrics of subglacial traction tills at the sea-cliff Dwasieden: evidence of polyphase syn- and post-depositional deformation, DEUQUA Spec. Pub., this volume, 2019.

Fossen, H. (Ed.): Structural Geology, Campridge University Press, New York, 2010.

Gehrmann, A., Hüneke, H., Meschede, M., and Phillips, E. R.: 3D microstructural architecture of deformed glacigenic sediments associated with large-scale glacitectonism, Jasmund Peninsula (NE Rügen), Germany, J. Quaternary Sci., 32, 213–230, https://doi.org/10.1002/jqs.2843, 2017.

Groth, K.: Zur glazitektonischen Entwicklung der Stauchmoräne Jasmund/Rügen, Schriftenreihe des Landesamtes für Umwelt, Naturschutz und Geologie Mecklenburg-Vorpommern, 3, 39–49, 2003.

Jaekel, O.: Neue Beiträge zur Tektonik des Rügener Steilufers, Zeitschrift der Deutschen Geologischen Gesellschaft, 69, 81–176, 1917.

Kenzler, M , Tsukamoto, S., Meng, S., Thiel, C., Frechen, M., and Hüneke, H.: Luminescence dating of Weichselian interstadial sediments from the German Baltic Sea coast, Quat. Geochronol., 30, 251–256, https://doi.org/10.1016/j.quageo.2015.05.015, 2015.

Kenzler, M., Tsukamoto, S., Meng, S., Frechen, M., and Hüneke, H.: New age constraints from the SW Baltic Sea area – implications for Scandinavian Ice Sheet dynamics and palaeoenvironmental conditions during MIS 3 and early MIS 2, Boreas, 46, 34–52, https://doi.org/10.1111/bor.12206, 2016.

Menzies, J.: Micromorphological analyses of microfabrics and microstructures indicative of deformation processes in glacial sediments, Geol. Soc. London Spec. Pub., 176, 245–257, https://doi.org/10.1144/GSL.SP.2000.176.01.19, 2000.

Müller, U. and Obst, K: Lithostratigraphie und Lagerungsverhältnisse der pleistozänen Schichten im Gebiet von Lohme (Jasmund/Rügen), Zeitschrift für geologische Wissenschaften, 34, 39–54, 2006.

Phillips, E. R., van der Meer, J. J. M., and Ferguson, A.: A new "microstructural mapping" methodology for the identification, analysis and interpretation of polyphaser deformation within subglacial sediments, Quaternary Sci. Rev., 30, 2570–2596, https://doi.org/10.1016/j.quascirev.2011.04.024, 2011.

Phillips, E. R., Lipka, E., and van der Meer, J. J. M.: Micromorphological evidence of liquefaction, injection and sediment deposition during basal sliding of glaciers, Quaternary Sci. Rev., 81, 114–137, https://doi.org/10.1016/j.quascirev.2013.10.005, 2013.

van der Meer, J. J. M.: Microscopic evidence of subglacial deformation, Quaternary Sci. Rev., 12, 553–587, https://doi.org/10.1016/0277-3791(93)90069-X, 1993.

Vaughan-Hirsch, D. P., Phillips, E. R., and Lee, J. R.: Micromorphological analysis of poly-phase deformation associated with the transport and emplacement of glaciotectonic rafts at West Runton, north Norfolk, UK, Boreas, 42, 376–394, https://doi.org/10.1111/j.1502-3885.2012.00268.x, 2013.

DEUQUA Spec. Pub., 2, 35–41, 2019
https://doi.org/10.5194/deuquasp-2-35-2019

Open Access DEUQUA Special Publications

Coastal cliff at Lenzer Bach on Jasmund Peninsula, Rügen Island (Pleistocene Stripe 4): reconstructed history of glacitectonic deformation based on fold geometry and microstructural mapping

Paul Mehlhorn[1], Laura Winkler[1], Franziska-Charlotte Grabbe[1], Michael Kenzler[1], Anna Gehrmann[1], Heiko Hüneke[1], and Henrik Rother[1,2]

[1]Institute for Geography and Geology, University of Greifswald, Greifswald, 14789, Germany
[2]Landesamt für Geologie und Bergwesen Sachsen-Anhalt (LAGB), State Geological Survey Saxony-Anhalt, Köthener Str. 38, 06118 Halle, Germany

Correspondence: Paul Mehlhorn (paul.mehlhorn@uni-greifswald.de)

Relevant dates: Published: 15 August 2019

How to cite: Mehlhorn, P., Winkler, L., Grabbe, F.-C., Kenzler, M., Gehrmann, A., Hüneke, H., and Rother, H.: Coastal cliff at Lenzer Bach on Jasmund Peninsula, Rügen Island (Pleistocene Stripe 4): reconstructed history of glacitectonic deformation based on fold geometry and microstructural mapping, DEUQUA Spec. Pub., 2, 35–41, https://doi.org/10.5194/deuquasp-2-35-2019, 2019.

Abstract: A thrust-bound footwall syncline located within the proximal part of the southern Jasmund Glacitectonic Complex is investigated, exploring the spatio-temporal relationship between glacitectonic macro- and microstructures. Orientation and geometry of macroscale folds and thrust faults reveal a two-phased deformation history recorded by the sedimentary sequence. The deformation is a result of glacitectonic imbrication and subsequent ice flow across Jasmund Peninsula during the late Weichselian. Clast microfabrics preserved within the folded glacial diamicts reveal that till-internal deformation is mainly related to subglacial shearing within the glacier bed, which predates large-scale imbrication and folding.

1 Introduction

The syncline of Pleistocene Stripe 4 (Streifen 4) is located at a coastal cliff section northeast of Lenzer Bach near the town Sassnitz (54°31′42.24″ N, 13°40′25.99″ E). The exposed sequence comprises tightly folded units of Upper Cretaceous chalk and (para-)conformably overlying Pleistocene sediments, comprising glacial diamicts (till units M1 and M2) and interbedded gravel, sand and silt (units I1 and I2) (Fig. 1). Above an angular unconformity, which truncates the large-scale glacitectonic structure, gravel-rich channel fills and a further glacial diamict (M3 unit) are deposited. Optically stimulated luminescence (OSL) dating supported by lithostratigraphic correlation indicates that the Pleistocene succession was mainly formed during the Weichselian advance of the Scandinavian Ice Sheet (see Kenzler et al., 2017; Kenzler and Hüneke, 2019).

Over the last century the locality at Stripe 4 has been investigated multiple times with a focus on reconstructing the depositional history and entangling the site's spectacular but complex glacitectonic history (e.g. Keilhack, 1914; Jaekel, 1917; Steinich, 1972; Kahlke, 1982). Based on ar-

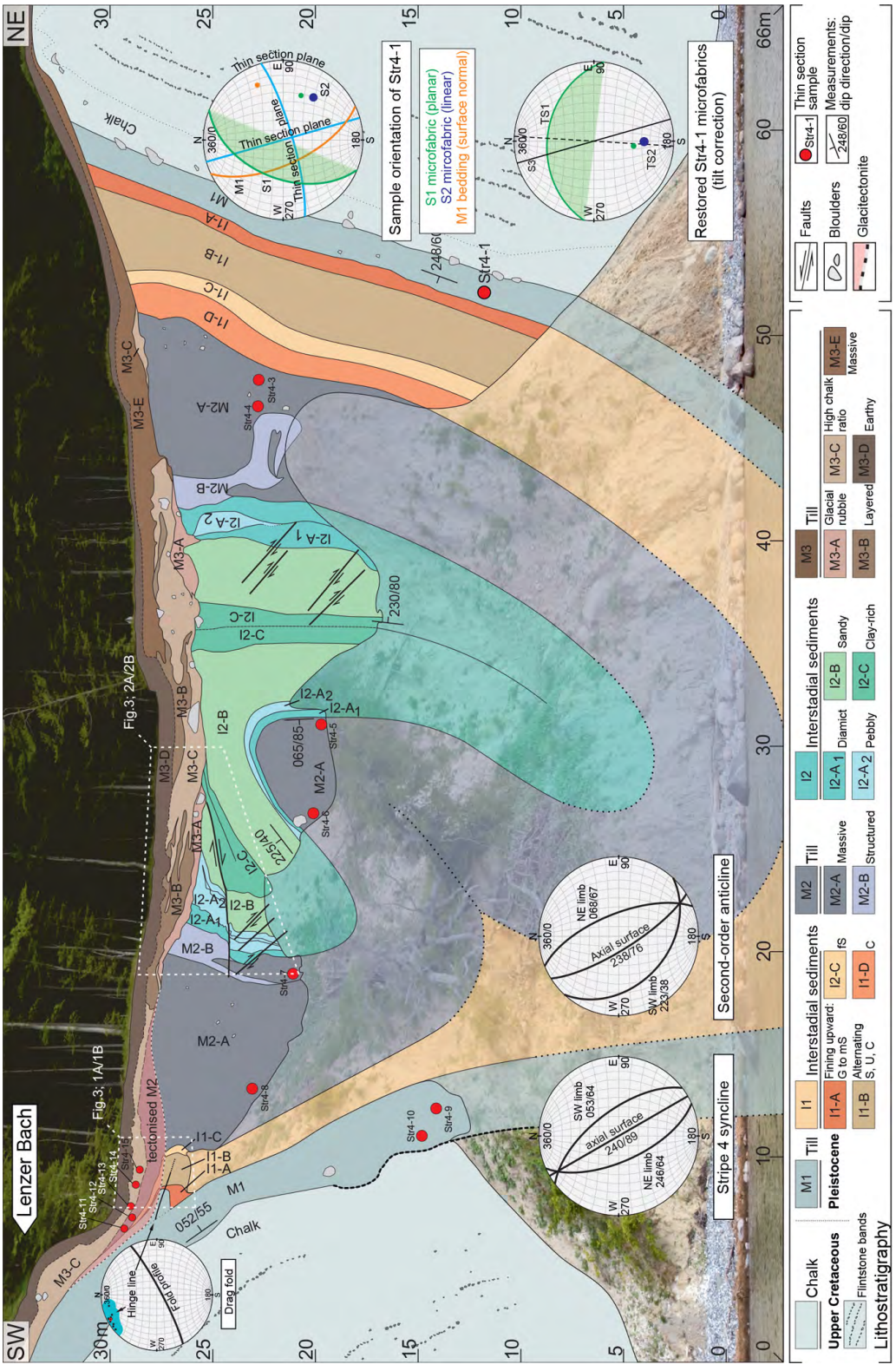

Figure 1. Geological cliff section of Pleistocene Stripe 4 (Streifen 4) northeast of Sassnitz on Rügen Island (Mehlhorn, 2016, modified), showing large-scale glacitectonic folding of Cretaceous chalk and Pleistocene glacial deposits of units M1 to I2, as well as the unconformably overlying late Weichselian M3 sediment complex. Structural data and sample locations from which thin sections were produced for clast microfabric analyses are indicated (red dots). Lower-hemisphere stereographic plots highlight orientation of the macroscopic folds (left) and results from the clast-microfabric analysis (right). Note that the coastal cliff is oriented almost perpendicular to the strike of the fold structures.

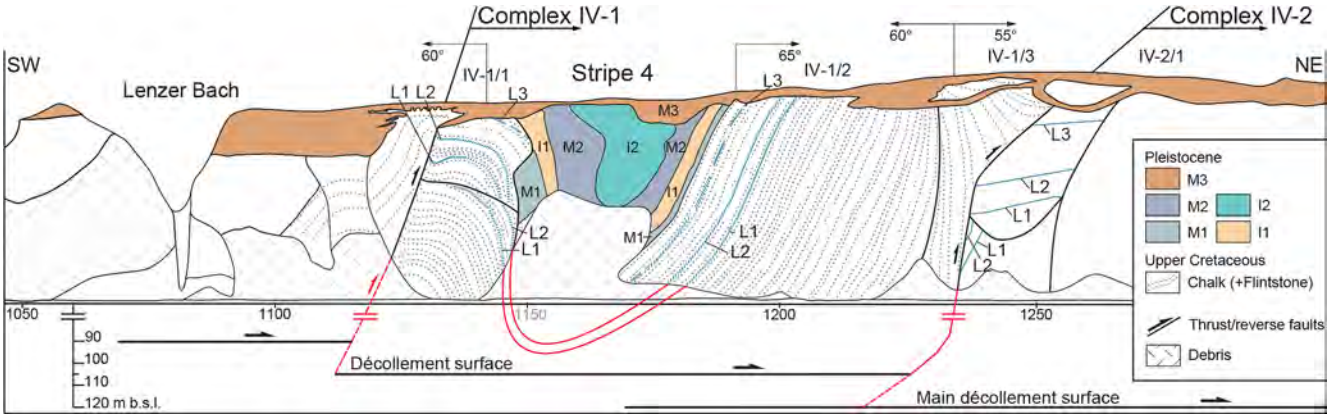

Figure 2. NE-verging syncline of Pleistocene Stripe 4 within a framework of imbricate thrust sheets exhibiting hanging-wall anticlines of chalk (based on Steinich, 1972, and Gehrmann, 2018). The depicted depth of the decollement (at 105–120 m b.s.l.) is not true to scale. Black dashed lines indicate flint layers. See Fig. 1 for stratigraphy of the Pleistocene units.

chitectural geometries, recognition of crosscutting relationships between the depositional units and identification of glacitectonic structures, an imbricate thrust-stack model was eventually developed for the glacitectonic evolution of the Jasmund Peninsula during the Weichselian glaciation (e.g. Steinich, 1972; Groth, 2003; Ludwig, 2011). More recently, Gehrmann and Harding (2018) and Gehrmann (2018) classified this area as a glacitectonic complex, where Stripe 4 is in a proximal position within the southern structural sub-complex of the overall Jasmund Glacitectonic Complex. The Pleistocene succession is preserved in the footwall syncline between the hanging-wall anticlines of two adjoining imbricate thrust sheets, which are separated by a steep ramp (Fig. 2).

In early 2012, a cliff failure formed a new exposure that exhibited the fold in modified geometry and detail including a metre-scale second-order parasitic fold at the centre of the syncline and a drag fold at its southern limb (Fig. 1). These circumstances allowed for a new in-depth macro- and microstructural investigation (Mehlhorn, 2016). The analysis of microstructures observed in thin sections from the glacial diamicts provided a relative chronology of deformational events, which is interpreted in the context of syn-depositional till-formation processes and post-depositional modifications (e.g. water escape, glacitectonic folding and imbrication) (Mehlhorn, 2016; Winkler, 2016; Grabbe, 2017). Note that all measurements of planes indicate direction and inclination of the dip.

2 Macro- and microstructural characteristics

2.1 Northeast-verging syncline and second-order anticline below the angular unconformity

The syncline comprises chalk beds and overlying Pleistocene deposits including units M1 to I2 (Fig. 1). The easily visible flint layers within the chalk allow for tracing of the deformed bedding and outline large-scale fold structures (Fig. 2). Fold axes and axial plane of the slightly asymmetric (tight) syncline strike NW–SE as documented by the orientation of bedding planes at both outer limbs (246/64, 053/64). Compared to the southwestern limb the northeastern limb dips distinctly steeper. The intersection point of the bedding-plane great circle (linear 330/13) indicates a gently plunging fold axis towards the NW. At the contact between the chalk and the Pleistocene units at the southwestern limb, we note some dislocation along an indistinct fault that runs along the stratigraphic boundary.

The southwestern limb of the syncline is characterised by a second-order fold (parasitic fold) that can be classified as an adventive anticline. It displays a distinct NE vergence, as documented by bedding-plane measurements within the I2 unit at both limbs (Fig. 1). The southwestern limb of the anticline dips at a low angle towards the SW (223/38), while the northeastern limb dips at a steeper angle towards the NE (068/67). The intersecting great circles of the bedding planes indicate a SE-directed plunge of the fold axis (linear 150/14). Thus, the fold axes of the main syncline and the second-order anticline plunge in opposite directions.

Within the southwestern limb of the syncline – above the parasitic anticline – the M2 and I2 units are offset by a flat SW-dipping reverse fault (Fig. 3 2A/2B; compare to Fig. 1) along which the hanging wall displays a NE-directed displacement of about 2 m. Smaller-scale associated subordinate normal faults within the I2 unit show minor displacements of 5–10 cm.

2.2 Drag fold associated with the angular unconformity

Along the above-mentioned angular unconformity near the top of the folded sequence, the chalk and Pleistocene units M1 to I2 are sharply truncated. An exception is a metre-scale (recumbent) drag fold at the southwestern limb of the syncline (Fig. 3 1A/1B, compare to Fig. 1). The subvertically oriented units M1, I1 and M2 are bent at right angles at their

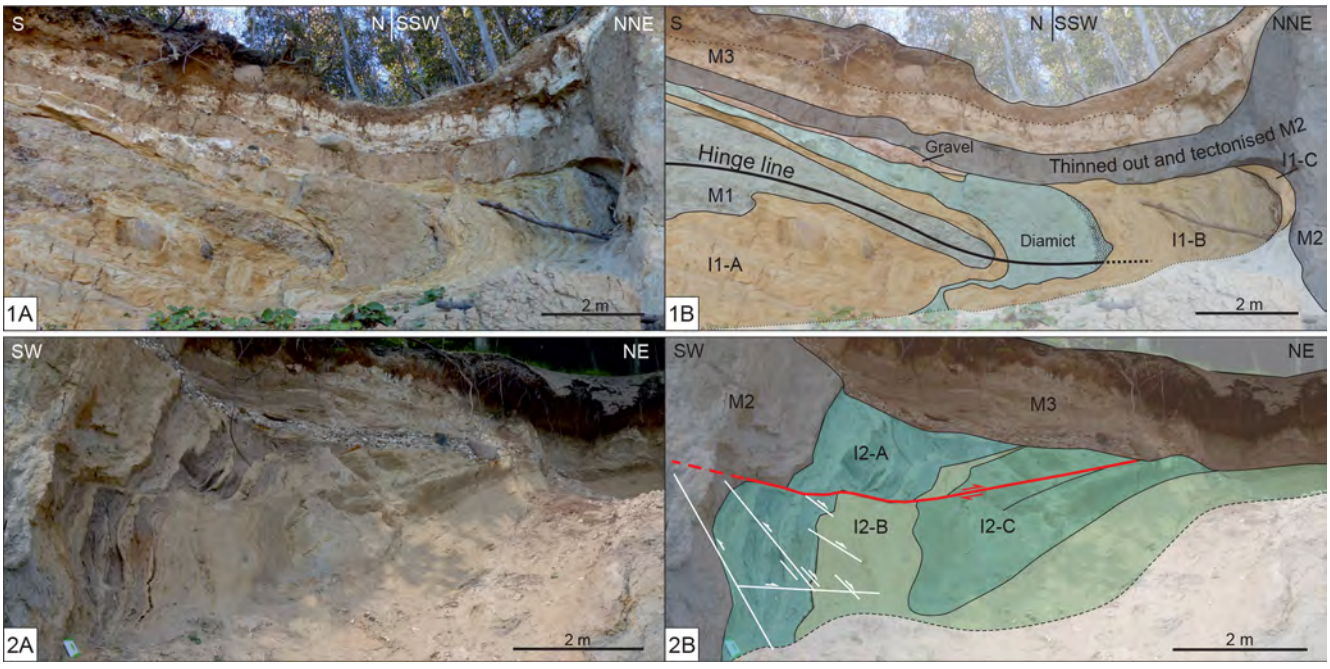

Figure 3. Outcrop details at Pleistocene Stripe 4. Photograph **(1A)** and sketch **(1B)** showing a drag fold associated with the angular unconformity at the southwestern limb of the syncline. Also shown is the hinge line (see Fig. 1). Photograph **(2A)** and sketch **(2B)** show the SW-dipping thrust fault. Note the distinct angular unconformity below the M3 sediment complex, which truncates the older units.

uppermost ends towards the SW and pinch out laterally over a distance of a few metres. The drag fold shows a nearly horizontal axial plane. Measurements along the hinge line (Fig. 1, top left) document a NW–SE-trending fold axis, gently plunging NW (linear 332/07). A glacial diamict (M3 unit) directly overlies the upper limb of the drag fold.

2.3 Microstructural mapping of till units

Thin-section-based mapping of clast microfabrics (Phillips et al., 2011) defined by the preferential alignment of detrital grains reveal the presence of up to four different till microfabrics (labelled S1 to S4) within these units. They can best be exemplified in vertical thin sections oriented parallel to the ice flow (Fig. 4). Directional data from thin sections – obtained from the M1 and M2 units – were reoriented according to subsequent glacitectonic tilt and folding. The majority reveal two dominant till fabrics; a planar S1 microfabric dipping at a low to moderate angle towards the NNE (i.e. "up-ice") and a linear S2 fabric plunging at a moderate angle towards the SSW (i.e. "down ice") (Brumme, 2015; Mehlhorn, 2016; Winkler, 2016; Grabbe, 2017). These fabrics, which formed early at the glacier bed during deposition, are cut by the later, subvertical to steeply inclined S3 and S4 fabrics (Fig. 4).

3 Interpretation of deformational events and kinematic frame

3.1 Formation of the NE-verging syncline and second-order anticline: large-scale glacitectonic folding and imbrication

Both the NW–SE-trending syncline and the subordinate second-order anticline (Fig. 1) exemplify structure and kinematics of the exposed portion of the Jasmund Glacitectonic Complex. Stripe 4 is located within the proximal zone of the southern sub-complex interpreted as an imbricate fan, featuring large-scale folding, particularly revealing distinct footwall synclines below moderately to steeply inclined thrust faults (Gehrmann et al., 2019). Based on cross-section restoration, Gehrmann (2018) deduced the decollement level at a depth of 105–120 m b.s.l. and calculated a horizontal shortening of about 40 % (∼ 400 m) in minimum for this sector (complex IV-1 to IV-3) (Fig. 2). The asymmetric geometry and vergence of the tight fold indicate a NE-directed growth of the imbricate thrust stacks at this location within the glacitectonic complex. The documented values correspond to the orientation of the syncline in the best-fit model constructed by Gehrmann (2018).

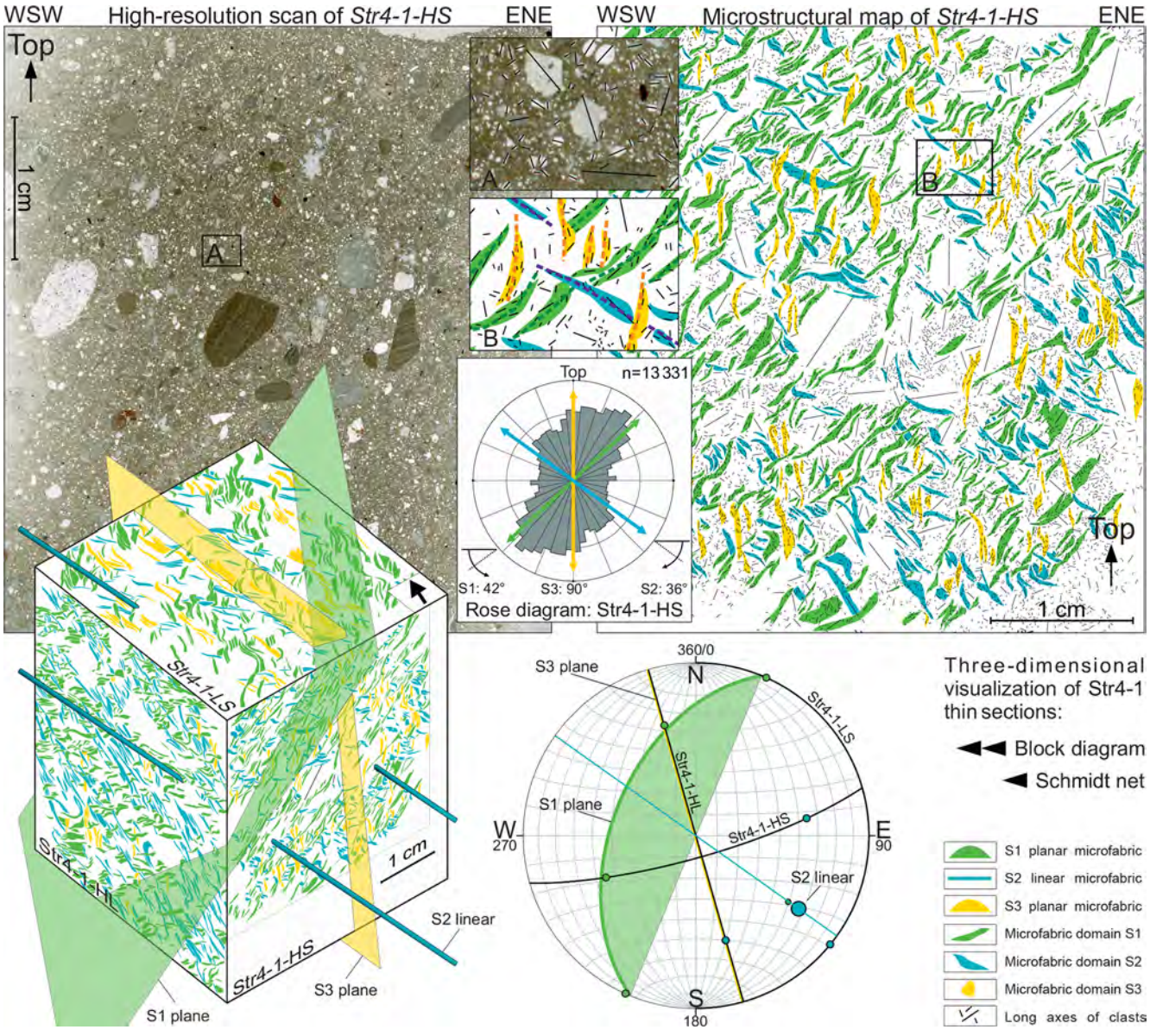

Figure 4. High-resolution scan and microstructural map of a thin section – Str4-1-HS – of sample Str4-1 (see Fig. 1 for sample location), exemplifying the microstructural mapping approach and till microfabric analysis following the methodology of Phillips et al. (2011). The orientation of the long axes of intra-diamict sand- to granule-sized clasts are shown by a rose diagram, stereogram (Schmidt net) and block diagram. Compare stereogram in Fig. 1 for restored data. Note the crosscutting relationship of at least three microfabric domains: the dominant planar fabric (S1) dips in a NNE direction (007/41, reoriented for glacitectonic tilt and folding) and is intersected by a linear fabric (S2) plunging towards the SSW (181/37, reoriented for glacitectonic tilt and folding). Both the planar S1 and linear S2 fabrics are related to subglacial deformation during deposition of the M1 till; their opposing orientations ("up-ice" versus "down-ice") indicate a sense of shear from the NNE to SSW, confirming findings by Brumme (2015). A later subvertical planar fabric (S3), trending NNW–SSE (075/89), cuts across these earlier fabrics. As this (youngest) fabric runs parallel to Str4-1-HL and corresponds with the axial surface of the large-scale syncline, it is thought to have formed by upward escape of porewater through the sediment induced by glacitectonic folding (see Gehrmann et al., 2017).

3.2 Origin of the SW-oriented drag fold: glacitectonite formed during deposition of the M3 unit

The recumbent drag fold below the angular unconformity at the base of the M3 unit (Fig. 3 1A/1B) can be best explained as part of a glacitectonite unit formed by subglacial deformation imposed by ice advancing from the NE. Although subglacial shearing folded and streamlined the pre-existing sediments (M1, I1 and M2), they retained some structural characteristics of their parent material (e.g. cross lamination in the I1 unit). The structural unit is thus classified as a type B glacitectonite (Benn and Evans, 1996), which has undergone largely non-penetrative deformation. The NW–SE-trending hinge line of the fold, the horizontally oriented upper limb and the thinning out of sedimentary beds away from the hinge zone all indicate drag by ice shear towards the SW.

The overlying M3 unit features a combination of erosional channel structures, glacigenic diamicts, and interbedded water-lain gravels and sands (Fig. 1). All sediments deposited above the unconformity contain large amounts of flint pebbles and chalk (granules and fine-grained mud).

3.3 Fabric development during deposition of the M1 (and M2) diamicts: subglacial formation of a traction till with polyphase deformation

The analysis of microstructures observed in thin sections obtained from glacial diamicts on Jasmund revealed a relative chronology of deformational events, which can be interpreted in the context of syn-depositional till-forming processes and subsequent post-depositional modification (Brumme, 2015; Brumme et al., 2019). In accordance with these results, clear evidence of subglacial deformation reveals the presence of a pervasive set of clast microfabrics within the M1 and M2 diamicts at Stripe 4 (Mehlhorn, 2016; Winkler, 2016; Grabbe, 2017), documenting polyphase deformation processes at the glacier bed (e.g. van der Meer, 1993; Phillips et al., 2018). Most of these fabrics predate the large-scale glacitectonic folding; i.e. their orientation cannot be related to established ice-flow directions until restoring their original position by rotation and back-tilting (Figs. 1, 4). The two dominant gently dipping clast microfabrics S1 and S2, exemplified within the M1 unit (Fig. 4), display preferred grain orientations towards the NNE (S1) and SSW (S2), respectively, as a result of shear at the glacier bed under ductile conditions (Brumme, 2015). The subvertical to steeply inclined S3 and S4 fabrics are thought to have developed during dewatering of the water-saturated diamicts. A more detailed description and interpretation of the polyphase deformation recorded by the till microfabrics are given by Brumme (2015) and Brumme et al. (2019).

4 Conclusion

The origin of the documented clast microfabrics within the glacial diamicts of units M1 and M2 are related to subglacial shear conditions during the advance of the Scandinavian Ice Sheet from the NNE (and NE). The presence of up to four microfabrics (labelled S1 to S4) results from polyphase deformation during till accumulation and penecontemporaneous (to post-depositional) dewatering. Subsequent large-scale glacitectonic folding and imbrication produced the NE-verging syncline together with the second-order anticline and thrust faults as part of the formation of the southern subcomplex within the Jasmund Glacitectonic Complex. The SW-oriented drag fold associated with the angular glacitectonic unconformity represents the shear-folded base (glacitectonite) of the deformational layer formed during deposition of the M3 till due to ice advance towards the SW; thus, its development postdates the large-scale folding and imbrication at Stripe 4.

Data availability. All underlying data are published in the figures of this article. Thin sections are stored in the thin section archive of the Institute of Geography and Geology at the University of Greifswald.

Author contributions. PM, LW and FCG carried out field work and processed, measured and analysed the samples. PM wrote the first draft of the paper and developed most of the illustrations. MK suggested the field site and joined the sampling. HH and MK designed the project, secured funding and supervised PM, LW and FCG during their bachelor theses. HH rewrote part of the paper. AG and HR contributed with text about the sampling site and the regional geology. All authors contributed to the discussion and interpretation of the presented research results.

Competing interests. The authors declare that they have no conflict of interest.

Acknowledgements. The authority of the National Park "Vorpommersche Boddenlandschaft" kindly granted the approval to work in the Jasmund district. We are grateful to Sylvia Weinert (University of Greifswald) for careful preparation of the thin sections. Martin Meschede and an unknown colleague are thanked for their constructive reviews. We acknowledge support for the article processing charge from the DFG (no. 393148499) and the Open Access Publication Fund of the University of Greifswald.

Financial support. This research has been supported by the DFG (German Research Foundation, grant no. 393148499) and the Open Access Publication Fund of the University of Greifswald.

References

Benn, D. I. and Evans, D. J. A.: The interpretation and classification of subglacially-deformed materials, Quaternary Sci. Rev., 15, 23–52, https://doi.org/10.1016/0277-3791(95)00082-8, 1996.

Brumme, J.: Three-dimensional microfabric analyses of Pleistocene tills from the cliff section Dwasieden on Rügen (Baltic Sea Coast): Micromorphological evidence for subglacial polyphase deformation, PhD thesis, University of Greifswald, Greifswald, Germany, 250 pp., 2015.

Brumme, J., Hüneke, H., and Phillips, E.: Micromorphology and clast microfabrics of subglacial traction tills at the sea-cliff Dwasieden: evidence of polyphase syn- and post-depositional deformation, DEUQUA Spec. Pub., this volume, 2019.

Gehrmann, A.: The multi-stage structural development of the Upper Weichselian Jasmund glacitectonic complex (Rügen, NE Germany), PhD thesis, University of Greifswald, Greifswald, Germany, 235 pp., 2018.

Gehrmann, A. and Harding, C.: Geomorphological Mapping and Spatial Analyses of an Upper Weichselian Glacitectonic Complex Based on LiDAR Data, Jasmund Peninsula (NE Rügen), Germany, Geosciences, 8, 208, https://doi.org/10.3390/geosciences8060208, 2018.

Gehrmann, A., Hüneke, H., Meschede, M., and Phillips, E. R.: 3D microstructural architecture of deformed glacigenic sediments associated with large-scale glacitectonism, Jasmund Peninsula (NE Rügen), Germany, J. Quaternary Sci., 32, 213–230, https://doi.org/10.1002/jqs.2843, 2017.

Gehrmann, A., Meschede, M., Hüneke, H., Pedersen, S. A. S.: Sea cliff at Kieler Ufer (Pleistocene stripes 11–16) – Large-scale architecture and kinematics of the Jasmund Glacitectonic Complex, DEUQUA Spec. Pub., this volume, 2019.

Grabbe, F.-C.: Fazies- und Strukturanalyse des glazitektonisch mehrphasig deformierten M2-Tills vom Streifen 4 auf Jasmund (Rügen), BSc thesis, University of Greifswald, Greifswald, Germany, 48 pp., 2017.

Groth, K.: Zur glazitektonischen Entwicklung der Stauchmoräne Jasmund/Rügen, Schriftenreihe des Landesamtes für Umwelt, Naturschutz und Geologie Mecklenburg-Vorpommern, 3, 39–49, 2003.

Jaekel, O.: Neue Beiträge zur Tektonik des Rügener Steilufers, Zeitschrift der Deutschen Geologischen Gesellschaft, 69, 81–176, 1917.

Kahlke, R.-D.: Verbreitung, Aufbau und Genese der I2-Ablagerungen der Halbinsel Jasmund (Rügen), thesis, Universität Greifswald, Greifswald, Germany, 108 pp., 1982.

Keilhack, K.: Die Lagerungsverhältnisse des Diluviums in der Steilküste von Jasmund auf Rügen, Jahrbuch der Preußischen Geologischen Landesanstalt, 33, 114–158, 1914.

Kenzler, M. and Hüneke, H.: Sea cliff at Glowe: Stratigraphy and absolute age chronology of the Jasmund Pleistocene sedimentary record, DEUQUA Spec. Pub., this volume, 2019.

Kenzler, M., Tsukamoto, S., Meng, S., Frechen, M., and Hüneke, H.: New age constraints from the SW Baltic Sea area–implications for Scandinavian Ice Sheet dynamics and palaeoenvironmental conditions during MIS 3 and early MIS 2, Boreas, 46, 34–52, https://doi.org/10.1111/bor.12206, 2017.

Ludwig, A. O.: Zwei markante Stauchmoränen: Peski/Belorussland und Jasmund, Ostseeinsel Rügen/Nordostdeutschland – Gemeinsame Merkmale und Unterschiede, E&G Quaternary Sci. J., 60, 31, https://doi.org/10.3285/eg.60.4.06, 2011.

Mehlhorn, P.: Makro- und mikrostrukturelle Analyse der Pleistozän-Sedimente am Streifen 4 von Jasmund (Rügen), BSc thesis, University of Greifswald, Greifswald, Germany, 64 pp., 2016.

Phillips, E. R., van der Meer, J. J. M., and Ferguson, A.: A new "microstructural mapping" methodology for the identification, analysis and interpretation of polyphaser deformation within subglacial sediments, Quaternary Sci. Rev., 30, 2570–2596, https://doi.org/10.1016/j.quascirev.2011.04.024, 2011.

Phillips, E. R., Spagnolo, M., Pilmer, A. C. J., Rea, B. R., Piotrowski, J. A., Ely, J. C., and Carr, S.: Progressive ductile shearing during till accretion within the deforming bed of a palaeo-ice stream, Quaternary Sci. Rev., 193, 1–23, https://doi.org/10.1016/j.quascirev.2018.06.009, 2018.

Steinich, G.: Endogene Tektonik in den Unter-Maastricht-Vorkommen auf Jasmund (Rügen), Geol. Beih. 20, 1–207, 1972.

van der Meer, J. J. M.: Microscopic Evidence of Subglacial Deformation, Quaternary Sci. Rev., 12, 553–587, https://doi.org/10.1016/0277-3791(93)90069-X, 1993.

Winkler, L.: Mikrostrukturelle Analyse des glazitektonisch mehrphasig deformierten M2-Tills vom Streifen 4 auf Jasmund (Rügen), BSc thesis, University of Greifswald, Greifswald, Germany, 54 pp., 2016.

DEUQUA Spec. Pub., 2, 43–50, 2019
https://doi.org/10.5194/deuquasp-2-43-2019

Open Access DEUQUA Special Publications

Sea cliff at Glowe: stratigraphy and absolute age chronology of the Jasmund Pleistocene sedimentary record

Michael Kenzler and Heiko Hüneke

Institute of Geography and Geology, University of Greifswald, Friedrich-Ludwig-Jahn-Str. 17a, Greifswald, 17487, Germany

Correspondence: Michael Kenzler (kenzlerm@uni-greifswald.de)

Relevant dates: Published: 15 August 2019

How to cite: Kenzler, M. and Hüneke, H.: Sea cliff at Glowe: stratigraphy and absolute age chronology of the Jasmund Pleistocene sedimentary record, DEUQUA Spec. Pub., 2, 43–50, https://doi.org/10.5194/deuquasp-2-43-2019, 2019.

Abstract: Four remarkable Pleistocene cliff outcrops scattered across the peninsula of Jasmund exhibit the dynamics of the Scandinavian Ice Sheet during the Weichselian glaciation in this area. The investigated sites display up to 30 m thick sequences of glacial tills with intercalated (glaci)fluvial to (glaci)lacustrine sediments. Based on detailed lithofacies analyses and a physical age chronology, we trace the reconstruction of the depositional sequences and their corresponding stratigraphic position within the Weichselian record.

1 The Weichselian glaciation in the southwestern Baltic Sea area

This article gives an overview of the current state of research on the peninsula of Jasmund, with special consideration given to the stratigraphy of the Pleistocene deposits. The Weichselian glaciation (115–12 ka) is characterised by alternating phases of warmer (interstadial) and colder (stadial) climate conditions. The response of large ice masses to this climatic fluctuation is one fundamental question that had to be answered to shape robust climate models. One of the most significant inland ice bodies in the Northern Hemisphere during the Quaternary glaciations was the Scandinavian Ice Sheet (SIS; Fig. 1a) as part of the Eurasian ice sheet. The southern maximum extent of the SIS during the Weichselian glaciation reached from Denmark across northern Germany through Poland and the Ukraine in the southeast of Europe. Repeated advances and retreats of the ice front shaped the landscape of much of northern and eastern Europe. However, after more than 130 years of Quaternary research, the timing and even the number of SIS advances into the southwestern Baltic Sea area during the last glaciation are still unclear and far away from being solved (Hughes et al., 2016). Hence, the dynamics of the SIS are for most of the last glaciation only fragmentarily understood, particularly for the early to mid-Weichselian period.

The Pleistocene cliff outcrops around the peninsula of Jasmund (SW Baltic Sea; Figs. 1b, 2a) constitute a significant geological archive of the complex interaction between the dynamics of a large-scale ice sheet and climate fluctuations. The glacigenic and related deposits in the area of Jasmund have been studied since the end of the 19th century (see Kenzler et al., 2010, and references therein). In addition to the depositional environment and the stratigraphic position of the distinct Pleistocene layers (Fig. 2b), the formation of the glacitectonic complex of Jasmund as a whole has been another focus of research (Gehrmann, 2018; Gehrmann and Harding, 2018; Gehrmann et al., 2019).

For the reconstruction of the Weichselian SIS oscillations and their response to climate signals, an accurate and absolute age constraint of the different ice extents is required. Until now, the distribution of available age data for the south-

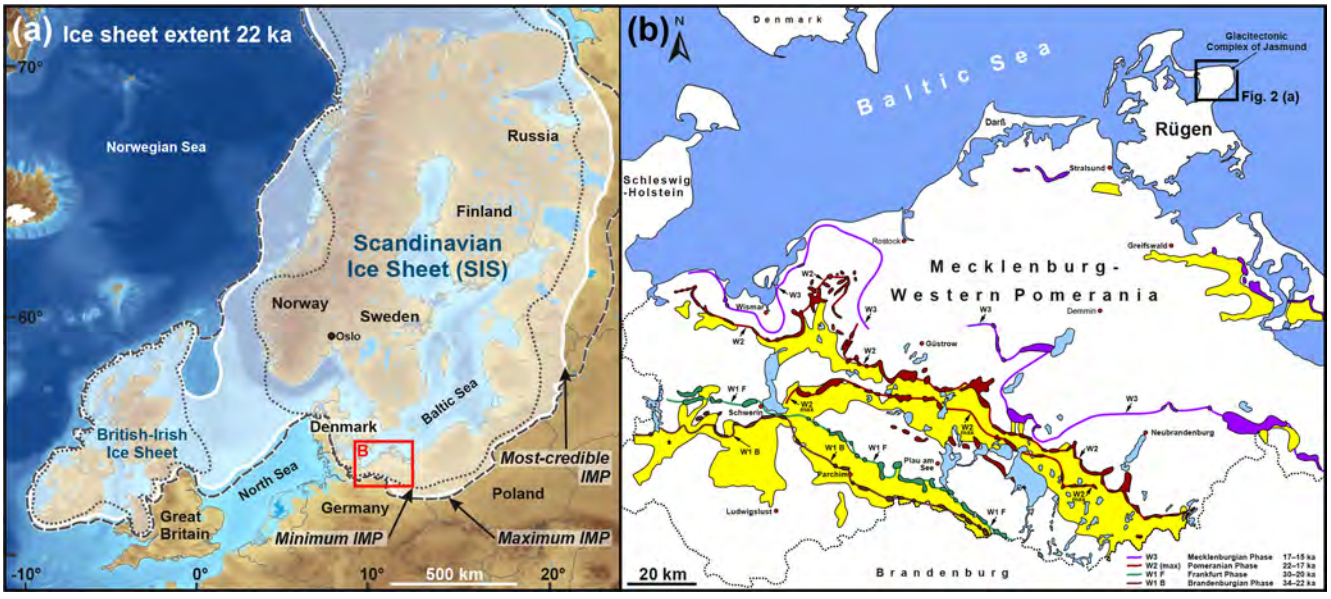

Figure 1. **(a)** Palaeogeographical map of NW Europe showing the ice extent at 22 ka (ice marginal position – IMP; modified after Hughes et al., 2016); **(b)** overview map of northeastern Germany with the suggested main Weichselian ice marginal positions (W1–W3), including age classification (based on Litt et al., 2007; Heine et al., 2009; Lüthgens et al., 2011; Börner et al., 2014; Rinterknecht et al., 2014; Toucanne et al., 2015; Hardt et al., 2016; Hardt and Böse, 2016) and associated sandur deposits (yellow area) (based on Landesamt für Umwelt, Naturschutz und Geologie Mecklenburg-Vorpommern, 2010, and Schulz, 2011).

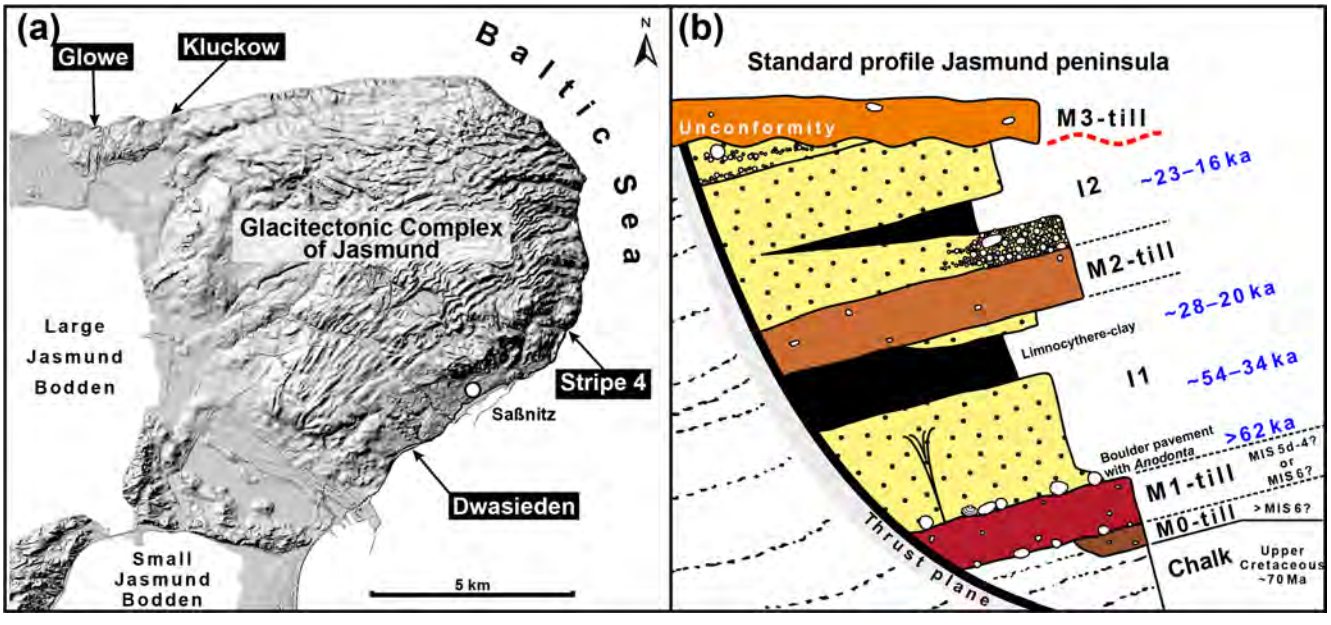

Figure 2. **(a)** Digital elevation model of Jasmund with cliff sections mentioned in the text; the hillshade relief with 10-fold exaggeration shows the glacitectonically structured morphology of the peninsula (based on @GeoBasis-DE/M-V 2015, processed by Jörg Hartleib). **(b)** Generalised stratigraphical profile of a glacitectonically rafted imbricate structure at Jasmund comprising Upper Cretaceous chalk and paraconformably overlying Pleistocene deposits including the disconformably overlying Late Weichselian till complex M3 (modified after Kenzler et al., 2017); age estimations in blue based on the luminescence results shown in Figs. 4 and 3 (based on Kenzler et al., 2015, 2017; Pisarska-Jamroży et al., 2018).

western Baltic Sea area has mainly focused on Denmark and Sweden (Hughes et al., 2016). For northern Germany, only sparse ages have been published, some of which contradict each other, which may be caused by the different dating techniques used in the studies. Recently, optically stimulated luminescence (OSL), infrared stimulated luminescence (IRSL), and terrestrial cosmogenic nuclide (TCN) dating methods have opened up new avenues to refine the chronology of single ice advances of the SIS during MIS 3 and 2 (e.g. Rinterknecht et al., 2014; Hardt et al., 2016; Kenzler et al., 2017).

2 Luminescence dating approach and its application to the peninsula of Jasmund

The main dating techniques for age constraint of the Weichselian ice marginal positions (IMPs) and associated deposits in NE Germany are surface exposure dating (SED; Heine et al., 2009; Rinterknecht et al., 2014), luminescence dating (e.g. Kenzler, 2017; Hardt, 2017), and radiocarbon dating (Steinich, 1992). In Mecklenburg-Western Pomerania, only a few of the SED-dated erratic boulders are related to Weichselian IMPs (e.g. Rinterknecht et al., 2014), and most of the radiocarbon ages are Late Glacial to Holocene (e.g. Lampe et al., 2016). Very few radiocarbon ages are available for the 50–20 ka timeframe (Steinich, 1992; Hughes et al., 2016), which is due to the very limited occurrence of in situ organic material in Weichselian deposits. The majority of the radiocarbon ages are related to the deglaciation period of the Late Weichselian, so they postdate an ice advance (minimum age estimations). Likewise, the SED of erratic boulders give the time of land stabilisation and thus yield a minimum age for an ice advance (Lüthgens et al., 2011). In contrast, with luminescence dating of (glaci)fluvial, (glaci)lacustrine, and aeolian sediments deposited in front of an active ice sheet, a direct age determination of the ice advance is possible. Several recent studies have clearly shown that luminescence dating can solve issues of the timing of the individual ice advances approaching NE Germany (e.g. Lüthgens et al., 2011; Kenzler et al., 2015, 2017; Hardt et al., 2016; Pisarska-Jamroży et al., 2018). These new luminescence age data raise the question of whether the traditional stratigraphy and interpretation of the main Weichselian ice advances of NE Germany have to be modified (Hardt, 2017; Kenzler, 2017).

Luminescence dating of quartz mineral grains (OSL) is well-suited to date silty to sandy sequences deposited in a sandur setting associated with ice marginal positions of Weichselian ice advances (e.g. Lüthgens et al., 2011; Hardt et al., 2016; Hardt, 2017). Furthermore, interstadial deposits of Weichselian age intercalated between till units have yielded reliable luminescence ages (Kenzler et al., 2015, 2017, 2018; Pisarska-Jamroży et al., 2018). Luminescence dating is based on the principle that the energy of the ionising radiation flux from the surrounding sediments (U / Th series nuclides, K and Rb – alpha, beta, and gamma radiation) and of cosmic radiation is stored within the crystal lattice of quartz and feldspar minerals, due to impurities and lattice defects (Aitken, 1985). This creates an accumulation of energy with time. The signal is zeroed (bleached) when exposed to sunlight, which allows us to date the last transportation event (exposure to sunlight). Several successful dating protocols have been obtained with quartz (e.g. Murray and Wintle, 2000) and K-rich feldspar mineral grains (e.g. Thiel et al., 2011) as well as quality criteria (Wintle and Murray, 2006) and statistical approaches (e.g. Galbraith and Roberts, 2012), which has secured the reliability of luminescence age data.

The Jasmund ages presented here are based mainly on OSL measurements of quartz mineral grains since a standard issue for (glaci)fluvial sediments deposited in a sandur setting is partial bleaching of the palaeo-luminescence signal, which results in an overestimation of the true burial age (Fuchs and Owen, 2008). A reason for this heterogeneous bleaching could be a short transport distance and therefore an insufficient exposure time for the palaeo-luminescence signal in the crystal lattice to be brought to zero. Since only well-bleached quartz grains are useful for age calculation, the insufficiently bleached grains need to be separated out. This can be achieved by reducing the grain number on a single aliquot up to one single grain (single grain measurement; Duller, 2008). By analysing the equivalent dose distribution, the heterogeneously bleached quartz grain populations can be identified and discarded.

An essential part of luminescence dating is a detailed and careful sedimentological logging and facies analysis, as a reliable base for the reconstruction of the depositional environments. This in turn enables the selection of the most suitable horizons (depositional environments) for luminescence sampling, to reduce potential difficulties such as partial bleaching as much as possible. The main sedimentological approaches are classification and interpretation of the lithofacies based on primary deposition and erosional features (e.g. composition, structure, texture, bedding, lamination, and bed boundaries).

3 The Weichselian glaciation in the southwestern Baltic Sea area

The general results of the four investigated cliff outcrops are summarised in Fig. 3. The geological succession at Jasmund peninsula includes Cretaceous bedrock (limestone), paraconformably overlain by Pleistocene deposits. Up to four till complexes (from bottom to top: M0, M1, M2, and M3) can be distinguished, which are separated from each other (with the exception of M0–M1) by mostly clayey to gravely units (I1 and I2). Age estimations of the lowermost till units M0 and M1 range from Elsterian to Saalian to mid-Weichselian (e.g. Steinich, 1992; Müller and Obst, 2006; Niedermeyer et al., 2010; Fig. 2b). Information about the early and mid-

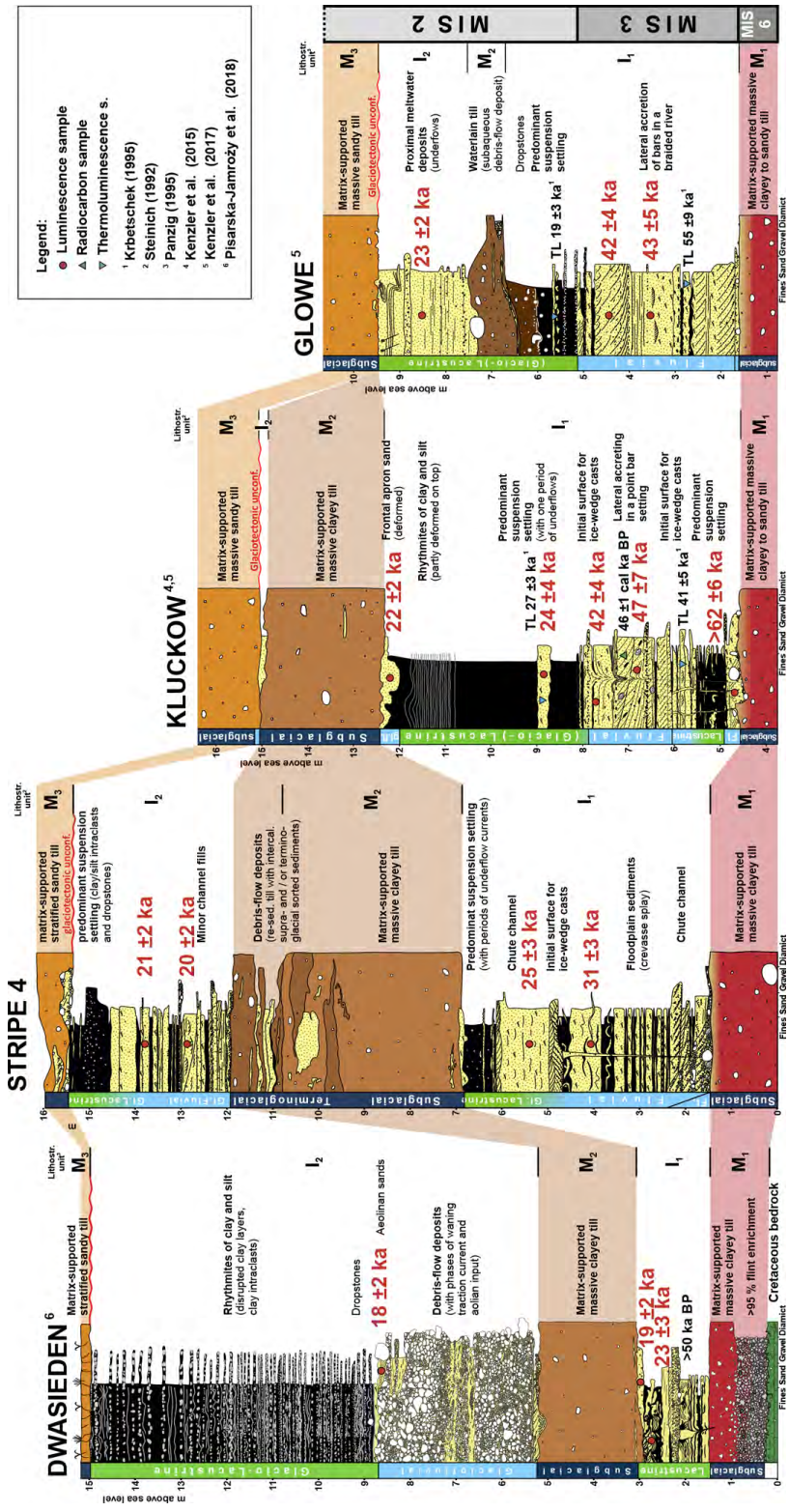

Figure 3. Summarised lithological profiles of four cliff outcrops around the peninsula of Jasmund. The correlation between the deposits of the outcrops was made by lithofacies analyses, physical age chronology, and fine-gravel analyses. Separated by till sheets, two distinct well-sorted sediment complexes (I1 and I2) of MIS 3 and MIS 2 age, respectively, are preserved in the outcrops. The lower one (I1) can be correlated across the whole of Jasmund, whereas the upper one (I2) is tailing out towards the northwest. The stratigraphical log from Glowe (profile metres 100–110, Fig. 5a; modified after Kenzler et al., 2017) indicates lithostratigraphical units, depositional environments, and OSL (red dots) and thermoluminescence (TL) ages (blue triangles). The lithological log of Kluckow (Fig. 3b) is based on Kenzler et al. (2017), whereas the log of Dwasieden is modified from Pisarska-Jamroży et al. (2018). Facies codes after Benn and Evans (2010).

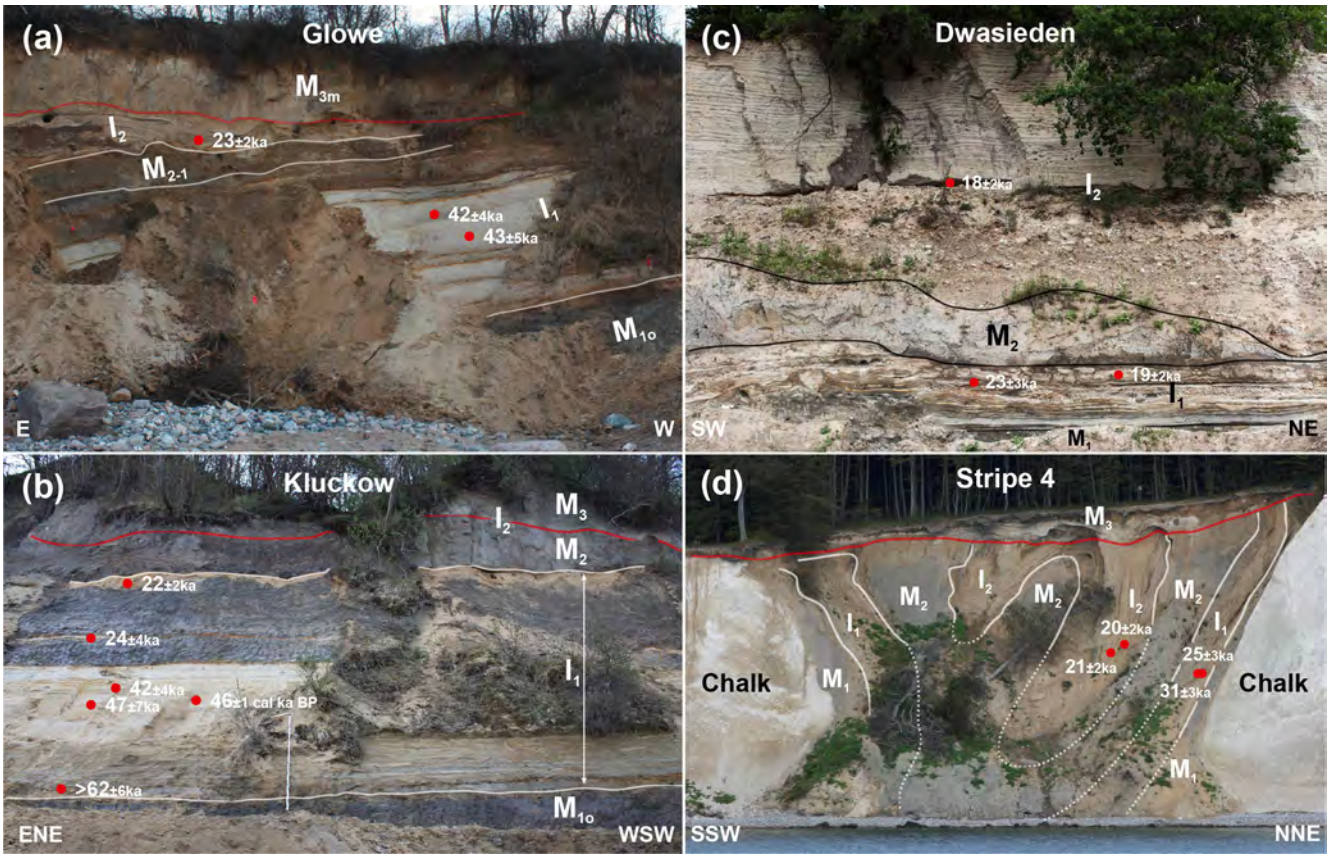

Figure 4. Photographs of **(a)** Glowe (profile metres 95–110, Figs. 2a and 5a; modified after Kenzler et al., 2017) and **(b)** Kluckow cliff sections (profile metres 50–70, Figs. 2a and 5b; modified after Kenzler et al., 2017). **(c)** Cliff section of Dwasieden with thick layers of glacifluvial and glacilacustrine units at the top (Figs. 2a and 3). **(d)** Pleistocene Stripe 4 sandwiched between two chalk complexes (Figs. 2a and 3). The filled dots highlight the sample position for luminescence dating including their age. The semi-transparent red lines represent the base M3 glacitectonic unconformity.

Weichselian time are very rare because sediments of this period are absent/eroded or were never deposited. The existence of an advance of the SIS between the end of the Eemian (115 ka) and the beginning of MIS 3 (57 ka) is unlikely but not impossible. The oldest luminescence ages from the base of the intercalated I1 unit (Figs. 2b, 3, 4, and 5) indicate a deposition of the underlying till (M1) older than 62 ± 6 ka. The landscape during the early MIS 3 was dominated by small lakes and arctic to subarctic climate conditions, including a change to moderate summers and cool winters. The deposition during the subsequent period (roughly between 54 and 34 ka; Fig. 2b) occurred in a fluvial environment (meandering/braided river systems) embedded in a steppe-like landscape. Palaeontological evidence indicates warmer interstadial climate conditions. Preserved ice wedge casts signal colder temperatures at the end of MIS 3. A correlation with the Klintholm advance documented in Denmark (Houmark-Nielsen, 2010) can be assumed (Kenzler et al., 2017). Indications for the existence of a MIS 3 ice advance reaching Jasmund are not available. The transition of MIS 3 and 2 was characterised by the deposition in a glacilacustrine basin, which can be formed due to the blocking effect of the Kattegat advance of the SIS between 29 and 26 ka (Houmark-Nielsen, 2010; Kenzler et al., 2017). The first dated Weichselian ice advance, which deposited the M2 till complex, occurred around 23 ± 2 ka (Brandenburgian Phase; Fig. 1a). The subsequent ice oscillations during the Pomeranian and Mecklenburgian phases took place between 20 and 15 ka (Toucanne et al., 2015; Kenzler et al., 2017; Hardt and Böse, 2016).

4 The Cretaceous–Pleistocene sequence of Glowe

The first stop of the day will lead us to the steep coast of Glowe (Fig. 1a). This cliff section illustrates the geological structure of the glacitectonic complex of Jasmund, as well as the Cretaceous–Pleistocene succession in this area (Figs. 2b and 3). Along the more than 300 m long coastal section, a chalk anticline deposit and a paraconformably overlying Pleistocene deposit crop out. A main feature is the very im-

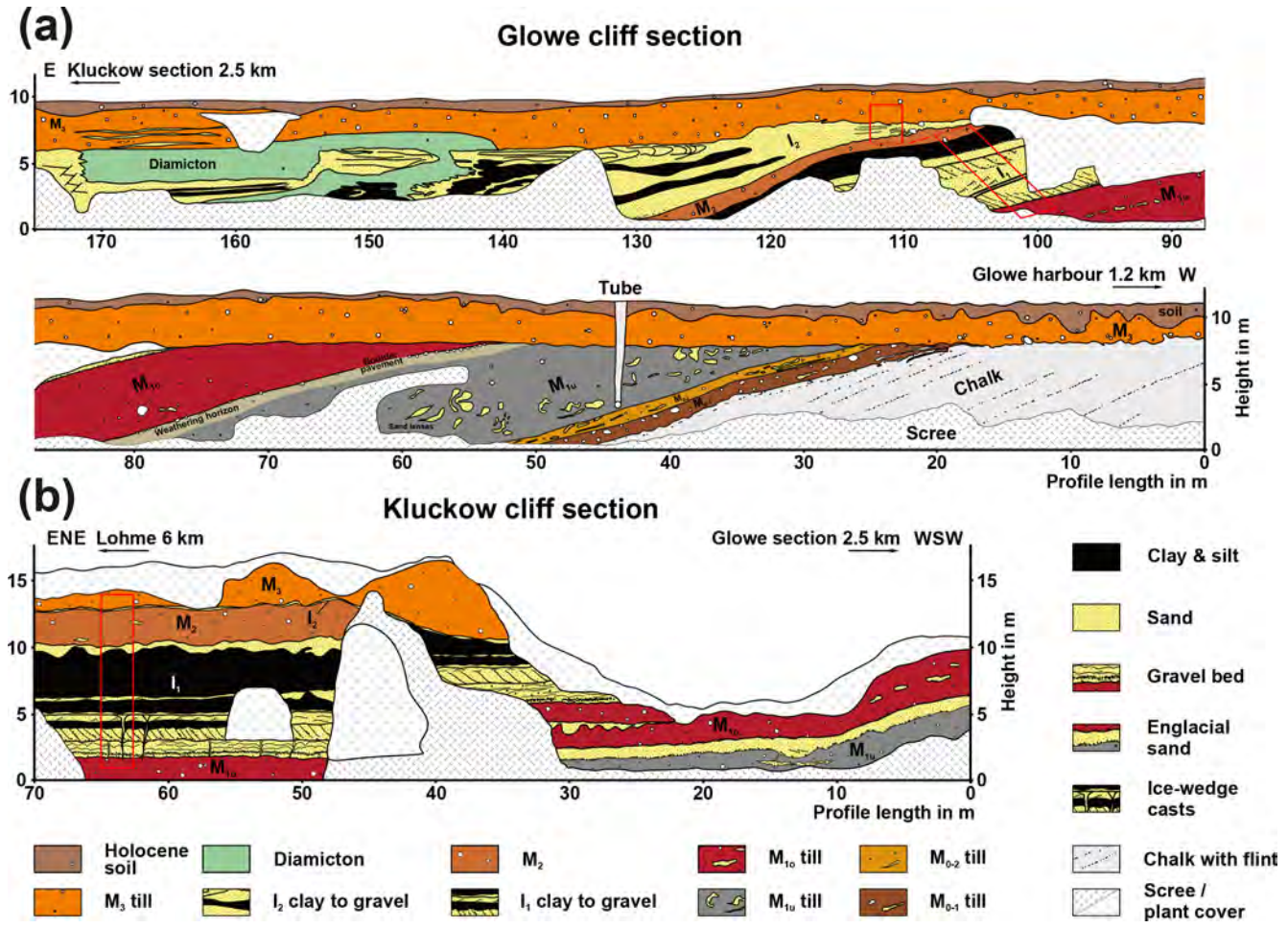

Figure 5. Sketches of the **(a)** Glowe and **(b)** Kluckow cliff sections (Fig. 2a for cliff locations). The sketches show the outcrop situation during the years 2010 and 2011, respectively (modified after Kenzler et al., 2017). The red boxes display the locations of the lithofacies analyses (Fig. 3).

pressive late Weichselian glacitectonic unconformity, visible in the upper part of the cliff (Fig. 4a). The Pleistocene sequence includes at least four diamictic units, which are correlated to advances of the SIS during the Elsterian, Saalian, and Weichselian glaciations (Panzig, 1995; Niedermeyer et al., 2010; Kenzler et al., 2017). The cliff also exhibits two horizons of well-sorted siliciclastic deposits intercalated between diamictic units (I1 and I2; Figs. 3, 4a, and 5). The depositional environment of about the last 50 kyr has been reconstructed with luminescence ages and sedimentological interpretations. Ice-free conditions dominated the study area during MIS 3 and early MIS 2. The deposition occurred in braided river systems under, at least partly, interstadial climate conditions. At the transition from MIS 3 to MIS 2, a cooling trend occurred, leading to the formation of a glaciolacustrine basin at the beginning of MIS 2. This cooling correlates with the Kattegat advance of the SIS known from Denmark (Houmark-Nielsen, 2010). The first advance of the SIS reached the area of Glowe during the Last Glacial Maximum (23 ± 2 ka; Kenzler et al., 2017). Variations in the meltwater supply from the nearby ice front dominated the deposition during this time, including debris flows (M2), which entered the ice-marginal basin. After the subsequent formation of the glacitectonic complex of Jasmund during the Pomeranian advance (ca. 20–18 ka), the glacitectonic unconformity was created together with the subsequent deposition of the youngest diamictic unit (M3).

In addition, the Pleistocene deposits outcropping at the cliffs of Kluckow, Stripe 4, and Dwasieden (Figs. 2a and 4) contain valuable sedimentological and stratigraphical information about the Weichselian glaciation (Fig. 3) that has improved our knowledge about the dynamics of the SIS in this area.

Data availability. All data relevant for this contribution are presented within the article itself or the publications cited.

Author contributions. MK and HH carried out fieldwork. MK processed, measured, and analysed the luminescence samples, as well as developed the illustrations. Both authors prepared the paper.

Competing interests. The authors declare that they have no conflict of interest.

Acknowledgements. This research was funded by the German Research Foundation (DFG projects HU 804/6-1, FR 877/16-1). Marie-Elaine van Egmond (Halle) is thanked for her professional English proofreading of a previous version of the paper. We are grateful to reviewer Kay Krienke (Llur Flintbek) for his valuable comments and feedback. We acknowledge support for the article processing charge from the DFG (no. 393148499) and the Open Access Publication Fund of the University of Greifswald.

Financial support. This research has been supported by the DFG (German Research Foundation, grant no. 393148499 and projects HU 804/6-1, FR 877/16-1) and the Open Access Publication Fund of the University of Greifswald.

References

Aitken, M. J.: Thermoluminescence dating, Academic Press, London, UK, 1985.

Benn, D. I. and Evans, D. J. A.: Glaciers and Glaciations, Hodder Education, London, UK, 802 pp., 2010.

Börner, A., Rinterknecht, V., Bourelès, D., and Braucher, R.: First results from surface exposure dating of glacial boulders in ice marginal belts of Mecklenburg-Western Pomerania (NE-Germany) using in-situ cosmogenic Beryllium-10, Journal for the Geological Science, 41, 123–143, 2014.

Duller, G. A. T.: Single-grain optical dating of Quaternary sediments: why aliquot size matters in luminescence dating, Boreas, 37, 589–612, 2008.

Fuchs, M. and Owen, L. A.: Luminescence dating of glacial and associated sediments: review, recommendations and future directions, Boreas, 37, 636–659, 2008.

Galbraith, R. F. and Roberts, R. G.: Statistical aspects of equivalent dose and error calculation and display in OSL dating: an overview and some recommendations, Quat. Geochronol., 11, 1–27, 2012.

Gehrmann, A.: The multi-stage structural development of the Upper Weichselian Jasmund Glacitectonic Complex (Rügen, NE Germany), PhD thesis, University Greifswald, Greifswald, Germany, 278 pp., 2018.

Gehrmann, A. and Harding, C.: Geomorphological Mapping and Spatial Analyses of an Upper Weichselian Glacitectonic Complex based on LiDAR Data, Jasmund Peninsula (NE Rügen), Germany, Geosciences, 8, 208, https://doi.org/10.3390/geosciences8060208, 2018.

Gehrmann, A., Meschede, M., Hüneke, H., and Schack Pedersen, S. A.: Sea cliff at Kieler Ufer (Pleistocene stripes 11–16) – Large-scale architecture and kinematics of the Jasmund Glacitectonic Complex, DEUQUA Spec. Pub., this volume, 2019.

Hardt, J.: Weichselian phases and ice dynamics of the Scandinavian Ice Sheet in northeast Germany, PhD thesis, FU Berlin, Berlin, Germany, 137 pp., 2017.

Hardt, J. and Böse, M.: The timing of the Weichselian Pomeranian ice marginal position south of the Baltic Sea: A critical review of morphological and geochronological results, Quatern. Int., 478, 51–58, 2016.

Hardt, J., Lüthgens, C., Hebenstreit, R., and Böse, M.: Geochronological (OSL) and geomorphological investigations at the presumed Frankfurt ice marginal position in northeast Germany, Quaternary Sci. Rev., 154, 85–99, 2016.

Heine, K., Reuther, A., Thieke, H. U., Schulz, R., Schlaak, N., and Kubik, P.: Timing of Weichselian ice marginal positions in Brandenburg (northeastern Germany) using cosmogenic in situ ^{10}Be, Z. Geomorphol., 53, 433–454, 2009.

Houmark-Nielsen, M.: Extent, age and dynamics of Marine Isotope Stage 3 glaciation in the southwestern Baltic Basin, Boreas, 39, 343–359, 2010.

Hughes, A. L. C., Gyllencreutz, R., Lohne, Ø. S., Mangerud, J., and Svendsen, J. I.: The last Eurasian ice sheet – a chronological database and time-slice reconstruction, DATED-1, Boreas, 45, 1–45, 2016.

Kenzler, M.: Ice-sheet dynamics and climate fluctuations during the Weichselian glaciation along the southwestern Baltic Sea coast, PhD thesis, University Greifswald, Greifswald, Germany, 169 pp., 2017.

Kenzler, M., Obst, K., Hüneke, H., and Schütze, K.: Glazitektonische Deformation der kretazischen und pleistozänen Sedimente an der Steilküste von Jasmund nördlich des Königsstuhls (Rügen), Brandenburg. geowiss. Beitr., 17, 107–122, 2010.

Kenzler, M., Tsukamoto, S., Meng, S., Thiel, C., Frechen, M., and Hüneke, H.: Luminescence dating of Weichselian interstadial sediments from the German Baltic Sea coast, Quat. Geochronol., 30, 215–256, 2015.

Kenzler, M., Tsukamoto, S., Meng, S., Frechen, M., and Hüneke, H.: New age constraints from the SW Baltic Sea area – implications for Scandinavian Ice Sheet dynamics and palaeoenvironmental conditions during MIS 3 and early MIS 2, Boreas, 46, 34–52, 2017.

Kenzler, M., Rother, H., Hüneke, H., Frenzel, P., Strahl, J., Tsukamoto, S., Li, Y., Meng, S., Gallas, J., and Frechen, M.: A multi-proxy palaeoenvironmental and geochronological reconstruction of the Saalian-Eemian-Weichselian succession at Klein Klütz Höved, NE Germany, Boreas, 47, 114–136, 2018.

Krbetschek, M. R.: Lumineszenz-Datierungen quartärer Sedimente Mittel-, Ost- und Nordostdeutschlands. PhD thesis, TU Bergakademie Freiberg, Freiberg, Germany, 122 pp., 1995.

Lampe, R., Janke, W., Schult, M., Meng, S., and Lampe, M.: Multiproxy-Untersuchungen zur Paläoökologie und -hydrologie eines spätglazial- bis frühholozänen Flachsees im nordostdeutschen Küstengebiet (Glowe-Paläosee/Insel Rügen), E&G Quaternary Sci. J., 65, 41–75, https://doi.org/10.3285/eg.65.1.03, 2016.

Landesamt für Umwelt, Naturschutz und Geologie: Geologische Karte von Mecklenburg-Vorpommern – Übersichtskarte 1 : 500 000 – Oberfläche, Güstrow, Germany, 2010.

Litt, T., Behre, K.-E., Meyer, K.-D., Stephan, H.-J., and Wansa, S.: Stratigraphische Begriffe für das Quartär des nord-

deutschen Vereisungsgebietes, E&G Quaternary Sci. J., 56, 7–65, https://doi.org/10.3285/eg.56.1-2.02, 2007.

Lüthgens, C., Böse, M., and Preusser, F.: Age of the Pomeranian ice-marginal position in northeastern Germany determined by Optically Stimulated Luminescence (OSL) dating of glaciofluvial sediments, Boreas, 40, 598–615, 2011.

Müller, U. and Obst, K.: Lithostratigraphy and bedding of the Pleistocene deposits in the area of Lohme (Jasmund/Rügen), Journal for the Geological Science, 34, 39–54, 2006.

Murray, A. S. and Wintle, A. G.: Luminescence dating of quartz using an improved single-aliquot regenerative-dose protocol, Radiat. Meas., 32, 57–73, 2000.

Niedermeyer, R.-O., Kanter, L., Kenzler, M., Panzig, W.-A., Krienke, K., Ludwig, A.-O., Schnick, H. H., and Schütze, K.: Rügen Island (I) – Facies, stratigraphy, structural architecture and geological hazard potential of Pleistocene deposits of the Jasmund cliff coast, in: Eiszeitlandschaften in Mecklenburg-Vorpommern, edited by: Lampe, R. and Lorenz, S., Geozon Science Media, Greifswald, Germany, 50–71, 2010.

Panzig, W.-A.: Zum Pleistozän von Rügen, Terra Nostra, 6, 177–200, 1995.

Pisarska-Jamroży, M., Belzyt, S., Börner, A., Hoffmann, G., Hüneke, H., Kenzler, M., Obst, K., Rother, H., and van Loon, A. J.: Evidence for glacio-isostatically induced crustal faulting in front of an advancing land-ice mass (Rügen Island, NE Germany), Tectonophysics, 745, 338–348, 2018.

Rinterknecht, V., Börner, A., Bourlès, D., and Braucher, R.: Cosmogenic ^{10}Be dating of ice sheet marginal belts in Mecklenburg-Vorpommern, Western Pomerania (northeast Germany), Quat. Geochronol., 19, 42–51, 2014.

Schulz, W.: Streifzüge durch die Geologie des Landes Mecklenburg-Vorpommern, Schwerin, Germany, 216 pp., 2011.

Steinich, G.: Die stratigraphische Einordnung der Rügen-Warmzeit, Journal for the Geological Sciences, 20, 125–154, 1992.

Thiel, C., Buylaert, J.-P., Murray, A. S., Terhorst, B., Hofer, I., Tsukamoto, S., and Frechen, M.: Luminescence dating of the Stratzing loess profile (Austria) – testing the potential of an elevated temperature post-IR IRSL protocol, Quatern. Int., 234, 23–31, 2011.

Toucanne, S., Soulet, G., Freslon, N., Silva Jacinto, R., Dennielou, B., Zaragosi, S., Eynaud, F., Bourillet, J.-F., and Bayon, G.: Millennial-scale fluctuations of the European Ice Sheet at the end of the glacial, and their potential impact on global climate, Quaternary Sci. Rev., 123, 113–133, 2015.

Wintle, A. G. and Murray, A. S.: A review of quartz optically stimulated luminescence characteristics and their relevance in single-aliquot regeneration dating protocols, Radiat. Meas., 41, 369–391, 2006.

DEUQUA Spec. Pub., 2, 51–60, 2019
https://doi.org/10.5194/deuquasp-2-51-2019

DEUQUA Special Publications

Micromorphology and clast microfabrics of subglacial traction tills at the sea cliff Dwasieden: evidence of polyphase syn- and post-depositional deformation

Johannes Brumme[1], **Heiko Hüneke**[1], **and Emrys Phillips**[2]

[1]Institut für Geographie und Geologie, Universität Greifswald, Greifswald 17487, Germany
[2]British Geological Survey, The Lyell Centre, Research Avenue South, Edinburgh, EH14 4AP, UK

Correspondence: Heiko Hüneke (hueneke@uni-greifswald.de)

Relevant dates: Published: 15 August 2019

How to cite: Brumme, J., Hüneke, H., and Phillips, E.: Micromorphology and clast microfabrics of subglacial traction tills at the sea cliff Dwasieden: evidence of polyphase syn- and post-depositional deformation, DEUQUA Spec. Pub., 2, 51–60, https://doi.org/10.5194/deuquasp-2-51-2019, 2019.

Abstract: A detailed thin-section-based micromorphological and microstructural study of the glacial diamicts exposed at the sea cliff of Dwasieden (M1, M2, M2) has revealed that all units can be related, in their entirety or in several parts, to subglacial conditions during the repeated readvance of the Scandinavian Ice Sheet. These readvances are characterised by polyphase deformation of the diamicts resulting in the development of ductile and brittle structures and localised water-escape structures. Subsequent alteration under periglacial conditions has been documented for the chalk and till units M1 and M2.

1 Introduction

In this contribution, the Pleistocene record exposed at the sea cliff of Dwasieden near Sassnitz (54°30′0.44″ N, 13°36′46.09″ E) is explored, focusing on the origin of the glacial diamicts. A detailed micromorphology study (Brumme, 2015) has allowed the unravelling of the complex depositional and deformation histories recorded by this sedimentary sequence with respect to ice flow across Jasmund. The analysis of the microstructures (Phillips et al., 2011; Brumme, 2015) observed in thin sections of the diamictons has revealed a chronology of deformational events which can be interpreted in the context of syn-depositional till-forming processes and post-depositional modification (e.g. permafrost, glacitectonic imbrication). More broadly, the geometry and cross-cutting relationships of the depositional units and glacitectonic (micro-)structures documented at this locality and other outcrops have enabled the construction of a tectono-stratigraphic model for the evolution of the Jasmund area during the Weichselian.

The cliff section at Dwasieden exposes the late Cretaceous (Maastrichtian) to late Pleistocene (Weichselian) record forming part of the Jasmund Glacitectonic Complex (Gehrmann et al., 2019). The site is located in a proximal position within the southern structural sub-complex (Gehrmann and Harding, 2018; Gehrmann, 2018) and is oriented parallel to strike of this imbricate thrust stack. The exposed succession largely occurs within a single imbricate thrust slice and shows sub-horizontal stratification. However, at the south-western end of the cliff, the steeply dipping chalk of the next, more proximal thrust sheet can be clearly seen thrust onto the much younger Pleistocene sediments. Previous work on the stratigraphy, sedimentary environmental conditions and glacitectonic deformation observed at Dwasieden has been published by Ludwig (1954/1955), Strahl (1988), Kanter (1989), Panzig (1989), Krienke (2004), Ludwig and

Panzig (2010), Beiche (2014), Brumme (2015), Kielczynski (2016) and Pisarska-Jamroży et al. (2018a, b).

The Pleistocene sedimentary sequence exposed at Dwasieden is representative of Jasmund (see Kenzler et al., 2019). The late Cretaceous chalk observed at the base of the cliff is overlain by three Pleistocene till units (M1, M2 and M3), which are interbedded by gravels, sands and silt-clay rhythmites (units I1 and I2) (Fig. 1). Although most of the lithostratigraphic boundaries are related to hiatuses resulting from breaks in sedimentation and/or erosion, two of these boundaries represent major regional unconformities: (i) an erosional disconformity at the base of the M1 till, which represents a major break of ~ 65 Myr between the latest Cretaceous and onset of Pleistocene sedimentation; and (ii) an angular unconformity at the base of the M3 till, which is formed during the late Weichselian and truncates the thrust sheets of the Jasmund Glacitectonic Complex.

The stratigraphic context aided by optically stimulated luminescence (OSL) dating indicates that the Pleistocene succession was mainly laid down during the Weichselian advance of the Scandinavian Ice Sheet. Pisarska-Jamroży et al. (2018a) concluded that the upper part of the I1 unit must have been deposited between 22.7 ± 1.9 and 19.0 ± 2.3 ka, i.e. shortly before the first late Weichselian ice advance reached the Jasmund peninsula (see Kenzler et al., 2017; Kenzler et al., 2019). Thus, the M2 till that directly overlies the I1 sedimentary record is thought to represent the Brandenburgian advance phase of the ice sheet during the Last Glacial Maximum (LGM). The I2 sedimentary record represents a short phase of ice retreat during post-LGM oscillations of the ice front around 17.9 ± 1.8 ka, which is derived form an OSL age of a thin aeolian sand layer at the base of a glacilacustrine sand-silt-clay rhythmite deposited during the subsequent ice advance, most likely the Pomeranian phase of the Weichselian glaciation (cf. Kenzler et al., 2017). This ice advance is interpreted as having caused the glacitectonic imbrication of Jasmund and subsequently deposition of the M3 till.

2 Micromorphological and microstructural characteristics of the Pleistocene units

Chalk. The uppermost part of the chalk is brecciated, comprising chalk clasts and randomly distributed clusters of flints within a soft chalky matrix. Large erratic boulders of crystalline rocks are found enclosed within the chalk up to 1.5 m below its upper boundary. Furthermore the chalk also contains isolated streaks of diamict material similar to the overlying M1 till. The top of the chalk is highly irregular and locally deformed by complex disharmonic folds and flame-like structures that extend into the overlying M1 diamicton.

Micromorphology. In this section (Fig. 2) the highly brecciated chalk consists of angular to subangular clasts, which locally show diffuse and/or corresponding boundaries, set within a micritic carbonate or chalk-rich siliciclastic matrix containing lithic fragments of magmatic and metamorphic rocks similar to those observed within the overlying till. Large isolated quartz grains were locally observed within both the matrix of the chalk breccia and even within the chalk clasts. Evidence of the flow of water through the breccia and involution of fine-grained material from the overlying M1 till into the altered chalk bedrock is provided by the presence of irregular pockets and veins of clay (cutan) which possess a well-developed unistrial plasmic fabric.

M1. The clast-rich, blue-grey M1 diamicton is approximately 1.5 m thick and contains stringers or lenses of medium sand to fine gravel. Red-brown Fe-stained patches indicate that this diamict has undergone at least some secondary alteration. The base of the till is deformed by flame structures and overturned drag folds, which show a distinct vergence towards the SW. Macrofabric analysis carried out on pebble- and boulder-sized clasts within the M1 till reveals that their *ab* planes typically dip towards the NE. Locally developed clusters of subvertically oriented clasts are also present. Large boulders locally occur on the M1 surface or are partially embedded within the diamicton.

Micromorphology. Thin sections of the M1 diamicton reveal that crushed grains are very common and that deformation structures include turbate structures (ductile) and microfaults (brittle). Water-escape structures are also common and contain fine, micritic carbonate translocated from the underlying chalk into the diamicton.

Detailed mapping of the clast microfabrics defined by the preferential shape alignment of detrital (skeleton) grains (Phillips et al., 2011) in thin sections oriented parallel to the ice flow (i.e. towards the SW) reveals the presence of up to four microfabrics formed in response to subglacial deformation (labelled S1 to S4 on Fig. 3); the dominant fabrics are a planar S1 microfabric which dips at a low to moderate angle towards the NE (i.e. up-ice) and a linear S2 fabric plunging at a moderate angle towards the SW (i.e. down-ice) (Brumme, 2015).

I1. The I1 unit is characterised by a sequence of horizontally interbedded fine sands, silts and clays. The unit also contains an irregular gravel layer (20 m long, 0.2 m thick) comprising clusters of boulder- to pebble-sized clasts. The gravel is occasionally covered by a thin drape of sand. Isolated outsized elongate boulders also occur elsewhere within the I1 unit in some cases orientated almost perpendicular to bedding within the host sediment. Sediments around these outsized clasts are deformed, showing down-warped lamination and lateral truncation.

In addition, soft-sediment deformation structures occur at three levels within the I1 unit. The well-laminated sands and silts display extremely well developed convolute bedding, load casts, ball-and-pillow structures, pseudo-nodules and water-escape structures. An ice-wedge cast extends from the top of the lowermost soft-sediment deformation structure down to the underlying M1 till.

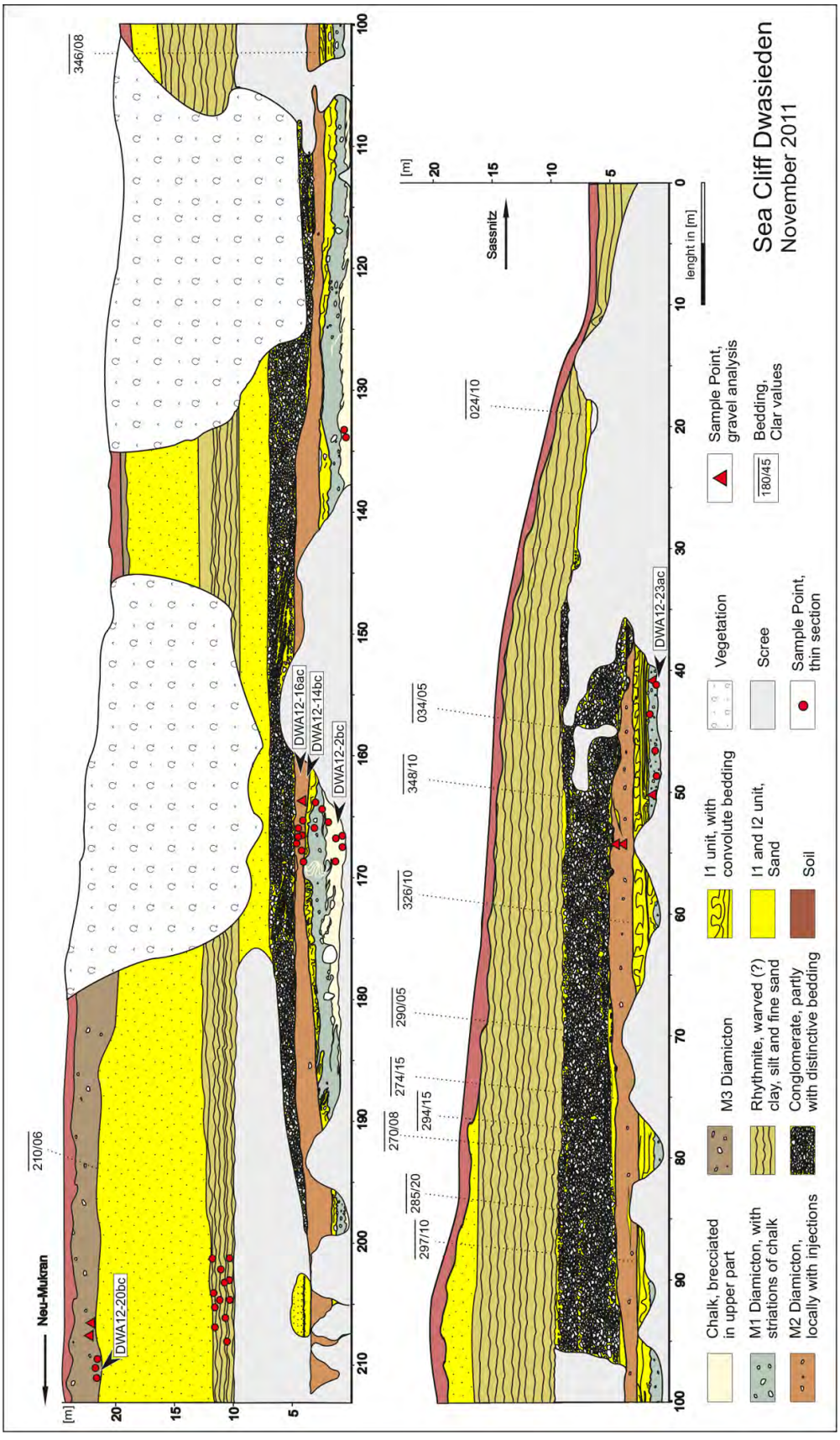

Figure 1. Simplified geological cliff section of Dwasieden southwest of Sassnitz (modified from Brumme, 2015).

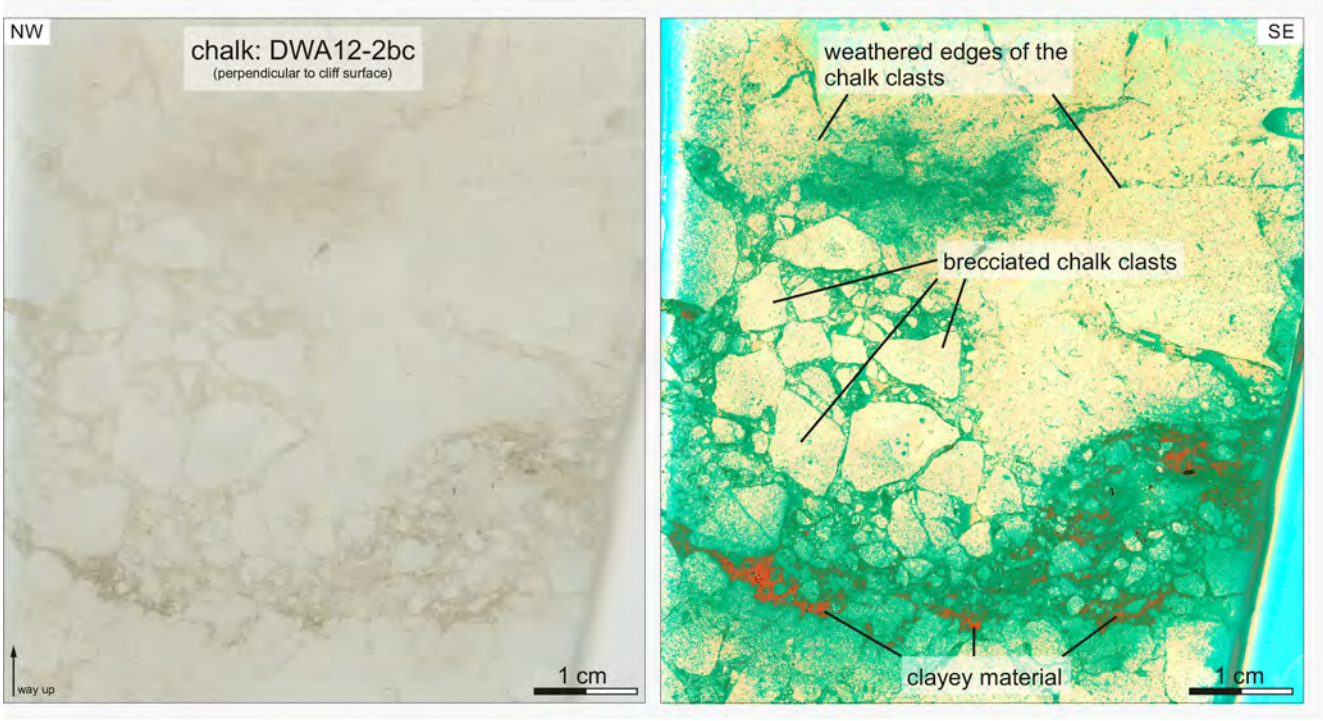

Figure 2. High-resolution scan and false-colour image of thin section DWA12-2bc taken from the brecciated uppermost part of the chalk at the Dwasieden cliff section (from Brumme, 2015).

M2. The M2 till is a massive, clast-poor deposit with sharp erosional lower and upper boundaries. At its base the diamicton includes a highly deformed glacitectonic mélange containing disrupted lenses (intraclasts) of well-bedded sand. These intraclasts are lithologically similar to, and therefore derived from, the underlying I1 unit. Furthermore, there are stringers of sand incorporated into the diamicton as a result of the attenuation of a drag folds which deform at the M1–I1 boundary. These sand stringers are deformed by SW-verging folds and sigmoidal strain markers recording a SE-directed sense of shear.

Micromorphology. In thin sections the clay-rich areas of the till possess a weakly to well-developed omnisepic plasmic fabric. Discrete shear zones which cross-cut the diamicton are marked by unistrial plasmic fabrics, while matrix-rich coating around larger grains show weak skelsepic plasmic fabrics. Microstructural mapping reveals the till possesses at least four microfabrics (S1, S2, S3, S4) (Figs. 4, 5), which is comparable to the underlying M1 diamicton and is therefore once again consistent with subglacial deformation imposed by ice advancing from the NE.

I2. The heterogeneous sedimentary unit I2 consists of interbedded gravels, sand-silt-clay rhythmites and well-sorted sands. The lower subunit (3–4 m thick) comprises crudely stratified boulder-rich sandy gravels which rest directly upon the M2 diamicton. In the northeastern part of the cliff section, the gravels are overlain by a subunit (2–5 m thick) of rhythmically bedded (? varved) fine-grained sands, silts and clays, which regularly include clay-intraclast layers (Beiche, 2014). Locally, the rhythmites are folded and contain outsized clasts (dropstones). Towards the southwest, they interfinger with a subunit (5–25 m) of cross-laminated and cross-bedded sand, which also possess climbing-ripple cross lamination, channelised cross bedding, upper plane bed lamination, antidunes and humpback dunes (Kielczynski, 2016). Furthermore, gravity-induced structures produced by sediment creep, slumping and sliding have been documented. In addition, outsized clasts (dropstones) occur.

M3. The brown M3 diamicton (2.5–3 m thick) is a sandy deposit rich in chalk stringers, which also contains a number of gravel lenses or intraclasts (10–20 cm long). This till also possesses a well-developed sub-horizontal set of joints.

Micromorphology. The common occurrence of crushed grains is obvious in thin sections. A district succession of microfabric domains has been documented by microstructural mapping (S1, S2, S3, S4) (Fig. 6).

3 Interpretation of sedimentary and deformational events

3.1 Periglacial versus subglacial soft-sediment deformation of the chalk and the M1 diamicton

The brecciated texture of the chalk is interpreted as resulting from a near-surface (in situ) fragmentation of the Pleistocene

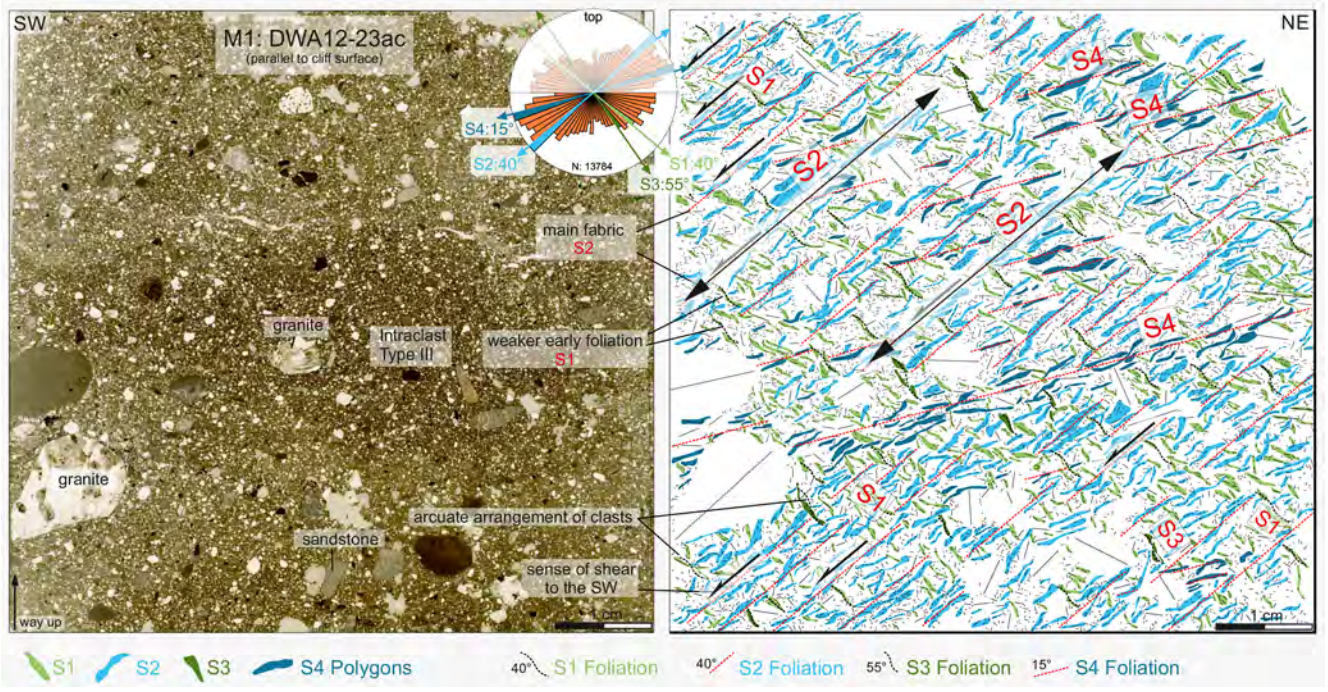

Figure 3. High-resolution scan and microstructural map of thin section DWA12-23ac taken from the upper part of the M1 diamicton at the Dwasieden cliff section (modified from Brumme, 2015). The rose diagram shows the maxima of grain long-axis orientation. The earliest clast microfabric (S1) represents a discontinuous and rough foliation defined by relatively short domains, which dip at ∼ 40° to the NE. The S1 domains typically exhibit a distinctive sigmoidal geometry which records an apparent sinistral sense of shear. This early foliation is cut by a younger clast microfabric (S2), which is more pervasively developed and dips at ∼ 40° towards the SW. The disjunctive and more planar S2 fabric is characterised by relatively continuous microlithons. The spacing of S2 domains varies across the thin section, indicating that deformation during the imposition of this fabric was heterogeneous, with the earlier S1 fabric being preserved within the wider S2 microlithons. S1 and S2 are locally cut by a weak S3 fabric, which dips at ∼ 55° to the NE and is defined by relatively short, irregular domains. In contrast to the earlier developed fabrics (S1 to S3), the locally well developed S4 clast microfabric occurs in discrete bands, which dip at ∼ 15° towards the SW. This foliation clearly cross-cuts S1, S2 and S3 and is the youngest fabric.

bedrock due to frost weathering by seasonal freeze and thaw associated with the development of an active layer above permafrost. Murton (1996) describes a similar disruption from the chalk of southeast England. The folded upper boundary provides evidence that the base of M1 and the top of the underlying chalk has undergone contemporaneous soft-sediment deformation. This may be caused by ductile subglacial deformation during ice advance from the NE and/or involutions caused by periglacial activity.

3.2 Origin of the M1 diamicton: subglacial traction till or reworked periglacial deposit?

Shear-sense indicators (drag folds, bladed boulders) have been used to reconstruct a SW-directed ice flow during deposition of the M1 till (Brumme, 2015). Macroscopic and micromorphological features give evidence of both ductile and brittle deformation within the M1 till, which is a well-known feature in till successions (e.g. Larsen et al., 2006). The common occurrence of crushed grains within the M1 diamicton is indicative of subglacial deformation (van der Meer, 1993), although those features were also described from mass flow deposits (Lachniet et al., 2001). Clear evidence of subglacial deformation, however, reveals the presence of a pervasive distinctive set of clast microfabrics within the M1 diamicton (Brumme, 2015), documenting a polyphase deformation at the glacier bed (e.g. van der Meer, 1993; Phillips et al., 2018). They record a gradual shift from ductile (C'-type shear bands related to S1 and S2) to brittle deformation due to a decrease in the water content (localised S4 shear bands), which is known as strain hardening (Hiemstra and Rijsdijk, 2003).

The clusters of vertically aligned cobble- and boulder-sized clasts (erratics) within glacial sediments typically indicate that the sediment has subsequently undergone periglacial activity; the clasts are displaced/rotated due to frost heave. This feature together with the involutions, partial mixing of M1 with the chalk, and the alteration of the chalk bedrock clearly reveal the impact of permafrost. The presence of water-escape structures are indications for an initial high-water content within the M1 till.

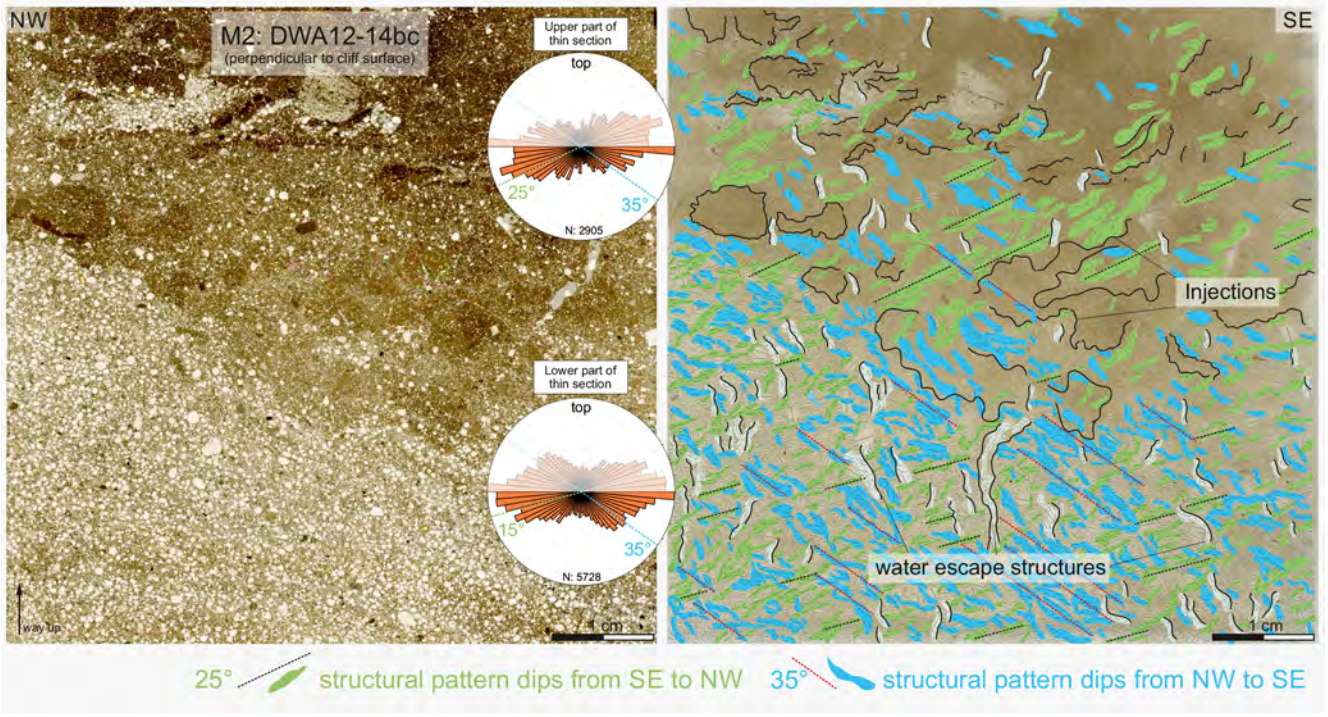

Figure 4. High-resolution scan and microstructural map of thin section DWA12-14bc, taken from the base of the M2 diamicton at the Dwasieden cliff section (modified from Brumme, 2015). The rose diagram shows the maxima of grain long-axis orientation. Note water-escape structures and injections into the upper part. Distinctly oriented microfabrics mainly characterise the more-coarse-grained lower part. The earliest clast microfabric (S1) represents a discontinuous foliation defined by relatively short domains, which show an apparent dip between ∼ 15 (lower part) and ∼ 15° (upper part) to the NW. A younger clast microfabric (S2), which is more pervasively developed, shows an apparent dip at ∼ 35° towards the SE. Steeply inclined grains form a third clast microfabric (S3), which is related to water-escape structures and cross-cuts the older S1 and S2.

3.3 The I1 sediment: evidence of periglacial activity

The fine-grained I1 sediments are regarded as having accumulated in a glacilacustrine environment close to the ice margin (Ludwig, 1954/55; Ludwig and Panzig, 2010; Brumme, 2015). The interbedded gravel layer and the outsized clasts represent ice-rafted debris formed by dumpstones and dropstones from drifting ice bergs (Pisarska-Jamroży et al., 2018b).

The soft-sediment deformation structures that occur together with an ice-wedge cast in the lower part (SSDS-1) are thought to provide evidence for periglacial activity during and after the accumulation of the I1 unit probably in response to annual (seasonal) freeze–thaw (Brumme, 2015). However, soft-sediment deformation in the upper part (SSDS-1, 2) have been interpreted by Pisarska-Jamroży et al. (2018a) as seismites potentially providing evidence for glacio-isostatically induced crustal faulting in front of the advancing Scandinavian Ice Sheet during the late Weichselian (Last Glacial Maximum, MIS-2).

3.4 Origin of the M2 diamicton: a subglacial mélange formed as a result of the deformation of soft permafrost

The macroscopic features are indicative of a glacitectonite at the base of the M2, which includes incorporated or plucked intraclasts and highly attenuated, folded and boudinaged laminae of the underlying sediment. The laminae are vertically stacked in the till and thereby represent tectonic slices produced during sequential phases of till accumulation. The preservation of primary lamination within the intraclasts is attributed to deformation of "warm" permafrost at temperatures slightly below the pressure-melting point, when pore ice cemented the intraclasts as rigid bodies (see Waller et al., 2011). Drag folds and sigmoidal strain markers indicate that the M2 till was laid down by ice advancing from the NE (Brumme, 2015).

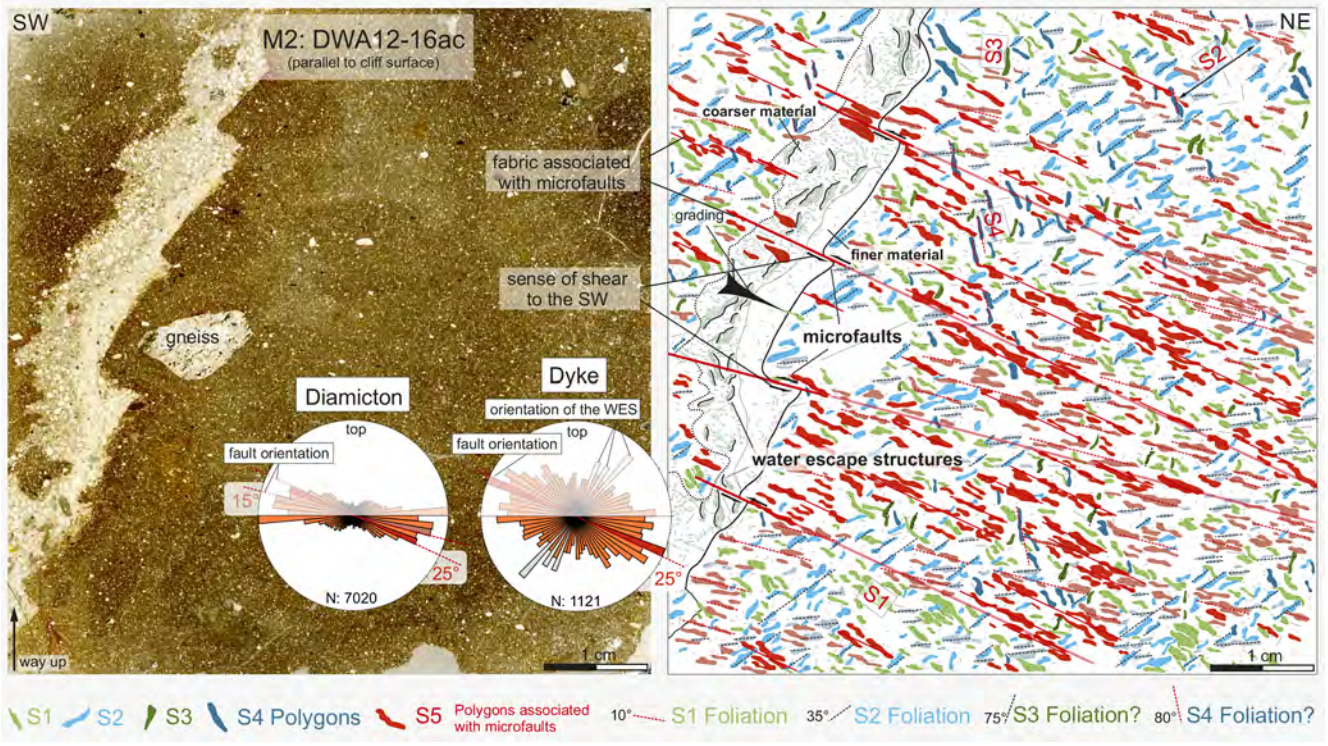

Figure 5. High-resolution scan and microstructural map of thin section DWA12-16ac, taken from the centre of the M2 diamicton at the Dwasieden cliff section (modified from Brumme, 2015). The rose diagram shows the maxima of grain long-axis orientation. Note the district set of five clast microfabric domains, which display strain hardening. The oldest S1 dips at ∼ 30° to the NE, while the main S2 dips at ∼ 35° to the SW. Both S1 and S2 are cut by younger clast microfabric domains, including the straight, parallel-oriented S5, which dips at ∼ 25° to the NE. The latter parallels and corresponds with reverse faults that dissect the subvertical dyke structure (sinistral sense of shear). Note high percentage of steeply inclined grain long axes within the dyke (see lower rose diagram).

3.5 Fabric development and dewatering during the deposition of the M2 diamicton: evidence for subglacial deformation of a water-saturated traction till

Micromorphological investigations show that both the shear-structured glacitectonic melange at the base and the homogenised-massive main M2 diamicton can be classified as a subglacial traction till (see Evans et al., 2006). Several thin sections from the M2 (e.g. Figs. 4, 5) reveal that there are two dominant gently dipping clast microfabrics omnipresent throughout this diamicton, forming a consistent pattern of short and discontinuous S1 domains (dip to the NNE), intersected by subparallel to anastomosing S2 domains (dip to the SSW, i.e. corresponding to the inferred ice flow). These microfabrics display preferred grain orientation as a result of shear at the glacier bed under ductile conditions (Brumme, 2015).

These early formed fabrics are cut by a subvertical to steeply inclined (? S3 and) S4 fabric (Figs. 4, 5) which is thought to have developed during dewatering of this water-saturated diamicton. The upward escape of the porewater through the sediment would have been concentrated into narrow zones or fluid pathways. Within these zones the finer-grained clasts were re-orientated by the escaping porewater.

Continuing deformation resulted in the imposition of the locally preserved S5 fabric (Fig. 5) that occurs coplanar to a set of small-scale faults offsetting a steeply inclined, sand-filled hydrofracture, which cuts the M2 diamicton.

Interestingly, the sense of displacement on these NE-dipping faults is consistent with the shear sense recorded by the sigmoidal, S–C-like fabric geometries of the S1 and S2 domains, with both sets of kinematic indicators indicating a sense of shear towards the SW/SSW (i.e. in response to an ice advance from the NE/NNE). This microstructural evidence can be used to suggest that the imposition of S1 and S2 under ductile conditions and the subsequent brittle faulting associated with the S5 imprint occurred as a result of the same overall stress regime. The deformation history recorded by M2 can therefore be considered to be polyphase, consisting of an early phase of more ductile deformation and the imposition of S1 and S2 when the M2 diamicton was probably water saturated, followed by more brittle deformation (due to water escape) leading to localised faulting and S5 fabric development. Micromorphological evidence clearly indicates that the earlier ductile phase of deformation (S1, S2)

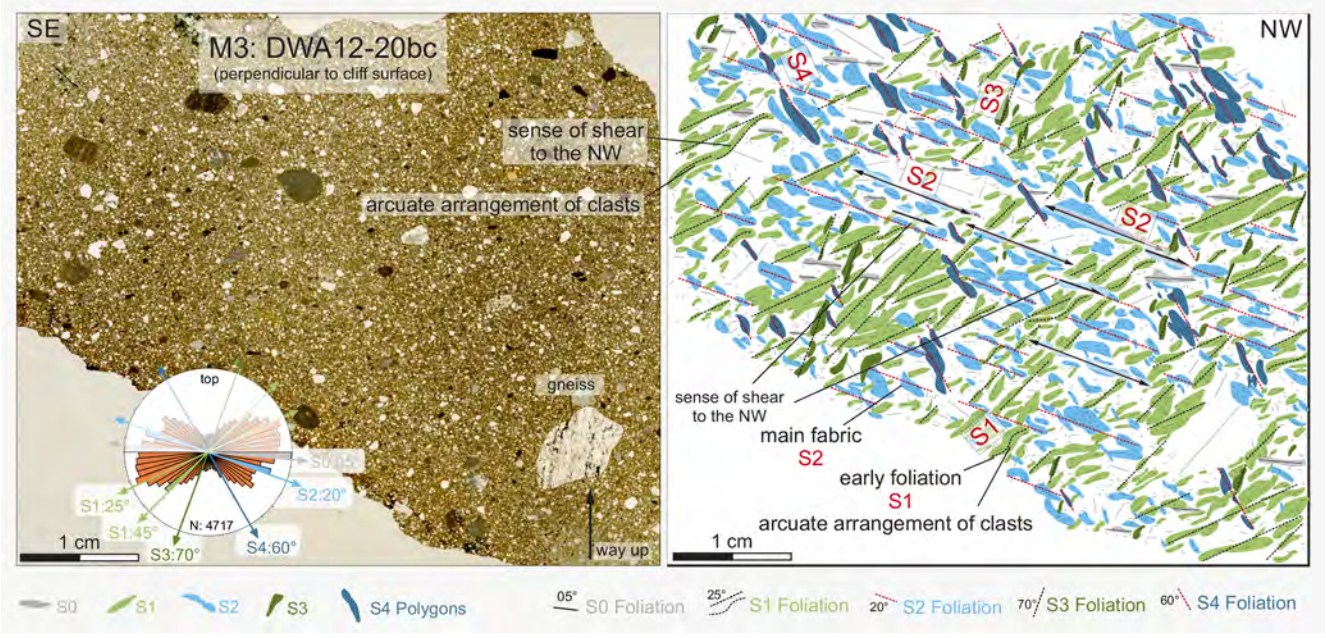

Figure 6. High-resolution scan and microstructural map of thin section DWA12-20bc (oriented perpendicular to the cliff), taken from the M3 diamicton at the Dwasieden cliff section (modified from Brumme, 2015). The structural rose diagram shows the maxima of grain long-axis orientation. There are two main microfabrics: the older S1 is represented by long and anastomosing domains that dip between ∼ 55 and ∼ 45° to the SE. Sigmoidal polygons indicate a dextral sense of shear. A younger, very distinct S2 fabric defined by parallel-oriented domains dips at ∼ 20° to the NW.

and later brittle phase were separated by a phase of dewatering and hydrofracturing, resulting in the formation of S3 and injection of the sand-filled veins (see Figs. 4, 5). Dewatering during the proposed progressive deformation events would have resulted in a change in the rheological properties and strain hardening of the diamicton.

3.6 Evidence for hydrofracturing and sediment injection during deposition of the M2

Macro- and microscale observations reveal that the M2 diamicton is cut by a number of sand-filled veins interpreted as hydrofractures. Microfabrics from the lower part (Fig. 4) indicate that liquefaction and injection of the underlying I1 sediments into M2 occurred penecontemporaneous to the deposition of the deformation till. Structurally higher within the M2 diamicton, the sand-filled veins are connected with larger, irregular patches of sand. Liquefaction and injection of the sand into M2 clearly indicate that the I1 was locally water saturated and, at least in part, unfrozen. Loading by the ice would have led to over-pressurised porewater within the locally melting permafrozen sand, leading to liquefaction, hydrofracturing of the basal part of the overlying diamicton and injection of the sand upward into the M2 as it was being deposited.

Within the upper, homogeneous part of M2, more brittle fabrics have been formed due to the ongoing dewatering during the advanced emplacement and consolidation of the diamicton. Cross-cutting relationships show that the formation of hydrofractures post-dates imposition of the ductile S1 and S2 clast microfabrics but occurred prior to the imposition of S5 and the associated faulting (Fig. 5).

3.7 The I2 sedimentary sequence: evidence for glacifluvial and glacilacustrine sedimentation

The I2 unit was deposited in glacifluvial and glacilacustrine environments at the ice margin (Ludwig, 1954/1955; Ludwig and Panzig, 2010; Beiche, 2014; Brumme, 2015). The heterogeneous interbedded facies has been interpreted as a glacial fan-delta complex developed at the margin of retreating ice sheet (Kielczynski, 2016). The crudely stratified gravels were deposited by debris flows and migrating transverse bed forms in a glacifluvial setting. In contrast, the rhythmically bedded sand-silt-clay couplets record sedimentation in a proglacial lake with temporal ice contact, as indicated by local folding, dropstones and characteristics of the varved lamination. The embedded in situ clay-intraclast layers are probably formed by annual freezing and thawing of the lake water and the lake bottom (Beiche, 2014). The varied sedimentary structures preserved within the thick sand subunit document rapidly changing flow conditions across the fan-delta cone (Kielczynski, 2016). The widely distributed gravity-induced folding structures may result from the steep depositional slope, liquefaction and even current drag.

3.8 Origin of the M3 diamicton: evidence of subglacial entrainment of chalk bedrock and formation of a traction till with polyphase deformation

The prominent chalk stringers within the M3 till provides clear evidence that the Cretaceous bedrock was exposed and prone to erosion during the advance of the Scandinavian Ice Sheet responsible for large-scale glacitectonism on the Jasmund peninsula and subsequent deposition of this subglacial till. The shape of sheared gravel intraclasts indicates a sense of shear towards the northwest. Macroscopic grain long-axis measurements show a preferred alignment of grain *a* axes to the NW, dipping to the SE (up-glacier). Microscopically, there is clear evidence of both ductile and brittle deformation during formation of the M3 diamicton (fabrics S1, S2, S3, S4), allowing a classification as traction till.

4 Conclusions

All till samples show evidence of polyphase deformation. There is predominantly pervasive ductile deformation in all thin sections, indicating a high initial water content under syndepositional conditions. Water-escape structures are typically related to late-stage ductile deformation. More local evidence of brittle deformation is indicative shear zones formed during later phases of deformation (syn- and post-depositional). The thin sections presented and discussed here are a small example of the potential when studying polyphase deformation at a microscale by means of a 2-D and 3-D microstructural mapping approach (see Phillips et al., 2011; Brumme, 2015).

Data availability. All underlying data are published in the figures of this article. Thin sections are stored in the thin-section archive of the Institute of Geography and Geology at the University of Greifswald.

Author contributions. JB carried out field work and processed, measured and analysed the samples. JB wrote the first draft of the manuscript and developed most of the illustrations. HH designed the project, secured funding and rewrote part of the manuscript. HH and EP supervised JB during his PhD. All authors contributed to the discussion and interpretation of the presented research results.

Competing interests. The authors declares that there is no conflict of interest.

Acknowledgements. The study has been financially supported by the DFG (German Research Foundation, projects HU 804/6-1, FR 877/16-1). We thank Sylvia Weinert (University of Greifswald) for careful preparation of thin sections. The constructive comments of Karsten Schütze and an unknown reviewer substantially improved our paper. We acknowledge support for the article processing charge from the DFG (no. 393148499) and the Open Access Publication Fund of the University of Greifswald.

Financial support. This research has been supported by the DFG (German Research Foundation, grant no. 393148499 and projects HU 804/6-1, FR 877/16-1) and the Open Access Publication Fund of the University of Greifswald.

References

Beiche, T.: Microfacies and depositional environment of Weichselian silt-clay rhythmites at the coastal cliff of Dwasieden (Jasmund, Rügen, Pomerania), Master-Thesis, University of Greifswald, 1–58, Greifswald, 2014.

Brumme, J.: Three-dimensional microfabric analyses of Pleistocene tills from the cliff section Dwasieden on Rügen (Baltic Sea Coast): Micromorphological evidence for subglacial polyphase deformation, Doctoral thesis, University of Greifswald, 1–250, 2015.

Evans, D. J. A., Phillips, E. R., Hiemstra, J. F., and Auton, C. A.: Subglacial till: Formation, sedimentary characteristics and classification, Earth-Sci. Rev., 78, 115–176, 2006.

Gehrmann, A.: The multi-stage structural development of the Upper Weichselian Jasmund glaciotectonic complex (Rügen, NE Germany), Doctoral thesis, University of Greifswald, 1–235, 2018.

Gehrmann, A. and Harding, C.: Geomorphological mapping and spatial analyses of an Upper Weichselian glacitectonic complex based on LiDAR data, Jasmund Peninsula (NE Rügen), Germany, Geosciences 8, 208, https://doi.org/10.3390/geosciences8060208, 2018.

Gehrmann, A., Meschede, M., Hüneke, H., and Pedersen, S. A. S.: Sea cliff at Kieler Ufer (Pleistocene stripes 11-16) – Large-scale architecture and kinematics of the Jasmund Glacitectonic Complex, DEUQUA Spec. Pub., this volume, 2019.

Hiemstra, J. F. and Rijsdijk, K. F.: Observing artificially induced strain: implications for subglacial deformation, J. Quarternary Sci., 18, 373–383, 2003.

Kanter, L.: Der M2-Till von Nordost-Rügen, Diploma-Thesis, University of Greifswald, Inst. of Geogr. and Geol., 1–62, Greifswald, 1989.

Kenzler, M. and Hüneke, H.: Sea cliff at Glowe: Stratigraphy and absolute age chronology of the Jasmund Pleistocene sedimentary record, DEUQUA Spec. Pub., this volume, 2019.

Kenzler, M., Tsukamoto, S., Meng, S., Frechen, M., and Hüneke, H.: New age constraints from the SW Baltic Sea area – implications for Scandinavian Ice Sheet dynamics and palaeoenvironmental conditions during MIS 3 and early MIS 2, Boreas, 46, 34–52, 2017.

Kielczynski, S.: Interpretation of bed forms from sedimentary structures: lateral and vertical facies relationships of the I2 sand deposits at Dwasieden (Island of Rügen), Master thesis, Universität Greifswald, 1–129, Greifswald, 2016.

Krienke, K.: Das Geschiebeinventar der weichselhochglazialen Tills von Südostrügen- Hilfsmittel zur Lithostratigraphie sowie zur Rekonstruktion von Ablagerungsbedingungen und glazialer Dynamik, Archiv für Geschiebekunde, 3, 701–710, 2004.

Lachniet, M. S., Larson, G. J., Lawson, D. E., Evenson, E. B., and Alley, R. B.: Microstructures of sediment flow deposits and subglacial sediments: a comparison, Boreas, 30, 254–262, 2001.

Larsen, E., Piotrowski, J. A., and Menzies, J.: Microstructural evidence of low-strain, time-transgressive subglacial deformation, J. Quarternary Sci., 22, 593–608, 2006.

Ludwig, A. O.: Eistektonik und echte Tektonik in Ost-Rügen (Jasmund), Wissenschaftliche Zeitschrift Universität Greifswald, 4, 251–288, 1954/1955.

Ludwig, A. O. and Panzig, W.-A.: Stopp 5: Das Pleistozän südlich Sassnitz – Fazies und Lagerung glazilimnischer/-fluviatiler Sedimente am Kliff bei Dwasieden, in: Eiszeitlandschaften in Mecklenburg-Vorpommern, edited by: Lampe, R. and Lorenz, S., 68–69, Geozon, Greifswald, 2010.

Murton, J. B.: Near-Surface Brecciation of Chalk, Isle of Thanet, South-East England a Comparison with Ice-Rich Brecciated Bedrocks in Canada and Spitsbergen, Permafrost Periglac., 7, 153–164, 1996.

Panzig, W.-A.: Das geschiebeinhaltliche Normalprofil des Till-Inventars von NE-Rügen und stratigraphische Konsequenzen im Ergebnis des Versuchs einer Tilldecken-Regionalkorrelation im SW-lichen Ostseegebiet auf geschiebekundlicher Grundlage, Habilitation-Thesis, University of Greifswald, Inst. of Geogr. and Geol., 1–149, Greifswald, 1989.

Phillips, E., van der Meer, J. J. M., and Ferguson, A.: A new "microstructural mapping" methodology for the identification, analysis and interpretation of polyphase deformation within subglacial sediments, Quaternary Sci. Rev., 30, 2570–2596, 2011.

Phillips, E., Spagnolo, M., Pilmer, A. C. J., Rea B. R., Piotrowski, J. A., Ely, J. C., and Carr, S.: Progressive ductile shearing during till accretion within the deforming bed of a palaeo-ice stream, Quaternary Sci. Rev., 193, 1–23, 2018.

Pisarska-Jamroży, M., Belzyt, S., Börner, A., Hoffmann, G., Hüneke, H., Kenzler, M., Obst, K., Rother, H., and van Loon, A. J.: Evidence from seismites for glacio-isostatically induced crustal faulting in front of an advancing land-ice mass (Rügen Island, SW Baltic Sea), Tectonophysics, 745, 338–348, 2018a.

Pisarska-Jamroży, M., van Loon, A. J., and Bronikowska, M.: Dumpstones as records of overturning ice rafts in a Weichselian proglacial lake (Rügen Island, NE Germany), Geol. Q., 62, 917–924, 2018b.

Strahl, U.: Über die "Ablationsmoräne" des M1- Geschiebemergels Jasmunds und Arkonas (Rügen), Diploma thesis, University of Greifswald, Sektion Geologische Wissenschaften, 1–65, Greifswald, 1988.

van der Meer, J. J. M.: Microscopic Evidence of Subglacial Deformation, Quarternary Sci. Rev., 12, 553–587, 1993.

Waller, R., Phillips, E., Murton, J., Lee, J., and Whiteman, C.: Sand intraclasts as evidence of subglacial deformation of Middle Pleistocene permafrost, North Norfolk, UK, Quaternary Sci. Rev., 30, 3481–3500, 2011.

DEUQUA Spec. Pub., 2, 61–67, 2019
https://doi.org/10.5194/deuquasp-2-61-2019

Open Access DEUQUA Special Publications

The sea cliff at Dwasieden: soft-sediment deformation structures triggered by glacial isostatic adjustment in front of the advancing Scandinavian Ice Sheet

Małgorzata Pisarska-Jamroży[1], Szymon Belzyt[1], Andreas Börner[2], Gösta Hoffmann[3], Heiko Hüneke[4], Michael Kenzler[4], Karsten Obst[2], Henrik Rother[5], Holger Steffen[6], Rebekka Steffen[6], and Tom van Loon[7]

[1]Geological Institute, Adam Mickiewicz University, B. Krygowskiego 12, 61-680 Poznań, Poland
[2]State Authority of Environment, Nature Conservation and Geology Mecklenburg-Western Pomerania, Goldberger 12, 18273 Güstrow, Germany
[3]Steinmann Institute for Geology, Bonn University, Nussallee 8, 53115 Bonn, Germany
[4]Institute of Geography and Geology, University of Greifswald, F.-L. Jahn 17a, 17487 Greifswald, Germany
[5]Landesamt für Geologie und Bergwesen, Sachsen Anhalt, Dezernat Landesaufnahme und Analytik, Köthener 38, 06118 Halle, Germany
[6]Geodetic Infrastructure, Lantmäteriet, Lantmäterigatan 2C, 80182 Gävle, Sweden
[7]College of Earth Science and Engineering, Shandong University of Science and Technology, Qingdao 266590, Shandong, China

Correspondence: Małgorzata Pisarska-Jamroży (pisanka@amu.edu.pl)

Relevant dates: Published: 15 August 2019

How to cite: Pisarska-Jamroży, M. G., Belzyt, S., Börner, A., Hoffmann, G., Hüneke, H., Kenzler, M., Obst, K., Rother, H., Steffen, H., Steffen, R., and van Loon, T.: The sea cliff at Dwasieden: soft-sediment deformation structures triggered by glacial isostatic adjustment in front of the advancing Scandinavian Ice Sheet, DEUQUA Spec. Pub., 2, 61–67, https://doi.org/10.5194/deuquasp-2-61-2019, 2019.

Abstract: Isostatic response of the Earth's crust as a consequence of the fluctuating extent of ice-sheet masses was accompanied by earthquakes probably due to local reactivation of pre-existing faults. Our study of a glacilacustrine and glacifluvial succession exposed on Rügen Island (SW Baltic Sea) indicates that some of the soft-sediment deformation structures within the succession must have formed shortly before the front of the Pleistocene Scandinavian Ice Sheet reached the study area (during the Last Glacial Maximum), thus during a stage of ice advance. Based on analysis of the textural and structural features of the soft-sediment deformation structures, the deformed layers under investigation are interpreted as seismites which formed as a result of seismically induced liquefaction and fluidisation.

1 Introduction

Bending of the Earth's lithosphere and mantle displacement can be induced by loading–unloading cycles resulting from alternating advances and retreats of an ice sheet (see, e.g. Mörner, 1990). Such glacial isostatic adjustment (GIA) may well induce earthquakes in the Earth's crust that leave traces in the form of layers with soft-sediment deformation structures (SSDSs) called "seismites" (van Loon, 2009). The link between deglaciation and neotectonics was described by many authors, e.g. Johnston (1996), Muir-Wood (2000), Kaufmann et al. (2005), Brandes et al. (2012), Hoffmann and Reicherter (2012), van Loon and Pisarska-Jamroży (2014), and van Loon et al. (2016). In contrast, there is only little evidence that the ice-sheet advance could cause earthquakes, too (Brandes et al., 2011; Pisarska-Jamroży et al., 2018a, 2019), and that corresponding SSDSs of seismic origin have been formed.

Pisarska-Jamroży et al. (2018a) documented two layers with abundant SSDSs in a glacilacustrine silty-sandy succession, in a coastal cliff near Dwasieden on Jasmund Peninsula of Rügen Island (Fig. 1a; 54°30′1.86″ N, 13°36′49.94″ E), which have been interpreted as seismites. The location under study is situated at the southernmost rim of the Trans-European Suture Zone (TESZ). The TESZ is a zone of crustal weakness and is characterised by numerous faults activated and reactivated during several late Palaeozoic and Mesozoic tectonic phases. The NW-trending faults (Fig. 1b, c) of the Tornquist Zone (Berthelsen, 1992), subdivided into the Sorgenfrei-Tornquist Zone (STZ) and the Tornquist-Teisseyre Zone (TTZ), and of the Tornquist Fan, occur in the area between Rügen and Bornholm (Thybo, 2000). Mesozoic transtension above the TESZ led to the formation of the Western Pomeranian Fault System (Krauss and Mayer, 2004). Compressional tectonics during the Late Cretaceous and the early Tertiary caused fault reactivation and anticline formation. Tertiary sediments are only locally preserved in graben structures bordered by WNW–ESE- to NW–SE-trending faults of the Western Pomeranian Fault System. This suggests reactivation of this fault system during the Cainozoic (particularly during the Oligocene–Miocene) due to changes in the stress field (compression) from NE to NW (Seidel et al., 2018).

2 Soft-sediment deformation structures interpreted as seismites

The succession of the cliff in Dwasieden, with an overall height of 20 m, is composed of Late Cretaceous (Early Maastrichtian) limestone overlain by five late Pleistocene units: three glacial diamict layers (M1–M3), separated from each other by glacifluvial and glacilacustrine silts, sands and gravels (see Brumme et al., 2019). Within the sandy silts, three deformed layers comprising SSDSs have been described (Fig. 2) by Pisarska-Jamroży et al. (2018a). The lowermost deformed level takes irregular positions; the SSDSs within it are concentrated in a few places, without any obvious lateral or vertical alignment. The top of this layer was exposed to periglacial conditions, which is indicated by the presence of an ice-wedge cast (Fig. 2c). Two deformed levels higher up show entirely different characteristics regarding both their distribution (laterally continuous over 150 m and vertically restricted to relatively thin levels) and structural nature; most SSDSs are relatively simple load casts and pseudonodules, with genetically related flame and fluid-escape structures (Fig. 2). A critical feature is that the two deformed levels are interbedded between undeformed layers. This excludes an origin of the deformations as a direct result of endogenic tectonics, periglacial processes or glacitectonics. A seismically induced origin of the SSDSs due to a GIA is therefore the only feasible explanation.

Some metres west of the main investigated profile, dumpstones and dropstones up to 0.8 m in size occur in the silty-sandy late Weichselian glacilacustrine succession. The dumping events are linked to iceberg rafting in a glacial lake (see Pisarska-Jamroży et al., 2018b).

3 Age and origin of the seismites

Based on their stratigraphic position and optically stimulated luminescence (OSL) dating, the two layers with SSDSs interpreted as seismites (Pisarska-Jamroży et al., 2018a) were deposited between 22.7 ± 1.9 ka and 19.0 ± 1.8 ka, and were formed in front of the Scandinavian Ice Sheet (SIS) (Heine et al., 2009; Kenzler et al., 2015, 2017). Kenzler et al. (2017) concluded that the first late Weichselian ice advance reached the Jasmund Peninsula at 22 ± 2 ka (Fig. 3a). This time roughly coincides with the maximum extent of the SIS in the SW Baltic Sea area during the Brandenburg Phase of the Weichselian glaciation (Houmark-Nielsen, 2010; Hughes et al., 2016). The lowermost till (M1) is interpreted to have formed during the Saalian glaciation during MIS 6, whereas the rest of the succession accumulated during the Weichselian glaciation (MIS 4–2; Panzig, 1995; Kenzler et al., 2015).

The study area is situated in a low-seismicity intraplate setting, which raises the question of which type of faulting may have resulted in the earthquakes that caused the formation of the seismites. Among the faults on Rügen Island, which are most likely to have been (re)activated by GIA during the Pleistocene, the NW-trending Schaabe fault (Fig. 1c) is situated only 2 km away from the studied cliff section. The fault strikes parallel to the ice margin of the advancing SIS at a distance of a few tens of kilometres and could easily have been (re)activated because of considerable slip variations in the moat area (Fig. 3b), as suggested by numerical model results of Hampel and Hetzel (2006). However, other nearby faults like the Parchow, Lietzow or Nord-Jasmund, Boldewitz, and Wiek faults (Fig. 1c) could also be related to GIA.

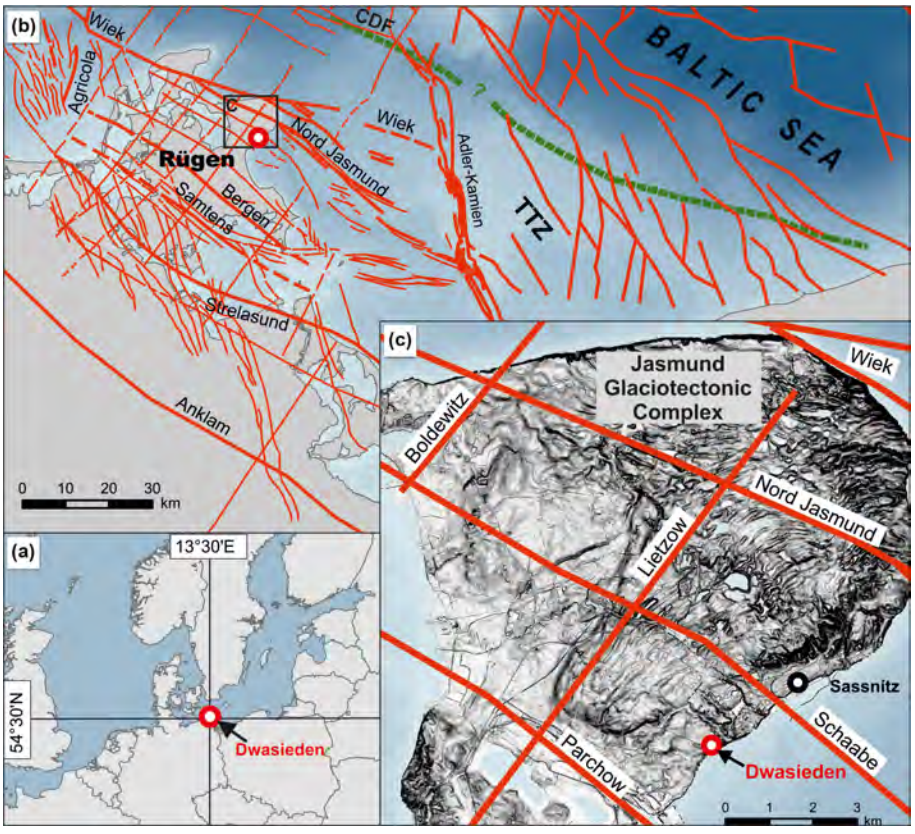

Figure 1. Location of the study area (modified from Pisarska-Jamroży, 2018a). **(a)** Position of Rügen Island within NW Europe. **(b)** Faults of the Tornquist Zone and Tornquist Fan recognised on Rügen Island and its vicinity (red lines); CDF: Caledonian Deformation Front (green dashed line); TTZ: Tornquist-Teisseyre Zone. **(c)** Rügen Island with main deep-rooted faults (Seidel et al., 2018, and references therein).

The GIA influence on the reactivation of the Schaabe fault has been tested with a three-dimensional finite-element model. As an ice load history model, the latest version of ANU-ICE was used (Lambeck et al., 2010), while several Earth model setups suggested for Fennoscandia (see Brandes et al., 2018) were tested. We analysed the Coulomb failure stress (δCFS) of each GIA model, which, put simply, shows for values above zero that fault (re)activation is possible, while below zero earthquakes solely due to GIA can be excluded (see Brandes et al., 2012, 2018). We assume optimal conditions, i.e. that the fault parameters including frictional behaviour are ideally placed in a given tectonic stress regime. In the case of northern Germany, a compressional regime (thrust faulting) is suggested in the World Stress Map (Heidbach et al., 2018).

At Dwasieden, fault instability is indicated after 16 ka (Fig. 4a), depending on the Earth model setup. However, in view of OSL dating results, the seismites could not be linked to stress changes induced by GIA – at ca. 23 ka, about 2 MPa difference in δCFS must be overcome to reach the instability zone. Changes in pore-fluid pressure in the upper crust during that time (not tested here), e.g. due to increased meltwater, may decrease this difference, but likely not completely. Hence, we also investigated a strike-slip tectonic stress regime, which cannot be completely excluded according to the World Stress Map (Heidbach et al., 2018) and because the regional geology is complex so that the overall stress field could be locally altered. For a strike-slip regime all tested models reach the instability zone between 24.5 and 23.5 ka (Fig. 4b), which supports a glacially induced origin of the seismites. We note though that these results are preliminary and subject to many assumptions and model uncertainties. The ice model has, for instance, no uncertainty assigned and has coarse 1000-year time steps during our period of interest. Further, the δCFS calculation does not yet allow the analysis of oblique-slip faults. The δCFS of such faulting could be found in between those for thrust and strike-slip faulting. Hence, thoroughly investigated and dated seismites such as at Dwasieden can help in GIA modelling by excluding or supporting certain GIA model setups, in historic ice-sheet development and in regional stress-field investigations.

Data availability. No data sets were used in this article.

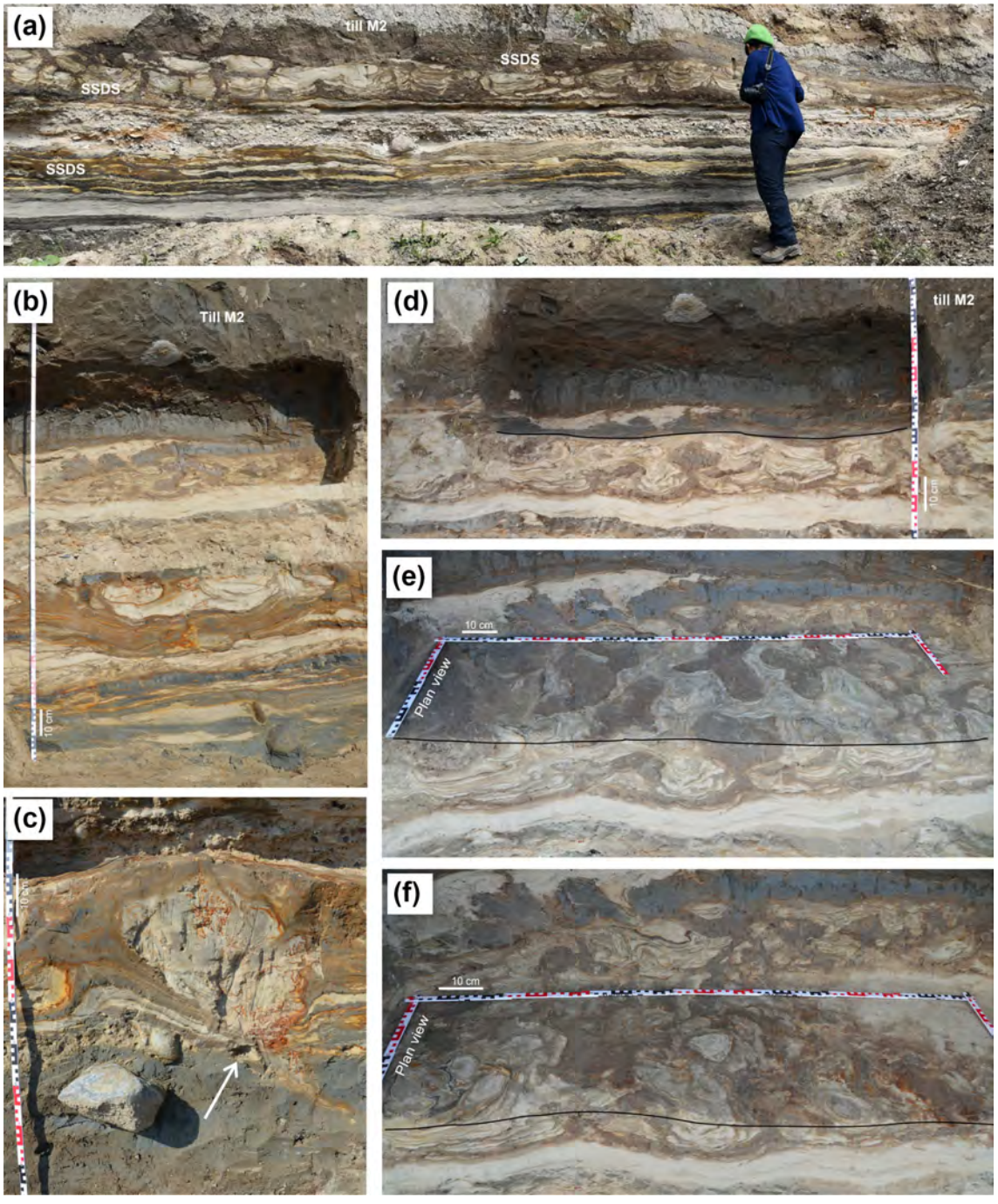

Figure 2. Details of the cliff section near the castle of Dwasieden. **(a)** The lateral extent of the soft-sediment deformation structures. **(b)** Vertical succession of the sediments below the till (M2) deposited during the Frankfurt/Brandenburgian advance of the SIS. The lowermost part contains glacilacustrine sediments with two dropstones; the upper part contains periglacially deformed sediments and deformations caused by seismic shocks. **(c)** Ice-wedge cast (white arrow) in the irregularly deformed sediments below the seismites. **(d)** Details of soft-sediment deformation structures. The yellowish sediments consist of silty fine-sandy material; the brownish sediments consist of silty clay and clayey silt. Sandy load casts and silty flame structures occur in the lower part of deformed layer. (**e**–**f**) Evolution of load structures in 3-D view using horizontal slicing of deformed layers.

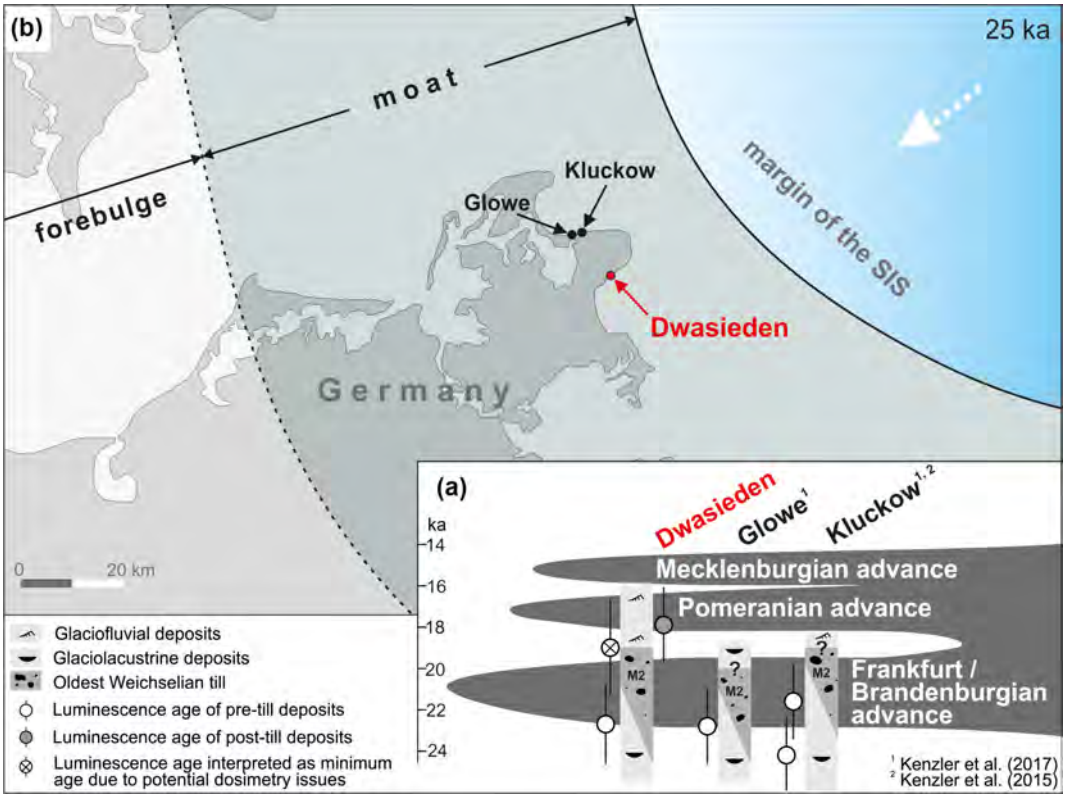

Figure 3. Palaeogeographical and lithostratigraphical reconstruction (modified from Pisarska-Jamroży, 2018a). **(a)** Luminescence ages of glacifluvial and glacilacustrine deposits below and above the first late Weichselian till (M2) on the Jasmund Peninsula in comparison to advances of the SIS. **(b)** Palaeogeographical map of the southwestern Baltic Sea area with the most likely extent of the SIS at 25 ka (based on Hughes et al., 2016), and reconstructed positions of the moat and the forebulge (based on the Peltier et al., 2015 model).

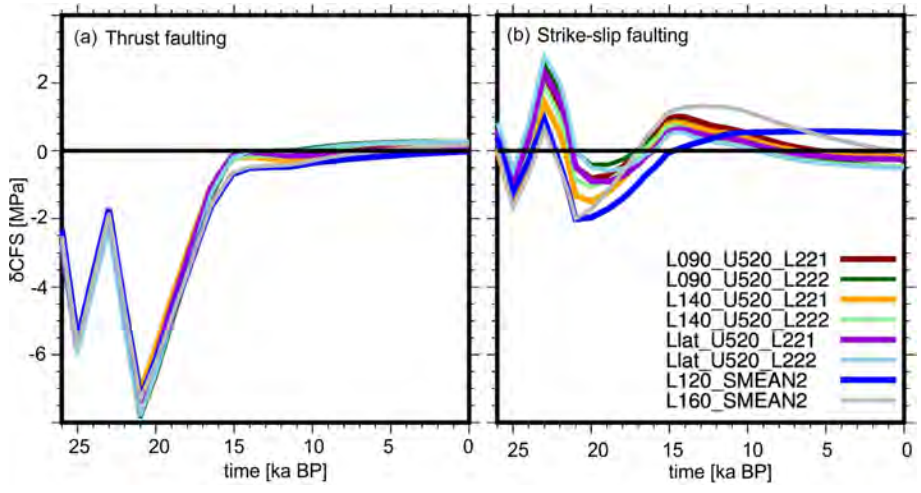

Figure 4. Changes in Coulomb failure stress (δCFS) at Dwasieden for **(a)** thrust and **(b)** strike-slip faulting over time for the last 26 kyr. The coloured curves represent eight different rheology models suitable for Fennoscandia (Brandes et al., 2018). δCFS values above zero indicate fault instability.

Author contributions. All authors discussed the results and contributed to the final paper. MPJ, SB, AB, GH, HH, MK, KO, HR and TVL participated in the fieldwork. HS and RS tested the GIA influence on the reactivation of faults with a three-dimensional finite-element model.

Competing interests. The authors declare that they have no conflict of interest.

Acknowledgements. We would like to thank Oxana Lunina and Piotr Paweł Woźniak for valuable comments. The study has been financially supported by a grant for the GREBAL project (no. 2015/19/B/ST10/00661) from the National Science Centre of Poland. We acknowledge support for the article processing charge from the DFG (no. 393148499) and the Open Access Publication Fund of the University of Greifswald.

Financial support. This research has been supported by the DFG (German Research Foundation, grant no. 393148499), the National Science Centre of Poland (grant no. 2015/19/B/ST10/00661) and the Open Access Publication Fund of the University of Greifswald.

References

Berthelsen, A.: From Precambrian to Variscan Europe, in: A Continent Revealed: The European Geotraverse, edited by: Blundell, D., Freeman, R., and Mueller, S., Cambridge University Press, Cambridge, 153–164, 1992.

Brandes, C., Polom, U., and Winsemann, J.: Reactivation of basement faults: interplay of ice-sheet advance, glacial lake formation and sediment loading, Basin Res., 23, 53–64, 2011.

Brandes, C., Winsemann, J., Roskosch, J., Meinsen, J., Tanner, D. C., Frechen, M., Steffen, H., and Wu, P.: Activity along the Osning Thrust in central Europe during the Lateglacial: Ice-sheet and lithosphere interactions, Quaternary Sci. Rev., 38, 49–62, 2012.

Brandes, C., Steffen, H., Sandersen, P. B. E., Wu, P., and Winsemann, J.: Glacially induced faulting along the NW segment of the Sorgenfrei-Tornquist Zone, northern Denmark: implications for neotectonics and Lateglacial fault-bound basin formation, Quaternary Sci. Rev., 189, 149–168, 2018.

Brumme, J., Hüneke, H., and Phillips, E.: Micromorphology and clast microfabrics of subglacial traction tills at the sea-cliff Dwasieden: evidence of polyphase syn- and post-depositional deformation, DEUQUA Spec. Pub., this volume, 2019.

Hampel, A. and Hetzel, R.: Response of normal faults to glacial-interglacial fluctuations of ice and water masses on Earth's surface, J. Geophys. Research, 111, B06406, 2006.

Heidbach, O., Rajabi, M., Cui, X., Fuchs, K., Müller, B., Reinecker, J., Reiter, K., Tingay, M., Wenzel, F., Xie, F., Ziegler, M. O., Zoback, M. L., and Zoback, M.: The World Stress Map database release 2016: Crustal stress pattern across scales, Tectonophysics, 744, 484–498, 2018.

Heine, K., Reuther, A. U., Thieke, H. U., Schulz, R., Schlaak, N., and Kubik, P. W.: Timing of Weichselian ice marginal positions in Brandenburg (northeastern Germany) using cosmogenic in situ Be-10, Z. Geomorphol. N.F., 53, 433–454, 2009.

Hoffmann, G. and Reicherter, K.: Soft-sediment deformation of Late Pleistocene sediments along the southwestern coast of the Baltic Sea (NE Germany), Int. J. Earth Sci., 101, 351–363, 2012.

Houmark-Nielsen, M.: Extent, age and dynamics of Marine Isotope Stage 3 glaciation in the southwestern Baltic Basin, Boreas, 39, 343–359, 2010.

Hughes, A., Gyllencreutz, R., Lohne, Ø. S., Mangerud, J., and Svendsen, J. I.: The last Eurasion ice sheets – a chronological database and time-slice reconstruction, DATED-1, Boreas, 45, 1–45, 2016.

Johnston, A. C.: A Wave in the Earth, Science, 274, 735, 1996.

Kaufmann, G., Wu, P., and Ivins, E. R.: Lateral viscosity variations beneath Antarctica and their implications on regional rebound motions and seismotectonics, J. Geodynam., 39, 165–181, 2005.

Kenzler, M., Tsukamoto, S., Meng, S., Thiel, C., Frechen, M., and Hüneke, H.: Luminescence dating of Weichselian interstadial sediments from the German Baltic Sea coast, Quat. Geochronol., 30, 215–256, 2015.

Kenzler, M., Tsukamoto, S., Meng, S., Frechen, M., and Hüneke, H.: New age constraints from the SW Baltic Sea area – implications for Scandinavian Ice Sheet dynamics and palaeoenvironmental conditions during MIS 3 and early MIS 2, Boreas, 46, 34–52, 2017.

Krauss, M. and Mayer, P.: Das Vorpommern-Störungssystem und seine regionale Einordnung zur Transeuropäischen Störung, Z. Geol. Wissenschaft., 32, 227–246, 2004.

Lambeck, K., Purcell, A., Zhao, J., and Svensson, N.-O.: The Scandinavian ice sheet: from MIS 4 to the end of the last glacial maximum, Boreas, 39, 410–435, 2010.

Mörner, N. A.: Glacioisostatic and long term crustal movements in Fennoscandia with respect to lithospheric and atmospheric processes and properties, Tectonophysics, 176, 13–24, 1990.

Muir-Wood, R.: Deglaciation seismotectonics: a principal influence on intraplate seismogenesis at high latitudes, Quaternary Sci. Rev., 19, 1399–1411, 2000.

Panzig, W.-A.: The tills of NE Rügen – lithostratigraphy, gravel composition and relative deposition directions in the southwestern Baltic region, in: Glacial Deposits in North-East Europe, edited by: Ehlers, J., Kozarski, S., and Gibbard, P., Balkema, Rotterdam, 521–533, 1995.

Peltier, W. R., Argus, D. F., and Drummond, R.: Space geodesy constrains ice-age terminal deglaciation: The global ICE-6G_C (VM5a) model, J. Geophys. Res.-Sol. Ea., 120, 450–487, 2015.

Pisarska-Jamroży, M., Belzyt, S., Börner, A., Hoffmann, G., Hüneke, H., Kenzler, M., Obst, K., Rother, H., and van Loon, A.J.: Evidence from seismites for glacio-isostatically induced crustal faulting in front of an advancing land-ice mass (Rügen Island, SW Baltic Sea), Tectonophysics, 745, 338–348, 2018a.

Pisarska-Jamroży, M., Van Loon, A. J., and Bronikowska, M.: Dumpstones as records of overturning ice rafts in a Weichselian proglacial lake (Rügen Island, NE Germany), Geol. Q., 62, 917–924, 2018b.

Pisarska-Jamroży, M., Belzyt, S., Bitinas, A., Jusienė, A., and Woronko, B.: Seismic shocks, periglacial conditions and glaciotectonics as causes of the deformation of a Pleistocene meandering river succession in central Lithuania, Baltica, 32, 63–77, 2019.

Seidel, E., Meschede, M., and Obst, K.: The Wiek Fault Zone east of Rügen Island: Origin, tectonic phases and its relation to the TransEuropean Suture Zone, Geol. Soc. London Spec. Pub., 469, https://doi.org/10.1144/SP469.10, 2018.

Thybo, H.: Crustal structure and tectonic evolution of the Tornquist Fan region as revealed by geophysical methods, Bull. Geol. Soc. Denmark, 46, 145–160, 2000.

Van Loon, A. J.: Soft-sediment deformation structures in siliciclastic sediments: an overview, Geologos, 15, 3–55, 2009.

Van Loon, A. J. and Pisarska-Jamroży, M.: Sedimentological evidence of Pleistocene earthquakes in NW Poland induced by glacio-isostatic rebound, Sediment. Geol., 300, 1–10, 2014.

Van Loon, A. J., Pisarska-Jamroży, M., Nartišs, M., Krievāns, M., and Soms, J.: Seismites resulting from high-frequency, high-magnitude earthquakes in Latvia caused by Late Glacial glacio-isostatic uplift, Journal of Palaeogeography, 5, 363–380, 2016.

DEUQUA Spec. Pub., 2, 69–75, 2019
https://doi.org/10.5194/deuquasp-2-69-2019

Open Access DEUQUA Special Publications

The Bronze Age battlefield in the Tollense Valley – conflict archaeology and Holocene landscape reconstruction

Gundula Lidke and Sebastian Lorenz

University of Greifswald, Institute of Geography and Geology, Friedrich-Ludwig-Jahn-Straße 16, 17487 Greifswald, Germany

Correspondence: Gundula Lidke (tollensetal-projekt@web.de)

Relevant dates: Published: 15 August 2019

How to cite: Lidke, G. and Lorenz, S.: The Bronze Age battlefield in the Tollense Valley – conflict archaeology and Holocene landscape reconstruction, DEUQUA Spec. Pub., 2, 69–75, https://doi.org/10.5194/deuquasp-2-69-2019, 2019.

Abstract: Archaeological discoveries in the Tollense Valley represent remains of a Bronze Age battle of ca. 1300–1250 BCE, documenting a violent group conflict hitherto unimagined for this period of time in Europe, changing the perception of the Bronze Age. Geoscientific, geoarchaeological and palaeobotanical investigations have reconstructed a tree- and shrubless mire characterised by sedges, reed and semiaquatic conditions with a shallow but wide river Tollense for the Bronze Age. The exact river course cannot be reconstructed, but the distribution of fluvial deposits traces only a narrow corridor, in which the Tollense meandered close to the current riverbed. The initial formation of the valley mire dates to the transition from the Weichselian Late Glacial to the early Holocene.

1 Introduction and history of archaeological research

The valley of the river Tollense in Mecklenburg-Western Pomerania (northeastern Germany, 53°44′53.25″ N, 13°18′19.84″ E, Fig. 1a) was the scene of dramatic events sometime during the first half of the 13th century BCE. Following chance finds in the riverbank by an amateur archaeologist in 1996 – among them, a human upper arm bone with embedded flint arrowhead and a wooden club – first trial excavation in the same year revealed a find layer close to the river with disarticulated skeletal remains, mostly human, some horse. A burial context could be excluded as there were neither related structures nor grave goods; in contrast even more indications for violence were detected, such as a skull with a large depressed fracture. The extraordinary find area has been the subject of intensive multidisciplinary research since 2009 (Jantzen et al., 2011, 2014). Skeletal remains of more than 130 individuals, likely all men, many of them evidently killed in violent conflict, are preserved at various sites in the valley; there are also all kinds of weaponry, ranging from bronze and flint arrowheads to now several wooden clubs and bronze weapons, such as a sword, spearheads and knives. The finds together attest a violent armed clash with at least several hundred (possibly thousands) participants, a conflict of a scale hitherto unexpected for the European Bronze Age. The neighbouring locations, i.e. the numerous archaeological sites representing the conflict, presumingly indicate different situations of deposition and implementation in sedimentary environments.

2 Archaeology in the river valley

Finds are spread over a stretch of the river more than 3 km long (Fig. 1b). They occur in different circumstances and

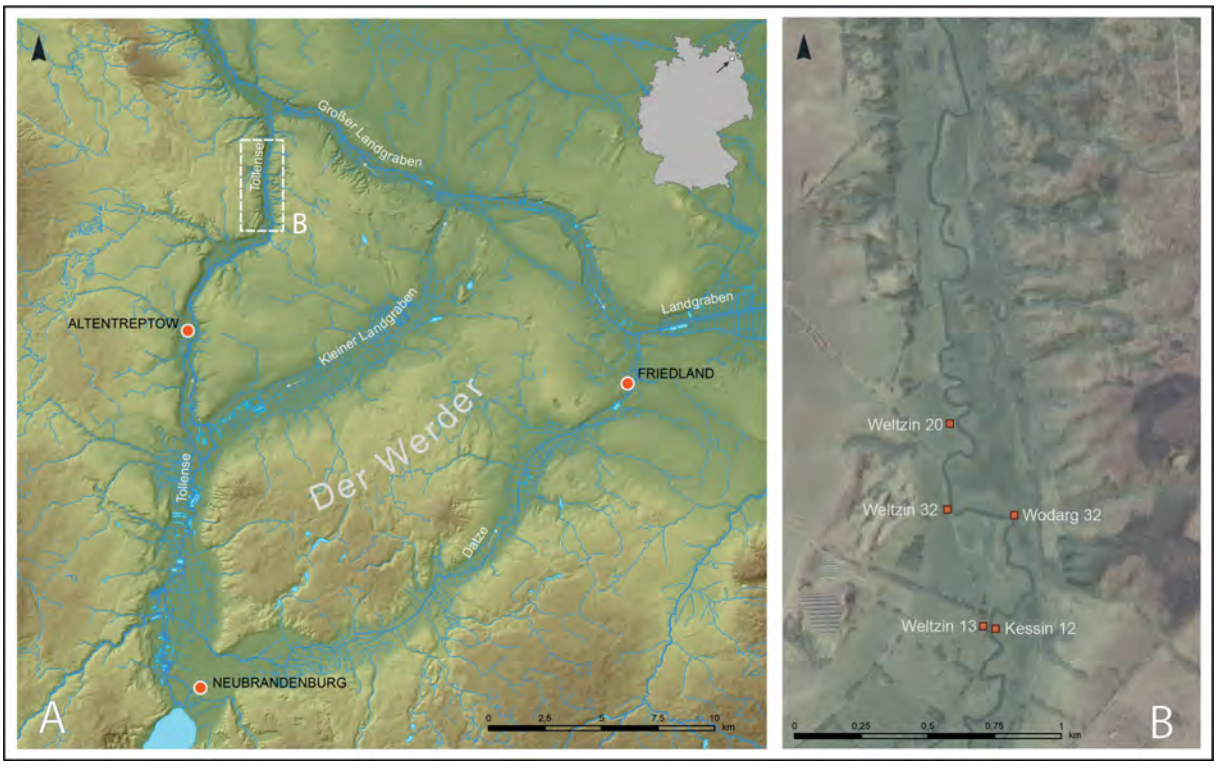

Figure 1. General shaded relief map with drainage system topography **(A)** and the location of the archaeological sites related to the conflict scenario **(B)**. Based on data from ©GeoBasis-DE/M-V 2016.

include mostly skeletal remains, but also weapons made of bronze, flint and wood. In situ finds, covered by a peat layer, can be found close to the river on the adjacent meadows as well as in riverbank sections exposed by erosional river dynamics. Furthermore, during dredging works in the 1970s and 1980s – to deepen the riverbed and to drain the mire – sediments including find material were taken out of the river and dispersed on the adjacent meadows, where skeletal remains and bronze objects can now be discovered displaced in secondary positions.

The most definite concentrations of human skeletal remains and weapon finds occur between sites Weltzin 13–Kessin 12 to the south and Weltzin 20 to the north (Terberger et al., 2014b). Nearly continuous find layers with human skeletal remains were documented there in sections of the riverbanks during diving surveys. Find intensity is especially high between sites Weltzin 32 and 20; in both areas in situ finds as well as finds from secondary contexts are documented. Further north of Weltzin 20 mostly dispersed skeletal remains have been discovered so far. Bones and remains of wooden shafts of arrows from several sites have been dated with accelerator mass spectrometry to ca. 1300–1250 BCE. These results together with the similarity of the sites and their find material, the state of preservation of the skeletal remains, the patterns of lesions, and the distribution of weapon finds indicate that all sites represent remains of one major conflict rather than several repeated minor ones (Terberger et al., 2018).

3 A causeway to conflict?

Sites Kessin 12 and Weltzin 13 represent the starting point of the "battlefield horizon" layer with human skeletal remains, partly with lesions, and bronze arrowheads. But finds from the Neolithic to the Middle Ages indicate that this area of the valley was – due to a favourable position in the valley layout – used as a river and valley crossing for several millennia (Jantzen et al., 2014). During diving surveys, remains of wooden constructions were detected in the eastern riverbank, dating to ca. 1300 BCE, indicating the use of the crossing during the time of the conflict, too. Geophysical measurements in the eastern floodplain showed linear structures over ca. 100 m, which during excavation turned out to be remains of a stone-flanked causeway built with wood, sand and turf at ca. 1900 BCE. This causeway (Fig. 2) likely made the crossing of the wet and at times possibly swampy floodplain possible during all seasons. Horse teeth discovered directly on the surface of the causeway were dated to ca. 1300 BCE again, indicating that this crossing was still known and used hundreds of years after its construction. Likely the causeway and valley crossing were the starting point of the conflict (Jantzen et al., 2014).

Figure 2. Kessin 12. Causeway with different methods of construction. **(a)** Stone-flanked causeway, excavated in 2013. **(b)** Causeway built with wood, sand and turf, excavated in 2014. Photos: Gundula Lidke.

4 Dead bodies in the river

At site Weltzin 32 the in situ find layer is situated ca. 2–3 m below the present surface in fluviatile sediments, likely those of the Bronze Age river. Extensive diving surveys have shown a continuous skeletal find layer over more than 60 m in the western river bank; there are also skeletal remains in the eastern river bank. Due to the depth of the in situ find layer only limited excavations on land have taken place so far. Interestingly, valuable finds like a gold spiral ring, two tin rings and four small bronze spirals were discovered in the find layer here, too. These are interpreted as personal belongings of combatants that could not be looted after battle due to the position of the bodies in the river (Krüger et al., 2012). A high number of bronze socketed arrowheads are attested here from the sediments displaced by dredging; one flint arrowhead stems from the in situ find layer in the riverbank section. The human bones show several perimortem lesions that originate from close as well as long-range weapons. Together, the finds indicate that fighting took place at this site. According to a hypothetical scenario (Lidke et al., 2018), the fighting might have moved northward from the causeway in a "running battle", with skirmishes and heavy fighting along the way.

5 A last stand and heavy casualties?

A little to the north, site Weltzin 20 is situated on an alluvial fan in the Tollense Valley. Here the in situ find layer is documented at ca. 0.8–1.7 m below the present surface. Taking off from the trenches of the 1996 excavation, which itself took place around the spot where the first discoveries had been made, ca. 460 m^2 had been excavated until 2015. More than 10 000 human remains, mostly found disarticulated, are documented from this site alone, partly in dense clusters, partly isolated (Fig. 3). In some cases there are horse bones, also disarticulated, indicating that these animals were involved in the conflict, too. Further finds within the skeletal find layer are very sparse and consist mostly of flint and bronze arrowheads; furthermore, there is just one bronze finger ring and a

Figure 3. Weltzin 20. Find layer with disarticulated human remains under excavation in 2013. Photo: Jana Dräger.

bone pin. More bronze socketed arrowheads were discovered during metal detecting in sediments displaced by dredging. According to the hypothetical scenario (Lidke et al., 2018), this site might have seen heavy fighting with a high number of casualties. The human bones again show a greater number of perimortem lesions, caused by close as well as long-range weapons, e.g. lesions by arrow shot; stabbing and cutting wounds perhaps caused by swords, knives or spearheads; and blunt traumata, probably caused by clubs or other blunt objects. The absence of other finds – apart from the few small objects mentioned above – indicates that the dead were looted thoroughly here.

6 Human skeletal remains and weapon lesions

More than 12 000 human skeletal remains are known from several sites in the Tollense Valley. Most of them stem from site Weltzin 20 where the most extensive research has taken place so far. More than 140 individuals can be reconstructed, most of them young adult males. A large number of bones show perimortem lesions, mostly caused by sharp force trauma, including arrowhead wounds as well as stabbing and cutting wounds. Blunt force lesions occur in lower numbers. There are also healed lesions, some of which stem from weapon use, which indicate that some individuals had also encountered violence in previous situations (Brinker et al., 2018). Analyses of aDNA and isotopes (Sr, C, N) point to a heterogeneous population group (Terberger and Heinemeier, 2014a; Price et al., 2017). Calculating from the number of the dead in the valley at least hundreds of battle participants are likely, representing a not purely local population. All in all, the remains of the conflict in the Tollense Valley help to draw a new picture of the European Bronze Age society.

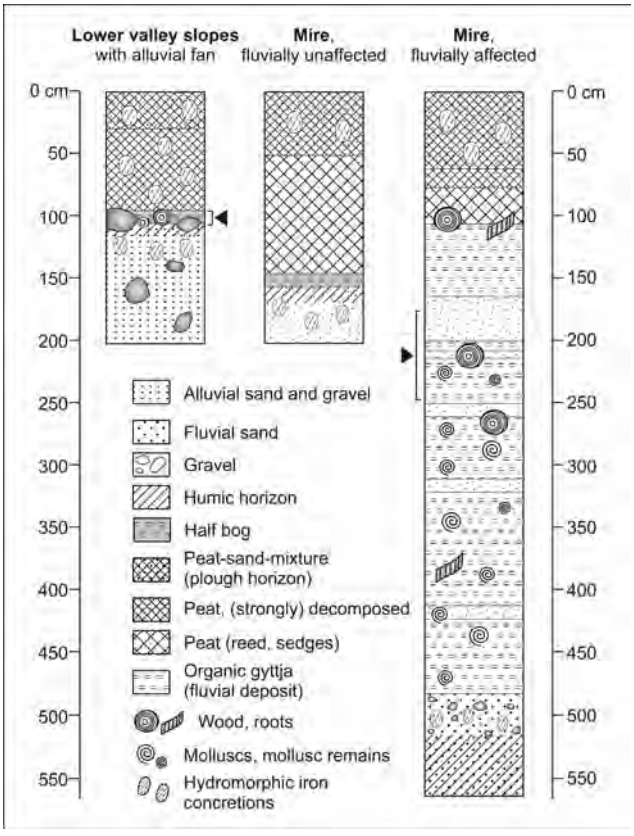

Figure 4. Standard profiles from the Tollense Valley near Weltzin (adapted from Lorenz et al., 2014).

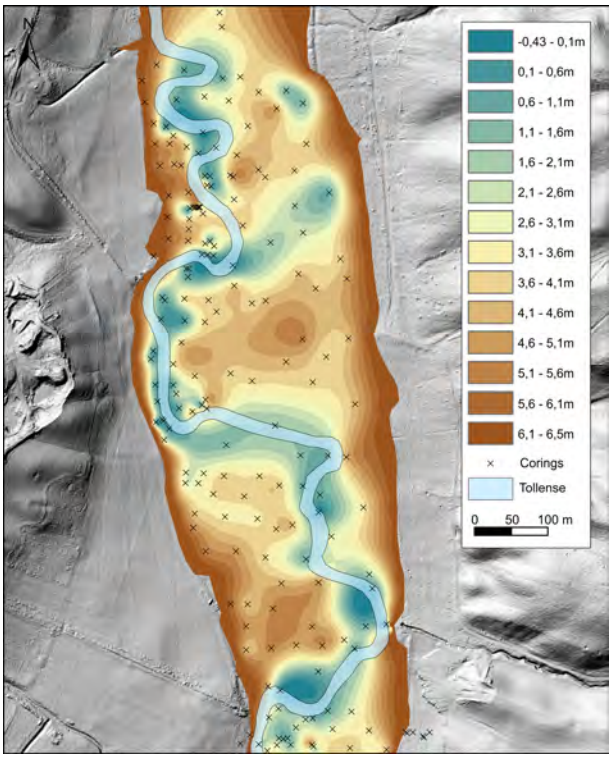

Figure 5. The minerogenic valley ground with incised palaeochannel derived from corings (adapted from Lorenz et al., 2014). Elevations are given in metres above sea level (m a.s.l.).

7 Weichselian Late Glacial to Holocene valley formation

The river Tollense, which is today 5–15 m wide and up to 4 m deep, flows in a 250–400 m wide incised valley of subglacial origin. The development of vast mires during the Holocene in the low river valleys south to the Baltic Sea was firstly associated with the rising Littorina Sea by Keilhack (1898). The current state of knowledge on the postglacial development of coastal river valleys and its mires has been comprehensively framed by Janke (2002, 1978), distinguishing 10 phases of valley formation from the deglaciation of the Mecklenburg Phase to the present (Börner et al., 2012, pp. 292–296). The valley of the river Tollense between Weltzin and its confluence with the river Peene in Demmin has been investigated with more than 250 corings and soil logs to reconstruct the Holocene palaeoenvironment with a special focus on the 1.5 km river course around the Bronze Age battlefield (Lorenz et al., 2014).

The Pleistocene ground of the valley consists of glaciofluvial sands and gravels. During the Pleniglacial and Preboreal/Boreal, deep gullies were fluvially eroded and subsequently filled with organic gyttjas and sand, rich in molluscs. Outside the gullies, the Pleistocene valley ground does not show a uniform gradient. In the Tollense Valley between Demmin and Weltzin the start of the limnic or organic sedimentation occurred from the Weichselian Late Glacial to Preboreal period (Lorenz et al., 2014, ca. 10 300–12 500 cal BP) and is therefore completely independent of the Baltic Sea level, which was at this time more than 15 m below (Lampe, 2005). A preferred direction of the onset of sedimentation against or along the decline of the valley is not recognisable. Furthermore no influence of the backlog caused by the Littorina transgression (Richter, 1968; Michaelis and Joosten, 2007) could be detected. The stratigraphies within the mire can be described as three standard profiles (Fig. 4): (1) alluvial fans, (2) fluvially influenced mire and (3) fluvially unaffected mire. Each has a decomposed peat at the surface, severely degraded by drainage and bearing iron concretions down to ca. 70 cm. Dumping of dredging materials from the river and ploughing in the recent past have also disrupted the mire surface.

The alluvial fans consist of morainic debris and belong to large gullies in the valley slopes, which were mainly created under periglacial conditions, but were fossilised with the onset of the Holocene and have been reshaped by colluvial sediments since the Subboreal. At some places, the alluvial fans narrow the valley and influence the river's course. This is the case for site Weltzin 20, where the surface of an alluvial fan with superimposed peat layers was excavated.

The fluvially unaffected mire is represented by peats of reed and sedges, which were initially formed by drowning, and then subsequently grew up with the rising groundwater table, overprinted by episodic floods of the river. This is indicated in particular by the absence of molluscs and minerogenic layers. Wood remains were rarely found in peat. At depths between 150 and 200 cm, the peat is underlain by buried humic gleyic soil. In contrast, the areas affected by fluvial sedimentation show no exclusive peat stratigraphy but interbedding with fluvial sands and organic gyttjas with numerous wooden remains and molluscs underneath a strongly decomposed peat. The alternating sequences reach thicknesses up to 4 m and represent deposits of slowly flowing to stagnant water. These sediments comprise many records of natural driftwood, but also artificial piles, wooden structures and fish fences, dating not only to the Bronze Age.

The reconstructed minerogenic valley ground reveals a 50–200 m wide channel, which is at least 2 m incised in the valley floor (Fig. 5). It runs in large meander loops, while a slope to the north or south cannot be derived. This structure is interpreted as a Weichselian Late Glacial riverbed, which can be attributed to the Dryas phases (Janke, 1978; Börner et al., 2012). The occurrence of the younger fluvial deposits is limited to this former riverbed, and today's river Tollense runs with smaller meanders within these boundaries (Fig. 5). The Weichselian Late Glacial riverbed has evidently been inherited and traced throughout the Holocene; younger river courses other than that channel are not recognisable.

8 The Bronze Age environment

The Bronze Age find layers in the Tollense Valley differ in depth and sedimentological composition, but are always connected to fluvial sediments and their distribution of the former riverbed, which has been relocated in the last 3000 years only to a small extent. In addition to the interpretation of sedimentological parameters, analyses of botanical remains, wood species identification and pollen analyses were carried out to reconstruct the Bronze Age environment. Sediments and microfossils indicate clear differences in groundwater level and vegetation between the Bronze Age environment and the present-day appearance of the landscape (Lorenz et al., 2014).

The river Tollense is considered to have formed a shallower, and presumably broader, riverbed for this period. The close proximity of sands and organic deposits suggests fluctuating but generally lower flow velocities. The river was overgrown with aquatic plants and only the respective current line transported sands. The mire surface at that time was still about 1 m lower, so the alluvial fans clearly outlined into the valley. During floods, they were obstacles where floating debris accumulated like proposed for site Weltzin 20, where numerous skeletal remains and wooden material have been excavated. Due to rearrangements by the fluctuating run-off, wooden branches and skeletal remains remained in the (semi)aquatic environment, were subsequently covered by sediments and conserved or rearranged on a small scale along the river banks. During the Bronze Age, the Tollense Valley was dominated by vast *Carex* reeds with open water surfaces. Today's meadows exist on meliorated and degraded peatlands that are extensively used for agriculture. In comparison, the hydraulic configuration of the river also stands in strong contrast. Today the river Tollense is strongly incised into the surrounding peatlands, due to straightening and shortening of the river course, as well as by annual river maintenance with the clearing and partly dredging of the riverbed. Increased flow velocities cause very steep embankments and the formation of a trough-like channel.

Data availability. Geological data can be requested from the authors.

Author contributions. GL and SL wrote the paper and prepared all figures.

Competing interests. The authors declare that they have no conflict of interest.

Acknowledgements. The research in the Tollense Valley and the results presented here involve a large number of people whom we would like to thank in this regard. We further acknowledge support for the Tollense Valley project from the German Research Foundation between 2010 and 2017 (DFG, nos. JA 1835/2 and TE 258/8). We would also like to thank the anonymous reviewer for helpful comments on the manuscript. We acknowledge support for the article processing charge from the DFG (no. 393148499) and the Open Access Publication Fund of the University of Greifswald.

Financial support. This research has been supported by the DFG (German Research Foundation, grant no. 393148499) and the Open Access Publication Fund of the University of Greifswald.

References

Brinker, U., Harten-Buga, H., Staude, A., Jantzen, D., and Orschiedt, J.: Prehistoric Warfare and Violence, chap. Perimortem Lesions on Human Bones from the Bronze Age Battlefield in the Tollense Valley: An Interdisciplinary Approach, 39–60, Springer International Publishing, Cham, https://doi.org/10.1007/978-3-319-78828-9_3, 2018.

Börner, A., Janke, W., Lorenz, S., Pisarska-Jamroży, M., and Rother, H.: Das Jungquartär im Binnenland Mecklenburg-Vorpommerns – glaziale Morphologie, Gewässernetzentwicklung und holozäne Landnutzungsgeschichte, in: Jahresberichte und Mitteilungen des Oberrheinischen Geologischen Vereins, N.F., 94, 287–313, 2012.

Janke, W.: Schema der spät- und postglazialen Entwicklung der Talungen der spätglazialen Haffstausee-Abflüsse, Wissenschaftliche Zeitschrift der Ernst-Moritz-Arndt-Universität Greifswald, Mathematisch-naturwissenschaftliche Reihe, 27, 39–43, 1978.

Janke, W.: The development of the river valleys from the Uecker to the Warnow, Greifswalder Geographische Arbeiten, 31, 101–106, 2002.

Jantzen, D., Brinker, U., Orschiedt, J., Heinemeier, J., Piek, J., Hauenstein, K., Krüger, J., Lidke, G., Lübke, H., Lampe, R., Lorenz, S., Schult, M., and Terberger, T.: A Bronze Age battlefield? Weapons and trauma in the Tollense Valley, north-eastern Germany, Antiquity, 85, 417–433, https://doi.org/10.1017/S0003598X00067843, 2011.

Jantzen, D., Lidke, G., Dräger, J., Krüger, J., Rassmann, K., Lorenz, S., and Terberger, T.: An early Bronze Age causeway in the Tollense Valley, Mecklenburg-Western Pomerania – The starting point of a violent conflict 3300 years ago?, Bericht der Römisch-Germanischen Kommission, 95, 13–49, https://doi.org/10.11588/berrgk.2017.0.44423, 2014.

Keilhack, K.: Die Entwicklung der glazialen Hydrographie Norddeutschlands, Zeitschrift der deutschen Geologischen Gesellschaft, 50, 77–83, 1898.

Krüger, J., Nagel, F., Nagel, S., Jantzen, D., Lampe, R., Dräger, J., Lidke, G., Mecking, O., Schüler, T., and Terberger, T.: Bronze Age tin rings from the Tollense valley in Northeastern Germany, Praehist. Z., 87, 29–43, https://doi.org/10.1515/pz-2012-0002, 2012.

Lampe, R.: Lateglacial and Holocene water-level variations along the NE German Baltic Sea coast: review and new results, Quatern. Int., 133, 121–136, 2005.

Lidke, G., Jantzen, D., Lorenz, S., and Terberger, T.: The Bronze Age battlefield in the Tollense Valley, Northeast Germany: conflict scenario research, in: Conflict archaeology: Materialities of collective violence in late prehistoric and early historic Europe, edited by: Fernández-Götz, M. and Roymans, N., vol. 5 of Themes in Contemporary Archaeology, 61–68, 2018.

Lorenz, S., Schult, M., Lampe, R., Spangenberg, A., Michaelis, D., Meyer, H., Hensel, R., and Hartleib, J.: Geowissenschaftliche und paläoökologische Ergebnisse zur holozänen Entwicklung des Tollensetals, in: Tod im Tollensetal – Forschungen zu den Hinterlassenschaften eines bronzezeitlichen Gewaltkonfliktes in Mecklenburg-Vorpommern, edited by: Jantzen, D., Orschiedt, J., Piek, J., and Terberger, T., vol. 50 of Beiträge zur Ur- und Frühgeschichte Mecklenburg-Vorpommerns, 37–60, Landesamt für Kultur und Denkmalpflege Mecklenburg-Vorpommern, 2014.

Michaelis, D. and Joosten, H.: Mire development, relative sea-level change, and tectonic movement along the Northeast-German Baltic Sea coast, Bericht der Römisch-Germanischen Kommission, 88, 101–134, 2007.

Price, D., Frei, R., Brinker, U., Lidke, G., Terberger, T., Frei, K., and Jantzen, D.: Multi-isotope proveniencing of human remains from a Bronze Age battlefield in the Tollense Valley in northeast Germany, Archaeol. Anthrop. Sci., https://doi.org/10.1007/s12520-017-0529-y, 2017.

Richter, G.: Fernwirkung der litorinen Ostseetransgression auf tiefliegende Becken und Flußtäler, Eiszeitalter und Gegenwart, 19, 48–72, 1968.

Terberger, T. and Heinemeier, J.: Die Fundstelle im Tollensetal und ihre absolute Datierung, in: Tod im Tollensetal – Forschungen zu den Hinterlassenschaften eines bronzezeitlichen Gewaltkonfliktes in Mecklenburg-Vorpommern. Teil 1: Die Forschungen bis 2011, edited by: Jantzen, D., Orschiedt, J., Piek, J., and Terberger, T., vol. 50 of Beiträge zur Ur- und Frühgeschichte Mecklenburg-Vorpommerns, 101–116, Landesamt für Kultur und Denkmalpflege Mecklenburg-Vorpommern, 2014a.

Terberger, T., Dombrowsky, A., Dräger, J., Jantzen, D., and Lidke, G.: Professionelle Krieger in der Bronzezeit vor 3300 Jahren? Zu den Überresten eines Gewaltkonfliktes im Tollensetal, Mecklenburg-Vorpommern, in: Gewalt und Gesellschaft. Dimensionen der Gewalt in ur- und frühgeschichtlicher Zeit, edited by: Link, T. and Peter-Röcher, H., vol. 259 of Universitätsforschungen zur Prähistorischen Archäologie, 93–109, 2014b.

Terberger, T., Jantzen, D., Krüger, J., and Lidke, G.: Das bronzezeitliche Kampfgeschehen im Tollensetal – ein Großereignis oder wiederholte Konflikte?, in: Bronzezeitliche Burgen zwischen Taunus und Karpaten: Beiträge der Ersten Internationalen LOEWE-Konferenz vom 7. bis 9. Dezember 2016 in Frankfurt/M., edited by: Hansen, S. and Krause, R., vol. 319 of Universitätsforschungen zur prähistorischen Archäologie, 103–123, 2018.

DEUQUA Spec. Pub., 2, 77–81, 2019
https://doi.org/10.5194/deuquasp-2-77-2019

Open Access DEUQUA Special Publications

The Müritzeum in Waren (Müritz): natural history museum and modern nature discovery centre

Mathias Küster[1,2]

[1]Institute of Geography and Geology, University of Greifswald, Friedrich-Ludwig-Jahn-Straße 16, 17487 Greifswald, Germany
[2]Department for Exhibition and Natural History Collections, Müritzeum gGmbH, 17192 Waren (Müritz), Germany

Correspondence: Mathias Küster (m.kuester@mueritzeum.de)

Relevant dates: Published: 15 August 2019

How to cite: Küster, M.: The Müritzeum in Waren (Müritz): natural history museum and modern nature discovery centre, DEUQUA Spec. Pub., 2, 77–81, https://doi.org/10.5194/deuquasp-2-77-2019, 2019.

Abstract: The Müritzeum is a nature discovery centre and a museum in the heart of the Mecklenburg Lake District. It is the first natural history museum in Mecklenburg-Vorpommern, with natural history collections that are over 150 years old, and are still growing today. The collections contain about 290 000 specimens from the fields of botany, zoology and geology. An extensive library and an archive are also part of the museum. Collecting, preserving and researching natural history are our main spheres of activity. The exhibition in the Müritzeum offers the visitor a comprehensive insight into the development of the nature and landscape of northeastern Germany and of Mecklenburg-Vorpommern and the Lake Müritz region in particular. The largest aquarium for indigenous freshwater species in Germany enables visitors to imagine themselves in the underwater world of the Mecklenburg Lake District.

1 History of the museum – an outline

The museum of natural history in Waren (Müritz) has existed for over 150 years. In the 18th and 19th centuries there were extensive natural history collections in private cabinets and at universities of varying sizes. However, these were not accessible to the public. In 1866, Freiherr Hermann von Maltzan (1843–1891) founded the "von Maltzan'sche Naturhistorische Museum für Mecklenburg" (the von Maltzan's museum of natural history for Mecklenburg, also known as the "Maltzaneum"). It was the first official museum of natural history in the then Grand Duchy of Mecklenburg-Schwerin (Seemann, 2018a). The founder's aim was to provide natural scientists a platform for professional exchange and to give the public the opportunity to find out about their local environment. The natural history collections laid the foundation for our museum. In the founding years and beyond, Hermann von Maltzan and the first curator and director of the museum, Carl Struck, were very active members of the "Verein der Freunde der Naturgeschichte in Mecklenburg" (Association of friends of natural history in Mecklenburg). In this way, many contacts were established with collectors, thus the natural history collections grew significantly.

By buying and selling real estate, the collection was housed in several locations in Waren (Müritz) in the years from 1884 to 1929. After that it arrived in its present location, in the present-day House of Collections, which was an old public school in 1929 (Fig. 1), through the support of the association "Vereinigung für Heimatschutz" (an organisation for regional conservation). In the coming years the museum's curatorial teams, who were members of the association, worked on a voluntary basis.

Figure 1. The historical building that is today the "House of Collections" (Photo: Müritzeum).

Figure 2. The new exhibition building "House of 1000 Lakes" (Photo: Mirko Runge).

During the Second World War the museum and the collections were largely spared from destruction, however, during the last days of the war several specimens of the bird collection were stored in the Sophienhof castle near Waren (Müritz). The castle and nearly all specimens were destroyed by arson (Seemann, 2018a). In the post-war years, the insect collection was considerably expanded and reorganised. A specialist library, among other things, was set up by Carl Hainmüller (1875–1956).

In 1957 the Maltzaneum was united with the local history museum under the name "Müritz-Museum". The exhibition was reorganised, and the focus was put on educational and nature conservation tasks. In 1973, the Museum got the status of a special museum for state culture, nature conservation and the environment. After excluding the prehistoric and historic collections, the renovation of the museum building between the years 1982 and 1991, and its reorganisation, the museum got its mission statement, making it the "Natural History Museum for the State of Mecklenburg-Vorpommern" (Seemann, 2018a).

In 1982 the "Müritz-Aquarium" was founded as a part of the Müritz-Museum. The construction of a large aquarium with native freshwater fish species was an absolute novelty in northeastern Germany. A total of 25 000 L of water were distributed in 16 aquariums, the largest of which contained 8000 L of water. More than 20 native species of fish were presented in the tanks.

In 2007, a project of remodelling, lasting several years, ended, accompanied by renovation work on the historic museum building, the House of Collections, and the construction of a new modern exhibition building, the "House of 1000 Lakes" (Fig. 2). Since the foundation of the Müritzeum gGmbH in 2007, visitors have been able to gain a lasting insight into nature from a modern exhibition, the largest aquarium for local freshwater species and the museum garden.

2 Natural history collections

Over a period of 150 years approx. 290 000 natural historical specimens have been collected. In one specimen several individuals of one species can be combined, thus there are several million natural history objects. The specimens are housed either in depots or in the exhibition. The collections consist of botanical, zoological and geological specimens. These collections are taken mainly from the area of Mecklenburg-Vorpommern but, with regard to the entire collection of individual collectors, some specimens from all over the world have been added to the collections.

In addition, over the years an extensive archive, with reference to the collections or the collectors, has been created. This includes field descriptions, collection catalogues, correspondence and maps. A recent census showed a stock of over 80 000 photos. The library holds over 16 000 books, 12 000 journals and 1200 special editions. Content from the fields of botany, zoology, geology, geography, forestry and hunting sciences, agriculture, landscape history and nature conservation is presented. A total of 1200 books are over 100 years old. The oldest book is from 1588.

The most extensive collection of the natural history collections is that of the insects (Fig. 3). Today it contains roughly 175 000 specimens. The collection of small butterflies and moths is especially worth mentioning here, with 7500 specimens it is the largest collection of its kind in Mecklenburg-Vorpommern. The coleopteran beetle collection, with 42 000 specimens, is also of great importance. The cerambycid collection with 6317 specimens from 505 species and 61 subspecies is the largest in Mecklenburg-Vorpommern (Seemann, 2018a). The most recent additions to the collection were in 2017 (Schemschat, 2017).

The bird collection includes 3030 mounted and prepared birds and bird bodies, 4115 clutches with more than 11 000

Figure 3. Insects form a large part of the natural history collection (Photo: Sebastian Köpcke and Volker Weinhold).

Figure 4. Subfossil record: historical specimen of a Mammoth molar tooth found in 1883 (Photo: Müritzeum).

eggs, 696 plucked birds, and around 300 skeletons (Seemann, 2018a). Nearly all breeding native bird species and birds of passage or vagrant species have been collected (Seemann and Seemann, 2011). For several years the Müritzeum has been a partner in the joint cause of the state project "Research into causes of death" together with the State Office for the Environment, Nature Conservation and Geology of Mecklenburg-Vorpommern and the Leibniz Institute for Zoo and Wildlife Research in Berlin. Investigated mortal finds, especially of white-tailed eagles and ospreys, are documented and included in the collection (Seemann and Seemann, 2011).

Other zoological collections are the mammal collection (including subfossil records, Fig. 4); the mollusc collection; and small collections of amphibians, reptiles, fish, crabs, leeches, and spiders. Nearly 35 000 plants, comprising flowering plants, ferns, mosses, algae and fungi, are also part of the biological collections.

About 25 000 specimens, including rocks, minerals and fossils belong to the geological collection. Above all, Nordic debris ("Geschiebe") from Scandinavia, the Baltic Sea region and Mecklenburg-Vorpommern are of great importance for the "ice age region" of northern Germany. The latest addition was a collection of Nordic debris in 2016 (Günther and Küster, 2018). Currently, a transfer to the museum is being prepared for a collection with numerous specimens, including holotypes from the Cambrian.

In addition to the preservation of the collections and the planning and realisation of exhibitions, research is carried out on the natural history collections by the scientific staff of the museum, external scientists and volunteers. Among other things, this research deals with natural history questions about specimens; Glacial, Holocene, and recent species distribution and species change; and studies of collectors and collection history (see Ukkonen et al., 2011; Küster and Günther, 2016; Seemann, 2018b, c; Thiele et al., 2018).

3 Exhibition

The permanent exhibition in the Müritzeum gives visitors a comprehensive insight into the nature and the development of the landscape of northeastern Germany. A wide range of interaction and exploration facilities are offered to the visitors. Especially in the House of the 1000 Lakes one can enjoy the bird exhibits, the forest, a journey through time from the Ice Age to the present, and the formation and the development of Lake Müritz with its underwater world. In the bird exhibition space, the visitor is shown the diversity of birdlife by, for example, listening to bird songs and calls in the concert hall. Interesting facts about bird migration and bird research are also shared. The newly designed "high-tech balloon room" realistically simulates a crossing over the Mecklenburg Lake District (Küster, 2018a).

The life of trees can be traced from the root to the treetop in the forest room. A 1000-year-old oak tree tells the history of the forest over centuries. The "forest at night" room offers the possibility of listening to the sound of the forest at night, a single button press and you are face-to-face with the animals. The new exhibition space for the UNESCO World Natural Heritage listed ancient beech forests of Germany explains the importance of these rare and unique habitats (Fig. 5, Küster, 2018a).

The largest aquarium for indigenous freshwater species in Germany, presenting the underwater world of the Mecklenburg Lake District, always causes astonishment. This 100 000 L fish tank that extends over two levels, with hundreds of whitefish moving in an unbroken circle attracting the visitors' attention (Fig. 6). In 26 "near-natural" large and small fish tanks, one can discover about 50 different types of fish, in addition to crabs, terrapins, mussels, snails and aquatic plants.

The House of Collections not only presents the collections of natural history in magazines, the library and the archive but also a permanent exhibition about collecting, preserv-

Figure 5. New exhibition – the UNESCO World Natural Heritage listed ancient beech forests of Germany (Photo: Mirko Runge).

Figure 6. The 100 000 L fish tank containing 300 whitefish is a highlight of the aquarium area of the museum (Photo: Werk3/Andreas Duerst).

ing and researching natural history as well as special exhibitions about environmental and historical topics. Around 1500 specimens of the natural history collection can be admired in the entirety of the Müritzeum.

A circular path leads you around the Herrensee in the museum garden. As a natural body of water it is the habitat of many species of breeding birds. An artificial island built in 2018 helps secure the population of a colony of black-headed gulls that has been breeding on the site for 50 years (Küster, 2018b). Large erratic boulders protected as geotops, as well as a boulder garden, give evidence of the geological past of the region and the origin of the rocks (Günther, 2010).

Data availability. All data relevant for this contribution are presented within the article itself.

Competing interests. The author declares that there is no conflict of interest.

Acknowledgements. I would like to thank Ralf Scheibe (Greifswald) for the review. We acknowledge support for the article processing charge from the DFG (no. 393148499) and the Open Access Publication Fund of the University of Greifswald.

Financial support. This research has been supported by the DFG (German Research Foundation, grant no. 393148499) and the Open Access Publication Fund of the University of Greifswald.

References

Günther, A.: Die Geologische Sammlung im Müritzeum in Waren (Müritz), Neubrandenburger Geologische Beiträge, 10, 131–144, 2010.

Günther, A. and Küster, M.: Gesteinssammlungen aus dem Strelitzer Land im Müritzeum, in: Zur Geologie und Landschaft des Strelitzer Landes, edited by: Naturschutzbund Deutschland e.V., Regionalverband Mecklenburg Strelitz, Labus – Sonderheft 25, Phönix Multimedia, Neustrelitz, Germany, 148–154, 2018.

Küster, M.: Neue Impulse in der Dauerausstellung des Müritzeums 2018, Mitteilungen des Museumsverbandes Mecklenburg-Vorpommern, 27. Jahrgang, 48–49, 2018a.

Küster, M.: Eine neue Brutinsel im Herrensee – aktiver Vogelschutz im Müritzeum, Mitteilungen des Museumsverbandes Mecklenburg-Vorpommern, 27. Jahrgang, 46–47, 2018b.

Küster, M. and Günther, A.: Aspekte zum Ichnofossil *Ophiomorpha nodosa* anhand eines norddeutschen Geschiebes, Geschiebekunde aktuell, 32, 113–119, 2016.

Schemschat, L.: Neues über die Käfersammlungen des Müritzeums in Waren (Müritz) (Coleoptera: Cerambycidae), Virgo, 19. Jahrgang, Heft 1, 33–35, 2017.

Seemann, F. and Seemann R.: Katalog der Vogelsammlung des Müritzeums, Präparate, Eier, Skelette, Rupfungen, Veröffentlichungen der Naturhistorischen Landessammlungen für Mecklenburg-Vorpommern im Müritzeum, 18, 270 pp., 2011.

Seemann, R.: Waren: Müritzeum with the Natural History Collections for the State of Mecklenburg-Vorpommern, in: Zoological Collections of Germany – The Animal Kingdom in its Amaz-

ing Plenty at Museums and Universities, edited by: Beck, L. A., Springer Nature, Cham, Switzerland, 647–658, 2018a.

Seemann, R.: Fundstücke – Seltene Druckwerke im Bestand der Naturhistorischen Landessammlungen für Mecklenburg-Vorpommern, Archiv Natur und Landeskunde Mecklenburg-Vorpommern, 55, 54–69, 2018b.

Seemann, R.: "Zwar weiß ich viel, doch will ich alles wissen..." – Die Geschichte(n) hinter den Sammlungen, Mitteilungen des Museumsverbandes Mecklenburg-Vorpommern, 27. Jahrgang, 16–20, 2018c.

Thiele, V., Blumrich, B., Gottelt-Trabandt, C., Schuhmacher, S., Eisenbarth, A., Berlin, A., Deutschmann, U., Tabbert, H., Seemann, R., and Steinhäuser, U., in cooperation with: Büsch, S., Duvekot, D., Schlomm, M., and Höfs, C.: Verbreitungsatlas der Makrolepidopteren Mecklenburg-Vorpommerns, Allgemeiner Teil und Artengruppen der Blutströpfchen, Schwärmer, Bären und Spinnenartigen, edited by: Landesamt für Umwelt, Naturschutz und Geologie Mecklenburg-Vorpommern and biota – Institut für ökologische Forschung und Planung GmbH, Steffen Media GmbH, Friedland, Berlin, Germany, 352 pp., 2018.

Ukkonen, P., Aaris-Sørensen, K., Arppe, L., Clark, P. U., Daugnor, L., Lister, A. M., Lõugas, L., Seppä, H., Sommer, R. S., Stuart, A. J., Wojtal, P., and Zupin, I.: Woolly mammoth (*Mammuthus primigenius* Blum.) and its environment in northern Europe during the last glaciation, Quaternary Sci. Rev., 30, 693–712, 2011.

DEUQUA Spec. Pub., 2, 83–88, 2019
https://doi.org/10.5194/deuquasp-2-83-2019

Open Access DEUQUA Special Publications

Late Glacial to Holocene dune development at southern Krakower See

Sebastian Lorenz[1], **Henrik Rother**[2], **Michael Kenzler**[1], **and Sara Kaphengst**[1]

[1]Universität Greifswald, Institut für Geographie and Geologie, Friedrich-Ludwig-Jahn-Straße 16–17, 17487 Greifswald, Germany
[2]Landesamt für Geologie und Bergwesen Sachsen-Anhalt, Köthener Straße 38, 06118 Halle, Germany

Correspondence: Sebastian Lorenz (sebastian.lorenz@uni-greifswald.de)

Relevant dates: Published: 15 August 2019

How to cite: Lorenz, S., Rother, H., Kenzler, M., and Kaphengst, S.: Late Glacial to Holocene dune development at southern Krakower See, DEUQUA Spec. Pub., 2, 83–88, https://doi.org/10.5194/deuquasp-2-83-2019, 2019.

Abstract: The site at the southern shore of Krakower See shows the Quaternary geology of the surrounding area. The local Quaternary sequence comprises a thickness of 50–100 m of Quaternary deposits while the surface morphology is dominated by the ice marginal position of the Pomeranian moraine, which passes through the area. The bathymetry of the lake basin of Krakower See indicates a predominant genesis by glaciofluvial erosion in combination with glacial exaration. Past research in this area has focussed on the reconstruction of Pleniglacial to Holocene environmental changes, including lake-level fluctuations, aeolian dynamics, and pedological processes and their modification by anthropogenic land use.

1 Quaternary deposits and geomorphological setting

The thickness of Quaternary sediments in the surrounding area of Krakow am See varies between 50 and 100 m due to a Mesozoic intrusion of a salt diapir into the Liassic and Lower Cretaceous record. Underneath the Pleistocene sediments, Liassic deposits directly occur (Schulz, 1963). There is evidence from the southern shore of Krakower See of (probably dislocated) Eemian lacustrine and telmatic sediments comprising a 6.4 m succession of organic gyttja rich in molluscs, and peat, overlying at least 22.4 m of Saalian deposits (Cepek, 1972). The Weichselian ice marginal positions of the Pomeranian Phase determine the morphological classification of the region. The maximum extent of the Pomeranian Phase represents an early Pomeranian advance, which is limited to the region west of Krakower See (Fig. 1 Rühberg et al., 1995). Overall, the region's morphogenesis reflects the interaction of ice marginal sedimentation and glacial thrusting within the context of a bulged salt diapir (Schulz, 1963).

Krakower See has been the subject of several geoscientific investigations since the end of the 19th century (Geinitz, 1886; Möckel, 1892; Ahrens, 1913; Schulz, 1963; Richter, 1963; Lorenz, 2007). It is situated within the terminal moraines of the Pomeranian Phase and finds its southern lake shore in the outwash plain (Fig. 1). Because of its position within the Pomeranian moraine belt and an adjacent glacial outwash plain to the south (Nossentiner Heide), the lake basin displays a complex morphology as a result of the combined influences of meltwater erosion and, to a lesser degree, of glacial exaration. In the past, geomorphological, palaeohydrological and palaeoecological research has focussed on the investigation of lake terraces, lake sediments and the genesis of the Nebel, which cuts across the moraines, draining

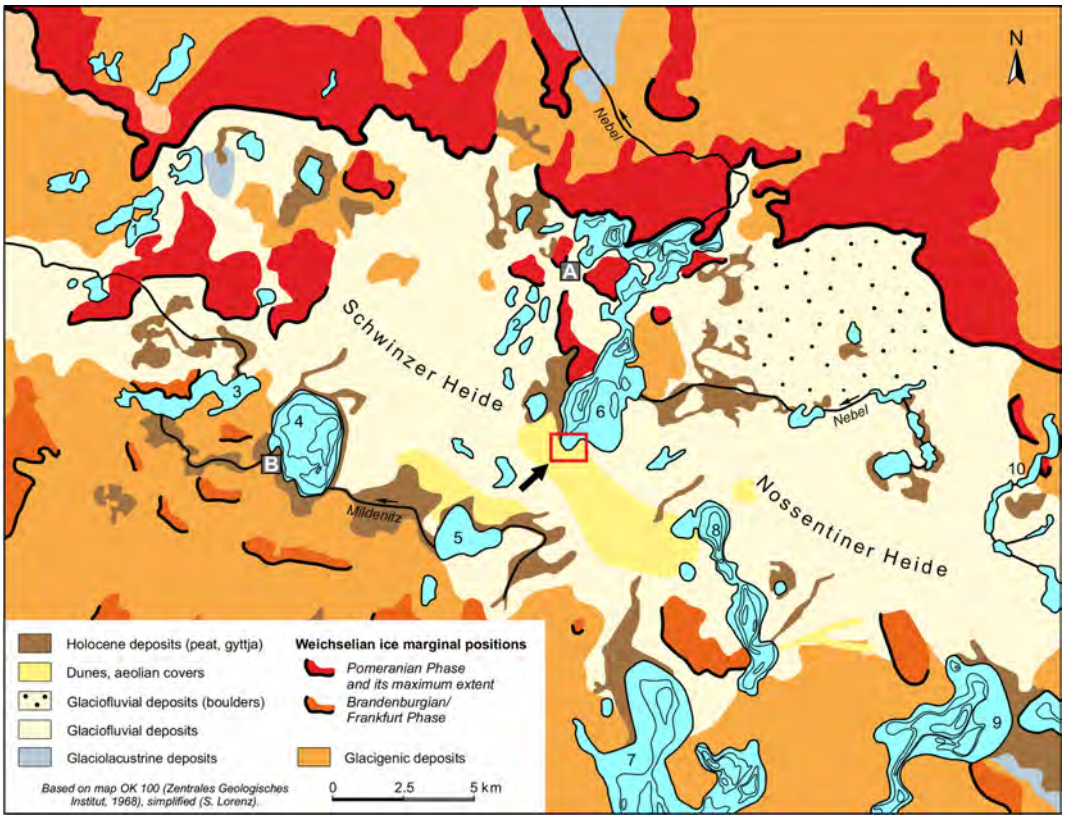

Figure 1. Simplified map of Quaternary sediments and landforms in central Mecklenburg after ZGI (1968a) and ZGI (1968b). Important lakes are numbered: 1 Woseriner See, 2 Langsee, 3 Dobbertiner See, 4 Goldberger See, 5 Damerower See, 6 Krakower See, 7 Plauer See, 8 Drewitzer See, 9 Fleesensee, 10 Tiefer See (Klocksiner Seenkette). Krakow am See (A) and Goldberg (B) are small towns in the mapped area.

Krakower See via the Warnow into the Baltic Sea (Rother, 2003; Viehberg, 2004; Hübener and Dörfler, 2004; Lorenz, 2003, 2007; Kaiser et al., 2007). Krakower See (16.48 km^2 with 21 islands, 47.5 m a.s.l., mesotrophic) is divided into five sub-basins orientated in a NNE–SSW direction. The proximity of the lake basin to the ice marginal zones and its morphometry suggest that the basin formation was predominantly forced by glacifluvial erosion (Schulz, 1963, 1994). An artificial dam, built in 1882, separates the lake at its narrowest part in the northern Untersee and southern Obersee. The river Nebel flows through the lake, entering Krakower See in the south-east and leaving it in the north-east using the aforementioned transverse valley across the Pomeranian moraine belt.

The 2 m lake terrace represents the highest reconstructed lake level of Lake Krakow at 51 m a.s.l., about 3 m above the present level. The terrace distribution varies between 1.5 and 3.2 m above the present water level and can be traced at a width of 200–500 m around the entire lake, with the best development observed on the southern lake shore (Fig. 3). The 2 m terrace shows an inclination of 0.6 % towards the lake and is built up by sandy substrates, and locally by gravel. Calcareous, mollusc-free glacilacustrine sediments occur at a depth between 60 and 180 cm frequently showing periglacial deformations (Fig. 3). Based on the distribution of the 2 m terrace and its associated stratigraphies and morphologies, such as fossil cliffs and glacilacustrine sediments, a late-glacial palaeo-lake of about 30 km^2 in size with a lake level at 51 m a.s.l. was reconstructed (Fig. 2). This palaeo-lake included 12 smaller and presently independent lakes in the vicinity, while the palaeo-lake itself had no drainage to the north. All islands of Krakower See show abrasion at the level of the 2 m terrace. So far, the age of the palaeo-lake has not been determined by absolute age dating. But the generally lower elevations, as well as the distinct differing content of microfossils (pollen, diatoms, ostracods, botanical remains) of lake sediments from the Allerød and the Younger Dryas in the littoral of the present lake, indicate an older Late Glacial palaeo-lake phase with more or less absent or not preserved microfossils displayed in lacustrine sediments incorporated in the 2 m terrace (Lorenz, 2007, pre-Allerød). The palaeo-lake phase ends during the final Younger Dryas with the incision of the transverse valley of the river Nebel causing a drop in the lake level (Rother, 2003; Kaiser et al., 2007). Lake terraces of Weichselian Late Glacial age are common features of Mecklenburgian lakes (Schulz, 1968; Kaiser et al., 2012).

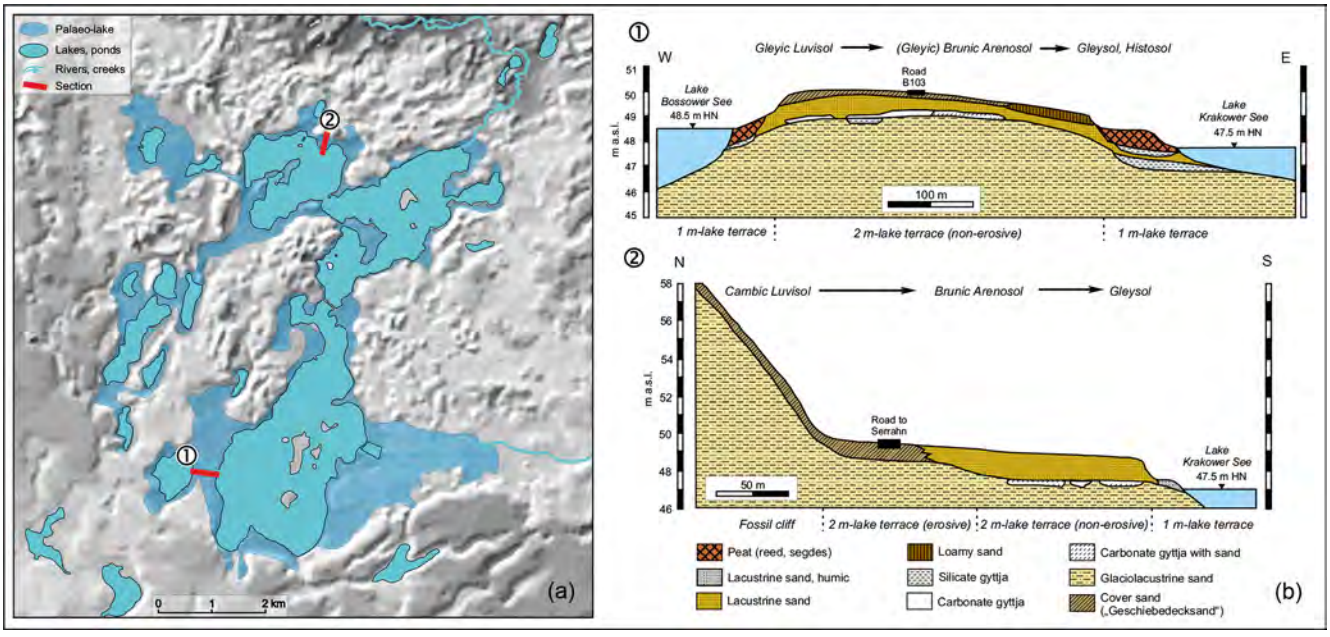

Figure 2. Extent of the Krakower See palaeo-lake during the Weichselian Pleniglacial to Late Glacial period **(a)** and pedo-geomorphic cross sections of associated lake terraces (**b**, modified, Lorenz, 2003).

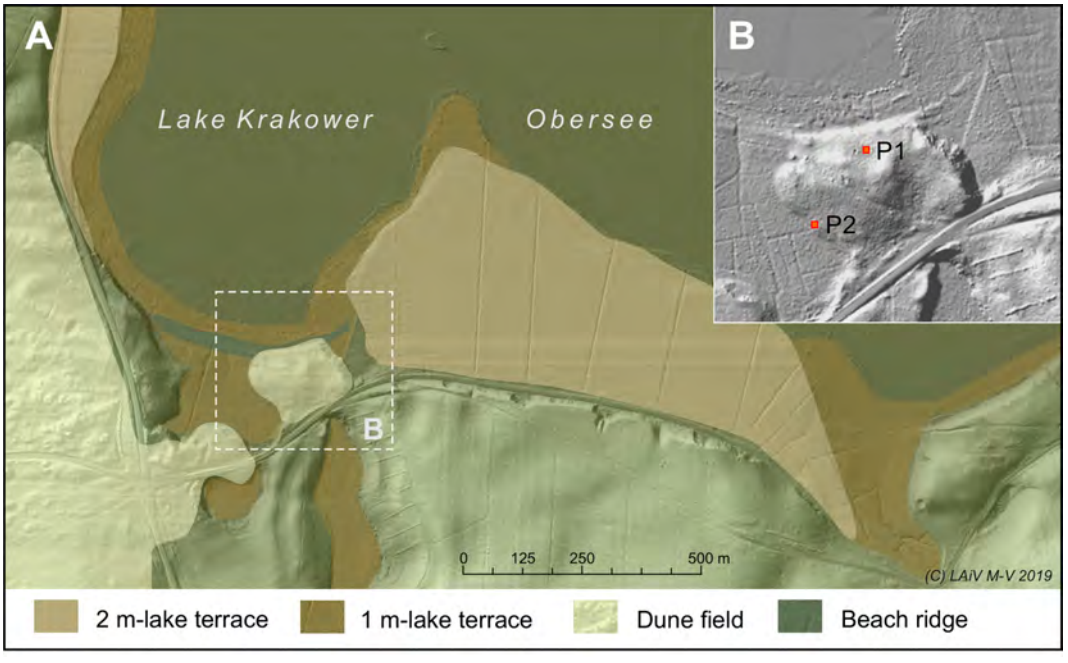

Figure 3. Lidar DEM showing littoral landforms and dune fields south of Krakower Obersee **(A)**. The inserted box **(B)** indicates the location of the presented soil profiles P1 and P2.

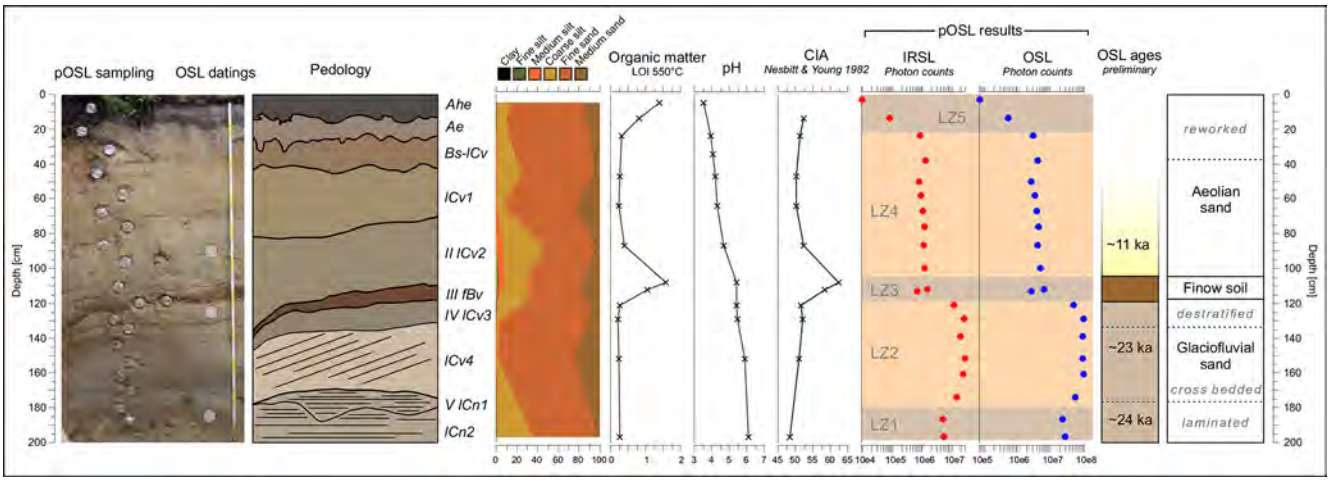

Figure 4. Lithology, stratigraphy and pedology after Eckelmann et al. (2006); luminescence zones (LZ) and geochronology of the Late Glacial to Holocene dune profile P1.

2 Dunes and palaeosols at southern Krakower See

The afforested dunes at southern Krakower See (Fig. 3, 53°35′32″ N, 12°15′59″ E) are of irregular shape and cover glacifluvial sands and gravels of the Pomeranian Phase. Their poorly developed or eroded top soils (predominantly podzolic Arenosols) include considerable amounts of incorporated charcoal, which points to a land-use history with deforestation resulting in a strong impact on the upper soil horizons (e.g. charcoal kilns). In addition to soils of late Holocene origin, a buried late glacial surface indicated by a Bwb horizon (brunic Arenosol) was revealed by pedological mapping (Lorenz, 2007; Kaiser et al., 2007). Based on its stratigraphic and pedological features, the brunic Arenosol has been classified as so-called Finow soil following Schlaak (1998, in German *Finowboden*). The Finow soil has been found and described by several authors in the northern parts of Germany and Poland and dates into the Allerød to Preboreal (e.g. Bussemer et al., 1998; Bogen et al., 2003; Kaiser et al., 2009; Küster and Preusser, 2010). Very close to a fossil cliff at the southern shore of Krakower See, a 10–20 cm thick Bwb horizon is preserved at depths between 60 and 120 cm. It represents a buried terrestrial surface without groundwater influence declining to the south. Thus, the buried surface at this location reveals a gradient orientated opposite to the present surface. A radiocarbon-dated charcoal particle from the Bwb horizon in profile P1 (Fig. 3) suggests the Late Glacial age of the palaeosol (12.9 ka calBP Kaiser et al., 2007), but further investigations with a portable optically stimulated luminescence (OSL) reader (pOSL Sanderson and Murphy, 2010) and common OSL datings have recently been carried out to gain an additional chronology for the formation of the overlying dunes (Fig. 4 Kaphengst, 2015).

The pOSL reader used for this study operates in continuous-wave stimulation mode with 880 nm for infrared stimulated luminescence (IRSL) and 470 nm for optical stimulated luminescence (OSL), where integrated IRSL and OSL signal intensities, depletion rates, and the IRSL / OSL ratio are measured. IRSL and OSL signal intensities respond to a combination of the post-depositional age of the sediment, the luminescence sensitivity of the tested mineral grains, the local dose rates, the completeness of bleaching and potentially inherited luminescence signals due to prior cycles of environmental irradiation (Sanderson and Murphy, 2010). A total of 20 samples have been measured without any chemical pretreatment. Based on the luminescence data (photon counts from the portable reader) profile P1 has five luminescence zones (LZs, Fig. 4). LZ1 relates to the lowermost part of the profile with laminated glacifluvial sediments. LZ2 comprises six samples, where the first and the last one indicate a mixed signal. The samples in between show similar photon counts, pointing to a rapid sedimentation of LZ1 and LZ2. Lamination and the cross-bedding in both luminescence zones give evidence for glacifluvial environments associated with the Pomeranian Phase. LZ3 represents the Bwb horizon of the brunic Arenosol from which two measurements were obtained. For this horizon clay, silt, organic content (LOI) and the chemical index of alteration (CIA Nesbitt and Young, 1982) have the highest values. The CIA is used as a geochemical indicator for the weathering of feldspar and the associated formation of clay minerals, which helps to detect palaeosol formation, e.g. in homogeneous sediment successions (p. 10 Sheldon and Tabor, 2009). LZ4 comprising predominantly unstratified fine sand with low organic content continues with nearly the same photon counts as in LZ3 and shows decreasing pH and CIA values. LZ4 is of aeolian origin. LZ5 represents the present A horizon in fine sand with a distinct podzolic influence and linearly decreasing photon counts from 25 cm upwards, which indicates a stratigraphic break probably related to hiatus. This section is characterised

by a minimum pH value of 3.6. However, the pOSL results illustrate nonuniform phases of sedimentation with the leaping photon counts.

The Bwb horizon of the brunic Arenosol lies in between laminated and cross-bedded glacifluvial deposits in the lower part and unstratified aeolian sediments in the upper part of profile P1. With similar stratigraphic position and lithology Küster and Preusser (2010) characterised the Bwb horizon for another site in southern Mecklenburg as a cover sand (GDS, *Geschiebedecksand*). The luminescence profiles show that the GDS has nearly the same photon counts as the overlying material. This indicates mixing of the material from the GDS and the aeolian coversands. The Finow soil shares properties with the cover sands (*Geschiebedecksand*), including poor sorting and a high content of finely grained aeolian sediment (Schlaak, 1998). Its depositional environment is assumed to have been influenced by weathering, but not by permafrost (p. 53 Bussemer et al., 1998). The preliminary OSL dates from profile P1 (Fig. 4) point to a Weichselian spectrum with Last Glacial Maximum ages for the well-stratified glacifluvial sediments and a Late Glacial age for the aeolian sands on top of the Finow soil. All three dates support the models of Finow soil formation mentioned above during the period from the Allerød to Preboreal.

The western fringe of the dune field comprises late Holocene dunes, which developed into the aggradational fringe of Krakower Obersee (Fig. 3, P2). Profile P2 shows a gleyic dystric Histosol covered by ca. 100 cm of aeolian sands. A remarkable feature in the profile is that organic soil horizons start 1 m above the present lake level. The dark and strongly organic fossil soil represents the lake level before the artificial lowering in 1836 by 1.05 m, which led to the formation of the 1 m lake terrace (Fig. 3 Lorenz, 2003). It is concluded that the dune field was built up by late glacial aeolian dynamics, as well as by the impact of historical land use. Both profiles indicate a constant reworking of the topsoils and late glacial aeolian sands.

Data availability. Laboratory data are available from the authors.

Author contributions. SL, HR, MK and SK participated in the fieldwork. SK performed the laboratory analyses and luminescence measurements. MK and HR conducted the luminescence datings. SL wrote the paper and prepared all figures. HR, MK and SK contributed to the paper.

Competing interests. The authors declare that they have no conflict of interest.

Acknowledgements. We would like to thank the anonymous reviewer for helpful comments on the paper. We acknowledge support for the article processing charge from the DFG (no. 393148499) and the Open Access Publication Fund of the University of Greifswald.

Financial support. This research has been supported by the DFG (German Research Foundation, grant no. 393148499) and the Open Access Publication Fund of the University of Greifswald.

References

Ahrens, H.: Terrassen an den Seen Mecklenburgs, Archiv des Vereins der Freunde der Naturgeschichte in Mecklenburg, 67, 1–55, 1913.

Bogen, C., Hilgers, A., Kaiser, K., Kühn, P., and Lidke, G.: Archäologie, Pedologie und Geochronologie spätpaläolithischer Fundplätze in der Ueckermünder Heide (Mecklenburg–Vorpommern), Archäologisches Korrespondenzblatt, 33, 1–20, 2003.

Bussemer, S., Gärtner, P., and Schlaak, N.: Stratigraphie, Stoffbestand und Reliefwirksamkeit der Flugsande im brandenburgischen Jungmoränenland, Petermann Geogr. Mitt., 142, 115–125, 1998.

Cepek, A.: Zum Stand der Stratigraphie der Weichsel-Kaltzeit in der DDR, Wissenschaftliche Zeitschrift der Ernst-Moritz-Arndt-Universität Greifswald, Mathematisch-Naturwissenschaftliche Reihe, 21, 11–21, 1972.

Eckelmann, W., Sponagel, H., Grottenthaler, W., Hartmann, K.-J., Hartwich, R., Janetzko, P., Joisten, H., Kühn, D., Sabel, K.-J., and Traidl, R.: Bodenkundliche Kartieranleitung. KA5, Schweizerbart Science Publishers, Stuttgart, Germany, 2006.

Geinitz, F. E.: Die Seen, Moore und Flußläufe Mecklenburgs – Ein Versuch zur Erklärung der Entstehung der Seen und Wasserläufe der norddeutschen Diluviallandschaft, sowie der Küstenbildung, Commissionsverlag Güstrow, 1886.

Hübener, T. and Dörfler, W.: Reconstruction of the trophic development of Lake Krakower Obersee (Mecklenburg, Germany) by means of sediment-diatom- and pollen-analysis, Studia Quaternaria, 21, 101–108, 2004.

Kaiser, K., Rother, H., Lorenz, S., Gärtner, P., and Papenroth, R.: Geomorphic evolution of small river-lake-systems in northeast Germany during the Late Quaternary, Earth Surf. Proc. Land., 32, 1516–1532, 2007.

Kaiser, K., Lorenz, S., Germer, S., Juschus, O., Küster, M., Libra, J., Bens, O., and Hüttl, R. F.: Late Quaternary evolution of rivers, lakes and peatlands in northeast Germany reflecting past climatic and human impact – an overview, E&G Quaternary Sci. J., 61, 103–132, https://doi.org/10.3285/eg.61.2.01, 2012.

Kaiser, K., Hilgers, A., Schlaak, N., Jankowski, M., Kuehn, P., Bussemer, S., and Przegietka, K.: Palaeopedological marker horizons in northern central Europe: characteristics of Lateglacial Usselo and Finow soils, Boreas, 38, 591–609, https://doi.org/10.1111/j.1502-3885.2008.00076.x, 2009.

Kaphengst, S.: Late Glacial and Holocene sedimentation and pedogenesis in the Pomeranian ice marginal zone (Mecklenburg): new insights from portable luminescence measurements and grain surface characterization, mathesis, University of Greifswald, Institute for Geography and Geology, 2015.

Küster, M. and Preusser, F.: Late Glacial and Holocene aeolian sands and soil formation from the Pomeranian outwash plain (Mecklenburg, NE-Germany), E&G Quaternary Sci. J., 58, 156–163, https://doi.org/10.3285/eg.58.2.04, 2010.

Lorenz, S.: Geomorphogenese, Sedimente und Böden der Terrassen am Krakower See in Mecklenburg – Untersuchungen zur jungquartären Paläohydrologie, Greifswalder Geographische Arbeiten, 29, 69–104, 2003.

Lorenz, S.: Die spätpleistozäne und holozäne Gewässernetzentwicklung im Bereich der Pommerschen Haupteisrandlage Mecklenburgs, Phd thesis, Universität Greifswald, Greifswald, available at: https://nbn-resolving.org/urn:nbn:de:gbv:9-000425-2 (last access: 8 July 2019), 2007.

Möckel, E.: Die Entstehung des Plauer Sees, des Drewitzer oder Alt-Schweriner Sees und des Krakower Sees, Druck der Rathsbuchdruckerei Güstrow, 1892.

Nesbitt, H. and Young, G.: Early Proterozoic climates and plate motions inferred from major element chemistry of lutites, Nature, 299, 715–717, https://doi.org/10.1038/299715a0, 1982.

Richter, G.: Untersuchungen zum spätglazialen Gletscherrückgang im mittleren Mecklenburg, Forschungen zur deutschen Landeskunde, 138, p. 98, Deutsche Akademie für Landeskunde, Bonn-Bad Godesberg, 1963.

Rother, H.: Die jungquartäre Landschaftsgenese des Nebeltales im Bereich der Pommerschen Hauptendmoräne bei Kuchelmiß (Mecklenburg), Greifswalder Geographische Arbeiten, 29, 105–141, 2003.

Rühberg, N., Schulz, W., von Bülow, W., Müller, U., Krienke, H.-D., Bremer, F., and Dann, T.: Mecklenburg–Vorpommern, in: Das Quartär Deutschlands, edited by Benda, L., Borntraeger, Berlin, 95–115, 1995.

Sanderson, D. and Murphy, S.: Using simple portable OSL measurements and laboratory characterisation to help understand complex and heterogeneous sediment sequences for luminescence dating, Quat. Geochronol., 5, 299–305, https://doi.org/10.1016/j.quageo.2009.02.001, 2010.

Schlaak, N.: Der Finowboden – Zeugnis einer begrabenen weichselspätglazialen Oberfläche in den Dünengebieten Nordostbrandenburgs, Münchener Geographische Abhandlungen, A49, 143–148, 1998.

Schulz, W.: Eisrandlagen und Seeterrassen in der Umgebung von Krakow am See in Mecklenburg, Geologie – Zeitschrift für das Gesamtgebiet der Geologie und Mineralogie sowie der angewandten Geophysik, 12, 1152–1168, 1963.

Schulz, W.: Spätglaziale und holozäne Spiegelschwankungen an den westlichen Oberen Seen Mecklenburgs, Archiv des Vereins der Freunde der Naturgeschichte in Mecklenburg, 12, 7–43, 1968.

Schulz, W.: Die geologische Situation im Naturpark Nossentiner-Schwinzer Heide, Naturschutzarbeit in Mecklenburg–Vorpommern, 37, 33–40, 1994.

Sheldon, N. D. and Tabor, N. J.: Quantitative paleoenvironmental and paleoclimatic reconstruction using paleosols, Earth-Sci. Rev., 95, 1–52, https://doi.org/10.1016/j.earscirev.2009.03.004, 2009.

Viehberg, F. A.: Paleolimnological study based on ostracods (Crustacea) in Late-glacial and Holocene deposits of Lake Krakower See (Mecklenburg-Vorpommern, NE-Germany), Studia Quaternaria, 21, 109–115, 2004.

ZGI: Zentrales Geologisches Institut – Geologische Karte der Deutschen Demokratischen Republik im Maßstab 1 : 100 000, Einheitsblatt 35 (Schwerin), 1968a.

ZGI: Zentrales Geologisches Institut – Geologische Karte der Deutschen Demokratischen Republik im Maßstab 1 : 100 000, Einheitsblatt 36 (Neubrandenburg), 1968b.

DEUQUA Spec. Pub., 2, 89–93, 2019
https://doi.org/10.5194/deuquasp-2-89-2019

DEUQUA Special Publications

Tiefer See – a key site for lake sediment research in NE Germany

Achim Brauer[1,2], **Markus J. Schwab**[1], **Brian Brademann**[1], **Sylvia Pinkerneil**[1], **and Martin Theuerkauf**[3]

[1]Section "Climate Dynamics and Landscape Evolution", GFZ German Research Centre for Geosciences, Potsdam, 14473, Germany
[2]Institute of Geosciences, Potsdam University, Potsdam, 14476, Germany
[3]Institute of Botany and Landscape Ecology, University of Greifswald, Greifswald, 17487, Germany

Correspondence: Achim Brauer (brau@gfz-potsdam.de)

Relevant dates: Published: 15 August 2019

How to cite: Brauer, A., Schwab, M. J., Brademann, B., Pinkerneil, S., and Theuerkauf, M.: Tiefer See – a key site for lake sediment research in NE Germany, DEUQUA Spec. Pub., 2, 89–93, https://doi.org/10.5194/deuquasp-2-89-2019, 2019.

Abstract: Tiefer See formed in a subglacial gully system at the end of the last glaciation in the northeast German lowlands. The lake has been selected as a focus site within the TERENO (Terrestrial Environmental Observatory) NE German observatory because it forms annual laminations (calcite varves) providing detailed information of past climate and environmental changes. Our research integrates palaeolimnology and limnology by combining high-resolution analyses of the sediment record with a comprehensive monitoring of the lake and its sedimentation processes since 2012. This allows evaluation of the observed effects of ongoing climate change in the context of the long-term history of the lake. The lacustrine sediment profile comprises the last 13 000 years and is dated by a multiple dating approach. The sedimentation is dominated by biochemical calcite formation and algal blooms. Detrital material from the catchment forms only a minor component even during times of increased human impact. Repeated changes between well-varved, poorly varved and homogeneous sediment intervals indicate that sedimentation processes in the lake are particularly sensitive to changes in lake circulation. The research at Tiefer See is embedded in ICLEA (https://www.iclea.de, last access: 2 August 2019) and BaltRap (https://www.io-warnemuende.de/projekt/167/baltrap.html, last access: 2 August 2019) projects.

1 Geomorphology and Geology

Tiefer See is part of the Klocksin lake chain, a subglacial gully system in a morainic terrain located in the natural park Nossentiner/Schwinzer Heide at 53°35.5′ N, 12°31.8′ E. The Klocksin lake chain extends from NNE to SSW and includes the four lakes Flacher See (64.4 m a.s.l.), Tiefer See (62.9 m a.s.l.), Hofsee (62.7 m a.s.l.) and Bergsee (62.6 m a.s.l.). The catchment geology of the northern part of the lake chain including Tiefer See is formed by tills while the southern part consists of glacifluvial sands. Numerous erratics along the shoreline of Tiefer See indicate the proximity of terminal moraines which formed during the Pomeranian ice advance W2 at around 16 kyr BP. Today, Tiefer See is connected to Hofsee in the south while the connection to Flacher See in the north has been channelised in a tunnel after construction of a railway dam between the two lakes. Tiefer See has a surface area of ca. 0.75 km^2 and the catchment area is about 5.5 km^2. With a maximum depth of 62 to 63 m Tiefer See is the deepest lake of the Klocksin lake chain (Fig. 1). It has no major inflow and outflow. The present-day lake water is mesotrophic and the circulation mode is

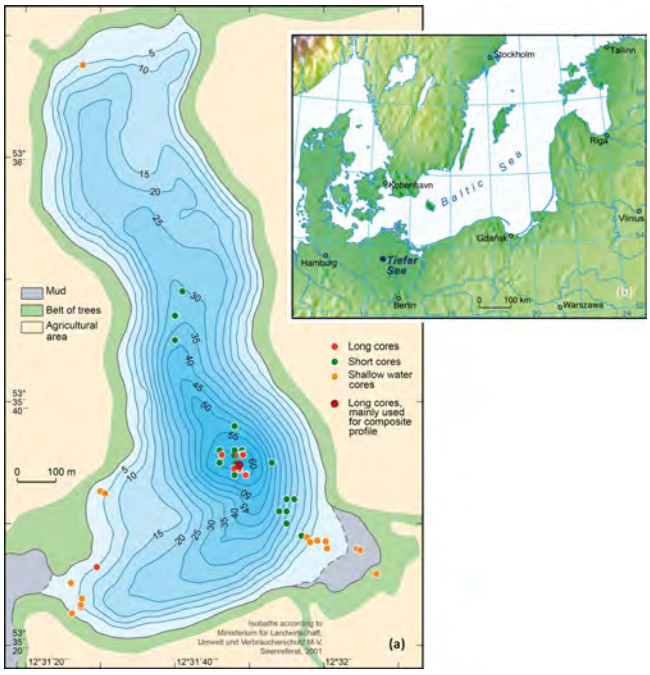

Figure 1. **(a)** Lake bathymetry and core locations (red: long cores; green: surface cores; orange: shallow water cores). **(b)** Tiefer See location.

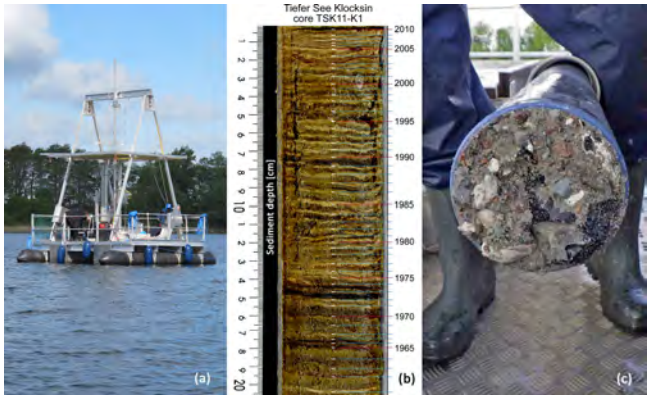

Figure 2. **(a)** GFZ lake sediment coring device (https://www.UWITEC.at, last access: 2 August 2019); **(b)** subrecent varves; **(c)** basal gravel and sand.

either mono- or dimictic, depending on the formation of a winter ice cover (Kienel et al., 2013). The climate is warm–temperate at the transition from oceanic to continental conditions. Mean monthly temperatures range from 0 °C in January to 17–18 °C in July with maxima up to 30 °C and minima down to −5 °C. Mean monthly precipitation varies between ca. 40 mm during winter and ca. 60 mm in summer with a mean annual precipitation of 560–570 mm. Although the catchment is mainly used for agriculture, the direct shoreline of the lake is covered by a fringe of trees without any buildings and roads.

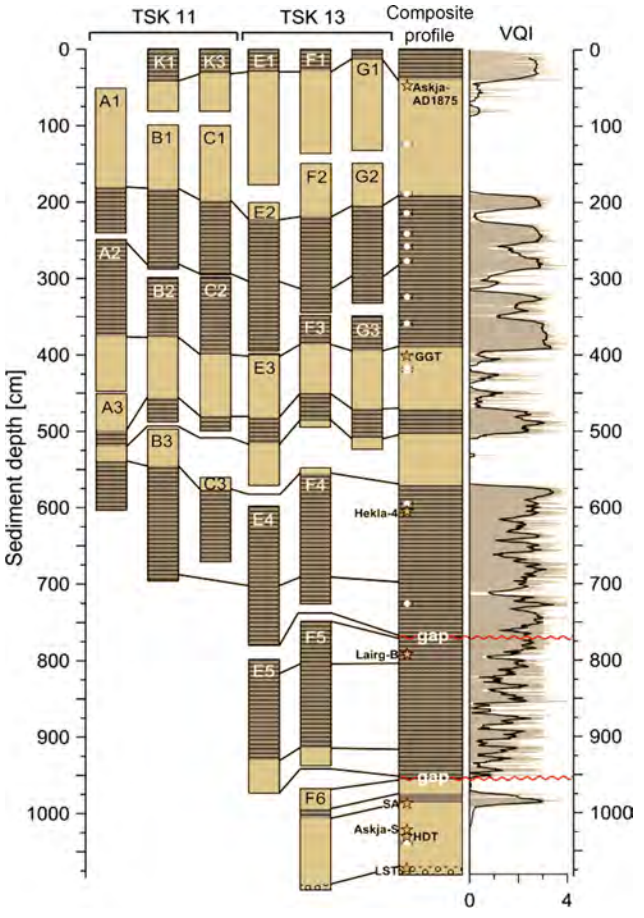

Figure 3. Schematic profiles of Tiefer See sediment cores and the respective composite profile with well-varved (dark) and non-varved (light) sections; white dots indicate AMS 14C dates, and orange stars show positions of cryptotephras (data from Wulf et al., 2016).

2 The sediment profile

In addition to several surface sediment cores from the entirety of the lake basin, a total of nine overlapping sediment cores have been obtained from the deepest part of the lake (Fig. 1a) with the GFZ piston coring device (Fig. 2a) during three field campaigns in 2011, 2013 and 2019. A composite profile has been established from six cores which includes two minor gaps below 7.5 m depth in the early Holocene (Dräger et al., 2017). These gaps have been closed with the new cores taken in 2019. The composite profile is about 11 m long and depicts a main lithological change from basal sands and gravel (Fig. 2c) to massive fine-grained and calcite-rich lacustrine sediments at about 10.7 m depth. At 10.4 m sediment depth (Fig. 3) a rapid transition to organic-rich sediments occurred. The organic-rich sediments vary in structure from finely laminated to poorly laminated and massive. The finely laminated sediments represent three different microfacies types of varves, (1) Ca-rhodochrosite varves, (2) or-

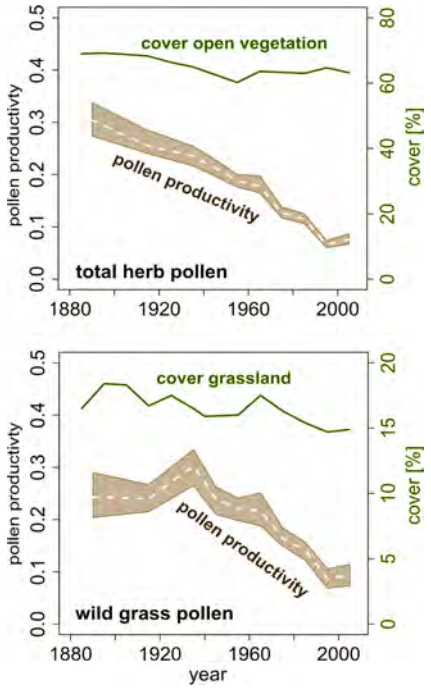

Figure 4. Changes in the cover of open vegetation and grasslands in the surroundings of Tiefer See, and changes in the mean pollen productivity of herbs and grasses since 1880 CE (after Theuerkauf et al., 2015).

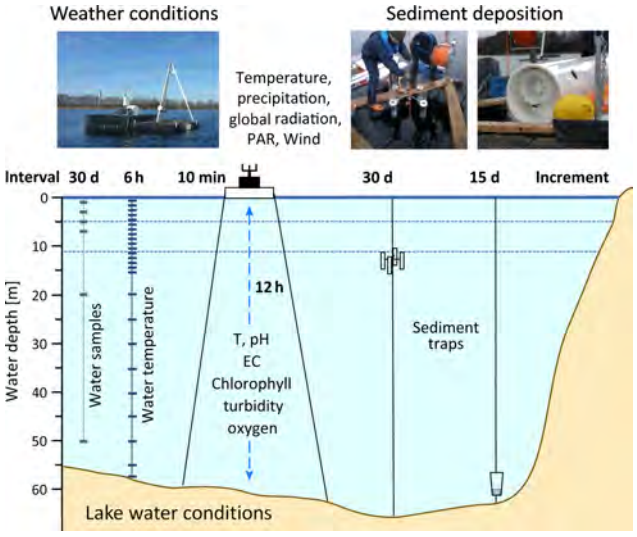

Figure 5. Sketch of installed lake sediment monitoring equipment in Tiefer See.

ganic varves and (3) calcite varves (Dräger et al., 2017). The most recent period of varve preservation began in 1924 CE (Kienel et al., 2017) with the formation of calcite varves (Fig. 2b). The alternation of varved and poorly or non-varved sediment intervals is also reflected in stable carbon isotope data of organic matter which is interpreted as variations between predominantly anoxic and oxic lake bottom waters (Dräger et al., 2019). The frequency and duration of poorly varved intervals increased during the late Holocene and has been related to either climatic changes (increased windiness) or human impact in the catchment (Dräger et al., 2017).

3 The age–depth model

Dating is crucial for robust reconstruction of past climate and environment changes. Therefore, a multiple dating approach has been applied for the sediment record from Tiefer See including varve counting, radiocarbon dating, tephrochronology and ^{10}Be analyses. Due to the minor gaps in the lower part of the sediment profile, a robust and continuous chronology could be established only for the last 6030 ± 85 yrs BP (ca. 7.5 m sediment depth). Varves have been counted using a petrographic microscope and non-varved intervals have been interpolated using sedimentation rate estimates based on microstructural analyses on thin sections. The resulting varve chronology has been confirmed by 12 radiocarbon dates of organic macroremains and by three cryptotephra horizons: (1) the Askja 1875 CE, (2) the Glen Garry (2088 ± 122 yrs BP) and (3) the Hekla 4 tephra (4293 ± 43 yrs BP). The identification of another five Holocene cryptotephras of Icelandic origin in the lower part of the sediment profile (Hässeldalen, Askja-S, Saksunarvatn, Lairg B; Wulf et al., 2016) provides a good estimate of the early Holocene age model. ^{10}Be data further confirmed the chronology and allowed an independent synchronisation with the varved sediment record from Lake Czechowskie a few hundred kilometres further east (Czymzik et al., 2015, 2018). The base of the profile is dated into the late Allerød through the detection of glass shards from the Laacher See eruption (12 880 yrs BP).

4 Pollen analyses

The seasonal resolution of the sediments allows for tracing historical land-use changes in great detail (Theuerkauf et al., 2015). Varve dating enabled us to accurately estimate pollen deposition of herbs and trees over the past 150 years, which has then been compared to the contemporaneous land cover documented in archival data (Fig. 4; Theuerkauf et al., 2015). Interestingly, the strong decline in herb pollen deposition since the 1950s did not reflect a change in the cover of arable land and grassland. Instead, pollen deposition of herbs and grasses was controlled by changes in pollen productivity in response to intensified land management. Today, grassland is mown earlier and more frequently, giving the grasses less time to flower and produce pollen than previously. This study demonstrated that the modern vegetation is not always a reliable reference for the past. Therefore, the ROPES approach without pollen productivity as a parameter has been developed for the long pollen record of the last 6000 years from Tiefer See (Theuerkauf and Couwenberg, 2018).

Pollen analyses in combination with sedimentological parameters as well as macrofossil and microfossil analysis from 20 sediment cores along the shore of Tiefer See and in adjacent peatlands were applied for Holocene lake level reconstruction. We found Holocene lake level fluctuations with an amplitude of about 10 m, which exceeds by far recently observed variations. Based on radiocarbon age modelling, the lowest lake levels occurred during the early Holocene and maxima in the medieval period. These changes are only partly related to climatic changes but we also observe a link to changes in forest cover. In particular during medieval times, large-scale forest opening likely increased groundwater formation and thus contributed to lake level increases.

5 Lake and sedimentation monitoring

A comprehensive lake monitoring instrumentation (Fig. 5) has been installed on Tiefer See since 2012 in order to decipher the response of the lake to ongoing climate change (Heinrich et al., 2018) and to study in detail the processes that transform weather signal into the sediment record. The instrumentation includes a permanent weather station on the lake measuring temperature, relative humidity, solar radiation, rainfall and wind speed in 10 min intervals. Attached to the weather station is an automatic probe that measures water parameters from the epilimnion to the lake bottom every 12 h. These measurements are complemented by temperature loggers permanently installed in 1 m apart down to 15 m water depth and 5 m apart down to 55 m depth. In addition, lake water is sampled monthly at water depths of 1, 3, 5, 7, 20 and 50 m for chemical analyses and stable oxygen and deuterium isotopes. Sediments are trapped in monthly intervals in two four-cylinder traps, one directly below the productive zone in the epilimnion and one in the hypolimnion. In the hypolimnion is a sequential trap with 15 d sample intervals installed. First results of the water isotope analyses revealed a seasonal 1.5 ‰ enrichment of δ^{18}O proving the expected evaporative loss of surface water of up to 10 % during the summer, which corresponds to the observed lake level drop of 50 cm. Interestingly, the deep water also generally has more positive δ^{18}O values than the annual rainwater mean collected on the weather station. The isotopic enrichment of the deep water indicates a long water residence time in the lake, which is likely due to the lack of major in- and outflows and low groundwater inflow. The intensive monitoring also allowed the investigation of the effects of the 2018 summer heatwave on the lake hydrology (Heinrich et al., 2019).

Data availability. No data sets were used in this article.

Author contributions. AB, MJS and MT wrote the text. SP, BB, MJS and MT participated in the fieldwork and took the photographs in Fig. 2. All authors contributed to the discussion and interpretation of the presented research results. Additional information and supplementary data about this project are published (Czymzik et al., 2015, 2018; Dräger et al., 2017, 2019; Heinrich et al., 2018, 2019; Kienel et al., 2013, 2017; Theuerkauf et al., 2015, Theuerkauf and Couwenberg, 2018; Wulf et al., 2016).

Competing interests. The authors declare that they have no conflict of interest.

Acknowledgements. This study is a contribution to the Virtual Institute of Integrated Climate and Landscape Evolution Analysis – ICLEA – of the Helmholtz Association (VH-VI-415) and to BaltRap: The Baltic Sea and its southern Lowlands: proxy-environment interactions in times of Rapid change (SAW-2017-IOW2). We acknowledge support for the article processing charge from the DFG (no. 393148499) and the Open Access Publication Fund of the University of Greifswald.

Financial support. This research has been supported by the DFG (German Research Foundation, grant no. 393148499) and the Open Access Publication Fund of the University of Greifswald.

References

Czymzik, M., Muscheler, R., Brauer, A., Adolphi, F., Ott, F., Kienel, U., Dräger, N., Słowiński, M., Aldahan, A., and Possnert, G.: Solar cycles and depositional processes in annual ^{10}Be from two varved lake sediment records, Earth Planet. Sc. Lett., 428, 44–51, 2015.

Czymzik, M., Muscheler, R., Adolphi, F., Mekhaldi, F., Dräger, N., Ott, F., Słowinski, M., Błaszkiewicz, M., Aldahan, A., Possnert, G., and Brauer, A.: Synchronizing 10Be in two varved lake sediment records to IntCal13 14C during three grand solar minima, Clim. Past, 14, 687–696, https://doi.org/10.5194/cp-14-687-2018, 2018.

Dräger, N., Theuerkauf, M., Szeroczynska, K., Wulf, S., Tjallingii, R., Plessen, B., Kienel, U., and Brauer, A.: A varve micro-facies and varve preservation record of climate change and human impact for the last 6000 years at Lake Tiefer See (NE Germany), Holocene 27, 450–464, https://doi.org/10.1177/0959683616660173, 2017.

Dräger, N., Plessen, B., Kienel, U., Słowiński, M., Ramisch, A., Tjallingii, R., Pinkerneil, S., and Brauer, A.: Relation Hypolimnetic oxygen conditions influence varve preservation and δ^{13}C of sediment organic matter in Lake Tiefer See, NE Germany, J. Paleolimnol., 62, 181–194, https://doi.org/10.1007/s10933-019-00084-2, 2019.

Heinrich, I., Balanzategui, D., Bens, O., Blume, T., Brauer, A., Dietze, E., Gottschalk, P., Güntner, A., Harfenmeister, K., Helle, G., Hohmann, C., Itzerott, S., Kaiser, K., Liebner, S., Merz, B., Pinkerneil, S., Plessen, B., Sachs, T., Schwab, M. J., Spengler, D., Vallentin, C., and Wille, C.: Regionale Auswirkungen des Globalen Wandels: Der Extremsommer 2018 in Nordostdeutschland, System Erde, 9, 38–47, https://doi.org/10.2312/GFZ.syserde.09.01.6, 2019.

Heinrich, I., Balanzategui, D., Bens, O., Blasch, G., Blume, T., Böttcher, F., Borg, E., Brademann, B., Brauer, A., Conrad, C., Dietze, E., Dräger, N., Fiener, P., Gerke, H. H., Güntner, A.,Heine, I., Helle, G., Herbrich, M., Harfenmeister, K., Heußner, K., Hohmann, C., Itzerott, S., Jurasinski, G., Kaiser, K., Kappler, C., Koebsch, F., Liebner, S., Lischeid, G., Merz, B., Missling, K. D., Morgner, M., Pinkerneil, S., Plessen, B., Raab, T., Ruhtz, T., Sachs, T., Sommer, M., Spengler, D., Stender, V., Stüve, P., and Wilken, F.: Interdisciplinary Geoecological Research across Time Scales in the Northeast German Lowland Observatory (TERENO-NE), Vadose Zone J., 17, 25, https://doi.org/10.2136/vzj2018.06.0116, 2018.

Kienel, U., Dulski, P., Ott, F., Lorenz, S., and Brauer, A.: Recently induced anoxia leading to the preservation of seasonal laminae in two NE-German lakes, J. Paleolimnol., 50/4, 535–544, 2013.

Kienel, U., Kirillin, G., Brademann, B., Plessen, B., Lampe, R., and Brauer, A.: Effects of spring warming and mixing duration on diatom deposition in the deep Tiefer See, NE Germany, J. Paleolimnol., 57, 37–49, 2017.

Theuerkauf, M. and Couwenberg, J.: ROPES Reveals Past Land Cover and PPEs From Single Pollen Records, Front. Earth Sci., 6, https://doi.org/10.3389/feart.2018.00014, 2018.

Theuerkauf, M., Dräger, N., Kienel, U., Kuparinen, A., and Brauer, A.: Effects of changes in land management practices on pollen productivity of open vegetation during the last century derived from varved lake sediments, Holocene, 25, 733–744, 2015.

Wulf, S., Dräger, N., Ott, F., Serb, J., Appelt, O., Gudmundsdottir, E., van den Bogaard, C., Słowinski, M., Błaszkiewicz, M., and Brauer, A.: Holocene tephrostratigraphy of varved sediment records from Lakes Tiefer See (NE Germany) and Czechowskie (N Poland), Quaternary Sci. Rev., 132, 1–14, 2016.

Acknowledgements

The organizers and participants of the Field Symposium of the INQUA Peribaltic Working Group 2019 in Greifswald would like to thank the following institutions for their support and cooperation:

GFZ - Helmholtz Centre Potsdam - German Research Centre for Geosciences

GREBAL-project team from University of Poznań (Poland)

Greifswald University, Institute for Geography and Geology

LUNG MV - State Authority for Environment Nature protection and Geology Mecklenburg-Western Pomerania, Geological Survey, Güstrow

Ministry of Agriculture and the Environment Mecklenburg-Western Pomerania, Schwerin

Müritzeum - Nature Discovery Center, Waren (Müritz)

Lower Saxony State Office for Cultural Heritage, Battlefield Archaeology, Tollense Valley Germany, Hannover

We thank the German Academic Exchange Service (DAAD) and the International Office of the Greifswald University for funding participants from partner universities.

We are grateful to the following sponsors for their financial support:

UmweltPlan GmbH Stralsund

GEO Projekt Schwerin GbR

Unternehmerverband Mineralische Baustoffe e. V.

Lagerstättengeologie-GmbH Neubrandenburg

GIG Gesellschaft für Ingenieurgeologie mbH Schwerin

Carlsberg Deutschland - Mecklenburgische Brauerei Lübz GmbH

issn 2625-8129